Hydrogen generation by the reaction of mechanochemically activated aluminium and water

SP du Preez

orcid.org/0000-0001-5214-3693

Dissertation submitted in fulfilment of the requirements for the degree *Master of Engineering in Chemical Engineering* at the North-West University

Supervisor: Dr DG Bessarabov

Co-supervisor: Prof HWJP Neomagus

Graduation ceremony: May 2019

Student number: 21220212

SOLEMN DECLARATION

I, **Stephanus Petrus du Preez**, declare herewith that the dissertation entitled:

Hydrogen generation by the reaction of mechanochemically activated aluminium and water,

which I herewith submit to the North-West University (NWU) as completion of the requirement set for the **Master of Engineering in Chemical Engineering** degree, is my own work, unless specifically indicated otherwise, has been text edited as required, and has not been submitted to any other tertiary institution other than the NWU.

Signature of the candidate:  University number: **21220212**

Signed at **Potchefstroom** on **20 November 2018**

PREFACE

Introduction

This dissertation was submitted in article format, as allowed by the North-West University (NWU) under the General Academic Rules (A-rules) set for post-graduate curricula. The A-rules prescribed that "... where a candidate is permitted to submit a dissertation in the form of a published research article or articles or as an unpublished manuscript or manuscripts in article format and if more than one such article or manuscript is used, the dissertation must still be presented as a unit, supplemented with an inclusive problem statement, a focused literature analysis and integration and with a synoptic conclusion….". Thus, due to the aforementioned, the articles included in this dissertation were added as they were published/submitted/drafted in/for a specific journal, depending at which stage the specific article was at the time the dissertation was submitted for examination. Some conventional chapters, i.e. experimental, as well as results and discussions, were therefore excluded from the dissertation, since the relevant information is presented in each respective article (Chapters 3 to 6). Separate motivation and objectives (Chapter 1), literature survey (Chapter 2), as well as project evaluation and conclusions (Chapter 7) chapters, were included along with the articles. Some repetition of ideas and similar text in some of the chapters and articles do occur, as some information presented in the motivation and objectives, literature survey, as well as project evaluation and future prospective chapter were summarized in the articles. This repetition is therefore a result of the format in which the dissertation is submitted and is beyond the candidate's control. Furthermore, the fonts, numbering, and layout of Chapters 3, 4, 5 and 6 (containing the research articles) are not consistent with the rest of the dissertation, since they were included as published (Chapter 3, 4 and 5), or in

generic article format (Chapter 6, submitted to or in preparation for submission to accredited peer reviewed journals).

A patent was granted by the Netherland patent office on the work presented in Chapters 3 to 5 on 19 October 2018 (Application number: NL2017962A, Publication number: NL2017962B1). Seeing as what the bulk of the patent consisted of work presented in Chapters 3 to 5, it was decided to only present the front page and claims in Appendix A.

Rationale in submitting dissertation in article format

Submitting a MEng dissertation in article format is allowed by the NWU; however, it is not a requirement of the NWU's A-rules. It is prescribed in the A-rules that with the submission of a non-article format dissertation, the faculty may require proof that at the time of submitting the dissertation for examination, the candidate has prepared a draft article ready for submission, or submit proof that a research article has already been submitted to an accredited journal. However, in practice, many of these draft articles are never submitted to accredited peer-reviewed journals.

Some advantages of submitting a MEng dissertation in article format include: (i) it increases the likelihood that the conducted work will be published, which is advantageous to the candidate, supervisor(s), and the university in general, (ii) articles submitted for publication are reviewed by experts in the respective field, which is implemented by the candidate to improve the article(s). This not only improves the dissertation's quality, but also gives the candidate (as well as supervisors and examiners) greater confidence in the conducted work, and (iii) it resolves the conflict between preparing articles for publication and the dissertation for examination, as the writing of the dissertation often enjoys priority, resulting in a lot of research results not getting published in the peer-reviewed public domain.

Letter of consent by co-authors

The listed co-authors hereby give consent that **Stephanus Petrus du Preez** may submit the following manuscripts as part of his dissertation, titled "**Hydrogen generation by the reaction of mechanochemically activated aluminium and water**" for the degree *Master of Engineering in Chemical Engineering* at the North-West University:

- Du Preez SP, Bessarabov DG. Hydrogen generation by means of hydrolysis using activated Al-In-Bi-Sn composites for electrochemical energy applications. International Journal of Electrochemical Sciences. 2017a;12:8663-82.
- Du Preez SP, Bessarabov DG. Hydrogen generation of mechanochemically activated Al Bi In composites. International Journal of Hydrogen Energy. 2017b;42:16589-602.
- Du Preez SP, Bessarabov DG. Hydrogen generation by the hydrolysis of mechanochemically activated aluminum-tin-indium composites in pure water. International Journal of Hydrogen Energy. 2018;43:21398-413.
- Du Preez SP, Bessarabov DG. Mechanochemical processing of aluminum-based composites for hydrogen generation purposes: Effects of bismuth and tin. Submitted to Journal of Alloys and Compounds.

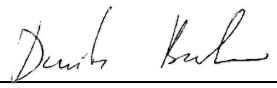

20 November 2018

Dmitri G. Bessarabov Date

LIST OF PUBLICATIONS

Journal articles

Du Preez SP, Bessarabov DG. Hydrogen generation by means of hydrolysis using activated Al-In-Bi-Sn composites for electrochemical energy applications. International Journal of Electrochemical Sciences. 2017a;12:8663-82. DOI: https://doi.org/10.20964/2017.09.22

Du Preez SP, Bessarabov DG. Hydrogen generation of mechanochemically activated Al Bi In composites. International Journal of Hydrogen Energy. 2017b;42:16589-602. DOI: https://doi.org/10.1016/j.ijhydene.2017.05.211

Du Preez SP, Bessarabov DG. Hydrogen generation by the hydrolysis of mechanochemically activated aluminum-tin-indium composites in pure water. International Journal of Hydrogen Energy. 2018;43:21398-413. DOI: https://doi.org/10.1016/j.ijhydene.2018.09.133

Du Preez SP, Bessarabov DG. Mechanochemical processing of aluminum-based composites for hydrogen generation purposes: Effects of bismuth and tin. Submitted to Journal of Alloys and Compounds.

Patent

Bessarabov, DG & Du Preez, SP, Activation compounds for hydrogen generation, Netherlands Patent Application No. NL2017962A, Publication No. NL2017962B1

Conference proceedings

Du Preez, SP and Bessarabov, D.G. Hydrogen Generation by Activated Aluminum and Water, Catalyst Society of South Africa, Hermanus, South Africa, November 2015 **(Poster presentation).**

Du Preez, SP and Bessarabov, D.G. Hydrogen Generation by means of Activated Aluminum hydrolysis, Catalyst Society of South Africa, Drakensberg, South Africa, November 2016 **(Poster presentation).**

Du Preez, SP and Bessarabov, D.G. Mechanochemical Processing of aluminum for Hydrogen Generation Purposes, Catalyst Society of South Africa, Legend Gold & Safari Resort, South Africa, November 2018 **(Poster presentation).**

ACKNOWLEDGMENTS

"I can do all this through Him who gives me strength"

Philippians 4:13

God almighty, thank you for the strength and perseverance to undertake each task that came across my path. Without your grace and love, I am nothing.

I would sincerely like to thank the following people for their help and support. They played a vital role in the completion of my dissertation and helped me to grow both academically and as a person.

My mentors Dr. Dmitri Bessarabov and Prof. Hein Neomagus for their guidance and expertize.

My parents Faan and Yvonne du Preez, and my siblings Johan, Bennie, and Yolandi, for their support, love and motivation.

My better half, Michelle Eagleton, for her unconditional love and support during the duration of this study.

TABLE OF CONTENTS

TABLE OF FIGURES

ABSTRACT

This dissertation presents a method to generate on-demand and pure hydrogen from neutral pH water using a hydrolysing material, i.e. mechanochemically activated aluminium (Al), under standard ambient conditions. The individual and combined effects of the considered activation compounds, i.e. bismuth (Bi), indium (In), and tin (Sn), on Al during mechanochemical processing were evaluated. Of importance in this study were i) composite hydrolysis reactivity towards water, ii) the effects of activation compounds on Al particle behaviour during mechanochemical activation, i.e. cold-welding, strain hardening, fracturing, and iii) the distribution of activation compounds in Al particles. Several activation compound combinations were considered for investigation, i.e. Bi-In-Sn, Bi-In, Sn-In and Bi-Sn. SEM and EDS analyses were applied to determine particle morphology and surface/sub-surface chemical compositions of Al particles pre- and post mechanochemical activation procedures. Scanning electron microscopy (SEM) energy dispersive x-ray spectrometer (EDS) results presented in this study suggests that the considered activation compounds could be distributed relatively homogeneously throughout Al particles by mechanochemical activation. Such a distribution promoted micro-galvanic activity between anodic Al and cathodic Bi, In, and Sn. X-ray diffraction indicated various intermetallic phase formation between Al-activation compound and activation compound-activation compound. These phases formed as a result of mechanochemical activation and in some cases affected the structural failure and/or reactivity of Al particles. Numerous high hydrogen yielding (>95%) composites were prepared. Furthermore, a preliminary method to recover activation compounds from hydrolysed Al using common acids was proposed.

Keywords: Aluminium; mechanochemical processing; activation compounds; hydrolysis; neutral pH water; bismuth; indium; tin.

CHAPTER 1: MOTIVATION AND OBJECTIVES

An overview of the project motivation is briefly discussed in Section 1.1, while general aims and specific objectives are listed in Section 1.2.

1.1. Background and motivation

Hydrogen is a suitable substitute for traditional carbon-based fuel sources. The majority of hydrogen currently produced contains carbon dioxide (CO_2) and carbon monoxide (CO) [1, 2]. CO_2 is the main green-house gas contributor, whereas CO in known to deteriorate proton exchange membrane fuel cells (PEMFCs) used to convert the chemical energies associated with hydrogen gas into electrical energy [3-6]. PEMFCs can offer a technology for clean energy production [7, 8], especially for mobile (transport sector), low-power (<1 kW), and portable electrical device applications [9, 10]. A limiting factor to hydrogens application is its low gaseous density of 0.089 $kg.m^{-3}$ [11], which greatly complicates its storage.

Several methods have been developed in recent years to generate on-demand pure hydrogen. One such a method is the hydrolysis of certain metals, such as Al, Mg and Zn [12-19], with various water qualities. Al was considered in this study as a hydrolyzing metal and water as the hydrogen source. Water has a hydrogen content of 111 $kg.m^{-3}$, whereas petrol and liquid hydrogen (at 20 K) has hydrogen contents of 84 and 71 $kg.m^{-3}$, respectively [20, 21].

Al's hydrolysis is a spontaneous reaction; however, a thin protective oxide layer on Al's surface prevents this reaction. Numerous studies have been performed to remove this oxide layer, e.g. submerging Al in acidic or alkaline solutions, amalgamation with Hg and Ga, hydrothermal processing, and thermal and mechanochemical activation with various materials. In most cases, these activated Al composites are limited to laboratory scale due to

several reasons, e.g. certain activation compounds are toxic/expensive, composites exhibit too high/low reactivities, expensive equipment required, and corrosive reaction conditions. This study focused on the development of an improved Al activation process, with emphasis on hydrogen yield and activation compound addition optimization.

1.2. Objectives

The overall objective of this study was to develop and optimize a process to produce a low-cost mechanochemically activated Al based composite, which may be combined with neutral pH water under standard ambient conditions, to generate on-demand, pure hydrogen for a variety of low power applications.

The specific objectives of this work were:

1. Identify suitable activation compounds to activate Al using a mechanochemical approach;
2. Determine the efficiency of identified activation compounds in terms of composite hydrolysis reactivity;
3. Investigate the various reaction parameters that may affect the performance of prepared composites;
4. Develop a method to recover activation compounds from hydrolyzed Al composites.

CHAPTER 2: LITERATURE SURVEY

This chapter reviews current, relevant literature relating to the dissertation topic, i.e. hydrogen generation by the reaction of mechanochemically activated aluminium and water. This chapter consist of general information on renewable energy (Section 2.1), hydrogen as an energy carrier (Section 2.2), current hydrogen production processes (Section 2.3), hydrogen storage methods (Section 2.4), an overview of the proposed hydrogen generation method (Section 2.5), and the known aluminium hydrolysis methods (Section 2.6). Finally, a concluding summary is provided (Section 2.7).

2.1. Introduction

The continuous development and expansion of industrial and commercial sectors over recent decades have placed increasing stress on the global energy demand, raising questions regarding the reserve capacity and sustainability of current fossil fuel resources [22]. The increase in energy demand and subsequent fossil fuel consumption is chaperoned by increased pollutant emissions. As a result, these factors are incentive for the development of renewable energy sources. Though a fossil-fuel free economy is many years away from becoming a reality, a reduction of fossil fuel dependence is an achievable objective. Renewable energy sources, e.g. solar, wind, geothermal and tidal, are infinite energy sources with relatively reliable and predictable patterns. Wind and solar energy production is comparatively safe and has minimal negative environmental consequences [23, 24]. Additionally, the use of solar energy for off-grid mining areas [25, 26] and off-grid islands [27, 28] has been adopted in the past [29].

A major limitation of large scale implementation of continuous off-grid renewable energy is daily intermittency, i.e. periods of low wind speeds and night-time. Additionally, such a power-grid may not be able to handle the total amount of energy produced during certain

periods, forcing it to forgo the excess energy generated, either by exporting excess energy to a neighbouring grid or by down-scaling the energy production capacity. Thus, it is evident that an energy storage method is required for a renewable energy grid to provide a continuous supply of energy. Several such methods exist, e.g. compressed air energy, fly-wheels, thermal energy, pumped hydro-storage, and electrochemical (batteries). These methods typically store energy on a small to medium scale, and only for a limited period of time [30].

2.2. Hydrogen as an energy carrier

The production of hydrogen may be a suitable energy storage solution. Unlike hydrocarbons, hydrogen cannot be destroyed when reacted with oxygen [31], and only yields water and energy according to Reaction 2-1:

$$H_2 + 0.5O_2 \rightarrow H_2O, \Delta H = -285.8 \text{ kJ/mol} \qquad \text{(Reaction 2-1)}$$

Hydrogen has been identified as the best candidate to replace fossil fuels [32, 33]. Per unit mass, hydrogen combustion yields three times more energy than natural gas and six times more energy than coal [34]. Hydrogen is typically applied in petroleum refining [35-37], ammonia production [33, 35, 38], refinement of various metals, e.g. copper, zinc, uranium, lead, nickel, and tungsten [35, 39, 40], hazardous waste hydrogenation (dioxins, polychlorinated biphenyls), and as rocket fuel [35]. Hydrogen is a renewable, non-polluting energy carrier with high specific energy and calorific density [41-43]. Furthermore, internal combustion engines can be converted with relative ease to facilitate hydrogen gas as a fuel source, increasing the efficiency by 25% if compared to petrol engines [34, 44]. However, the compatibility of hydrogen gas with fuel cells (FCs) is its most appealing factor. FCs can serve as an alternative form of clean energy production [7, 8]. A major advantage of FC application is the decentralization of power generation, implying that electricity does not have to be imported from the point of generation by transformers and high tension, long

distance power lines where losses usually occur [34]. Various different FCs exist, e.g. proton-exchange membrane (PEM), alkaline, phosphoric, solid oxide, and molten carbonate [9]. PEMFCs convert the chemical energies associated with hydrogen into electrical energy without combustion [3, 4], and are considered advantageous over other FC types for mobile power applications (such as vehicles), stationary power units, and portable electrical devices [9, 10, 45, 46]. The transport sector have adopted PEMFCs due to its fast start-up and lower operational temperature characteristics [34]. PEMFCs are the ideal replacements for internal combustion engines due to its temperature tolerance, high power density, and rapid load responses. Approximately half of the globally produced oil is consumed by road vehicles [2], and considering the likelihood that fossil fuel production will decrease over-time [47], PEMFC operated vehicles seems inevitable. In addition to this, the global projected energy demand will double or triple by 2050 and it is highly unlikely that gas and oil supplies will meet this demand [48]. Thus, the need for alternative, renewable fuels is further expedited by these trends.

2.3. Hydrogen production

Hydrogen is the most abundant element in the universe, but is rarely found in its elementary form on earth. Hydrogen can be produced from non-renewable (hydrocarbon) and renewable sources. The majority of hydrogen is currently produced from non-renewable sources [2, 35], and it is estimated that 48% of hydrogen is produced from natural gas, 30% from oil, 18% from coal, and 4% from electrolysis [2]. Hydrogen obtained from hydrocarbons produces carbon dioxide (CO_2) as a by-product, which is subsequently released into the atmosphere [1, 49]. Additionally, carbon monoxide (CO) may be present in hydrogen obtained from hydrocarbon sources and may have detrimental effects on fuel cells utilized to convert the chemical energies of hydrogen to electrical energy [5]. Thus, if hydrogen were to be obtained from hydrocarbons it cannot be truly considered as renewable. Ideally, the process

applied to obtain hydrogen should only produce hydrogen (and no other gasses such as CO_2 and/or CO) from a renewable sources [50]. The most commonly applied industrial hydrogen production methods are discussed in short in the following texts [35]:

2.3.1. Steam methane reforming

This process consists of reacting natural gas or other methane (CH_4) rich gas streams with steam in the presence of a catalyst, mainly producing hydrogen and CO_2. The obtained hydrogen rich gas typically consists of 70 to 75 % hydrogen, 2 to 6 % CH_4, 6 to 14 % CO_2, and 7 to 10 % CO. This method of hydrogen production is however not an attractive route for a mature hydrogen economy. A reason being is that natural gas reforming produces as much CO_2 as direct natural gas combustion. Additionally, this route would starve the global CH_4 reserve, resulting in natural gas being as sensitive as oil [35, 51].

2.3.2. Hydrocarbon gasification

Gasification, also termed partial oxidation process, produces hydrogen gas from various hydrocarbon sources, e.g. coal, low-value refinery products, heavy residual oil, and petroleum coke [52]. Gasification is performed by reacting the hydrocarbon source with oxygen at a less than stoichiometric ratio at between 1200 and 1350 ºC, yielding a mixture of hydrogen and CO [53].

2.3.3. Hydrogen from biomass

Two biomass-to-hydrogen conversion technologies are typically utilized, i.e. thermochemical and biochemical processes [35]. These processes involve either pyrolysis or gasification to obtain syngas, which is a mixture of hydrogen and CO [35, 53]. Biomass gasification has been identified as a possible approach towards renewable hydrogen production. Additionally, various hydrogen from biomass production processes yield other useable by-products, e.g. ethanol, methanol, activated carbon, and fertilizer [54].

2.3.4. Hydrogen from nuclear energy

Hydrogen can be produced from water by electrochemical and/or thermochemical processes utilizing nuclear energy as the primary thermal energy source [55]. Notwithstanding the attractiveness of hydrogen production from a carbon-limiting perspective, the use of nuclear power raises other serious health and environmental concerns with regard to uranium mining and processing, radioactive waste disposal and management, and the potential for devastating accidents [54].

2.3.5. Water electrolysis

This hydrogen production method entails splitting water molecules into hydrogen and oxygen by utilizing an electrolyzing device operating on electricity. Two types of water electrolysers are most commonly utilized, i.e. alkaline using potassium hydroxide as an electrolyte and PEM which utilizes a solid polymer membrane electrolyte. Electrolysers currently being utilized ranges from a few kW to up to 2 MW per electrolyser [35]. A major benefit of hydrogen obtained in such a way is that only pure oxygen and hydrogen are produced [52, 53, 56]. Nevertheless, large volume hydrogen production plants implementation has yet to be realized due to economic considerations.

2.4. Hydrogen storage

The storage of hydrogen is complicated by its low boiling point (-252.95ºC), low gaseous density (0.089 $kg.m^{-3}$), and high liquidus density (71 $kg.m^{-3}$) [11, 35]. In fact, hydrogen storage is a critical issue that has to be resolved prior to establishing an economically and technically viable hydrogen fuel economy [49]. For instance, on-board vehicular hydrogen storage requires much larger storage tanks, if compared to petrol/diesel tanks [2]. According to Sharma and Ghoshal (2015), three competing requirements are considered as challenges in finding a suitable storage material, i.e. high hydrogen density, reversibility of the

release/charge cycle at temperatures compatible with current generation fuel cells, and fast release/charge kinetics with minimum energy barriers with regard to hydrogen release/charge procedures [35]. Hydrogen can be stored by manipulating its state conditions (phase, temperature, pressure), and chemically by various compounds, e.g. metal hydrides, methane, carbon nanostructures, methanol, and liquid organic hydrogen carriers [57-59]. Currently, hydrogen is mainly stored as a pressurized gas, in its liquid state, or as a metal hydride [11]. Of these methods, pressurized gas is the cheapest and least complicated storage method [60]. Figure 2-1 illustrates the various hydrogen storage methods [35].

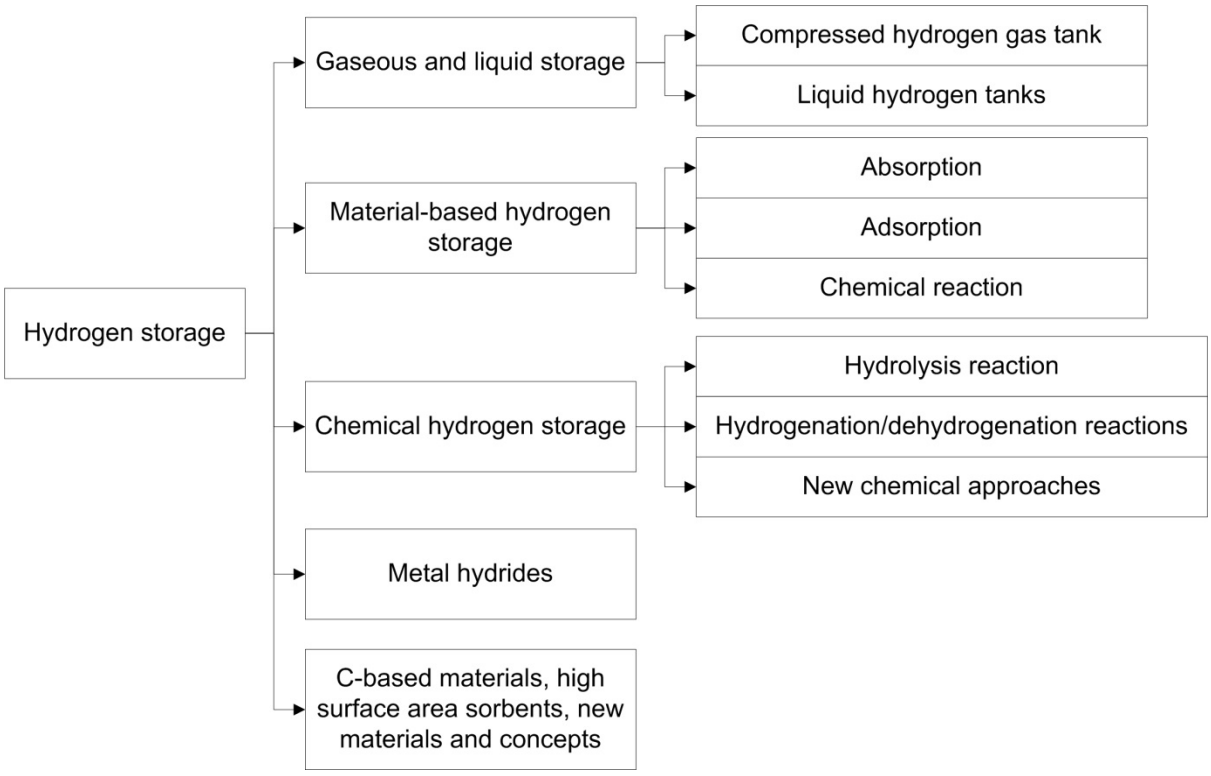

Figure 2-1: Illustration of the various hydrogen storage methods (Reprinted from Sharma and Ghoshal, Hydrogen the future transportation fuel: From production to applications, 2015, 43, 1151-1158, with permission from Elsevier).

Hydrogen's storage in a solid or liquid matrix is a viable alternative to compressed and liquid hydrogen storage methods. The most promising storage methods are in solid materials that either form chemical bonds or physically adsorb hydrogen at volume densities greater than

liquid hydrogen [35]. Considering the latter mentioned, the following hydrogen generation method is proposed.

2.5. Proposed hydrogen generation method

In this dissertation, hydrogen generation by means of Al-water hydrolysis reaction was investigated. Water was selected as the hydrogen source material. Per unit volume, water has a hydrogen content of 111 $kg.m^{-3}$, exceeding that of gasoline (84 $kg.m^{-3}$) and pure liquid hydrogen (71 $kg.m^{-3}$) [20, 21, 61]. Various methods exist to produce hydrogen from water, e.g. water photo-catalysis [62-65], water electrolysis [56, 59, 66, 67], metal-hydride hydrolysis [68-70], and metal hydrolysis [12, 71-73]. Furthermore, when considering hydrogen's low gaseous density, it would be beneficial to store it as water, and break the hydrogen-oxygen bond when the demand for it presents itself.

In recent years, several metals have been considered for metal hydrolysis hydrogen generation, i.e. Al, Mg, and Zn [12, 16, 18, 19, 74, 75]. Al is considered as the most viable metal due to several attractive properties, i.e. high hydrogen generation potential of 1.36 $L.g^{-1}$ Al under standard ambient conditions [76, 77], low volumetric mass density of approximately 2700 $kg.m^{-3}$, high energy density, and abundance. No carbon is released during the hydrolysis of Al, and only yields pure hydrogen gas and Al-hydroxides. These hydroxides are considered environmentally benign and may be used in various applications, i.e. flocculation, fire retardation, papermaking [78, 79]. Furthermore, Al can be fully re-metallized to its metallic state, i.e. Al^0, by the Hall-Héroult process [14, 61]. Al's volumetric mass density and high energy density significantly reduce the total weight of an Al-based energy system. An example of the use of Al in the field of energy is its application in high pH electrolyte batteries. Pure Al discharge reaction potential can be as low as -2.33 V with respect to the standard hydrogen electrode [80]. Additionally, the lightweight of Al and its tri-valence (Al^{3+}) yields an electrochemical equivalence of 2.98 $Ah.g^{-1}$ [81]. All the

foregoing properties of Al indicate it to be a suitable anode material. Many investigators began studying Al's corrosion as a hydrogen generator. Due to the fact that pure Al is highly electronegative; it is easily subjugated to corrosion by changing into ion forms. According to Dražić and Popić (1999) the electrochemical corrosion of Al-based materials cannot be predicted using Wagner-Traud mixed potential model, due to existence of the negative difference effect. This effect states that the hydrogen evolution rate will increase with increasing anodic polarization [82]. Normally, practical uses of Al based materials are recognized for its resistance to corrosion, e.g. construction material. This is due to a thin, dense, protective oxide layer on the surface of Al (and its alloys) caused by the strong affinity between Al and oxygen. This layer protects Al from corrosion under ambient conditions and it is the main limiting feature when corrosion applications of Al are considered, especially if continuous hydrogen generation is the end-goal.

2.6. Aluminium hydrolysis methods

Al may be hydrolysed by either manipulating the reaction conditions, i.e. water pH, reaction temperature, or by manipulating Al's physical and chemical properties. This section discusses some of the most relevant hydrolysis methods.

2.6.1. Al's exposure to harsh pH environments

Submerging Al in alkaline or acidic solutions to generate hydrogen has been widely investigated [83-97]. This method involves the dissolution of the coherent oxide layer Al's surface, as well as preventing reformation thereof, by means of acidic/alkaline solutions. Boukerche et al. (2014) found that the dissolution rate of Al was greater in NaOH than in HCl [88]. This was ascribed to the presence of hydroxide ions (OH^-) in alkaline environments, which actively dissolved the protective oxide layer. NaOH is the most commonly utilized alkali, and the Al-NaOH reaction occurs as follow [83, 98-100]:

$$2Al + 6H_2O + 2NaOH \rightarrow 2NaAl(OH)_4 + 3H_2 \quad \text{(Reaction 2-2)}$$

$$NaAl(OH)_4 \rightarrow NaOH + Al(OH)_3 \quad \text{(Reaction 2-3)}$$

$$2Al + 6H_2O \rightarrow 2Al(OH)_3 + 3H_2 \quad \text{(Reaction 2-4)}$$

NaOH consumed in Reaction 2-2 is regenerated by $NaAl(OH)_4$ decomposition (Reaction 2-3). Thus, only water is consumed during this reaction if the reaction is properly controlled. The overall reaction (Reaction 2-4) is a well-known parasitic reaction, which is considered undesirable during alkaline Al-air batteries. Soler et al (2007b) investigated the effects of NaOH, KOH and $Ca(OH)_2$ on Al's dissolution, and it was found that NaOH was superior to KOH and $Ca(OH)_2$ when promoting Al's dissolution [84]. Several hydrogen generating devices have been developed based on the Al-NaOH reaction [85, 90, 101-103].

This method of hydrogen generation typically requires extreme pH values and elevated temperatures (approximately 100°C) in order to achieve high hydrogen generation rates. The use of such harsh pH solutions is considered far from ideal due to the rapid equipment deterioration. Addition, the use of harsh pH solutions for mobile application should be avoided.

2.6.2. Hydrothermal process

Hydrogen may be generated by reacting Al with water at elevated temperatures and pressures. In recent years, several studies have been conducted [104-110]. Under the correct conditions, Al powder can react with neutral pH waters according to the following reaction [105]:

$$2Al + 3H_2O \rightarrow Al_2O_3 + 3H_2 \quad \text{(Reaction 2-5)}$$

An attractive prospect of the Reaction 2-5 is the application thereof in space and underwater propulsion systems [111, 112], and explosives [113]. Typically, nano-scaled Al is best suited

for this type of reactions as such particles have high chemical activity, comparable to that of alkali metals, due to their larger reaction surfaces. However, a draw-back of this method is the requirement of expensive equipment and unfavourable reaction conditions [104, 105].

2.6.3. Combination with dissimilar metals

A mechanism was proposed by Reboul et al. (1984) explaining Al's activation by alloying elements, also known as dissimilar metals [114]. Initially, anode dissolution is induced by galvanic coupling, which oxidized Al and the alloying element, according to Reaction 2-6:

$$Al(M) \rightarrow Al^{3+} + M^{n+},\ M = \text{alloying element/dissimilar metal} \qquad \text{(Reaction 2-6)}$$

M^{n+} cations re-deposits onto the surface of Al due to the cathodic nature of the alloying element relative to Al, according the electrochemical exchange reaction:

$$Al + M^{n+} \rightarrow Al^{3+} + M \qquad \text{(Reaction 2-7)}$$

Simultaneous local Al-oxide layer separation occurs during Reaction 2-7, shifting Al's anodic potential towards that of bare Al. As for point defect formation, retention and agglomeration of mobile metallic species on alloy surfaces attributes to the localized de-filming process [115]. Thus, Al may be activated with small quantities of various alloying element/dissimilar metals to enable the Al anodic dissolution process [116]. Al's activation by dissimilar metals may be divided into three groups: amalgamation, thermal alloying, and mechanochemical activation. The following texts discuss these activation routes.

2.6.3.1. Amalgamation

Smith (1972) stated that Hg addition to a Al-water system could continuously produce hydrogen at temperatures <100°C [117], until Al is consumed. This approached avoids the use of corrosive chemical and unfavourable reaction conditions. Al's amalgamation with Hg and Hg-based composites and hydrolysis occurs according to Reactions 2-8 and 2-9, respectively [118-122].

$$Al + Hg \rightarrow Al(Hg) \quad \text{(Reaction 2-8)}$$

$$Al(Hg) + 6H_2O \rightarrow Al(OH)_3 + H_2 + Hg \quad \text{(Reaction 2-9)}$$

Here, Al's corrosion/dissolution mechanism may been ascribed to a combination of physical and electrochemical processes [123]. Reaction 2-8 presents the physical corrosion of Al where Al's atomic bond strength is reduced as Hg penetrates the surface of Al particles, which caused Al's embrittlement. This occurrence is known as the Rebinder effect, defined as the effect of adsorptive decrease in solid strength under physical-chemical influences of the medium [124]. Consequently, a Hg-based amalgam is formed on the surface of Al [125]. Subsequently, electrochemical corrosion takes place as described by Reaction 2-9 [118]. This reaction occurs via the transport of Al through the amalgamated layer, towards the amalgam-water boundary were Al is hydrolysed and Al-hydroxide and hydrogen gas is produced. Al is continuously dissolved and transported via the amalgam to the amalgam/water boundary, allowing continuous hydrogen generation until Al is consumed. This process is schematically presented in Figure 2-2 [120].

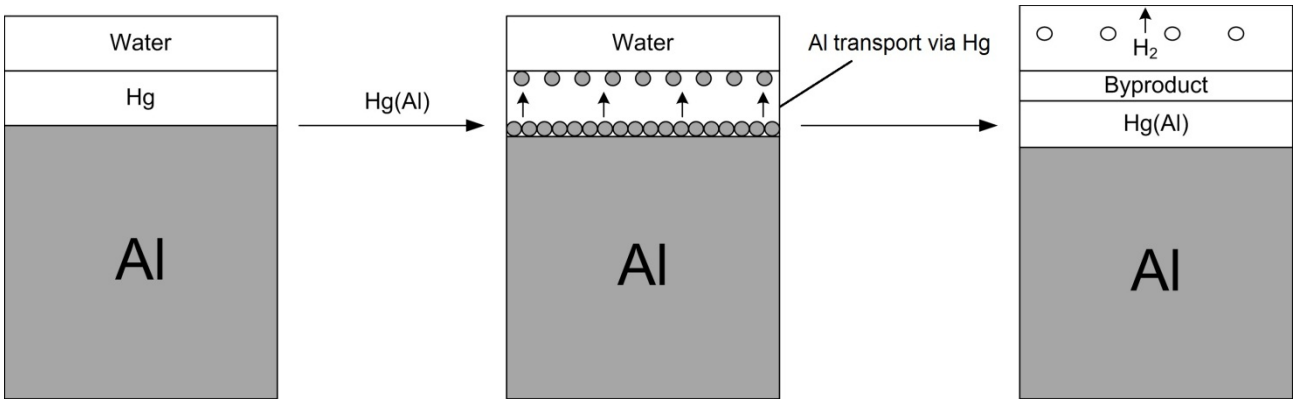

Figure 2-2: Proposed aluminium hydrolysis induced by Hg (Reprinted from Huang et al. Effects of amalgam on hydrogen generation by hydrolysis of aluminium with water, 2011, 36(23), 15119-15124, with permission from Elsevier).

Seo et al. (1988) stated that the reactivity of amalgamated Al was influenced by the amalgam composition [126]. Huang et al. (2011) prepared a Hg-Zn amalgam and determined its

effects on Al's hydrogen generation, and found that the addition of Zn to the amalgam increased the hydrogen generation rate and yield. In addition, the activation energy of the Hg-Zn amalgam was 43.4 $kJ.mol^{-1}$, whereas the Hg amalgam was 74.8 $kJ.mol^{-1}$ [120]. Though Hg, and Hg-based materials, has been proven successful in activating Al, its use has been limited due to the toxicity associated with Hg. In its elemental and methylated forms, Hg is highly toxic to humans and animals [127]. Consequently, this method is typically avoided.

Ga has a similar effect than Hg on Al particles, and is known to induce structural failure of Al matrixes [12, 72, 73, 128]. For instance, a Ga-In-Sn material has a melting point of 10.4°C, and in its liquid state, can cover and amalgamate the surface of Al to remove the coherent oxide layer [129]. However, Ga is an expensive compound and the use thereof to activate Al increases the cost of such Al composites. Thus, the use thereof limits the application of Ga-containing composites for hydrogen generation purposes.

2.6.3.2. Thermal alloying

Thermal alloying entails melting Al together with various activation compounds. Al has a relatively low melting point, i.e. 660°C, so treatment temperatures are typically in this range. However, depending on the activation compounds considered, the thermal treatment temperature may be well below that. Numerous studies have been performed on the activation of Al by thermal treatment with metals, e.g. Ga [124, 130, 131], Ga-In [132, 133], Ga-In-Sn [131, 134, 135], Ga-In-Zn [136], Ga-In-Sn-Bi [137], Ga-In-Sn-Mg [138, 139]. Though, high hydrogen yielding alloys could be prepared using this method, it has been proven that mechanochemical method produces more reactive composites than composites prepared by thermal treatment. For instance, Fan et al. (2007) compared the reactivities of Al-5.3% Ga-2.0% In-5.4% Sn-7.3% Zn composite (wt.%) prepared by thermal and

mechanical activation methods. They found that the composite prepared by mechanochemical processing had a shorter total reaction time and higher hydrogen yield than the thermally prepared composite [143]. In addition to this, thermal treatment consumes more energy that mechanochemical activation methods, due to inevitably heat loss during treatment procedures. Furthermore, one has to consider the solubilities of activation compounds in Al during thermal treatment procedures. For instance, Bi has no appreciable solubility in Al and forms a segregated layer on an Al melt [140], whereas Sn has a 0.1% solubility in Al at 600°C [141, 142]. Thus necessitating additional homogenization of Al melts to allow composite distribution through the melt until solidification occurs, further complicating such an activation route.

2.6.3.2. Mechanochemical activation

This activation route may be summarized as the coupling of chemical and mechanical phenomena on a molecular scale. It entails chemical behavior of stressed solids, mechanical breakage, tribology, stress-corrosion cracking, and material degradation under continuous deformation conditions. Mechanochemical activation gains its novelty as it is completely different from traditional chemical methods (e.g. does not include dissolving, solution agitation, heating), enabling environmentally friendly, and low contamination material preparation methods.

The general particle size and morphological changes of ductile, brittle, and ductile-brittle metals occurring during mechanochemical processing are explained in Refs. [143-145], and are summarized in the following text. During mechanochemical processing procedures (e.g. ball milling), metals undergo repetitive plastic deformation and are subjected to radical changes in particle shape, residual stress, which redistributes constituents. During ball milling of ductile and malleable particles, several mechanisms are at play. As ball milling

commences, particles cold weld as they are caught between the impacts of milling equipment, forming larger coagulated particles consisting of an unequal distribution of the initial constituents. After a certain period of milling, the coagulated particles will reach a stress-to-strain point due to work hardening, followed by strain-induced fracturing of coagulated particles. The result is a decrease in particle size as a result of particle fracturing. Of importance in this dissertation is Al's behavior during mechanochemical processing in the presence of certain metals. Du Preez and Bessarabov (2018) illustrated Al's behavior in the presence of Sn and In in Figure 2-3 during mechanochemical activation [146].

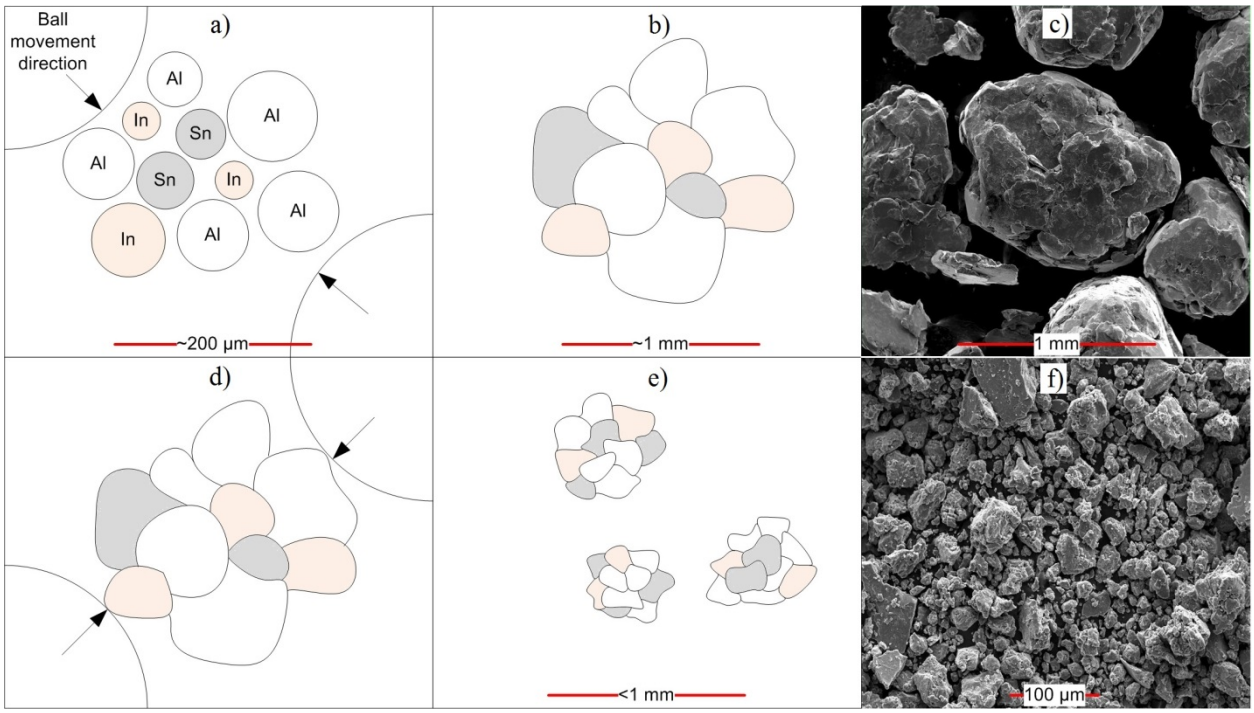

Figure 2-3: Illustration of Al's behavior in the presence of other compounds. Figures (c) and (f) shows Al-5 wt.% Sn-5 wt.% In micrographs, which where ball-milled for 5 and 30 min, respectively [146].

A benefit of Al's mechanochemical processing with dissimilar metals is that such metals may be relatively evenly distributed throughout Al particles, which promotes micro-galvanic activity between Al and the metal during hydrolysis reactions. Du Preez and Bessarabov

(2018) presented sub-surface micrographs of a mechanochemically activated Al-5 wt.% Sn-5 wt.% In as shown in Figure 2-4.

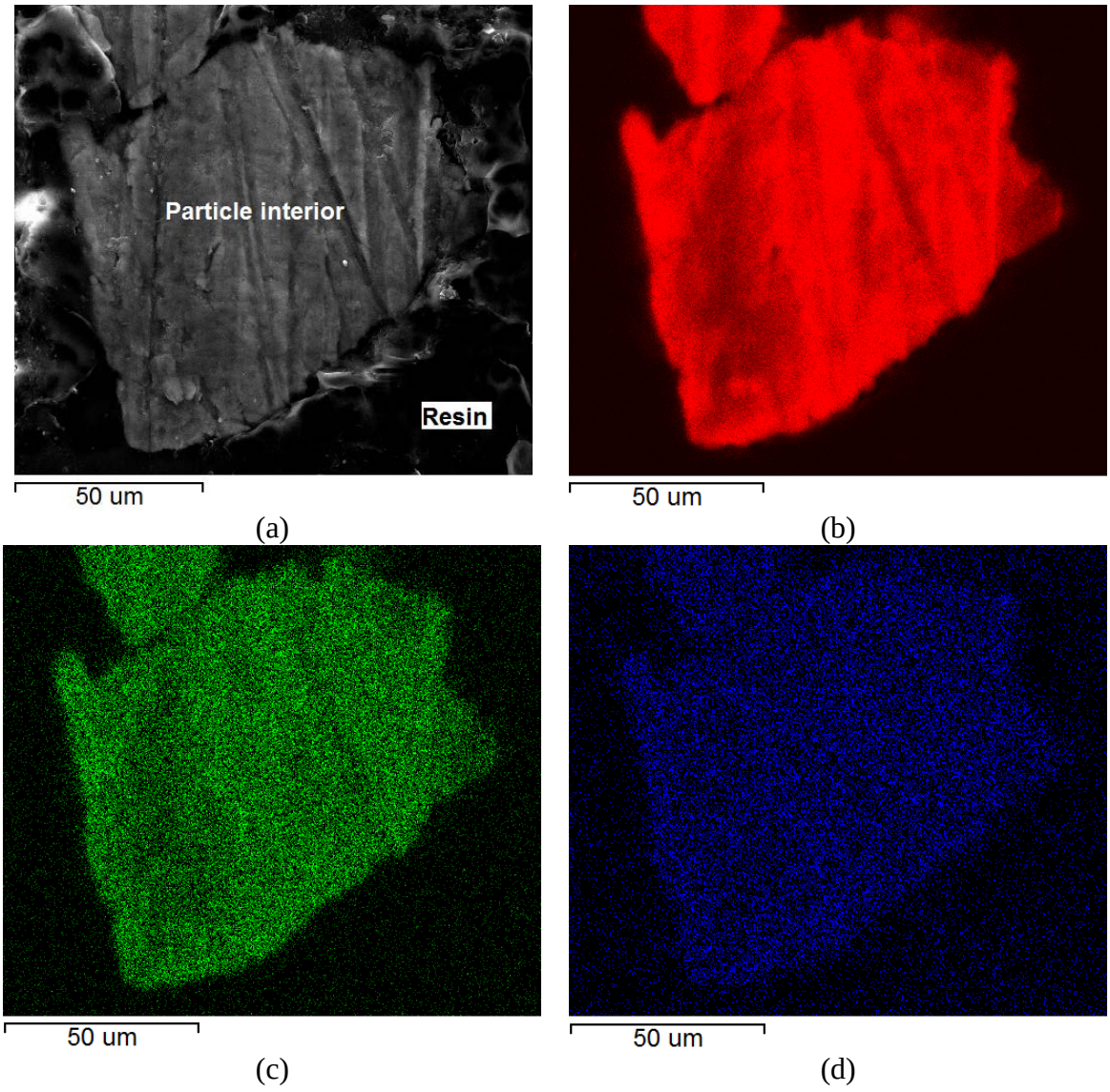

Figure 2-4: A SEM micrograph of a mechanochemically processed Al-5 wt.% Sn-5 wt.% In composite (a) and the corresponding EDS mappings for Al (b), Sn (c) and In (d) [146].

Numerous studies have been performed on the mechanochemical activation of Al with a series of dissimilar metals, e.g. Ga-In [71, 147], Ga-In-Sn [128, 148], Ga-In-Sn-Zn [72], Ga-Bi-Zn [149]. In most cases, high hydrogen yielding composites were prepared. When considering the total cost per volume unit hydrogen produced, the activation route and materials used to activate Al are the main determining factors. The major benefit of this

activation route is its simplicity and low energy requirements, allowing for the fabrication of a cheap hydrogen producing material.

2.6.4. Mechanochemical activation by metal oxides

A method to activate Al includes milling Al with metal oxides. Such metal oxides includes compounds capable of independent, highly exothermic thermite reactions (MoO_3, Bi_2O_3, CuO) [150], as well as chemically inert oxides (MgO, Al_2O_3, TiO_2) [150, 151]. Even though the addition of metal oxides to Al during ball milling increased the reactivity and hydrogen yield of Al during hydrolysis, the decrease in potential hydrogen generation (caused by a large fraction of Al being replaced by metal oxide), low availability of effective metal oxides [84], and increased complexity of seeding processes, makes metal oxide based Al activation less attractive than other, well established methods [110, 152].

2.6.4. Mechanochemical activation by water soluble salts

The use of water soluble inorganic salts (e.g. NaCl, KCl) individually or in conjuration with other additives to activate Al via mechanochemical activation has gained attention due to the relative ease and simplify of this Al activation method [20, 79, 153, 154]. The salts used during this activation method fulfil various crucial roles: i) salts prevents Al particles from cold-welding to each other, forming large agglomerates, ii) salts act as grinding media, reducing Al's particle size, iii) certain salts react with water to release heat, which promotes Al's hydrolysis, and iv) salt particles can become lodged in the surface of Al particles as indicated in Figure 2-5 [79]. Here, a NaCl particle has been lodged into an Al particle. When introduced to water, the salt particles dissolve and underlying metallic Al is hydrolysed. Per wt%, this type of composite typically requires a large fraction of salt to appreciably activate Al, reducing the hydrogen generation potential.

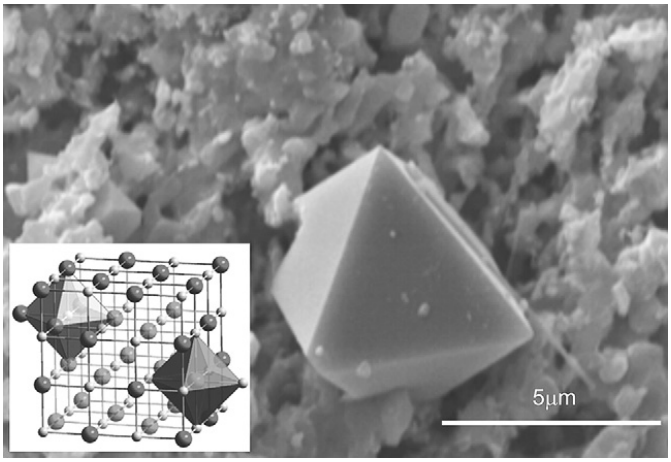

Figure 2-5: SEM micrograph of a NaCl particle lodged into an agglomerate of mechanochemically activated Al particles (Reprinted from Alinejad and Mahmoodi, A novel method for generating hydrogen by hydrolysis of highly activated aluminium nanoparticles in pure water, 2009, 34(19), 7934-7938, with permission from Elsevier).

2.6.5. Mechanochemical activation by carbon-based additives

Al's activation by C-based materials does not form chemical bonds; rather the interaction between Al and C-based materials may be ascribed as an adhesive/adsorptive type. Primarily, Al's mechanochemical activation by C-based materials prevents the reformation of the protective oxide layer on fresh Al surfaces due to C preventing contact between oxygen and the fresh Al surface [155]. In some cases where high energy mechanochemical activation was applied, Al_4C_3 formation occurred. The hydrolysis of Al_4C_3 yields methane, instead of hydrogen gas, according to the following reaction [156]:

$$Al_4C_3 + 12H_2O \rightarrow 4Al(OH)_3 + 3CH_4 \qquad \text{(Reaction 2-10)}$$

However, the formation of Al_4C_3 can be minimized by a low energy mechanochemical activation route [156], or formed Al_4C_3 can be converted to Al(C) by prolonged milling [157]. A major disadvantage of this method is that the heat released by Al/C composite hydrolysis exceeds the rate of heat transfer to the environment, which results in explosion-

like reactions [158]. Additionally, without specialized storage, Al/C composites are readily pacified by air [156, 159] and atmospheric moisture [156].

2.6.6. Activation of Al by Group 1 and 2 metals

Al composites activated by alkali and alkali earth metals (Mg is excluded from this section), such as Li and Ca, have been considered for hydrogen generation purposes. Alkali metal hydrolysis is similar to that of Al (in the absence of the protective layer), yielding hydrogen and an alkali solution. Compared to the other alkali metals, Li hydrolysis is relatively mild, and the hydrolysis reaction is systematically slowed and eventually stopped due to the formation of an insoluble Li-hydroxide layer on its surface. A major advantage of a Li or Ca activated Al composite is that Li and Ca increase the hydrogen volume obtainable per gram of composite hydrolysed. This is due to the fact that Li and Ca undergoes hydrolyses, whereas other typical activation compounds do not. Assuming complete hydrolysis and standard ambient conditions, Al, Li and Ca will generate 1360, 1760 and 610 mL of hydrogen per gram of metal, respectively. Zhao et al. (2011) mechanochemically prepared Al- x wt.% Ca (x = 5, 10, 15, 20) composites achieving 93.5 to 100% hydrogen yields [160]. Fan et al. (2011) mechanochemically prepared an Al-40% Li composite which achieved a hydrogen yield of 94.5%. In addition to this, the authors thermally prepared a Al-30% Li composite at 650 and 550°C, which yielded less hydrogen if compared to the mechanochemically prepared composite [161]. Rosenband and Gany (2014) thermally prepared a high hydrogen yielding Al-Li composite [162]. Fan et al. (2011) and Chen et al. (2014) mechanochemically produced Al-Li based composites reaching hydrogen yields of >90% [163]. However, a short-coming of Al-Li composites is that they are highly reactive with air, and that special storage measures have to be implemented. Furthermore, certain Al-Li composites have such high hydrolysis reactivity, that in-situ generated heat my cause the generated hydrogen to combust as it is generated.

2.7. Possible application

On-demand, pure hydrogen generation by the hydrolysis of Al with neutral pH water is an attractive source of hydrogen for various low power (<1 kW) applications. One such an application is in the unmanned aerial vehicle (UAV) market. PEMFCs are good candidates to replace Li-ion battery powered UAVs, providing such UAVs with longer flying times due to their low weight and high durability (https://ieeexplore.ieee.org/document/6749817). According to the U.S. Department of Energy, suitable fuel cells and UAVs are available; the limiting factor to fuel cell powered UAVs is low-cost, practical H_2 fuelling (https://www.energy.gov/sites/prod/files/2016/05/f32/fcto_webinarslides_h2_fc_small_unmanned_air_vehicles_052616.pdf). Some differences between battery and fuel cells powered UAVs include the following: i) fuel cells do not need to be recharged and only require hydrogen and air to function, ii) batteries store energy while fuel cells generate energy on-demand, and iii) in a fuel cell, anode (hydrogen) and cathode (air) gases are kept separate making it safer to operate. In addition to this, battery powered UAVs require large batteries for prolonged operation; whereas fuel cell powered UAVs mass remain static and only fuel storage increases to add runtime. For comparison sake, a 16 kg UAV system operating on battery power can operate for approximately 5 h, whilst the same system can operate for 28 and 48 h if powered by a fuel cell consuming gaseous or liquid hydrogen, respectively (https://www.unmannedsystemstechnology.com/wp-content/uploads/2017/02/White-Paper-Fuel-Cell-Energy-Systems-for-UAVs.pdf).

According to a study by PricewaterhouseCoopers (PwC) on the commercial applications of UAV technologies, the emerging global markets for drone-based business services are as follow: infrastructure (asset inventory, maintenance, investment monitoring) and agricultural (soil and drainage analysis, crop health assessment) sectors account for 45.2 and 32.3 billion USD, respectively. Other sectors (e.g. transport, security, entertainment, insurance,

telecommunication, and mining) collectively accounts for 49.7 billion USD (https://www.pwc.pl/en/publikacje/2016/clarity-from-above.html). Philip du Preez, general manager of ExecuJet Cape Town flight operations stated that the drone technology market has been increasing in recent years and is expected to grow by >19% from 2017 to 2020. Economist and economic adviser to the Commercial Aviation Association of South Africa, Roelof Botha, forecasts that the South African UAV industry will contribute 2 billion ZAR to the economy and create more than 24 000 jobs by the end of 2018 (http://www.miningweekly.com/print-version/aviation-company-adds-drones-to-african-offering-2017-07-19). Thus, a large market exists for on-demand hydrogen generation applications. The hydrolysis of Al can produce up to 11 wt% hydrogen (relative to the weight of Al), and if combined with a standard commercially available PEMFC, approximately 2200 $Wh.kg^{-1}$ Al of specific energy can be produced [11]. Though, a feasibly study has to be conducted, this method of on-demand hydrogen generation may be suitable for UAV applications.

2.8. Conclusion

In short, the ideal activated Al composite should contain the minimum wt.% of activation compound, and preferably, the activation compounds should be readily available, inexpensive, and safe/easy to handle. Thought numerous studies have been performed on the activation of Al with various materials, a mechanochemical Al activation method using dissimilar metals that excludes Ga as an activation compound is relatively unexplored. A study by Parmuzina and Kravchenko (2008) mechanochemically prepared an Al composite containing a certain wt.% of 70% Ga-30% In and 60% Ga-25% In-10% Sn-5% Zn. Both composites achieved approximately 99% hydrogen yields, suggesting that Sn and Zn could replace a fraction of the Ga content [72]. Furthermore, Bi has been proven to increase the reactivity of mechanochemically activated Al [20, 149, 164-166]. Moreover, the use of Bi in

combination with other low melting point metals to activate Al by a mechanochemical method for hydrogen generation purposes is also relatively unexplored. Thus, the use of Bi, Sn and In, and combinations thereof, to mechanochemically activate Al were considered as activation compounds in this dissertation. By monovariance experimentation and subsequent activation compounds addition optimization, the fabrication of high hydrogen yielding composites containing the minimum activation compounds was the focus of this dissertation.

CHAPTER 3: ARTICLE 1

Hydrogen generation be means of hydrolysis using activated Al-In-Bi-Sn composites for electrochemical energy applications

3.1 Author list and contributions

Authors list

S.P. du Preez[a] and D.G. Bessarabov[a,*]

[a] HySA Centre of Competence, North-West University (NWU), Potchefstroom Campus, Private Bag X6001, Potchefstroom, 2520, South Africa

Contributions

Contributions of the various co-authors were as follows:

Experimental work, data processing and interpretation, research, and writing of the scientific paper, was performed mainly by the candidate, SP du Preez. DG Bessarabov (supervisor) made conceptual contributions and assisted with article preparation.

3.2 Formatting and current status of the article

The article presented in Chapter 4 was published in *International Journal of Electrochemical Sciences* in 2017, Vol. 12, pages 8663-8682 (DOI: http://dx.doi.org/10.20964/2017.09.22). The journal details can be found at http://www.electrochemsci.org/ (Date of access: 13 September 2018).

Int. J. Electrochem. Sci., 12 **(2017)** 8663 – 8682, doi: 10.20964/2017.09.22

International Journal of
ELECTROCHEMICAL
SCIENCE
www.electrochemsci.org

Hydrogen Generation by Means of Hydrolysis Using Activated Al-In-Bi-Sn Composites for Electrochemical Energy Applications

S.P. du Preez and D.G. Bessarabov[*]

HySA Centre of Competence, North-West University (NWU), Potchefstroom Campus, Private Bag X6001, Potchefstroom, 2520, South Africa
[*]E-mail: dmitri.Bessarabov@nwu.ac.za

Received: 12 April 2017 / *Accepted:* 30 June 2017 / *Published:* 13 August 2017

Effective activation compounds are developed to produce hydrogen via hydrolysis of ball-milled Al-In-Bi-Sn composites in tap water at room temperature. Al-In-Bi-Sn composites are successfully activated by 3 h of milling. These composites exhibit hydrogen yields > 85% between 2.5 min (fastest reaction time) and 14 min (slowest reaction time). The intermetallic phases responsible for Al activation, $InSn_4$, InBi and In_3Sn, are selectively synthesized, identified and characterized. The reaction kinetics of each intermetallic phase are determined after ternary composite preparation, i.e., milling Al with In and Bi or Sn. Quaternary composites are also prepared to determine the formation kinetics of the intermetallic phases. These quaternary composites have high hydrogen yields (> 90%) and the reactions are complete within 170 s. The formation of intermetallic phases is responsible for the structural failure of Al, resulting in the size reduction of Al particles. The following are also investigated and quantified: the effects of water volume and reaction temperature on hydrolysis kinetics, and the activation energies of ternary Al composites.

Keywords: Activated aluminum; Hydrogen generation; Mechanochemical activation

1. INTRODUCTION

Hydrogen is a nonpolluting, clean and renewable energy carrier [1]. It has been identified as the most promising future alternative to traditional fossil fuels [2,3] due to its high calorific values [4], abundance and renewability [5]. The majority of hydrogen gas is produced from hydrocarbon sources [6], which produce large quantities of CO_2 gas as a by-product [7]. In addition, traces of CO may be present in hydrogen produced from hydrocarbons and may deteriorate proton exchange membrane fuel cells (PEMFCs) used to convert hydrogen's chemical energy to electrical energy [8]. Hydrogen can be

generated from various hydrocarbon sources, such as biogas [9], natural gas [4], and petroleum [10], whereas non-hydrocarbon hydrogen generation methods includes water electrolysis [9,11], water photo-catalysis [12], metal hydrolysis [11,13], and metal hydride hydrolysis [14]. Combining hydrogen with fuel cells to devices that are able to transform chemical energy into electricity and heat has yet to reach wide-scale application due to certain limitations, e.g., low efficiency, and high costs of hydrogen storage and transport [15]. For example, hydrogen has a low gaseous density of 0.089 kg m^{-3}, making the storage (and transport) of hydrogen gas a major limiting factor to the application thereof [4,16]. Ideally, hydrogen should be generated as it is required and consumed as soon as possible after being generated, removing the need for long term storage.

In recent years, research has focused on hydrogen generation by the reaction between a hydrogen source and a metal as hydrolyzing material [17-19]. Water is the most promising candidate as a hydrogen source [20] because it has a high hydrogen content of 111 kg m^{-3}, whereas gasoline and pure liquid H_2 have hydrogen contents of 84 and 71 kg m^{-3}, respectively [4,21]. Group IIA and IIIA light metals hold promise as hydrolyzing materials [22]. One such a promising and sustainable metal is aluminum (Al), the most abundant crustal metal on earth [4,23,24]. Al is a lightweight metal with a low density of 2700 kg m^{-3} and it can be fully recycled after hydrolysis through the Hall-Héroult process [25]. Furthermore, solid Al is much easier and safer to store than chemical hydrides and other hydrogen carriers [26].

Thus, hydrogen generation via hydrolysis of Al composites has attracted much interest from the scientific community because of the relative simplicity of the system and the high hydrogen storage capacity [27]. The reaction related to hydrogen generation is expressed as follows [5,25,26,28]:

$$2Al + 4H_2O \rightarrow 2AlOOH + 3H_2 \quad (1)$$

or

$$2Al + 6H_2O \rightarrow 2Al(OH)_3 + 3H_2 \quad (2)$$

The by-products produced in Reactions (1) and (2) are eco-friendly and they have many industrial applications, e.g., in alumina production [26], water treatment, paper making and fire retardation [25].

A major problem during Al hydrolysis, however, is the formation of a thin coherent oxide layer on the surface of Al and its composites, preventing further oxidation and corrosion of the Al [29]. Many methods have been proposed to remove and/or disrupt the oxide layer in efforts to increase the Al reactivity. One such method is the immersion of Al in an alkaline NaOH and/or KOH environment, which causes corrosion of the oxide layer and exposure of fresh Al to water [30-33]. However, due to the corrosive conditions, alternate methods were developed. One such a method is the amalgamation of the surface of Al with Hg, Hg-Zn amalgam [34] or eutectic Ga-In [22,35]. A less expensive and nontoxic method for removing the passive film includes the mechanical milling of Al with water soluble inorganic salts [36,37], carbon [38], metal oxides [39,40], iron [41] or lithium [42]. However, some of these methods have limitations, e.g., manufacturing processes are time consuming, the addition of large quantities (high wt%) of activation compounds is required, and initial and/or overall hydrogen generation rates are low.

Alloying Al with low melting point metals, e.g., Ga, In, Zn, Sn and Bi, has been found to be successful in activating Al for hydrogen generation under mild conditions [4,13,22,36,43]. During Al

composite preparation, melting methods require more energy than mechanochemical methods, hence increasing the cost of such composites. Furthermore, the inclusion of expensive activation compounds (Ga and In) reduces the economic feasibility of the large scale application. To the best of our knowledge, very limited literature is available in the public peer-reviewed domain on the successful mechanochemical activation of Al by means of low melting point metals (excluding Ga) for hydrogen generation purposes. Wang et al. (2013) achieved hydrogen conversion efficiency of close to 100% using a mechanochemically activated Al-Ga-In-Sn 89-3-3-5 wt% composite. The intermetallic phases In_3Sn and $InSn_4$ were observed during mechanochemical preparation of the Al-Ga-In-Sn composite. They are suspected to be the major compounds contributing to the activation of Al [44]. A recent study by du Preez and Bessarabov (2017) prepared high hydrogen yielding Al-Bi-In composites by a mechanochemical activation method dissimilar to the one applied in this study [45].

In this study, we attempted to activate Al by a mechanochemical activation method using Bi, In and/or Sn. Activation of Al was successfully achieved using only Bi-In and In-Sn. InBi, In_3Sn and $InSn_4$ were selectively synthetized and the reaction kinetics for each of the composites containing intermetallic phases, i.e., Al-BiIn, Al-In_3Sn and Al-$InSn_4$, were investigated. X-ray diffraction (XRD) was used to confirm the presence of *in-situ* formed intermetallic phases. Formation and reactivity of quaternary Al-In-Bi-Sn was also investigated. The activation metals (Bi, In and Sn) were found to be present on the surface of Al particles, indicating complete consumption of the as-received In, Bi and Sn during the mechanochemical activation process.

2. MATERIALS AND METHODS

2.1. Materials

The following starting materials were supplied by Sigma-Aldrich (South Africa): Al powder (< 200 μm, 99.5% purity), In shots (+5–2 mm, > 99.9% purity), Bi granules (> 99.99% purity) and Sn powder (< 150 μm, 99.5% purity). Hydrolysis reactions were performed using tap water. Pure nitrogen (99.99%) (Afrox, South Africa) was used during all purging steps.

2.2. Aluminum composite compositions and their mechanochemical preparation

Various Al composites with different compositions were prepared. Different amounts of Bi, In and Sn were added to a constant amount of Al (86.91 wt%). The amounts of the respective activation compounds varied between 0 and 10.55 wt%. The total amount of the activation compound was kept at 13.09 wt%. The compositions of ball-milled Al composites are given in Table 1.

Ball milling of Al composite powders was performed in a Retsch PM100 planetary ball mill (Retsch, Germany) under a nitrogen atmosphere. The as-received metals (Al, Bi, In and Sn) were weighed and placed in a 250 mL stainless steel grinding pot with 5 mm stainless steel grinding balls. The grinding ball to powder mass ratio was 30:1. For all composite preparations, the as-received metals were milled for 3 h at 450 rpm.

Table 1. Al composite compositions (wt%).

Composite	Compound (wt%)			
	Al	Bi	In	Sn
Al-$InSn_4$	86.91	0	2.54	10.55
Al-InBi	86.91	8.38	4.71	0
Al-In_3Sn	86.91	0	9.82	3.27
A	86.91	3.93	3.93	5.24
B	86.91	6.54	3.93	2.62
C	86.91	3.93	6.54	2.62
D	86.91	3.93	2.62	6.54

After each milling procedure, the ball-milled samples (still in the sealed grinding pots) were allowed to cool to room temperature. To avoid unwanted atmospheric oxidation, hydrolysis experiments with the cooled ball-milled samples were carried out as soon as possible. Composites were stored in an airtight container until required for use. Each composite was ball milled in duplicate. Only composites that displayed a repeatable trend in terms of physical change and size reduction after 3 h of ball milling were investigated, in triplicate. The particles of some Al composites agglomerated to form large particles with low reactivity. These were excluded from this study.

2.3. Hydrolysis set-up and hydrogen measurements

Hydrolysis reactions were carried out at standard temperature and pressure in a 100 mL flask reactor with two openings, one for hydrolysis solution addition (by means of a pressure equalizing addition funnel) and the other for hydrogen to escape. The generated hydrogen passed through a gas drier containing a combination of Drierite™ ($CaSO_4$) and SiO_2 to remove water vapor prior to hydrogen measurements. The hydrogen volume was measured using the water trap method, as described by Zhao et al. [46]. Hydrogen measurements were performed using 0.2 g composite and 10 mL of reaction solution, unless specified otherwise. The reaction mixtures were left unagitated during all hydrolysis reactions.

2.4. Expression of hydrogen generation

Hydrogen production is expressed as conversion yield (%), defined as the volume of hydrogen produced over the theoretical value of hydrogen that should be released assuming that the entire Al content is hydrolyzed. Applying the ideal gas law, approximately 1360 mL per gram of Al can be achieved under standard atmosphere and temperature conditions. The hydrogen generation rate is defined as the amount of hydrogen produced per minute and is expressed as mL min^{-1}, with mL referring to the volume of hydrogen generated from 0.2 g Al composite. All hydrolysis reactions had repeatable hydrogen generation values. The data are presented in triplicate. Error bars are not included for ternary composites as the error spread for all hydrolysis reactions was < 3%.

2.5. Sample characterization by XRD and SEM

XRD was performed using a Röntgen diffraction system (PW3040/60 X'Pert Pro). A back-loading preparation method was used to determine the crystalline phases present in the Al composites and hydrolysis residues. The samples were scanned using X-rays generated by a copper (Cu) Kα X-ray tube. Measurements were carried out between variable divergence slits and fixed receiving slits. The phases were identified using X'Pert HighScore Plus software (PANalytical).

Surface analysis of the as-received Al powder and ball-milled Al powders was performed using scanning electron microscopy (SEM). A FEI Quanta 200 scanning electron microscope with an integrated Oxford Instruments INCA 200 energy dispersive X-ray spectroscopy (EDS) microanalysis system was used. SEM micrographs were obtained (at various magnifications) to characterize the physical attributes of the investigated materials. Magnification (μm scale) is indicated on all micrographs presented (Figs 1–3). SEM-EDS were used to confirm the distribution of activation compounds on the surface of Al particles.

3. RESULTS AND DISCUSSION

3.1. Effects of ball milling on characteristics of Al composite particles

Repetitive plastic deformation of metals generally changes their microstructure, affects the magnitude of residual stresses and redistributes the constituents [47]. Initially, the Al composites described in this paper were milled for various periods of time and then contacted with water to determine an optimal milling time. Al composites milled for < 3 h (0.5, 1 and 2 h) had hydrogen yields of 5–35%. Visually, it was clear that the fine powders of the as-received Al powder and the activation compounds coagulated during the first 2 h of ball milling to form large flake-like particles. It was accepted that initial ball milling of fine Al powder with In, Bi and/or Sn caused particles to undergo cold welding, which increased the particle size of the powders dramatically. Some reactivity was observed, which is indicative of initial Al composite activation, but it was considered to be insignificant.

After 3 h of milling, particles changed from a flake-like morphology to a fine powder, coupled with a large increase in reactivity. Although it is unclear what causes this key change in morphology, this phenomenon can be explained on the basis of two mechanisms. (1) Ductile and malleable particles will agglomerate due to cold welding as a result of Al composite particles caught between milling ball impacts, i.e., ball–ball and ball–milling chamber, and undergo elastic deformation, until a certain stress-to-strain point is reached. (2) The Al particles then become deformed during the milling process, consequently increasing the hardness of these particles due to work hardening. The work hardened particles will then plastically deform and fracture, resulting in a decrease in particle size [48,49]. A similar trend was observed by Razavi-Tousi and Szpunar [50]; high energy ball-milled Al powder particles cold welded together, followed by a sudden decrease in particle size after a certain period of

ball milling. The fine Al composite powders produced by ball milling indicated that the as-received materials were milled into a homogenous powder with regard to particle size and distribution.

Fig. 1a shows a SEM image of the as-received Al powder and Fig. 1b an image of a 3 h ball-milled Al-9.82 wt% In-3.27 wt% Sn mixture before hydrolysis. The shape of the as-received Al powder changed from the initial 100–300 μm strand-like morphology to platelet morphology 7–70 μm in size. Fig. 1b shows that small fractured particles of the composite are embedded onto larger particles, leading to an increase in the deformities and defects of both types of particles, i.e., the smaller fractured and larger welded particles.

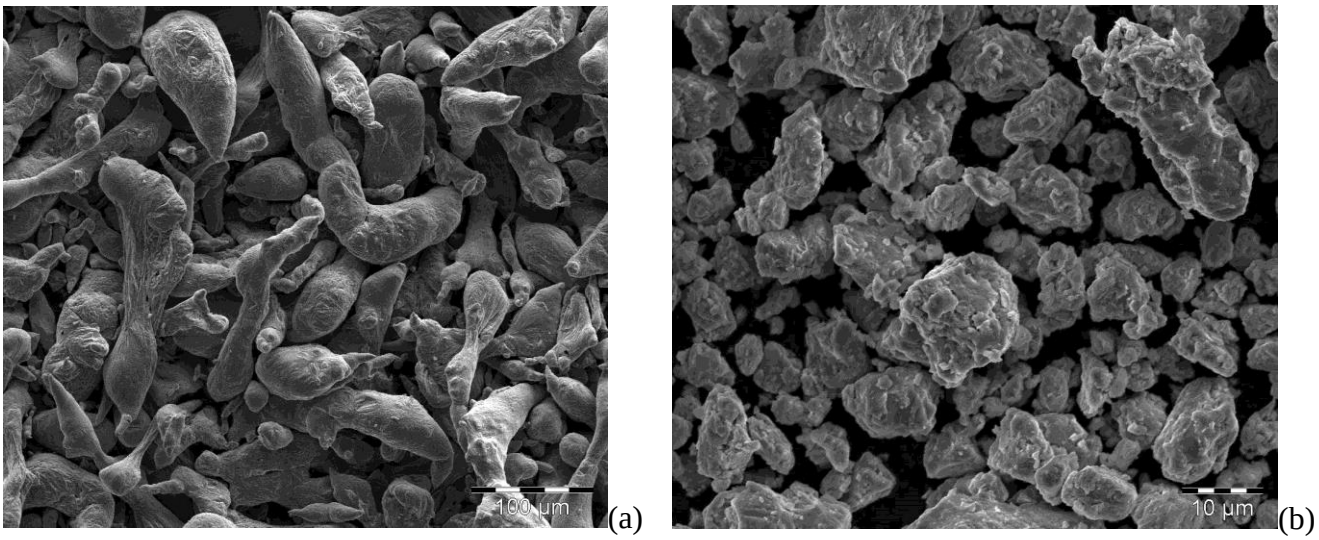

Figure 1. SEM micrographs of (a) as-received Al powder and (b) 3 h milled Al-9.82 wt% In-3.27 wt% Sn mixture.

After a certain period of ball milling, steady state equilibrium was reached between the rate of cold welding and the rate of fracturing; cold welding increases the average particle size and fracturing decreases it. Smaller particles are able to resist deformation without fracturing and they tend to weld onto larger particles, with an overall tendency to drive both very fine and very large particles towards an intermediate size [49,51]. A relatively large change in particle size, accompanied by the presence of both small and large particles, is shown in Fig. 1b. It indicates the presence of steady state equilibrium between the rate of welding and fracturing.

Fig. 2 shows various SEM micrographs illustrating ball-milled Al-In-Sn/Bi composite particles and quaternary Al Composite A (Al-3.93 wt% Bi-3.93 wt% In- 5.24 wt% Sn). The clustered particle encircled in Fig. 2a clearly indicates cold welding of smaller Al particles onto each other, forming a larger clustered particle. These clustered particles contain numerous deformities and irregularities, enabling water to freely penetrate deep within the particle. The majority of particles consist of larger solid particles, with smaller particles embedded on their surfaces. The reaction surface of clustered particles presented in Fig. 2 facilitates a larger surface area than single, smoother particles. This is due to the presence of previously mentioned deformities and irregularities. A larger reaction surface

implies a greater particle surface:water contact boundary, which will expedite the Al hydrolysis reaction. All of the reported composites prepared in this study had similar morphologies to the composites presented in Fig. 2 (confirmed by SEM), but these micrographs were not included in this paper.

It is evident from Figs 1 and 2 that the particle size of the as-received Al powder was successfully reduced. However, for the Al particles to act as hydrolyzing materials under ambient conditions, the reduction of particle size alone will not suffice. As previously mentioned, the formation of a thin coherent oxide layer on the surface of the Al particles has to be disrupted, exposing the underlying fresh Al to water. Thus, successful activation of Al particles depends on the distribution of the activation compounds (Bi, In and Sn) over the entire surface of the Al particles.

Fig. 3a shows a SEM image of the mechanochemically prepared composite A (Al-3.93wt% Bi-3.93wt% In-5.24wt% Sn). Fig. 3b, c, d and e depicts the corresponding EDS elemental map for Al, Bi, In and Sn, respectively. Red represents Al atoms; purple, orange and green represent Bi, In and Sn, respectively.

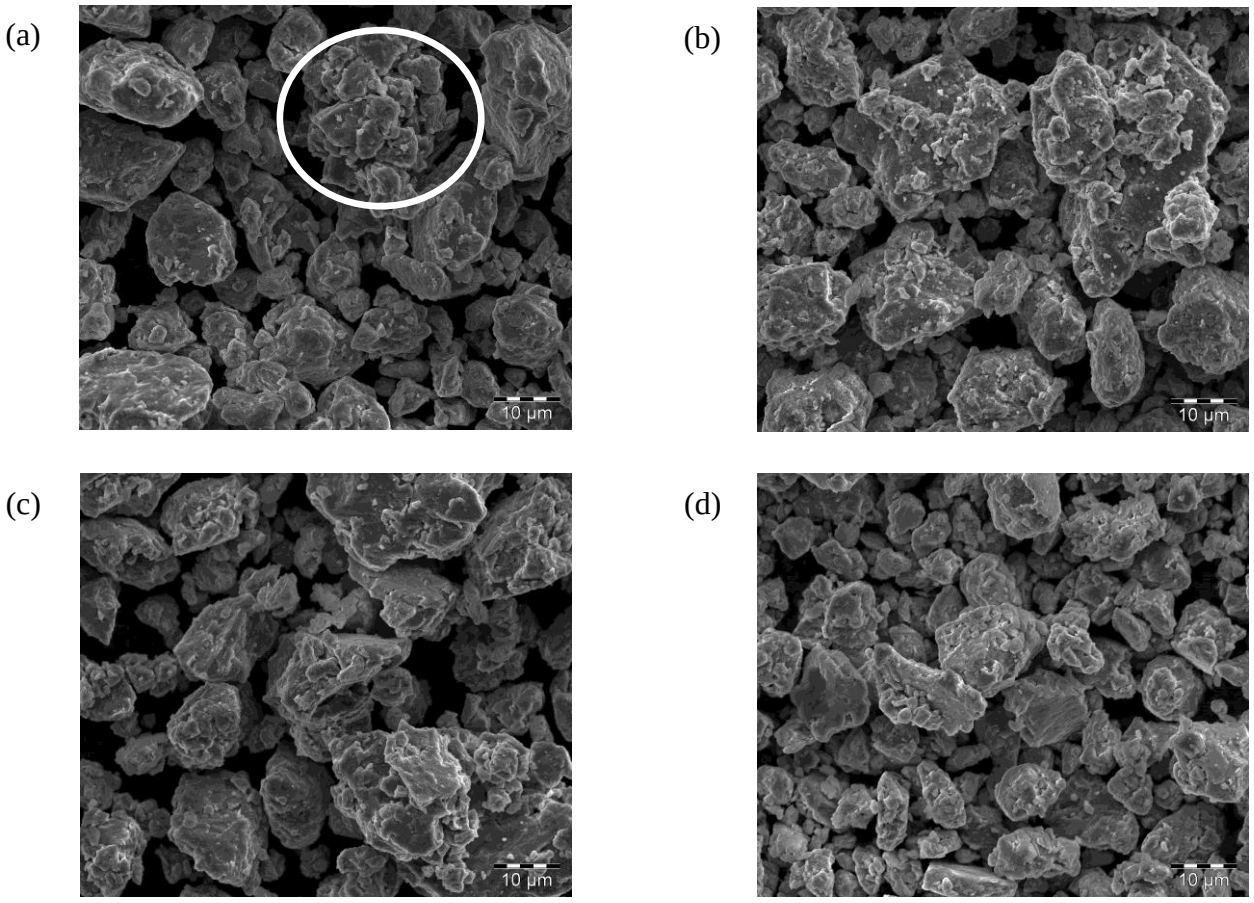

Figure 2. SEM micrographs of composites (a) Al-InBi, (b) Al-$InSn_4$, (c) Al-In_3Sn and (d) quaternary Composite A (Al-3.93 wt% Bi-3.93 wt% In- 5.24 wt% Sn), showing cold welding of smaller Al particles onto each other and onto larger particles.

Fig. 3 clearly shows that the activation compounds (Bi, In and Sn) were equally distributed on the Al surface and did not aggregate at certain points. Furthermore, the complete distribution of Sn and Bi on the Al surface is important for the composite combinations of Al-Sn and Al-Bi. Both these combinations offer easy electron transfer from Al (anode) to Sn and Bi (cathodes) in the micro-galvanic cell when the hydrolysis reaction of Al and water occurs [13,52,53]. Bi and Sn has a positive effect on Al hydrolysis, as an Al-Bi/Sn composites has an open circuit potential of -1.85 V, which is lower than the -1.77 V of pure Al [36]. Though, Sn does not form intermetallic phases with Al [54], the presence of Sn in Al-Sn composites has indicated an increase in the thermodynamic activity of Al [55]. Al-In composites displayed limited reactivity during hydrolysis with pure water at room temperature [56]. Additionally, it is highly likely that intermetallic phases (InBi, In_3Sn, and $InSn_4$) would occur on the surface of Al particles.

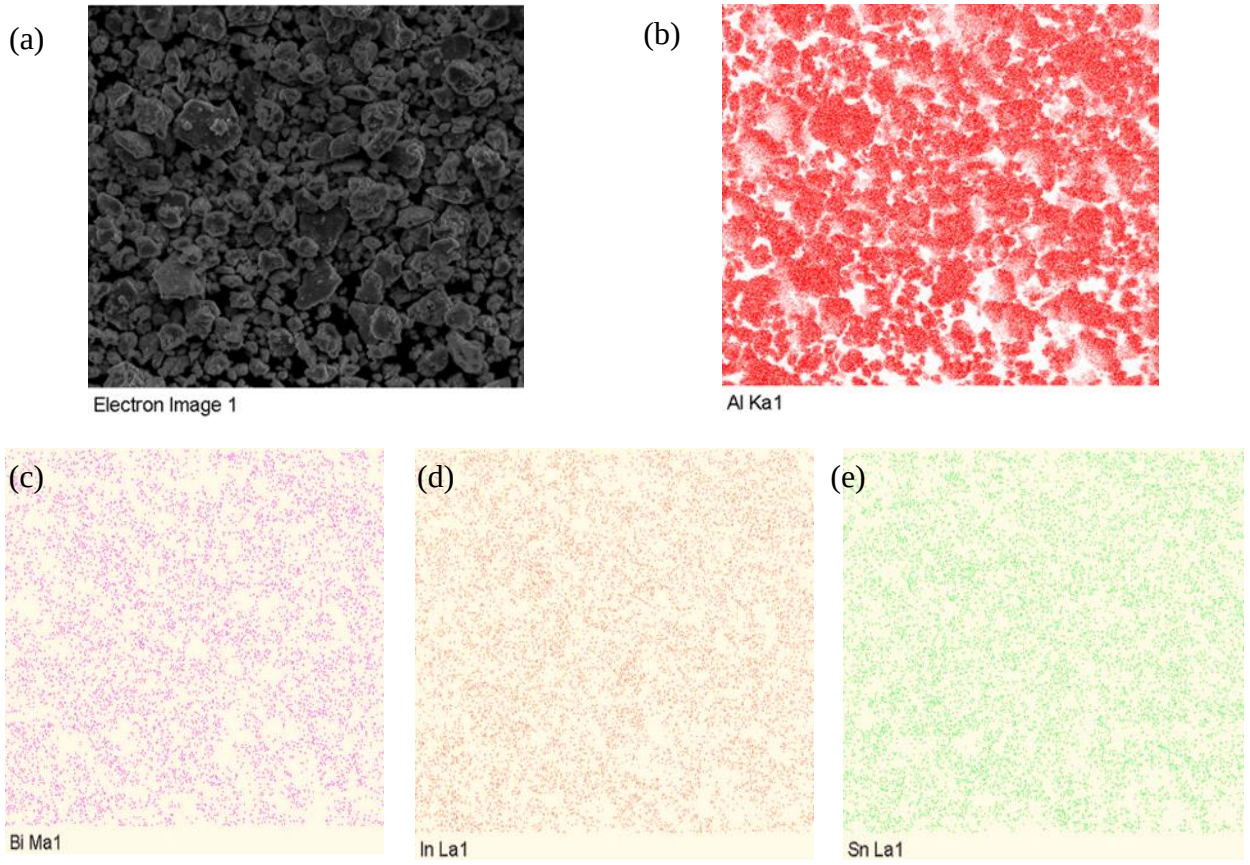

Figure 3. (a) SEM micrographs of quaternary composite A (Al-3.93 wt% Bi-3.93 wt% In-5.24 wt% Sn), and the corresponding EDS mapping for (b) Al, (c) Bi, (d) In and (e) Sn.

3.3. Characterization and hydrolysis kinetics of ternary Al-In-Bi and Al-In-Sn composites

XRD analysis of Al-In-Bi and Al-In-Sn was performed to investigate the intermetallic phases present in the ternary composites. Three prominent intermetallic phases formed during the mechanochemical preparation of Al composites: InBi, In_3Sn and $InSn_4$. They are believed to be

responsible for the activation of Al and/or partake in the work hardening of Al particles, which induces structural failure of Al particles.

Fig. 4 shows XRD patterns of the Al composites Al-$InSn_4$, Al-InBi and Al-In_3Sn. The wt% values of these composites are presented in Table 1. The wt% value of each of the composites coincided with the mole ratio of their corresponding intermetallic phases. Composites Al-$InSn_4$ and Al-In_3Sn had In:Sn mole ratios of 1:4 and 3:1, respectively, while composite Al-InBi had a In:Bi mole ratio of 1:1. In each case, intermetallic phases formed according to the predesignated mole ratios. Composites Al-$InSn_4$ and Al-In_3Sn only formed $InSn_4$ and In_3Sn, respectively. It was expected that some competition should exist between the formation of the two intermetallic phases; however, no competition was observed, and $InSn_4$ and In_3Sn were selectively synthesized. In the case of composite Al-InBi, InBi formed exclusively. No intermetallic Al-In and Al-Bi phases were detected. This may be ascribed to the low solubility of In and Bi in the Al matrix [57,58].

A study by Wang et al. (2012) indicated the presence of In_3Sn and $InSn_4$ (determined by XRD) in Al-Ga-In-Sn-Fe composites prepared by an arc melting method. Some composites had close to 100% yields, when hydrolyzed in hot (50 °C) water [59]. However, an objective of this study included to selectively synthesize In-Bi and In-Sn intermetallic phases on the surface of Al particles, using a mechanochemical preparation method. Additionally, the study by Wang et al. (2012) included Ga, which could be completely excluded from composites prepared in this study.

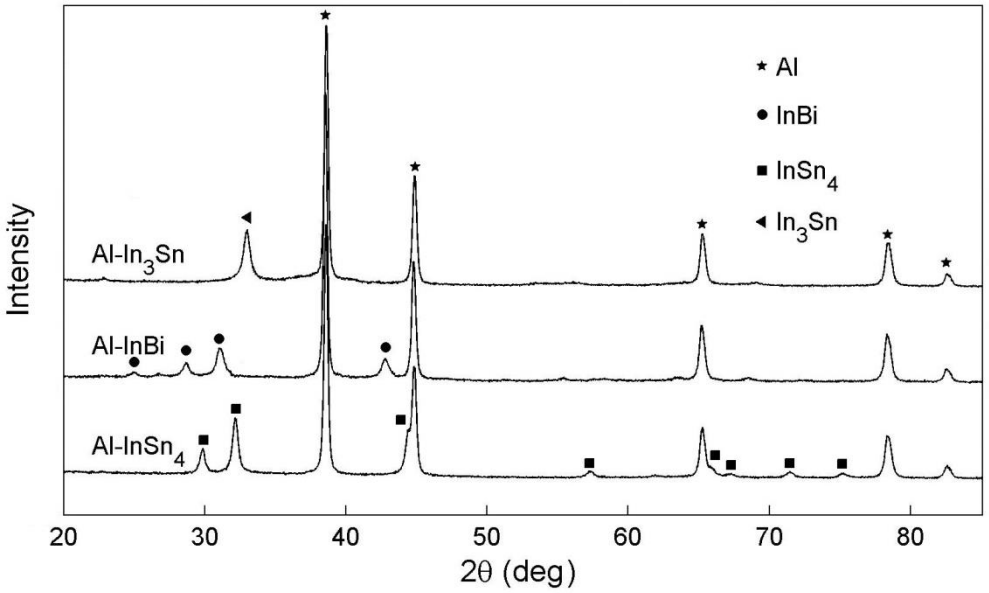

Figure 4. XRD patterns of ternary composites Al-$InSn_4$, Al-InBi and Al-In_3Sn. Experimental conditions used for ball milling of composites: 3 h, 450 rpm, nitrogen atmosphere. Amounts (wt%) of activation compounds (Bi, In and Sn) varied, in the range 2.54–10.55 wt%. Al was kept at 86.91 wt%.

The selectively synthesized intermetallic phase containing composites were hydrolyzed to investigate the respective effects of $InSn_4$, InBi and In_3Sn during Al hydrolysis. Fig. 5 shows the

hydrogen generation rates of the Al composites Al-$InSn_4$, Al-InBi and Al-In_3Sn under ambient conditions.

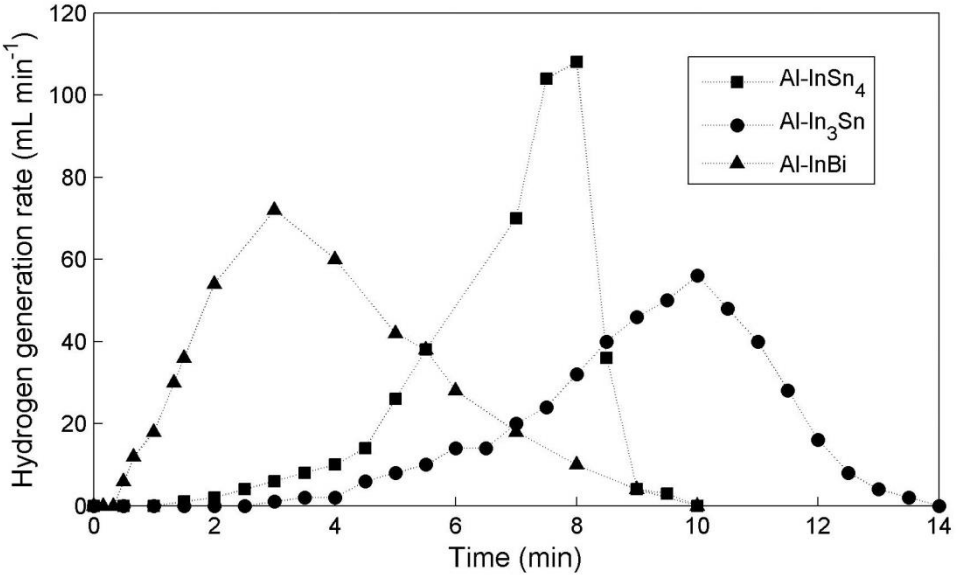

Figure 5. Hydrogen generation rates of ternary composites Al-$InSn_4$, Al-InBi and Al-In_3Sn. Hydrolysis parameters were kept constant: 10 mL tap water as hydrolysis solution, standard temperature and pressure.

Fig. 5 shows that Al-InBi reached its peak hydrogen generation rate of approximately 76 mL min^{-1} after 3 min of coming into contact with water. The average hydrogen generation rate (for 0.2 g Al composite) was 24 mL min^{-1}. Al-$InSn_4$ peaked at 120 mL min^{-1} after 8 min and rapidly decreased thereafter. Al-In_3Sn had a generation rate of 56 mL min^{-1} after 10 min. Al-$InSn_4$ and Al-In_3Sn had average hydrogen generation rates of 22 and 15 mL min^{-1}, respectively. It is evident that each intermetallic phase present in the composites (InBi, $InSn_4$ and In_3Sn) had unique hydrolysis kinetics.

The different induction times, i.e., delay before the initiation of hydrolysis, of each Al composite, due to the presence of different intermetallic phases, can be utilized to control the rate of hydrogen release. Al-InBi had the fastest hydrogen generation rate and an approximate hydrogen yield of 95%, whereas Al-In_3Sn and Al-$InSn_4$ had slower hydrogen generation rates and approximate hydrogen yields of 93%. Al-InBi had an induction time of 20 s before hydrolysis was initiated, whereas the induction times of Al-$InSn_4$ and Al-In_3Sn were 60 and 150 s, respectively. The composites thus had different induction times and different reaction kinetics. Al-$InSn_4$ had a peak hydrogen generation rate of 108 mL min^{-1} after 8 min of coming into contact with water, but reactivity rapidly decreased after reaching this peak. Al-InBi reached a peak hydrogen generation rate 72 mL min^{-1} after 3 min, whereafter the reactivity steadily decreased. Al-In_3Sn had a peak generation rate of 56 mL min^{-1} after 10 min. It had the slowest reaction kinetics and it displayed similar reaction kinetics to Al-$InSn_4$.

It was observed that the composite Al-InBi generated particles with high reactivity surfaces, whereas composites Al-$InSn_4$ and Al-In_3Sn generated particles with a protective layer on the surface of

the particles. It is possible that during hydrolysis, water had to diffuse through the coinciding intermetallic phases, i.e., $InSn_4$ and In_3Sn, before hydrolysis of the underlying Al could commence. Water diffused through $InSn_4$ faster than through In_3Sn, as indicated by the different induction times of the two composites Al-$InSn_4$ and Al-In_3Sn. Another possible reaction mechanism may be ascribed to micro-galvanic activity between Al-Sn, and that Al-$InSn_4$ had a shorter induction period due to an increased Sn content compared to the slower reacting Al-In_3Sn composite. Al-InBi reacted with water upon contact, which is indicative of a chemically reactive surface. It is likely that the short induction time may be ascribed to the high micro-galvanic activity of Al-Bi, resulting in the almost instantaneous hydrolysis of Al.

3.4. Formation kinetics of intermetallic phases during quaternary composite preparation

During ternary Al composite hydrolysis, the hydrogen yield (%) of the investigated composites was relatively constant, but the quaternary composites displayed some differences in terms of hydrolysis kinetics. Hydrolysis parameters were kept constant throughout, meaning that the only possible reason for variations in hydrolysis kinetics was the presence of different intermetallic phases and/or the amounts thereof.

Fig. 6 shows the XRD patterns of composites A, B, C and D. Ball milling parameters were kept constant. Composites B, C and D had different amounts of the activation compounds Bi, In and Sn: 2.62, 3.93 and 6.54 wt%.

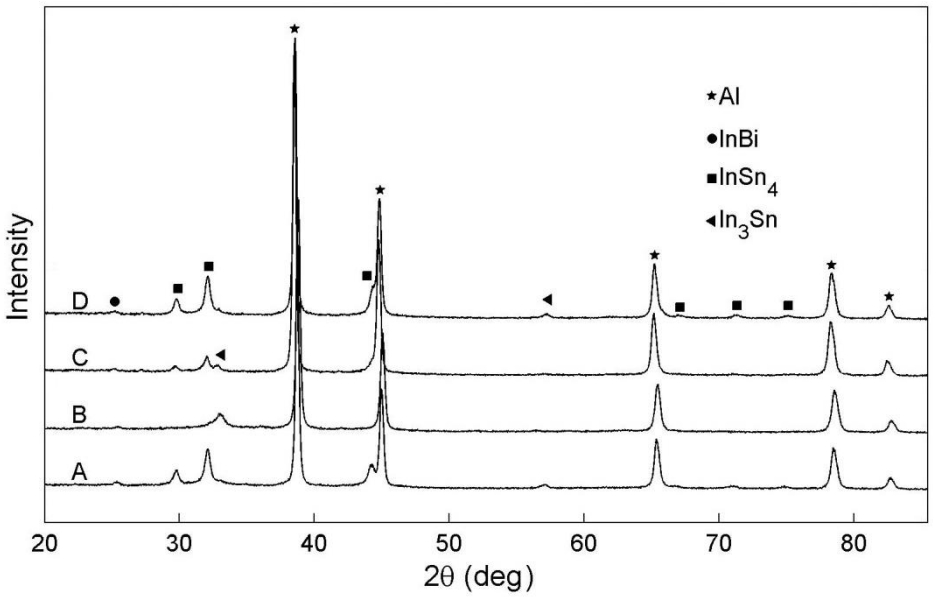

Figure 6. XRD patterns of quaternary Al composites A (Al-3.93 wt% Bi-3.93 wt% In-5.24 wt% Sn), B (Al-6.54 wt% Bi-3.93 wt% In-2.62 wt% Sn), C (Al-3.93 wt% Bi-6.54 wt% In-2.62 wt% Sn) and D (Al-3.93 wt% Bi-2.62 wt% In-6.54 wt% Sn). Experimental conditions used for ball milling of composites: 3 h, 450 rpm, nitrogen atmosphere. Amounts (wt%) of activation compounds (Bi, In and Sn) varied, in the range 2.62–6.54 wt%. Al was kept at 86.91 wt%.

It is evident from Fig. 6 that InBi, In_3Sn and $InSn_4$ formed during ball milling of the quaternary composites. Composite B had the largest fraction of Bi present (6.54 wt%). Only InBi and In_3Sn were observed. It was accepted that, on an atomic scale, the formation of InBi consumed the majority of the In and Bi atoms, followed by In_3Sn consuming the remainder of the In atoms.

InBi, In_3Sn and $InSn_4$ intermetallic phases were present in composite C. Bi atoms were consumed to form InBi, whereas the remainder of the In and Sn atoms competed to form In_3Sn and $InSn_4$. In the case of composite D, prominent peaks of all three intermetallic phases were observed. A possible reason for the three prominent peaks is that an increase in the number of Sn atoms could easily consume the In atoms to form In_3Sn and $InSn_4$. Composites A and D had similar XRD patterns. The small wt% increase in In and decrease in wt% Sn resulted in the peak drift observed at the 2θ position 44. This is due to the more complete formation of In_3Sn, which can be explained by an increase in In atoms that are readily available to composite with Sn atoms.

It also emerged from Fig. 6 that InBi had slightly faster formation kinetics than In_3Sn and $InSn_4$. The formation kinetics of In_3Sn and $InSn_4$ depended on the availability of both In and Sn atoms and the absence of Bi atoms. In Fig. 4, where Bi atoms were not present during ball milling, no competition was observed between In_3Sn and $InSn_4$ due to the atomic ratios of In:Sn; a 3:1 In:Sn ratio led to the formation of In_3Sn while a 1:4: In:Sn ratio led to the formation of $InSn_4$. Fig. 6 displays clear evidence of competitive formation between In_3Sn and $InSn_4$, which, to a certain extent, can be controlled by manipulating the mole ratios of In:Sn.

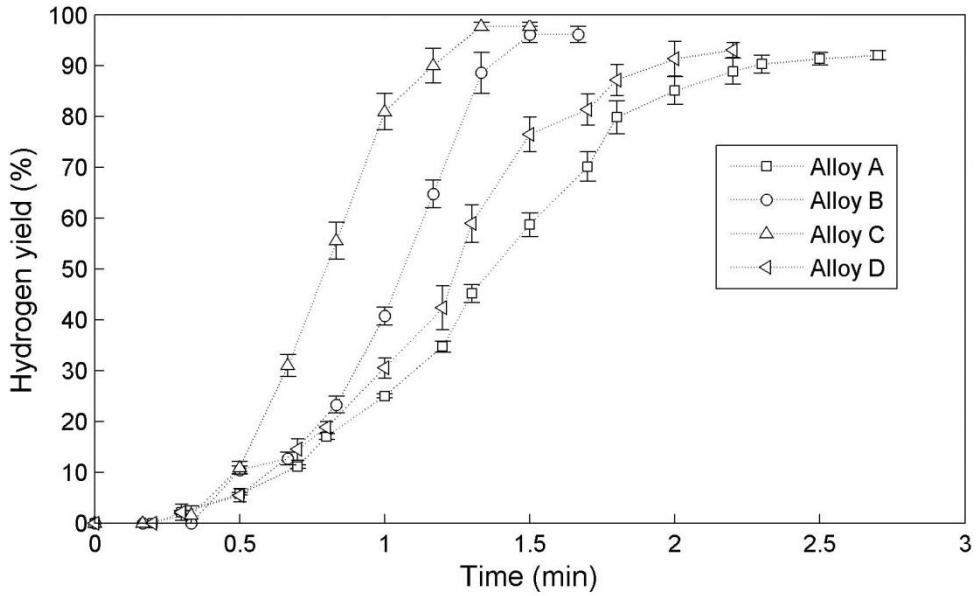

Figure 7. Average hydrogen yield (%) of quaternary Al composites A (Al-3.93 wt% Bi-3.93 wt% In-5.24 wt% Sn), B (Al-6.54 wt% Bi-3.93 wt% In-2.62 wt% Sn), C (Al-3.93 wt% Bi-6.54 wt% In-2.62 wt% Sn) and D (Al-3.93 wt% Bi-2.62 wt% In-6.54 wt% Sn). Experimental conditions used for ball milling of composites: 3 h, 450 rpm, nitrogen atmosphere. Amounts (wt%) of activation compounds (Bi, In and Sn) varied, in the range 2.62–6.54 wt%. Al was kept at 86.91 wt%.

Fig. 7 presents the average hydrogen yield (%) of quaternary Al composites A, B, C and D, respectively. In most cases, reactivity of quaternary Al composites did not differ substantially. Reported reactivities had approximate hydrogen yields of 91.2–98%. Induction times were relatively short and ranged from 20 to 30 s. The hydrolysis reactions were completed within 90 s (fastest) and 170 s (slowest) after coming into contact with water.

Results of the hydrolysis of quaternary Al composites were compared with results of the hydrolysis of the ternary Al composites. It is clearly evident that combinations of intermetallic phases displayed a synergetic effect with regard to reaction kinetics. The ternary composite Al-InBi had the shortest induction time (Fig. 5). This resulted in InBi containing quaternary composites displaying reduced induction periods, due to the *in situ* generated heat being released by the fast reacting InBi containing Al particles. The released heat catalyzed the slower reacting $InSn_4$ and In_3Sn containing Al particles. As far as the authors could assess, no literature is available in the peer-reviewed public domain on hydrogen generation of Al-In-Bi-Sn composites (excluding Ga) prepared through a mechanochemical activation method. Though, a study by Huang et al. (2015) prepared high hydrogen yielding Al-Ga-In_3Sn and Al-Ga-InBi composites, as well as a relatively low hydrogen yielding Al-Ga-$InSn_4$ composites, prepared through a melting method [60].

3.5. Proposed formation mechanism with regards to intermetallic phase formation

The authors propose the following two mechanisms that could play a role in intermetallic formation of InBi, In_3Sn and $InSn_4$. (1) During ball milling of ternary composites containing Al-Bi-In or Al-In-Sn, the atomic ratio will determine which intermetallic phases will form. For instance, if a 1:4 In:Sn atomic ratio is present, $InSn_4$ will form exclusively. A possible explanation for this is that, during ball milling, there will be a greater chance that a predetermined ratio of atoms will be caught between composite-forming milling-ball collisions. The same can be accepted for a 3:1 In:Sn atomic ratio. In the case of Al-Bi-In, InBi will form until either In and/or Bi is consumed. (2) During quaternary composite Al-In-Bi-Sn preparation, the formation of all three intermetallic phases (InBi, In_3Sn and $InSn_4$) may be present. In this study, small InBi peaks were observed in all Al composites containing Bi as a starting material. The presence of Bi induces a degree of competitive formation between In and Sn containing intermetallic phases, i.e., In_3Sn and $InSn_4$. Thus, the second mechanism for quaternary composite ball milling can be summarized as the formation of either InBi, In_3Sn and/or $InSn_4$, which is tantamount to the coincidental presence of atoms during collisions of milling balls and can be controlled by manipulating the quantity (wt%) of each of the activation compounds added.

3.6. Effects of mass ratio ($m_{Al\ powder}/m_{water}$) and temperature on the hydrolysis reaction

Al-$InSn_4$ was chosen to depict the effects of mass ratio and temperature as it represents a ternary composite with a reactivity between the fast reacting Al-InBi and slower reacting Al-In_3Sn. Here, a mass ratio of 1:20 is defined as 1 g of Al powder reacting with 20 mL of water. All mass ratios

were derived similarly. Fig. 8 depicts the effect of different mass ratios on (a) hydrogen yield and (b) reaction temperature. The mass ratio ranged from 1:20 to 1:500.

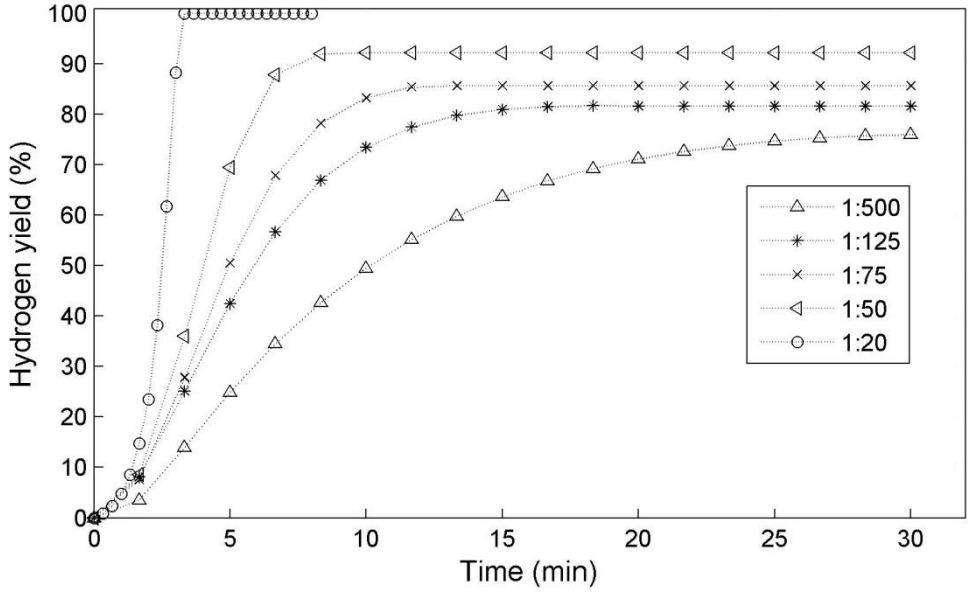

(a)

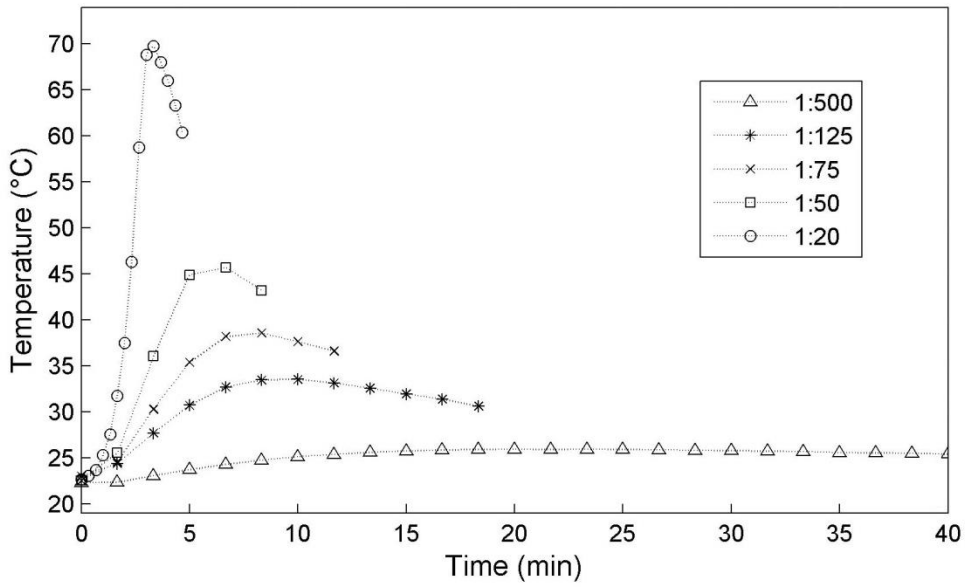

(b)

Figure 8. Effect of different mass ratios ($m_{Al\text{-}InSn4}/m_{water}$) on (a) hydrolysis kinetics of Al-$InSn_4$ and (b) change in reaction temperature during the hydrolysis reaction.

Results presented in Fig. 8a indicate an increase in the hydrolysis reaction rate and hydrogen yield as the mass ratio $m_{Al\text{-}InSn4}/m_{water}$ decreased from 1:500 to 1:20. The hydrogen yield for the 1:20 mass ratio hydrolysis reaction was 100% and it decreased to 76.2% as the mass ratio was increased to 1:500. The Al hydrolysis reaction is dependent on reaction temperature [13,61]. Thus, the decrease in hydrogen yield was caused by the decrease in reaction temperature. Fig. 8b depicts the effect that water volume has on the change in reaction temperature during hydrolysis reactions of ternary Al composite Al-$InSn_4$. The reaction temperature of the 1:20 mass ratio hydrolysis reactions increased by

48.0 ± 2.8 °C, whereas a 5.6 ± 0.8 °C increase was observed during the 1:500 hydrolysis reactions. During the hydrolysis reaction, heat ($\Delta H = -444.4$ kJ mol^{-1}) [42] is released and, in turn, catalyzes the hydrolysis reaction. An increase in water volume decreased the reaction temperature during hydrolysis as the *in situ* generated heat mitigates away from the immediate reaction sites (Al particles undergoing hydrolysis). This resulted in a slower hydrogen generation rate and a decrease in hydrogen yield. As expected, a similar trend was observed for all Al composites investigated in this study.

If the Al composites prepared in this study were to be considered for PEMFC applications, hydrogen has to be generated at a relatively steady rate, due to the fact that PEMFCs require a steady supply of hydrogen gas to operate optimally. Thus, the Al hydrolysis reaction has to be manipulated in such a way to ensure a controllable rate of hydrogen generation. It is clear from Figure 8 that larger hydrolysis mass ratios resulted in a decrease in reaction temperature, which in turn reduces the hydrogen generation rate (and hydrogen yields). For example, Al-$InSn_4$ hydrolysis performed at a 1:20 mass ratio had a 100% hydrogen yield, a reaction temperature increase of 48 °C, and a peak hydrogen generation rate of approximately 280 mL min^{-1}. Such reaction temperatures and hydrogen flow rates may cause complications during PEMFC applications. However, the same hydrolysis reaction performed at a 1:500 mass ratio will result in a reaction temperature increase of 5.6 °C, and a peak hydrogen generation rate of 18 mL min^{-1}. Thus, it is indicative that a certain amount of the Al-$InSn_4$ composite may be hydrolyzed to provide a PEMFC with a steady hydrogen stream. Though, hydrolysis at such a large mass ratio, i.e. 1:500, did result in a decrease in hydrogen yield, the hydrogen generation rate would be sufficient for PEMFC application.

Energy applications (PEMFC application) using this method of hydrogen generation is still under development and requires further improvements and developments, it may be utilized by several sectors. An advantage of this method is the ability to generate hydrogen on-demand and on-site, removing the need for hydrogen storage and transport. According to the Russian Skolkovo Foundation (web reference: https://sk.ru/news/m/wiki/14838/download.aspx) the portable charging devices market is an estimated $34bn market. Additionally, markets for unmanned aerial vehicles (UAVs), various military and emergency energy applications, portable low power electronic devices, and underground mining equipment are large, and the value yet to be determined. Al hydrolysis (Reactions 1 and 2) has a theoretical hydrogen mass yield of 11% based on the mass of Al. Considering the high hydrogen yields obtained from composites prepared in this study, an approximate 2.2 kWh kg^{-1} specific electric energy may be generated through a PEMFC [62]. It is worth mentioning that electrochemical energy systems, such as hydrogen fuel cells, require hydrogen of a high purity. "Al-to-hydrogen" system descried in this paper generates PEM-grade purity hydrogen. At this stage we envisage that the described technology could be used for power tools at construction sites, cell phones, laptops, professional digital video cameras, etc., in other words, niche, small-scale applications. For military applications, typical requirements would include, but not limited to, low noise level, low heat signature, lower weight, etc. and power rating not exceeding 1 kW. "Al-to-hydrogen" system could address all these requirements.

Fig. 8a and b reflects the major influence of reaction temperature on hydrogen generation. The following Arrhenius equation was used to determine this effect:

$$k = A\, exp^{(-Ea/RT)} \quad (1)$$

It gives the dependence of a rate constant (*k*) on temperature (T) and activation energy (E_a). By determining *k* from the maximum flow rates obtained at different temperatures (23–50 °C) and using eqn. (1), the activation energies of the ternary Al composites were calculated to be 47.2 kJ mol^{-1} for Al-InBi, 57.5 kJ mol^{-1} for Al-$InSn_4$ and 62.1 kJ mol^{-1} for Al-In_3Sn from the plot of reaction rate *k* against the reciprocal temperature, as presented in Fig. 9. The coefficient of determination (R^2) ranged between 0.9674 and 0.9927.

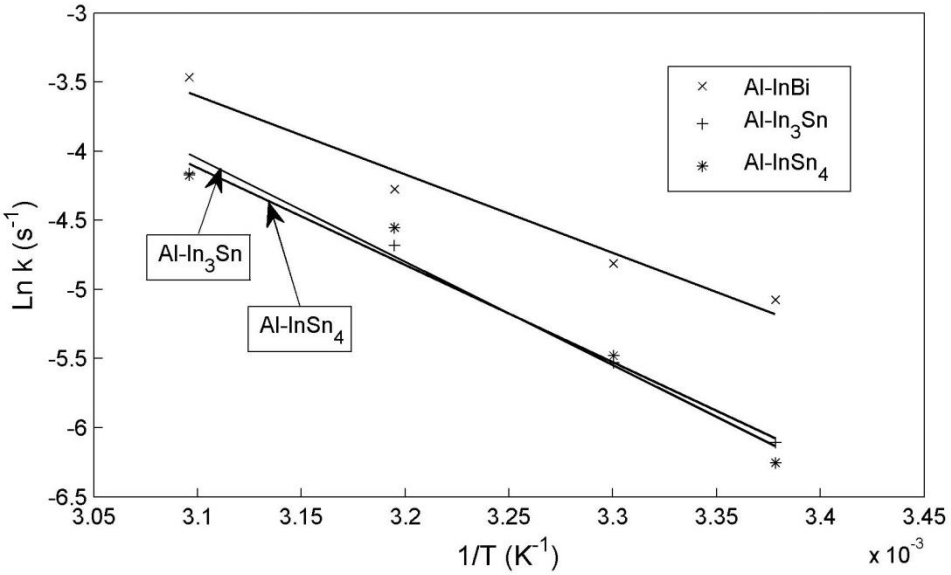

Figure 9. The Arrhenius plot for the maximum hydrolysis reaction rates of the reaction between ternary Al composites (Al-InBi, Al-In_3Sn and Al-$InSn_4$) and water.

The ternary Al composite activation energies coincide with the activation energies of Al activated by mechanochemical preparation methods using NaCl (63.1 ± 3.1 kJ mol^{-1}) [63] and graphite (61 ± 10 kJ mol^{-1}) [64]. The lower activation energy of Al-InBi, compared with Al-$InSn_4$ and Al-In_3Sn, corresponds with the induction times of all three ternary composites, e.g., Al-InBi had the lowest activation energy and the shortest induction time, whereas Al-$InSn_4$ had the highest activation energy and the longest induction time.

3.7. Analysis of hydrolysis residues

The hydrolysis residues of ternary Al composites and of Composite A, hydrolyzed at different water volumes, were characterized by XRD. Results are presented in Fig. 10a and b, respectively. XRD spectra of hydrolyzed residues were more detailed than spectra of unhydrolyzed Al composites (Figs 4 and 6) due to the absence of large, overshadowing Al peaks.

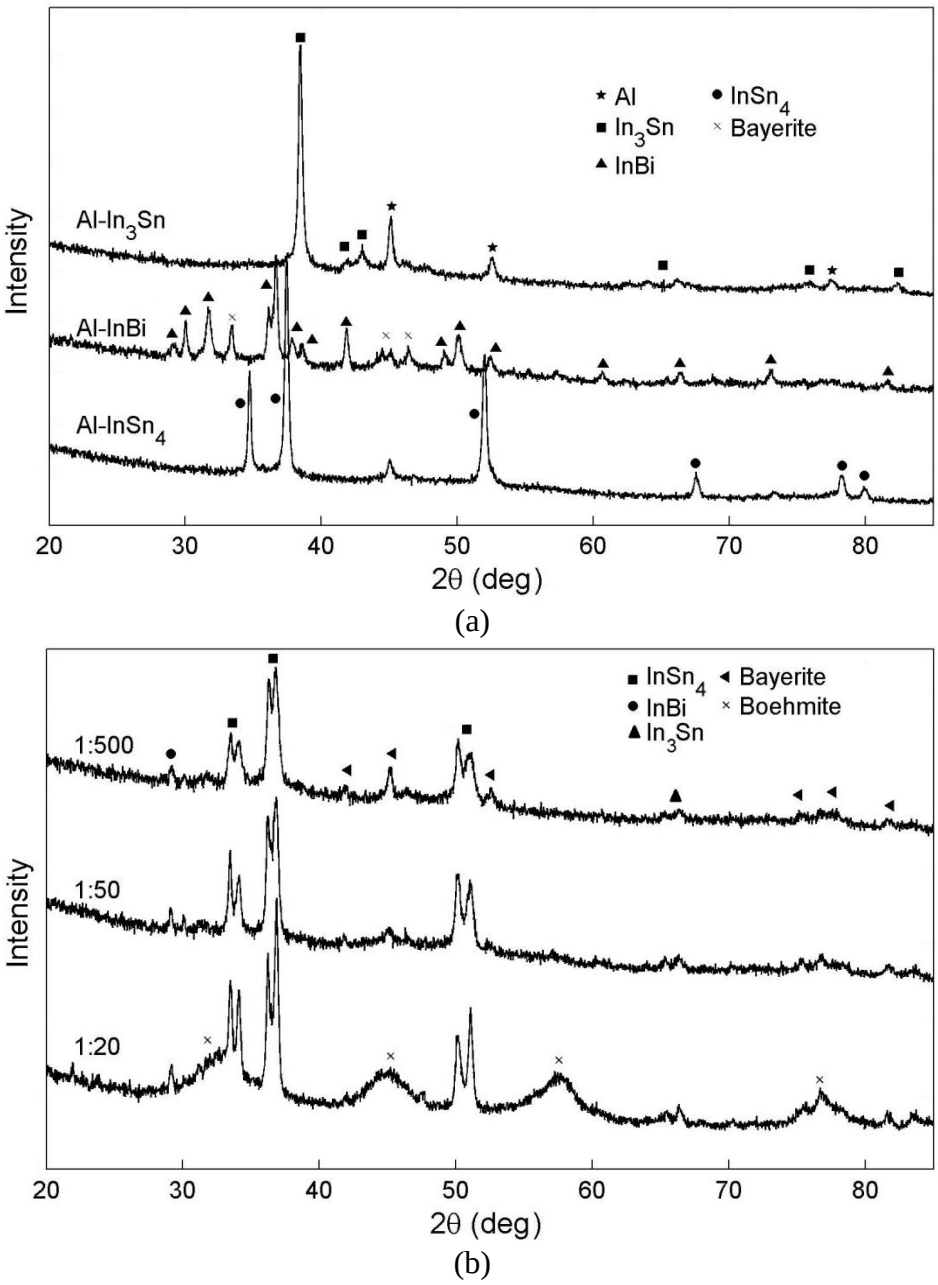

Figure 10. Hydrolysis residues of (a) ternary Al composites and (b) quaternary Composite A at various $m_{Al\ powder}/m_{water}$ ratios.

It is evident from Fig. 10a and b that the residues mainly consisted of two Al hydroxide phases (bayerite and boehmite), each of the composites coinciding intermetallic phases (InBi, In_3Sn and/or $InSn_4$), and some unreacted Al peaks. Fig. 10a shows many small bayerite peaks (some too small to indicate) and the intermetallic phases present. Small Al peaks indicate that some of the Al did not undergo hydrolysis. The presence of the intermetallic phases indicates that they did not react with water; hence, the total volume of hydrogen originated from the hydrolysis of Al.

It is evident from Fig. 10b that a decrease in water volume led to a decrease in bayerite peak intensity and an increase in boehmite peak intensity. This is due to the large increase in temperature as

the $m_{Al\ power}/m_{water}$ increased. At low temperatures, Al hydrolyzes to form bayerite. At higher temperatures, the bayerite decomposes to form boehmite. Both of these Al hydroxide phases are considered to be environmentally benign. This observation is in agreement with observations made by Huang et al. [60] and du Preez and Bessarabov (2017) [45].

4. CONCLUSIONS

A mechanochemical activation method was used to prepare various Al composites containing Bi, In and Sn as activation compounds. The hydrogen generation of activated Al upon reacting with tap water was investigated under standard temperature and pressure conditions. It was concluded that the hydrogen generation of ball-milled Al depended on the activation compounds, *in situ* generated intermetallic phases of the activation compounds and the amounts of *in situ* generated intermetallic phases.

Experimental results of this study can be summarized as follows:

(1) High yield ternary composites were successfully prepared, without the use of Ga. The intermetallic phases responsible for the activation of Al were successfully synthesized, identified and characterized. InBi containing composites had the shortest induction time and slightly higher hydrogen yields than the $InSn_4$ and In_3Sn containing composites. InBi containing composites had the fastest reaction time, followed by the $InSn_4$ and In_3Sn containing composites.

(2) Highly reactive quaternary composites were successfully prepared. Characterization revealed that all prepared quaternary composites contained InBi, and $InSn_4$ and/or In_3Sn, depending on the amount of activation compounds added. Hydrolysis reactions were relatively fast due to the presence of InBi. The heat released from InBi containing Al particles catalyzed the slower reacting $InSn_4$ and In_3Sn containing Al particles.

(3) The activation energies of ternary composites were determined to be between 47.2 and 62.1 kJ mol^{-1}. Al-InBi had the lowest activation energy, which suggests it follows a different reaction path to Al-$InSn_4$ and Al-In_3Sn.

(4) The hydrolysis reactions had a relatively large dependence on reaction temperature. Increased reaction temperatures expedited reaction rates and hydrogen yields. Thus, the hydrogen generation rate could be altered by controlling the reaction temperature, possibly at the expense of the hydrogen yield.

(5) XRD analysis of hydrolysis residues indicated that the intermetallic phases present in each of the composites did not hydrolyze, hence the total hydrogen content originated from the hydrolysis of Al. Low temperature hydrolysis produced boehmite whereas higher temperatures induced decomposition of boehmite to bayerite. Boehmite and bayerite are considered to be environmentally benign.

ACKNOWLEDGMENTS
Department of Science and Technology (DST) HySA Infrastructure Center of Competence at the North West University, South Africa, is acknowledged for financial support.

References

1. C. C. Elam, C. E. G. Padró, G. Sandrock, A. Luzzi, P. Lindblad and E. F. Hagen, *Int. J. Hydrogen Energ.*, 28 (2003) 601.
2. Y. Liu, X. Wang, Z. Dong, H. Liu, S. Li, H. Ge and M. Yan, *Energy*, 53 (2013) 147.
3. J. Macanás, L. Soler, A. M. Candela, M. Muñoz and J. Casado, *Energy*, 36 (2011) 2493.
4. H. Z. Wang, D. Y. C. Leung, M. K. H. Leung and M. Ni, *Renew. Sust. Energ. Rev.*, 13 (2009) 845.
5. Y. J. Chai, Y. M. Dong, H. X. Meng, Y. Y. Jia, J. Shen, Y. M. Huang and N. Wang, *Energy*, 68 (2014) 204.
6. M. Balat, *Int. J. Hydrogen Energ.*, 33 (2008) 4013.
7. M. Ball and M. Wietschel, *Int. J. Hydrogen Energ.*, 34 (2009) 615.
8. P. V. Gosavi and R. B. Biniwale, *J. Power Sources*, 222 (2013) 1.
9. J. A. Turner, *Science*, 305 (2004) 972.
10. X. Chen, Z. Zhao, M. Hao and D. Wang, *J. Power Sources*, 222 (2013) 188.
11. D. Bessarabov, G. Human, A. J. Kruger, S. Chiuta, P. M. Modisha, S. P. du Preez, S. P. Oelofse, I. Vincent, J. Van Der Merwe, H. W. Langmi, J. Ren and N. M. Musyoka, *Int. J. Hydrogen Energ.*, 42 (2017) 13568.
12. A. J. Esswein and D. G. Nocera, *Chem. Rev.*, 107 (2007) 4022.
13. A. V. Ilyukhina, A. S. Ilyukhin and E. I. Shkolnikov, *Int. J. Hydrogen Energ.*, 37 (2012) 16382.
14. B. Sakintuna, F. Lamari-Darkrim and M. Hirscher, *Int. J. Hydrogen Energ.*, 32 (2007) 1121.
15. B. C. Steele and A. Heinzel, *Nature*, 414 (2001) 345.
16. S. Elitzur, V. Rosenband and A. Gany, *Int. J. Hydrogen Energ.*, 42 (2017) 14003.
17. K. Wegner, H. C. Ly, R. J. Weiss, S. E. Pratsinis and A. Steinfeld, *Int. J. Hydrogen Energ.*, 31 (2006) 55.
18. M.-H. Grosjean, M. Zidoune, L. Roué and J.-Y. Huot, *Int. J. Hydrogen Energ.*, 31 (2006) 109.
19. M.-H. Grosjean and L. Roué, *J. Alloy Compd.*, 416 (2006) 296.
20. K. Mahmoodi and B. Alinejad, *Int. J. Hydrogen Energ.*, 35 (2010) 5227.
21. E. Tzimas, C. Filiou, S. D. Peteves and J. Veyret, Hydrogen storage: state-of-the-art and future perspective, Institute of Energy, Petten, The Netherlands, 2003.
22. O. V. Kravchenko, K. N. Semenenko, B. M. Bulychev and K. B. Kalmykov, *J. Alloy Compd.*, 397 (2005) 58.
23. A. V. Parmuzina and O. V. Kravchenko, *Int. J. Hydrogen Energ.*, 33 (2008) 3073.
24. E. David and J. Kopac, *J. Hazard. Mater.*, 209–210 (2012) 501.
25. B. Alinejad and K. Mahmoodi, *Int. J. Hydrogen Energ.*, 34 (2009) 7934.
26. H. Zou, S. Chen, Z. Zhao and W. Lin, *J. Alloy Compd.*, 578 (2013) 380.
27. X. Huang, T. Gao, X. Pan, D. Wei, C. Lv, L. Qin and Y. Huang, *J. Power Sources*, 229 (2013) 133.
28. H. Teng, T. Lee, Y. Chen, H. Wang and G. Cao, *J. Power Sources*, 219 (2012) 16.
29. M. Baniamerian and S. Moradi, *J. Alloy Compd.*, 509 (2011) 6307.
30. D. Belitskus, *J. Electrochem. Soc.*, 117 (1970) 1097.
31. L. Soler, J. Macanás, M. Muñoz and J. Casado, *Int. J. Hydrogen Energ.*, 32 (2007) 4702.
32. S. S. Martinez, L. Albañil Sánchez, A. A. Álvarez Gallegos and P. Sebastian, *Int. J. Hydrogen Energ.*, 32 (2007) 3159.
33. E.-D. Wang, P.-F. Shi, C.-Y. Du and X.-R. Wang, *J. Power Sources*, 181 (2008) 144.
34. X. Huang, C. Lv, Y. Huang, S. Liu, C. Wang and D. Chen, *Int. J. Hydrogen Energ.*, 36 (2011) 15119.
35. J. T. Ziebarth, J. M. Woodall, R. A. Kramer and G. Choi, *Int. J. Hydrogen Energ.*, 36 (2011) 5271.
36. M. Q. Fan, F. Xu and L. X. Sun, *Int. J. Hydrogen Energ.*, 32 (2007) 2809.

37. S. Liu, M.-Q. Fan, C. Wang, Y.-X. Huang, D. Chen, L.-Q. Bai and K.-Y. Shu, *Int. J. Hydrogen Energ.*, 37 (2012) 1014.
38. A. N. Streletskii, I. V. Kolbanev, A. B. Borunova and P. Y. Butyagin, *J. Mater. Sci.*, 39 (2004) 5175.
39. H.-W. Wang, H.-W. Chung, H.-T. Teng and G. Cao, *Int. J. Hydrogen Energ.*, 36 (2011) 15136.
40. P. Dupiano, D. Stamatis and E. L. Dreizin, *Int. J. Hydrogen Energ.*, 36 (2011) 4781.
41. J. L. López-Miranda and G. Rosas, *Int. J. Hydrogen Energ.*, 41 (2016) 4054.
42. M. Q. Fan, L. X. Sun, F. Xu, D. Mei, D. Chen, W. X. Chai, F. L. Huang and Q. M. Zhang, *Int. J. Hydrogen Energ.*, 36 (2011) 9791.
43. A. Ilyukhina, O. Kravchenko, B. Bulychev and E. Shkolnikov, *Int. J. Hydrogen Energ.*, 35 (2010) 1905.
44. H. Wang, Y. Chang, S. Dong, Z. Lei, Q. Zhu, P. Luo and Z. Xie, *Int. J. Hydrogen Energ.*, 38 (2013) 1236.
45. S. P. du Preez and D. G. Bessarabov, *Int. J. Hydrogen Energ.*, (2017) http://dx.doi.org/10.1016/j.ijhydene.2017.05.211
46. Z. Zhao, X. Chen and M. Hao, *Energy*, 36 (2011) 2782.
47. E. Czech and T. Troczynski, *Int. J. Hydrogen Energ.*, 35 (2010) 1029.
48. S. S. Razavi-Tousi and J. A. Szpunar, Metall. *Mater. Trans. E.*, 1 (2014) 247.
49. C. Suryanarayana, *Prog. Mater. Sci.*, 46 (2001) 1.
50. S. S. Razavi-Tousi and J. A. Szpunar, *Int. J. Hydrogen Energ.*, 38 (2013) 795.
51. J. Benjamin, *Sci. Am.*, 234 (1976) 40.
52. M. Q. Fan, L. X. Sun and F. Xu, *Renew. Energy*, 36 (2011) 519.
53. M. Q. Fan, F. Xu, L.-X. Sun, J.-N. Zhao, T. Jiang and W.-X. Li, *J. Alloy Compd.*, 460 (2008) 125.
54. R. Parsons, Handbook of electrochemical constants, Butterworths Scientific Publications, (1959) Preston, London.
55. N. Y. Taranets, V. Nizhenko, V. Poluyanskaya and Y. V. Naidich, *Acta Mater.*, 50 (2002) 5147.
56. M.-Q. Fan, L.-X. Sun and F. Xu, *Energy Convers. and Manage.*, 51 (2010) 594.
57. F.-Q. Wang, H.-H. Wang, J. Wang, J. Lu, P. Luo, Y. Chang, X.-G. Ma and S.-J. Dong, *Trans. Nonferrous Met. Soc. China*, 26 (2016) 152.
58. V. Bhattacharya and K. Chattopadhyay, *Mater. Sci. Eng. A*, 375 (2004) 932.
59. W. Wang, W. Chen, X. M. Zhao, D. M. Chen and K. Yang, *Int. J. Hydrogen Energ.*, 37 (2012) 18672.
60. T. Huang, Q. Gao, D. Liu, S. Xu, C. Guo, J. Zou and C. Wei, *Int. J. Hydrogen Energ.*, 40 (2015) 2354.
61. J. Skrovan, A. Alfantazi and T. Troczynski, *J. Appl. Electrochem.*, 39 (2009) 1695.
62. S. Elitzur, V. Rosenband and A. Gany, *Int. J. Appl. Sci. Technol.*, 5 (2015) 112.
63. A. K. Narayana Swamy and E. Shafirovich, *Combus. Flame*, 161 (2014) 322.
64. A. Streletskii, I. Kolbanev, A. Borunova and P. Y. Butyagin, *Colloid J.*, 67 (2005) 631.

CHAPTER 4: ARTICLE 2

Hydrogen generation of mechanochemically activated Al-Bi-In composites

4.1 Author list and contributions

Authors list

S.P. du Preez[a] and D.G. Bessarabov[a,*]

[a] HySA Centre of Competence, North-West University (NWU), Potchefstroom Campus, Private Bag X6001, Potchefstroom, 2520, South Africa

Contributions

Contributions of the various co-authors were as follows:

Experimental work, data processing and interpretation, research, and writing of the scientific paper, was performed mainly by the candidate, SP du Preez. DG Bessarabov (supervisor) made conceptual contributions and assisted with article preparation.

4.2 Formatting and current status of the article

The article presented in Chapter 3 was published in *International Journal of Hydrogen Energy* in 2017, Vol. 42, pages 16589-16602 (DOI: http://dx.doi.org/10.1016/j.ijhydene.2017.05.211). The journal details can be found at https://www.journals.elsevier.com/international-journal-of-hydrogen-energy/ (Date of access: 13 September 2018).

Available online at www.sciencedirect.com

ScienceDirect

journal homepage: www.elsevier.com/locate/he

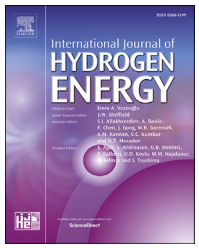

Hydrogen generation of mechanochemically activated Al–Bi–In composites

S.P. du Preez, D.G. Bessarabov*

HySA Centre of Competence, North-West University (NWU), Potchefstroom Campus, Private Bag X6001, Potchefstroom, 2520, South Africa

ARTICLE INFO

Article history:
Received 31 January 2017
Received in revised form
18 May 2017
Accepted 30 May 2017
Available online 19 June 2017

Keywords:
Activated aluminum
Hydrogen generation
Mechanochemical activation
Bismuth
Indium

ABSTRACT

The individual and combined effects of Bi and In on the morphology change and reactivity towards hydrogen release of Al during mechanochemical preparation of binary and ternary Al composites were determined. Subsequently, successfully prepared reactive composites were hydrolyzed with neutral pH waters under ambient conditions with the purpose of hydrogen generation. Reactive ternary composites were analyzed by scanning electron microscopy and X-ray diffraction. Results showed that phases found in the Al–Bi–In composites were Al, BiIn, $BiIn_3$, and Bi_3In_5. In some cases Bi and In that did not partake in intermetallic Bi–In phase formation were also found. The intermetallic phases between Bi and In were identified and characterized. It was concluded that the reactivity of ternary composites towards hydrogen yield were governed by the *in situ* formed intermetallic phases, and the remaining Bi and In that did not undergo intermetallic phase formation.

Introduction

The need for sustainable energy has been a critical topic for researcher during the last decade. Hydrogen has been identified as the best suitable candidate to replace traditional fossil fuels [1,2]. The reason being is that hydrogen is an abundant [3], renewable [3], clean, and non-polluting energy carrier with a high calorific and specific energy density [4–7]. A large fraction of hydrogen is produced from hydrocarbon sources [8], releasing large quantities of the greenhouse gas CO_2 into the atmosphere [9,10]. Additionally, the presence of CO in hydrogen obtained from hydrocarbons may seriously deteriorate fuel cells used to convert the chemical energy of hydrogen to electrical energy [11,12]. Thus, hydrogen obtained in such a manner cannot be considered as truly renewable if obtained from non-renewable sources. Ideally, hydrogen has to be obtained by clean processes from renewable sources, totally avoiding any CO_2 emissions [6]. Water is considered an alternative to hydrocarbons as a source of hydrogen due to its high hydrogen content of approximately 111 kg m^{-3}, whereas liquid hydrogen and gasoline have hydrogen contents of 71 and 84 kg m^{-3}, respectively [7,13,14]. Hydrogen can be produced from water by several different processes, e.g. water electrolysis [15], water photo catalysis [16], metal hydrolysis [17], and metal hydride hydrolysis [18]. Additionally, feasible storage of hydrogen gas is a critical issue limiting the use of hydrogen as an energy carrier due to its very low gaseous density (0.089 kg m^{-3}) [7,19]. Three main methods of hydrogen storage are currently applied, i.e. pressurized gas, liquid hydrogen, and metal hydrides [19]. Of these three methods, pressurized gas is the simplest and least expensive method

* *Corresponding author.*
E-mail address: dmitri.Bessarabov@nwu.ac.za (D.G. Bessarabov).
http://dx.doi.org/10.1016/j.ijhydene.2017.05.211

[20]. Ideally, hydrogen should be generated on demand and consumed as it is generated, removing the need for storage. Thus, the only the compounds partaking in hydrogen generation are stored.

Considering the above mentioned issues, the production of hydrogen by reacting water and metals (Mg, Li, Al, etc.) under mild or ambient conditions have received a lot of attention in recent years. Al is considered to be the best suited metal for such applications as is it an abundant [7], lightweight metal with a density of approximately 2700 kg m^{-3} [21], and a high hydrogen generation potential [22]. In addition, storage of solid Al is safer than metal hydrides and other hydrogen generators [23]. Al hydrolysis produces Al hydroxides and (to a lesser extent) oxides according to the following reactions [3,21–25]:

$$2Al + 6H_2O \rightarrow 2Al(OH)_3 + 3H_2 \quad (1)$$

$$2Al + 4H_2O \rightarrow 2AlOOH + 3H_2 \quad (2)$$

$$2Al + 3H_2O \rightarrow Al_2O_3 + 3H_2 \quad (3)$$

The produced by-products in reactions (1)–(3) are considered to be environmentally benign, fully recyclable through the Hall-Héroult process [26], and may be used in several industrial applications [21]. The Al hydrolysis reaction is thermodynamically favorable, but the formation of a passive oxide layer on the surface of Al prevents it from continuously producing hydrogen since it prevents Al–H_2O contact [27]. Considerable efforts have been made to solve this problem, i.e., removal/disruption of the oxide layer. One such a method includes the immersion of Al in alkaline or acidic solutions, removing the protective oxide layer [28–36]. However, high reaction rates are only reached at extreme pH values and at elevated temperatures (approximately 100 °C). Hydrothermal Al oxidation is a high hydrogen yield (100%) method, but requires very high reaction temperatures of 400 °C, pressures of >200 atm, and expensive equipment [37–39]. To mitigate the use of harsh experimental conditions, other methods were developed to increase the reactivity of Al. Hg and Hg-based compounds may be used to amalgamate Al surfaces to enable Al hydrolysis under mild conditions, but its application is restricted due to the toxicity of Hg [40–43]. Ga may be used to replace Hg as it has a similar effect on Al particles, i.e. enabling Al reactivity under ambient conditions. Ga in combination with metals such as In, Sn, Zn, and/or Bi produces compounds with the potential to activate Al particles. Considerable efforts have gone into the use of Ga and Ga-based activation compounds to produce reactive Al by thermal or mechanochemical activation methods, e.g. Ga [44], Ga-In Refs. [22,45,46], Ga-In-Sn [47–49], Ga-In-Sn-Zn [50–52], and Ga–In–Sn–Bi [53]. Though Ga removes the toxicity aspect of Al activation, it does however significantly increase the cost thereof. Additionally, thermal methods require more energy than mechanochemical methods, increasing the production cost of activated Al. Several studies have indicated that Al could be successfully activated by means of mechanochemical using activation compounds other than low melting point metals, e.g. carbon [54], metal oxides [55,56], water soluble salts [57,58], lithium [59], metal hydrides [60,61], and iron/magnesium [27,62]. However, some of these methods are restricted to laboratory scale due to limitations such as cost and instability of activation compounds, corrosiveness of chemicals used for Al activation, time consuming Al activation processes, and hydrogen flow rates being too low or too high for certain applications.

To the best of our knowledge, the successful mechanochemical activation of Al by means of low melting point metals, without the use of Ga, has yet to be realized. Wang et al. (2013) achieved a close to 100% hydrogen conversion yield using a mechanochemically prepared Al activated by 3 wt% Ga-3 wt% In-5 wt% Sn [47]. Whereas, Wang et al. (2016) achieved high hydrogen yields with mechanochemically activated Al by 1 wt% Ga-3 wt% In-6 wt% Sn [48]. Both studies included relatively minute quantities of Ga, though, even small additions of Ga will increase the production cost of Al composites. Additionally, the use of relatively cheap Bi has been proven to increase the reactivity of mechanochemically activated Al [14,57,58,63,64]. Moreover, the use of Bi in combination with other low melting point metals to activate Al by a mechanochemical method for hydrogen generation purposes is also relatively unexplored. Huang et al. (2015) achieved high hydrogen yields using an Al–Ga–In–Sn–Bi composited prepared by a melting method [53].

In spite of relatively large amount of publications on hydrogen generation from mechanochemically activated Al, there is a very limited number of papers that excluded Ga as an activation compound when considering low melting point metals. In this study, the individual roles of Bi and In (of which both are low melting point metals) during ball milling of Al were determined. Subsequently, ternary Al composites (containing Bi and In) were prepared and hydrolyzed. Several ternary Al composites were successfully prepared, in yields of >93%. X-ray diffraction (XRD) was used to determine the intermetallic phases present, as well as the presence of In and Bi. Scanning electron microscopy (SEM) was used to investigate morphology changes of un-milled and milled Al particles.

Materials and methods

Materials

The following starting materials were supplied by Sigma-Aldrich (South Africa): Al powder (<200 μm, 99% purity), In shots (+5-2 mm, >99.9% purity), and Bi granules (>99.99% purity). Ultrapure deionized water (resistivity, 18.2 MΩ cm^{-1}), produced by a Milli-Q water purification system, was used for all hydrolysis reactions. Pure Ar (99.99%) (Afrox, South Africa) was used during all purging procedures.

Aluminum composite compositions and their mechanochemical preparation

Binary and ternary composites were prepared. Binary composites (Al–Bi and Al–In) consisted of 10–30% of the activation compounds (Bi or In), with the balance being Al. Ternary

composites (Al–Bi–In) contained various amount of the activation compounds, in the range 0.62–9.38%, with Al kept at 90%. The compositions of ternary composites are indicated in Table 1.

Ball milling of Al composites powders was performed in a Retsch Emax high-energy ball mill (Retsch, Germany) under an Ar atmosphere. The as-received metals (Al, Bi, and In) were weighed and placed in a 125 mL stainless steel grinding pot with 5 mm stainless steel grinding balls. The grinding ball to powder mass ratio was 30:1. For all composite preparations, the as-received metals were milled for 30 min at 1500 rpm. The fine Al powders obtained after ball milling indicated that the as-received materials were milled into a homogenous powder, and represented a powder consisting of an equal distribution of constituents. Each composite was ball milled in triplicate. In order to avoid unwanted atmospheric oxidation, hydrolysis experiments with the ball-milled powders were carried out as soon as milling was completed. Composites were stored in an airtight container until required for use.

Hydrolysis setup and hydrogen measurements

Hydrolysis reactions were carried out at standard temperature and pressure in a 100 mL flask reactor with two openings, one for hydrolysis solution addition (by means of a pressure equalizing addition funnel) and the other for hydrogen escape. The generated hydrogen passed through two Drierite™ ($CaSO_4$) gas driers to remove water vapor prior to hydrogen measurements. Generated hydrogen was measured using a digital thermal gas mass flow meter to measure gas mass flow (Model GH-32654-12; Cole-Parmer, South Africa). Hydrogen measurements were performed using 0.5 g composite and 25 mL of pure water, unless specified otherwise. The reaction mixtures were left unagitated during all hydrolysis reactions. Each prepared sample was hydrolyzed in triplicate.

Expression for hydrogen generation

Hydrogen generation is expressed as a conversion yield (%), which is defined as the volume of hydrogen produced over the theoretical value of hydrogen that should be released assuming the entire Al content is hydrolyzed. Applying the ideal gas law, approximately 1360 NmL per gram Al is achievable under standard atmospheric conditions. Thus, the hydrogen yield (%) reflects the generated hydrogen volume measured as a fraction of the obtainable 1360 NmL. The hydrogen generation rate (mL min^{-1}) is defined as the volume of hydrogen (NmL) produced per minute from the hydrolysis of 0.5 g Al composite.

Table 1 – Composition of ternary Al composites.

Composite	Compound (wt%)	
	Bi	In
Al-9.38% Bi-0.62% In	9.38	0.62
Al-8.76% Bi-1.26% In	8.76	1.26
Al-7.5% Bi-2.5% In	7.5	2.5
Al-5% Bi-5% In	5	5
Al-3.74% Bi-6.26% In	3.74	6.26
Al-2.5% Bi-7.5% In	2.5	7.5
Al-1.26% Bi-8.76% In	1.26	8.76
Al-0.62% Bi-9.38% In	0.62	9.38

Sample characterization by XRD and SEM

XRD was performed using a Röntgen diffraction system (PW3040/60 X'Pert Pro). A back-loading preparation method was used to determine the crystalline phases present in the Al composites and hydrolysis residues. The samples were scanned using X-rays generated by a copper (Cu) Kα X-ray tube. Measurements were carried out between variable divergence slits and fixed receiving slits. The phases were identified using X'Pert HighScore Plus software (PANalytical). Structural refinement was performed using the Rietveld method (Autoquan programme) to confirm the abundance of phases present in ball-milled Al composites.

Scanning electron microscopy (SEM) with energy dispersive x-ray spectroscopy (EDS) detectors was used to perform morphological and chemical characterization of as-received Al powder and ball-milled Al composites. A FEI Quanta 200 scanning electron microscope with an integrated Oxford Instruments INCA 200 energy dispersive X-ray spectroscopy microanalysis system was used. SEM micrographs were obtained (at various magnifications) to characterize the physical attributes of the investigated materials. Magnification is indicated on each micrograph (μm scale). SEM-EDS was used to confirm the distribution of activation compounds on the surface of Al particles.

Results and discussion

Effects of Bi and In additions on ball-milled Al composite particles

Metals that undergo repetitive plastic deformation are subjected to radical changes in particle shape, residual stress, and the redistribution of constituents. During ball milling of ductile and malleable particles, several mechanisms are at play. These may be described as follows. As soon as ball milling commences, particles will undergo cold welding as they are caught between the impacts of milling equipment (ball–ball and ball–milling chamber), which leads to the formation of larger coagulated particles consisting of an unequal distribution of the initial constituents (Al, Bi, and/or In). After a certain period of milling, the coagulated particles will reach a stress-to-strain peak due to work hardening, followed by plastic deformation of coagulated particles. The result is a decrease in particle size as a result of particle fracturing [65,66].

During ball milling of Al, different metals will have varying effects on the behavior of Al particles. To determine the individual roles of Bi and In in Al particle morphology changes during ball milling, the binary Al composites containing 10–20% of Bi or In were investigated. Backscatter SEM micrographs in Fig. 1 present unmilled Al powder morphology (a) and the ball-milled morphology of binary composites containing 10% Bi (b), 20% Bi (c), 10% In (d), and 20% In (e). Milling parameters were kept constant, i.e., 30 min milling

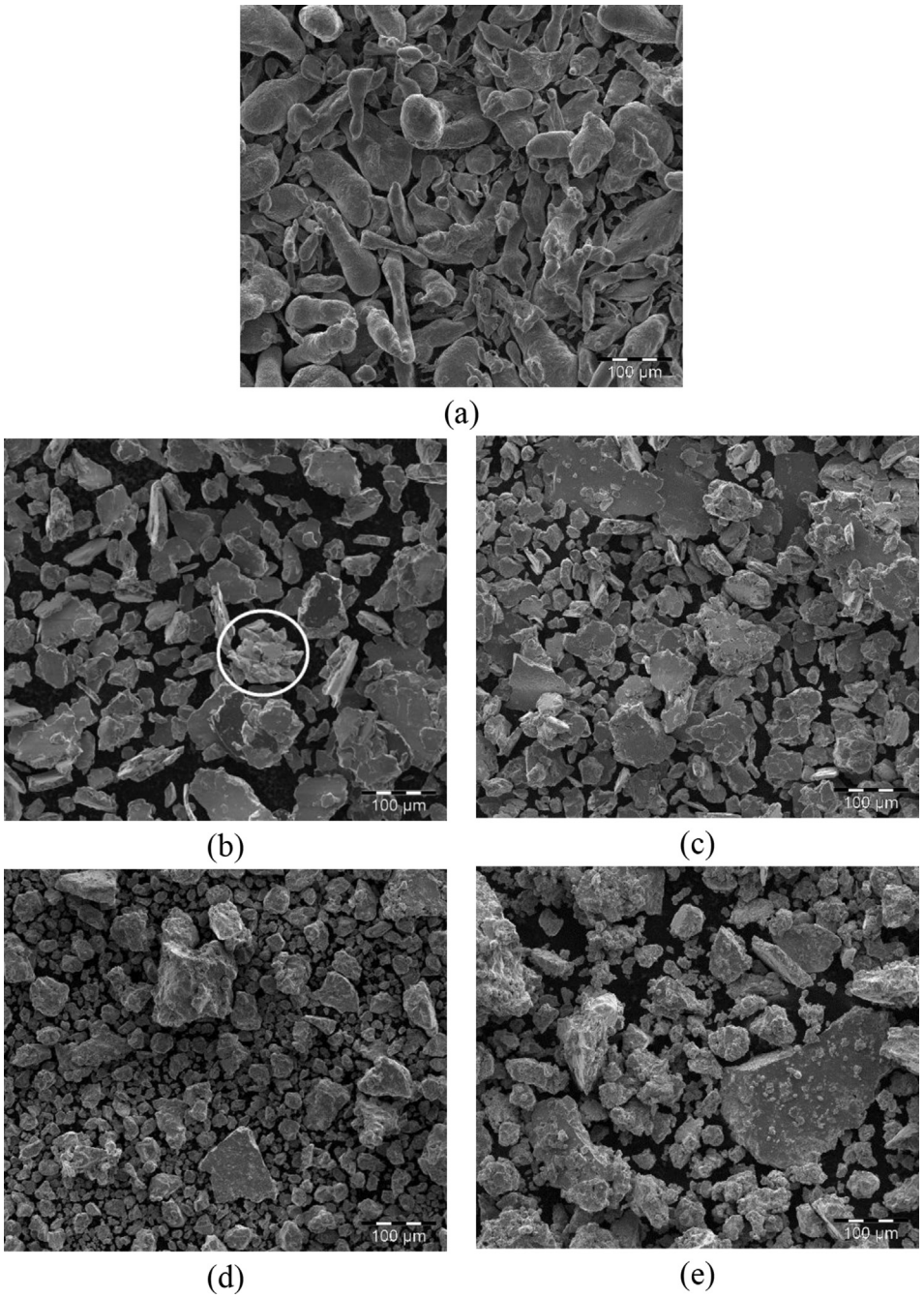

Fig. 1 – Backscatter SEM micrographs of (a) unmilled Al, (b) Al-10% Bi, (c) Al-20% Bi, (d) Al-10% In, and (e) Al-20% In composites.

time, 30:1 milling ball–powder ratio, 1500 rpm, and an Ar atmosphere.

It is evident from Fig. 1 that the milled Al–Bi and Al–In composites (b–e) underwent significant particle size reduction compared to the unmilled Al powder (a). The differences in Al morphology changes caused by Bi and In during individual ball milling are clearly visible. As received Al particles had a strand-like morphology and a particle size of between 100 and 300 μm. The Al-10% Bi alloy consisted of small fractured particles of 40–120 μm, whereas Al-10% In composite contained a large fraction of 10–40 μm particles and some larger 80 μm particles. All milled samples contained a fraction of relatively large particles, but to a much lesser extent than the finer particle fraction. Increasing the activation compound addition (%) to 20% resulted in a decrease in composite particle size. The presence of both small and large particles can be ascribed to a drive towards steady state equilibrium between cold welding (increasing average particle size) and fracturing (decreasing average particle size) of Al particles. Smaller particles are able to resist further deformation and fracturing, whereas larger particles are more susceptible to deformation and fracturing. Subsequently, smaller particles tend to weld onto each other (see encircled particle in Fig. 1b) and onto larger particles, driving the overall particle size distribution

towards an intermediate size [67,68]. Large particles, consisting of agglomerated finer particles, contain numerous morphological irregularities and deformities, enabling water to freely penetrate deep within these particles. The presence of small and large particles in Fig. 1, accompanied by the relatively large decrease in particle size, is indicative of a steady state equilibrium between the cold welding of particles and the fracturing thereof.

Fig. 1 confirms the successful size reduction of unmilled as-received Al particles. However, size reduction alone does not guarantee that Al will undergo hydrolysis under ambient conditions. It is well know that the protective oxide layer has to be disrupted to expose the underlying fresh Al to water. Thus, for good Al activation, the activation compounds (Bi and In) have to be dispersed equally over the entire surface of the Al particles. The distribution of activation compounds on the surface of Al particles was determined by SEM-EDS mapping of the Al, as presented in Fig. 2. (Red represents Al atoms; blue and green represent Bi and In, respectively.)

It is evident from Fig. 2 that Bi and In were equally distributed on the surface of Al particles and that no activation compound aggregation took place. Al corrosion in neutral or near-neutral pH waters increases when alloyed with certain metals. Localized micro-galvanic corrosion is governed by the potential difference between Al and the alloying metals [69,70]. The distribution of Bi on the surface of Al increases the micro-galvanic activity of Al–Bi composite as it offers the potential for electron transfer from the anodic Al to cathodic Bi during Al hydrolysis reactions [17,71,72]. Al–Bi composite have an open circuit potential of −1.85 V, which is 0.08 lower than that of pure Al [57]. In addition to the lower current potential of Al–Bi, the Bi disrupts the protective oxide layer on the surface of the Al particles. Al–In composites exhibited limited to no reactivity in pure water at room temperature. However, Al–In composites showed high reactivity in hot electrolyte solutions [42], which was not investigated in this study. The objectives of this study were not limited to the reactivity of the various ternary composites (Al–In and Al–Bi). Morphology changes of Al ball milled with the In and Bi was also considered as an objective. According to Fig. 2, it is highly likely that any phase formations between Bi and In would occur on the surface of Al particles.

Hydrolysis of ternary Al–Bi and Al–In composites

Once the roles of Bi and In on Al particle morphology changes during ball milling were determined, the effects of Bi and In on Al hydrolysis activity could be determined. As mentioned in Section Effects of Bi and In additions on ball-milled Al composite particles, Al–In hydrolysis experiments displayed limited reactivity in pure water at room temperature. This was in accordance with observations made by Fan et al. (2010) [63]. Al–In alloy has a potential of −1.1 V higher than the −1.29 V potential of water decomposition [73]. Al–Bi composites, on

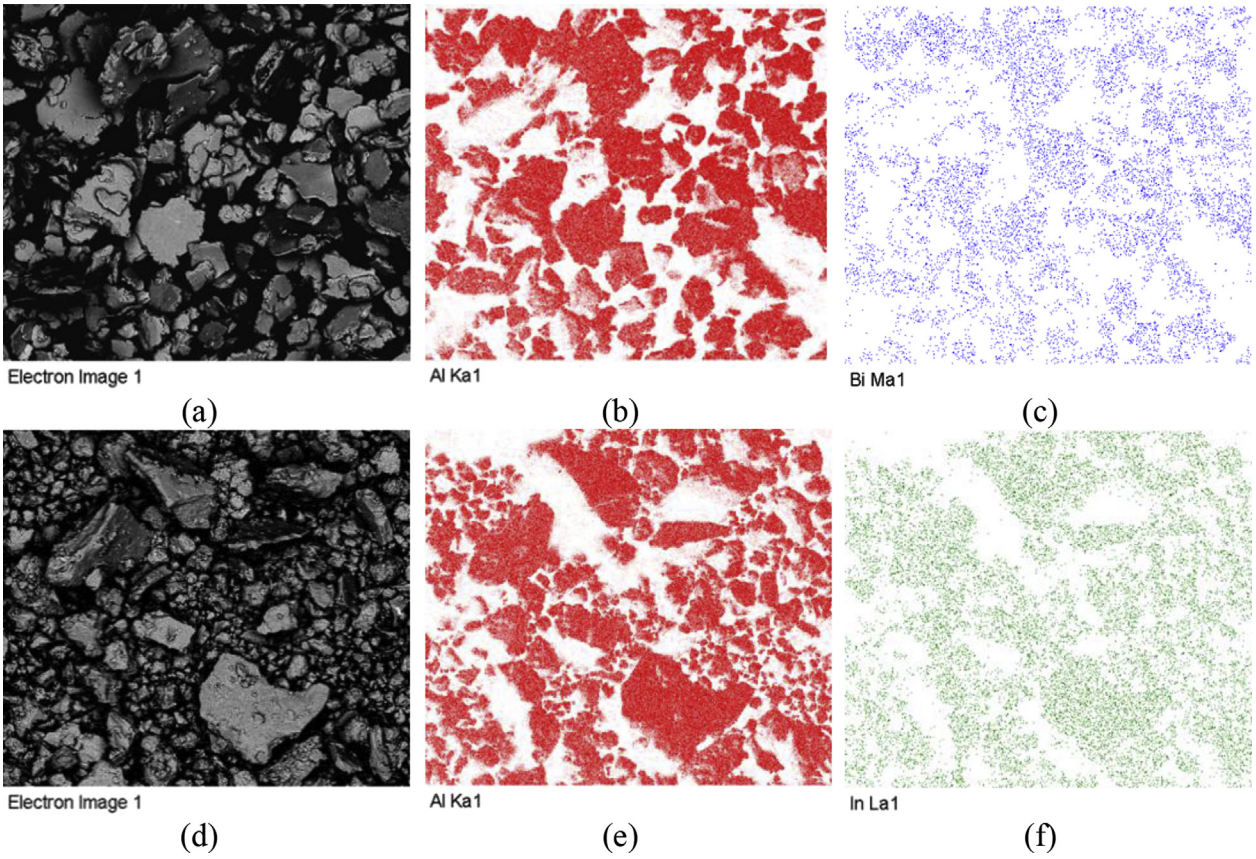

Fig. 2 – A backscatter SEM micrograph of (a) Al-10% Bi and the corresponding EDS mapping for (b) Al and (c) Bi; a SEM micrograph of (d) Al-10% In, and the corresponding EDS mapping for (e) Al and (f) In.

the other hand, can be hydrolyzed in pure water at room temperature. The deceasing Al content present in binary composites containing 15, 20, and 30% Bi (compared to Al-10% Bi) will result in milder water temperatures increases during hydrolysis, which may reduce the reactivity of Al–Bi composites. Thus, hydrolysis reactions were performed in 25 and 10 mL of pure water to determine the effect of reaction temperature on hydrogen yield. Fig. 3 presents Al–Bi hydrolysis reactions performed in 25 mL (a) and 10 mL (b) of pure water.

Fig. 3a shows the hydrogen yields of Al–Bi composites containing 10–30% Bi hydrolyzed in 25 mL pure water. The hydrogen yield increased from 82 to 86% as the Bi content increased from 10 to 15%, followed by a slight decrease to 85% as the Bi content was further increased to 20%. Increasing the Bi content to 30% resulted in a hydrogen yield of 66%. Hydrolysis reactions were completed after 32–42 min of coming into contact with water. Increasing the Bi content will increase the amount of Al–Bi contact point, which subsequently increases the micro-galvanic potential between anodic Al and cathodic Bi [72]. In addition, Al hydrolysis is dependent on reaction temperature [17,74]. Due to the decrease in Al content (as the Bi content was increased), the heat released during Al hydrolysis (−444.4 kJ mol^{-1}) [59] may result in an decrease in hydrogen yield.

Fig. 3b shows the hydrogen yields of Al–Bi composites hydrolyzed in 10 mL pure water. Al-10, 15, and 20% Bi displayed hydrogen yield increases of 4–9%, whereas Al-30% Bi had an increase of approximately 15%. Increases in hydrogen yields were not as substantial as decreases in hydrolysis reaction completion times. Decreasing the water volume from 25 mL to 10 mL resulted in reactions being completed 3.8–4.8 times faster. The shorter reaction times may be ascribed to increases in reaction temperature, which accelerated the hydrolysis reaction. On average, the reaction temperature increased by a factor of 2.70 ± 0.16 when the water volume decreased from 25 to 10 mL. The small increases in hydrogen yields of Al–Bi 10, 15, and 20% indicated that the reactivities of these alloy were not as dependent on reaction temperature as

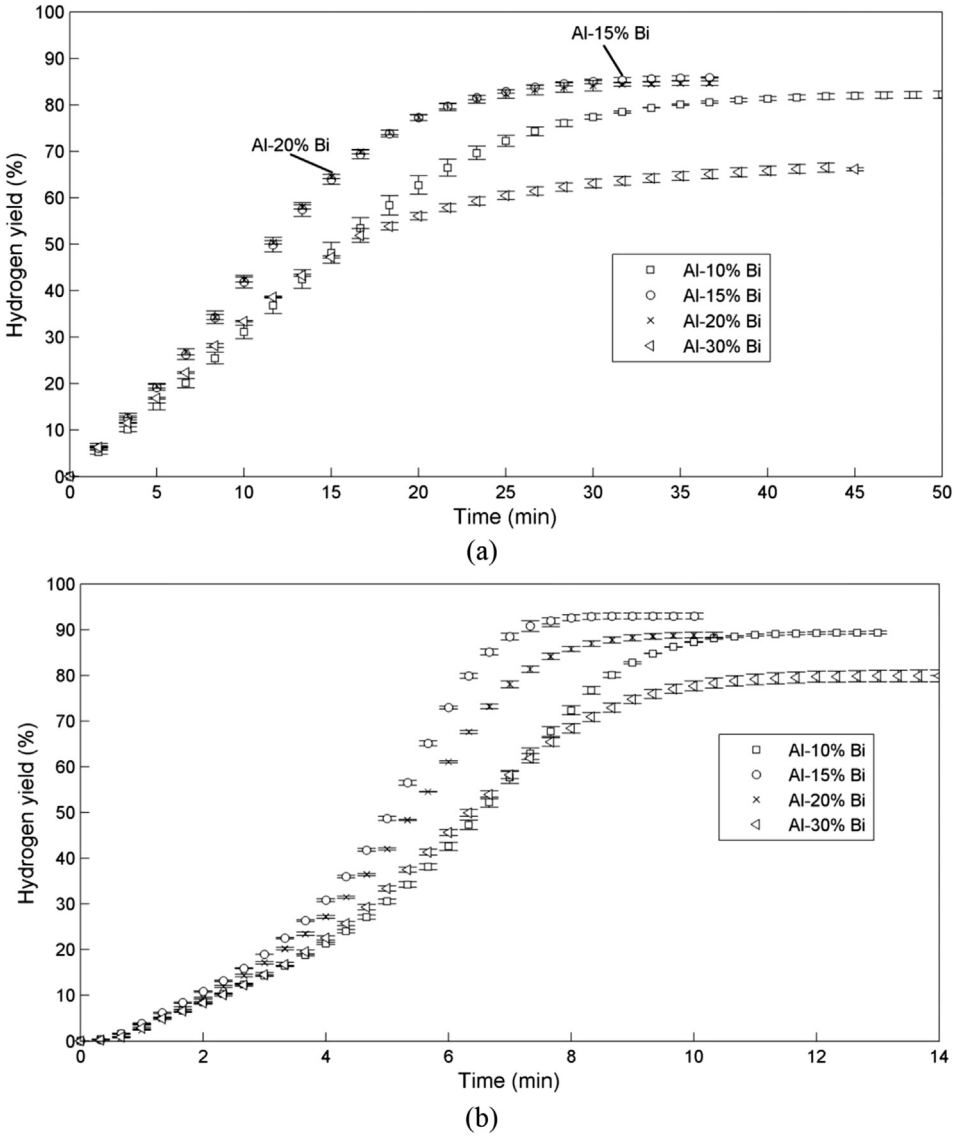

Fig. 3 – Hydrogen yields of binary Al–Bi composites, containing 10–30% Bi, hydrolyzed in (a) 25 mL and (b) 10 mL water.

Al-30% Bi. Based on results presented in Fig. 3, the activation compound addition and water volume for hydrolysis, for use in ternary composite investigations, were selected as 10% and 25 mL, respectively.

Hydrolysis of ternary Al–Bi–In composites

To investigate the synergetic effects of Bi and In on Al during composite preparation, composites containing various amounts of Bi and In (see Table 1) were prepared and hydrolyzed. Fig. 4 presents the hydrogen yields of ternary Al–Bi–In composites. Ternary composites were divided into two sets and are referred to as Al–Bi > In and Al–Bi < In, with Al–Bi > In being defined as the addition of Bi being greater than that of In. Al–Bi < In may be defined similarly. Al-5% Bi-5% In was included in both Fig. 4a and b, and served as reference in Fig. 4b. To avoid overcrowding the graphs presented in Fig. 4, no standard deviations for experimental results are included. The maximum hydrogen yield standard deviations did not exceed 2.9%.

Fig. 4a presents the hydrogen yields (%) of ternary Al–Bi > In composites. Al-7.5% Bi-2.5% In and Al-5% Bi-5% In had the highest hydrogen yields of approximately 95.5% and 93.1%, respectively, and the reaction was completed within 7.5 min. A reduction in hydrogen yield was observed when increasing the Bi content to >7.5%, and subsequently reducing the In content to <2.5%. Al-8.76% Bi-1.26% In and Al-9.38% Bi-0.62% In had yields of 82.5 and 81.5%, respectively, which is similar to that of Al-10% Bi (82%). SEM micrographs (not presented) of Al-8.76% Bi-1.26% In and Al-9.38% Bi-0.62% In showed similar morphology to that of Al-10% Bi, but with a particle size distribution comparable to that of Al-10% In.

Fig. 4b shows the hydrogen yields (%) of ternary Al–Bi < In composites. All ternary composites here had reduced

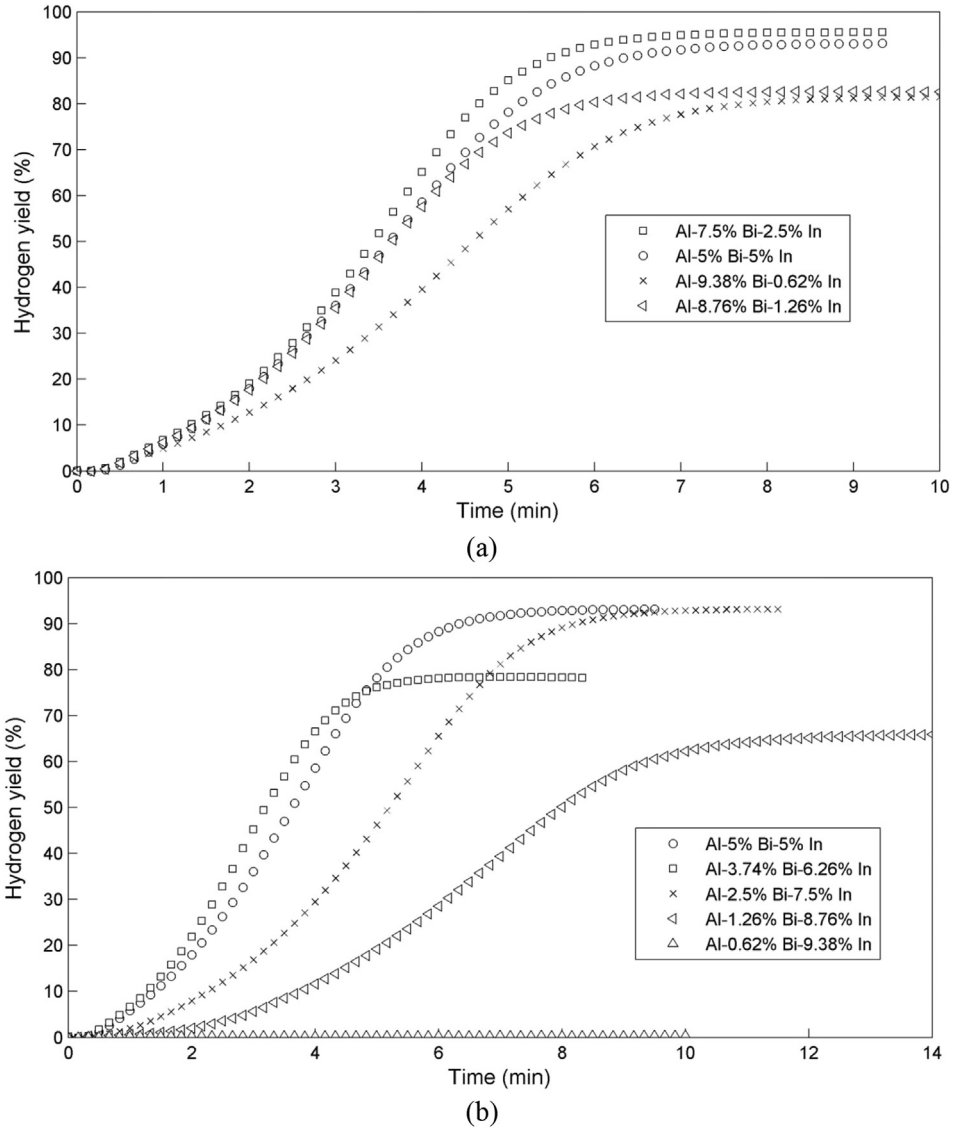

Fig. 4 – Hydrogen yields of composites Bi > In (a) and Bi < In (b). Hydrolysis parameters were kept constant: 25 mL pure water, room temperature. Milling parameters were kept constant: 30 min milling time, 30:1 milling ball:powder ratio, 1500 rpm.

hydrogen yields compared to the composites presented in Fig. 4a. Except for Al-2.5% Bi-7.5% In, which achieved a hydrogen yield of 93% within 10 min. A slight increase in Bi and a decrease in In content resulted in a large reduction in hydrogen yield. This is evident from the hydrolysis of Al-3.74% Bi-6.26% In, which achieved a hydrogen yield of 77% within 6.3 min. Furthermore, increasing the In content from 8.76 to 9.38%, and subsequently decreasing Bi content from 1.26 to 0.62%, resulted in an a nonreactive alloy; no hydrogen was produced after 10 min of the powder coming into contact with water.

It is clear from Fig. 4 that, during ball milling, certain combinations of Bi and In have a synergetic effect on Al reactivity. Combining the effects that Bi and In has on Al particles resulted in a high reaction surface composites with an abundance of galvanic-corrosion prompting Al–Bi contact points. These effects were best exploited in the Al-7.5% Bi-2.5% In composite. Additionally, surface defects and irregular morphologies associated with fine particles agglomerated onto other fine and large particles allowed a large water-composite contact boundary.

EDS mapping was used to determine whether both the activation compounds (Bi and In) were simultaneously distributed onto the surface of Al particles during ball milling procedures. Fig. 5 presents a backscatter SEM micrograph and the EDS mapping of Al-7.5% Bi-2.5% In. (Red represents Al atoms; blue and green represent Bi and In, respectively.)

The activation compound (Bi and In) distribution presented in Fig. 5 coincides with EDS mapping presented in Fig. 2. All ternary Al composites had similar EDS mappings, i.e., the complete distribution of activation compounds. This indicated that activation compound distribution onto the surface of Al particles was not the only factor that had an impact on the reactivity of composites presented in Fig. 4, suggesting that intermetallic phases of Bi–In may be a contributing factor to the reactivity of ball-milled Al composites.

XRD analysis of ternary Al composites

XRD was performed on ternary Al composites to determine the presence of intermetallic phases between Al, Bi, and In. Intermetallic phases between Bi and In will influence the hydrolysis kinetics of Al composites. Either in terms of particle size reduction, via the induction of work hardening, or Al particle surface reactivity. In addition to the formation of micro-galvanic cells between Al and Bi (as discussed in Section Effects of Bi and In additions on ball-milled Al composite particles), intermetallic phases may form on the surface of the Al particles, resulting in a layer of water permeable material. However, judging from the short induction periods (time before hydrolysis initiates), diffusion of water through a water permeable layer on the surface of Al particles may not be the case. Hydrolysis reactions are initiated within 20–40 s of Al coming into contact with water. Fig. 6 presents the Rietveld refined XRD patterns of (a) Al–Bi > In and (b) Al–Bi < In composites. Qualitative phase analysis using the Rietveld method was performed to confirm the presence of detected phases. Ternary Al composites are presented as A–H to avoid

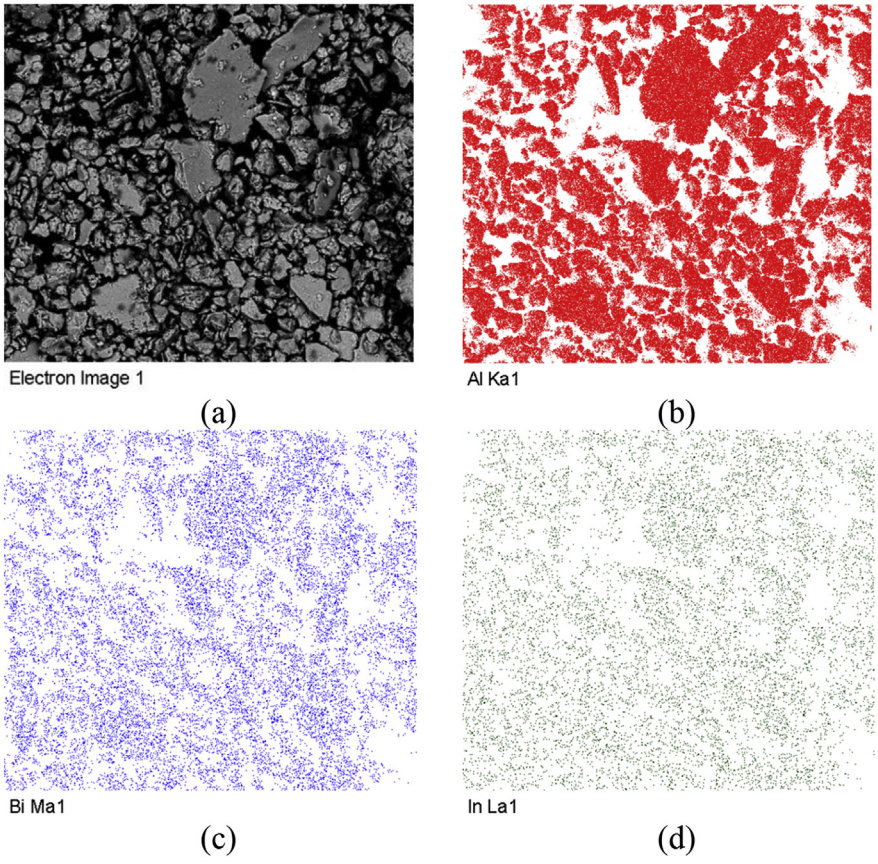

Fig. 5 – A backscatter SEM micrograph of Al-7.5% Bi-2.5% In (a), and the corresponding EDS mappings for Al (b), Bi (c), and In (d).

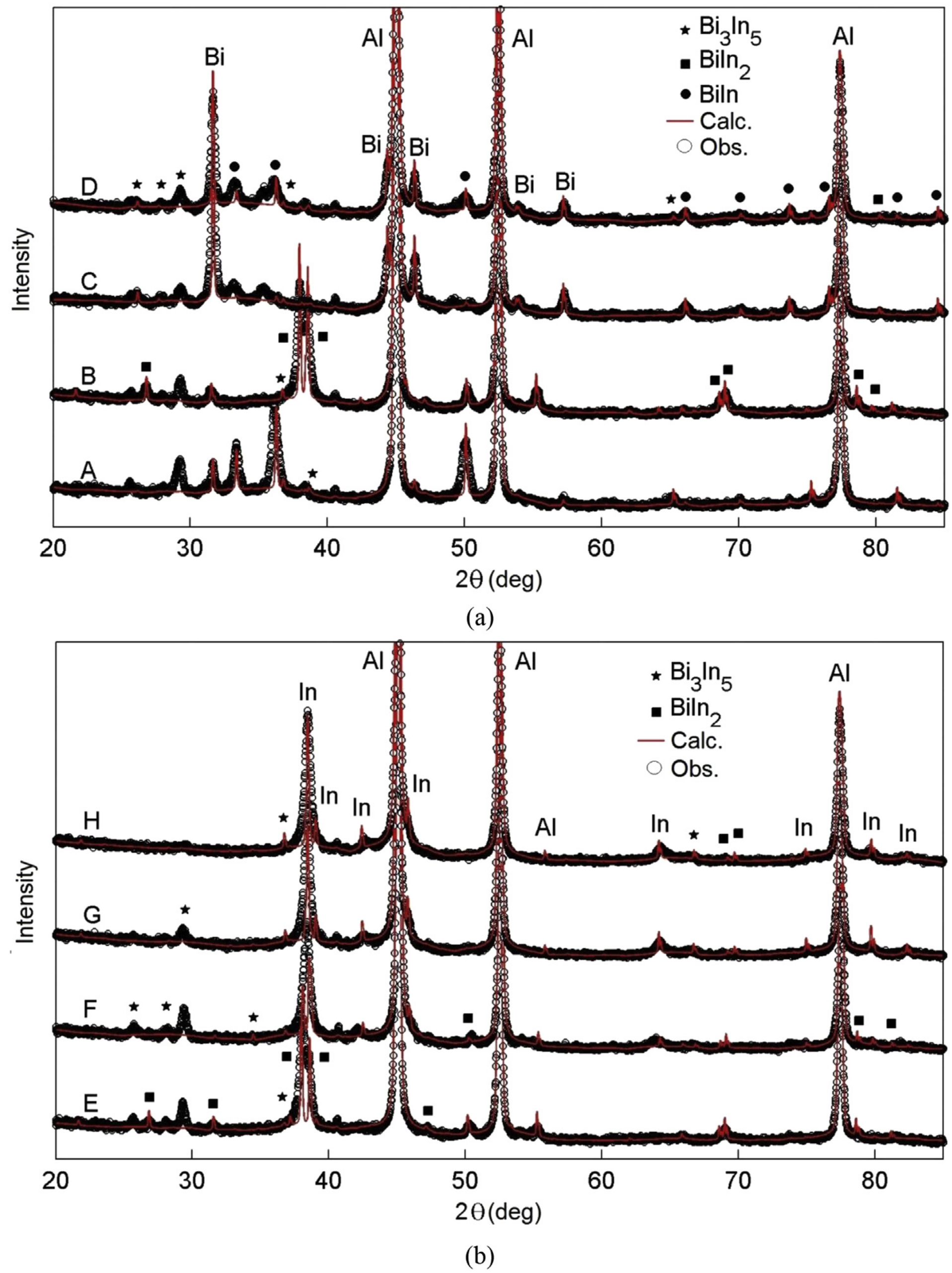

Fig. 6 – The Rietveld refinement of the XRD patterns of ternary (a) Al–Bi > In and (b) Al–Bi < In composites. Al composites presented are indicated as A (Al-7.5% Bi 2.5% In), B (Al-5% Bi-5% In), C (Al-9.38% Bi-0.62% In), D (Al-8.76% Bi-1.26% In), E (Al-3.74% Bi-6.26% In), F (Al-2.5% Bi-7.5% In), G (Al-1.26% Bi-8.76% In), and H (Al-0.62% Bi-9.38% In).

cluttering of presented data and are defined in the figure caption of Fig. 6. Observed values were indicated with black circles, whereas the calculated values were indicated by the solid red line. The entire Al peaks at 2θ positions 44 and 53 are not presented, in an effort to rather increase the detail of surrounding peaks. The R-factors (R_{exp}, R_p, R_{wp}) and GoF (Goodness-of-fit) values obtained from Rietveld analysis of the prepared composites (A–H) are summarized in Table 2.

It is evident from Fig. 6 that Bi and In formed several Bi–In intermetallic phases during high-energy ball milling of ternary composites. Observed Bi and In peaks were indicative that either one of the activation compounds was consumed

Table 2 – Parameter values of Rietveld structural refinement analysis of prepared Al composites.

Sample	Parameter (%)			
	R_{exp}	R_p	R_{wp}	GoF
A	3.94	8.34	13.27	3.37
B	4.08	8.44	12.96	3.16
C	3.92	7.73	11.28	2.88
D	3.87	7.42	10.62	2.74
E	4.10	7.89	12.55	3.06
F	4.29	8.38	12.86	2.99
G	4.26	8.32	13.09	3.07
H	4.25	8.11	12.60	2.96

during intermetallic phase formation and that the remaining activation compound could no longer partake in any intermetallic phase formation process. Fig. 6 also indicates that no other intermetallic phases with Al (Al–Bi and Al–In) could be formed under the experimental conditions used in this study. This may be ascribed to the low solid solubility of Bi and In in the Al matrix [48,75]. As far as the authors could assess, no other literature currently exists in the public, peer-reviewed domain on the in-situ formation of Bi–In intermetallic phases on the surface of Al during mechanochemical procedures.

However, the Bi–In intermetallic phases BiIn, $BiIn_2$, and Bi_3In_5 could be formed. Bi_3In_5 peaks were present in all of the ternary composites, except for Al-0.62% Bi-9.38% In. To date, the Bi_3In_5 formation kinetics are unclear. Considering the presence of Bi_3In_5 in each of the ternary composites, some intermetallic phases were likely to form at certain Bi:In atom ratios. Al-7.5% Bi-2.5% In had a Bi:In atomic ratio of 1.648 and contained several prominent BiIn peaks, whereas Al-5% Bi-5% In had a Bi:In atomic ratio of 0.549 and contained several $BiIn_2$ and some BiIn peaks. As expected, large fractions of Bi or In resulted in less reactive composites, as the composites revert to Al–Bi or Al–In reactivities, discussed in Section Hydrolysis of ternary Al–Bi and Al–In composites.

As indicated in Fig. 4, Al-7.5% Bi-2.5% In, Al-5% Bi-5% In, and Al-2.5% Bi-7.5% In were the most reactive composites. The reactivity of composites Al-7.5% Bi-2.5% In, and Al-5% Bi-5% In may be ascribed to the prominent presence of the intermetallic phases BiIn and $BiIn_2$, respectively. The reactivity of Al-2.5% Bi-7.5% In facilitated a fine particle size distribution (caused by In) and particles with reactive surfaces (caused by Bi). Composites Al-3.74% Bi-6.26% In and Al-1.26% Bi-8.76% In exhibited approximately the same peaks (and abundances) as alloy Al-2.5% Bi-7.5% In, but did not have equally high hydrogen yields. It is unclear what hydrolysis mechanism applies here. It is however accepted that a certain In content will result in very fine particles, which may simultaneously be activated by Bi during ball milling. Alloy 0.62% Bi-9.38% In did not exhibit any prominent peaks, which explains the alloy's inability to undergo hydrolysis under ambient conditions.

Effects of mass ratio ($m_{Al\ powder}/m_{water}$) and temperature on the hydrolysis reaction

Al-7.5% Bi-2.5% In was selected to investigate the effects of mass ratio (mass of Al powder to mass of water) and temperature on hydrolysis kinetics. Besides it being the best performing alloy, it contained a relatively low In content, making it inexpensive to produce. Here, a mass ratio of 1:50 is defined as 1 g of Al powder reacting with 50 mL of pure water. All mass ratios were derived similarly. Fig. 7 shows the effect of varying mass ratios on (a) hydrogen yield and (b) reaction temperature. The mass ratios investigated ranged from 1:20 to 1:200. The maximum hydrogen yield standard deviations did not exceed 3.4%.

Fig. 7a shows a steady decrease in reactivity when the mass ratio was increased from 1:20 to 1:200. The hydrogen yield for the 1:20 mass ratio hydrolysis was 100% and decreased to approximately 87.6% when the mass ratio was increased to 1:200. The decreased hydrogen yield was caused by the decrease in water temperature associated with larger mass ratios. A larger mass ratio will result in a greater volume of water, into which the *in situ* heat generated ($\Delta H = -444.4$ kJ mol^{-1}) during hydrolysis may disperse.

Fig. 7b shows an increase in reaction temperature as a function of increasing mass ratio. *In situ* released heat catalyzed the Al hydrolysis reaction and if the heat is allowed to mitigate away from the immediate reaction sites (i.e., Al particles undergoing hydrolysis) then a milder reaction will take place. The reaction temperature of the 1:20 mass ratio hydrolysis reaction increased by approximately 75 ± 2.3 °C, whereas the temperature of the 1:200 mass ratio reaction increased by 9 ± 0.2 °C. The large increase in reaction temperature did result in an increase in hydrogen yield. However, it may not be considered practical to achieve a 100% yield under such extreme conditions. A large temperature increase will cause several complications if this Al alloy (Al-7.5% Bi-2.5% In) is considered for proton exchange membrane fuel cell (PEMFC) applications.

Ideally, a PEMFC will require a steady flow of hydrogen. Hence, the controlled release of hydrogen (accompanied by lower reaction temperatures) may be considered more valuable than a close to 100% hydrogen yield. For example, hydrolysis of 1 g Al-7.5% Bi-2.5% In alloy at a 1:100 mass ratio resulted in a 89% hydrogen yield, approximately 18 °C increase in reaction temperature, and a maximum hydrogen generation rate of 97 mL min^{-1}. This is indicative that a certain amount of this alloy may be hydrolyzed at a 1:100 mass ratio to provide a PEMFC with a steady hydrogen stream. The PEMFC size will subsequently determine the amount of alloy required to be hydrolyzed. Whereas hydrolysis of the same alloy hydrolyzed at a 1:20 mass ratio resulted in a 100% hydrogen yield, a temperature increase of approximately 75 °C, and a maximum hydrogen generation rate of >1200 mL min^{-1}, which will result in some operational complications during PEMFC applications. Though this method of hydrogen generation for energy applications, such as in hydrogen fuel cells, is still in its early stages and requires further development and improvements, it may already be applied to address needs in several sectors. Some of the advantages of this method to produce hydrogen include, but not limited to, production of hydrogen on-demand and on-site, ability to reach hydrogen pressure that meets requirements of customers. These markets include portable low power devices for consumer electronics for to be used for charging electronic gadgets, UAV (unmanned aerial vehicles) market, military applications, emergency energy market, and even as hydrogen source for underground mining equipment. For example, according to the Russian Skolkovo Foundation (web reference: https://sk.ru/news/m/wiki/14838/download.aspx), the market of all portable charging devices is estimated to be $34bn. Considering the high hydrogen yield of the best performing composite presented in this study (Al-7.5%-2.5% In), up to 11 wt% of hydrogen may be produced compared to the aluminum weight. Thus, approximately 2200 Wh kg^{-1} Al of specific electric energy can be generated via a PEMFC [76].

Effects of water quality on hydrolysis

Al-7.5% Bi-2.5% In was selected to investigate the effects of water quality on hydrolysis kinetics. The water qualities

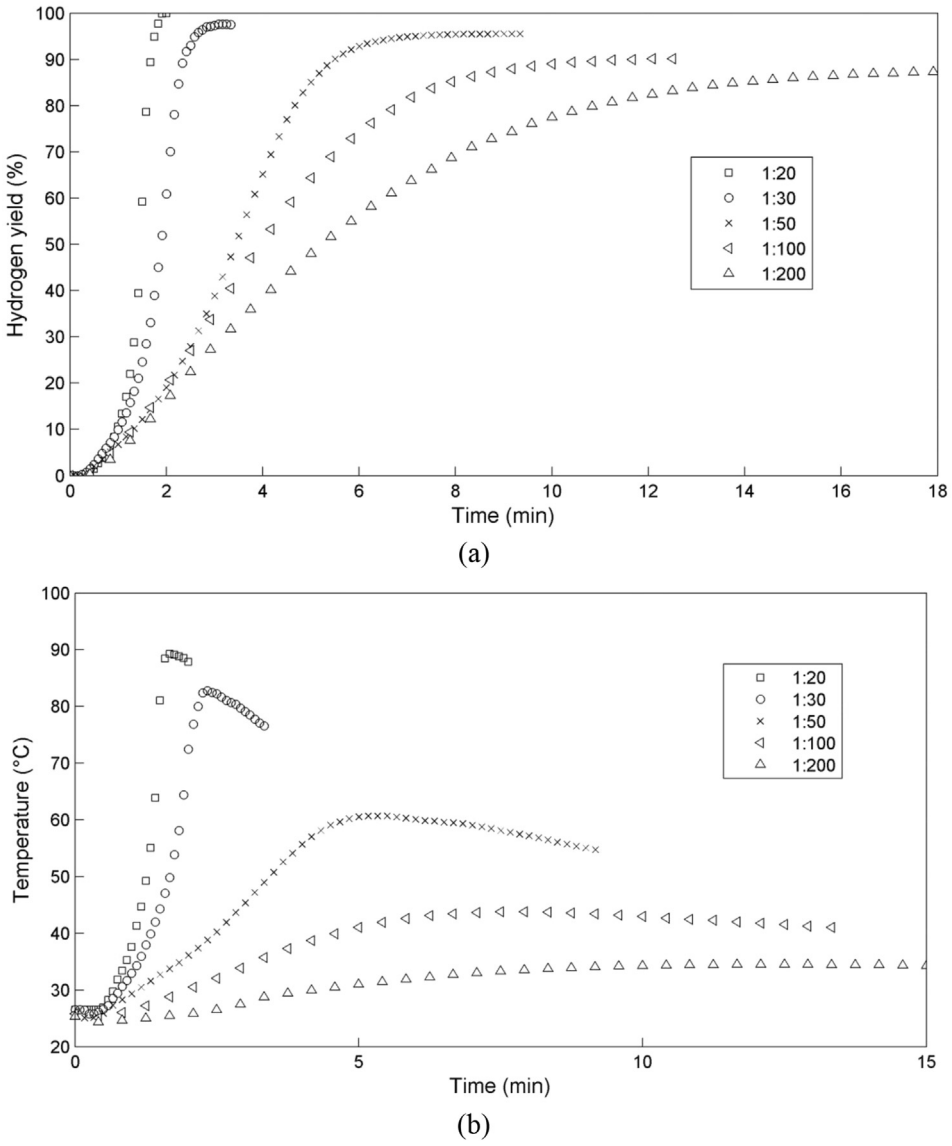

Fig. 7 – Hydrogen yields of Al-7.5% Bi-2.5% In hydrolyzed at various mass ratios of Al powder to mass water (a) and the change in reaction temperature during hydrolysis (b).

investigated were deionized, filtered and tap. Fig. 8 shows the effects that water quality has on hydrogen yields. The maximum hydrogen yield standard deviations were did not exceed 3.2%.

It is evident from Fig. 8 that the water quality used during hydrolysis did not appreciably affect the hydrogen yield of Al-7.5% Bi-2.5% In. All three water qualities (deionized, filtered, and tap) achieved hydrogen yields of approximately 95%. Al-7.5% Bi-2.5% In hydrolysis kinetics did show some differences when hydrolyzed in the various water qualities. Hydrolysis performed in filtered water displayed the fastest hydrolysis kinetics, followed by tap and deionized water. Considering the differences in hydrolysis kinetics, deionized water would be the preferred water quality during PEMFC applications due to its milder reactivity, when compared to that of filtered water, ensuring a steady release of hydrogen gas. Though, tap water may also be considered for PEMFC application as it does not require treatment prior to hydrolysis reactions and possesses a relatively similar reactivity when compared to that of deionized water hydrolysis.

Analysis of hydrolysis residues

The residue of Al-7.5% Bi-2.5% In hydrolyzed at different mass ratios (1:20, 1:50, and 1:200) were characterized using XRD and Rietveld structural refinement. Fig. 9 presents the Rietveld refined patters. The R-factors (R_{exp}, R_p, R_{wp}) and GoF values obtained from Rietveld analysis of Al-7.5% Bi-2.5% In hydrolyzed at different mass ratios are summarized in Table 3. All the investigated residues consisted mainly of two Al hydroxide phases, i.e., bayerite ($Al(OH)_3$) and boehmite (AlOOH), the intermetallic phases (BiIn, $BiIn_2$, and Bi_3In_5), Bi_2O_3, and some non-prominent Al peaks. These Al peaks indicated that a small quantity of Al did not undergo hydrolysis (except for the 1:20 mL hydrolysis residue). The intermetallic phases detected coincide with the phases detected in Fig. 6a, indicating that

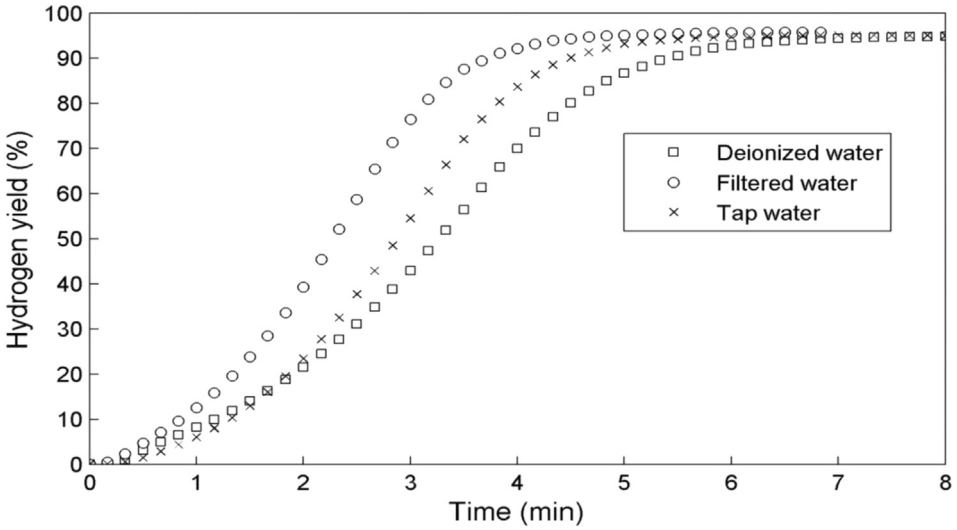

Fig. 8 – Effects of water quality on hydrolysis kinetics. Hydrolysis parameters were kept constant: 25 mL water, room temperature.

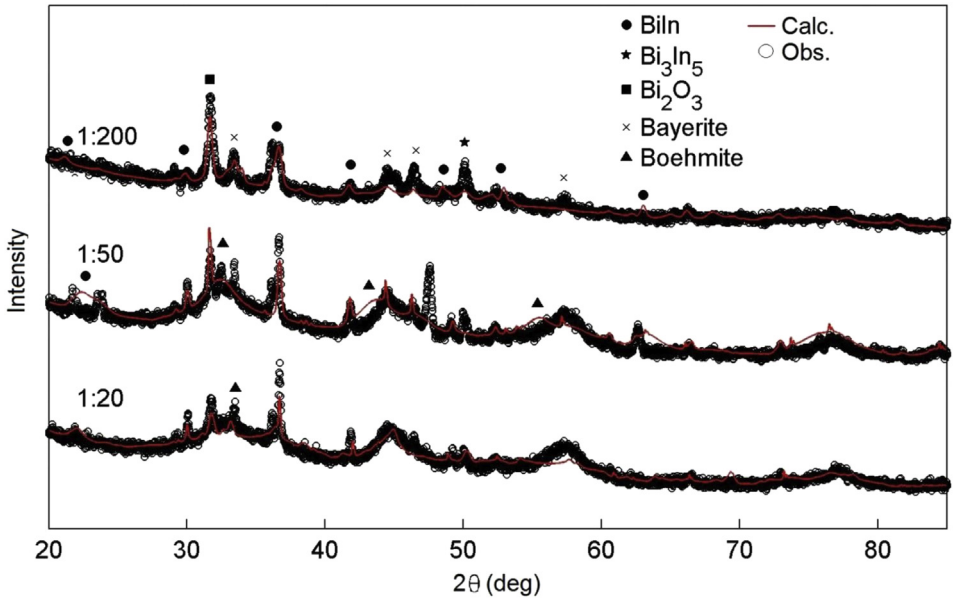

Fig. 9 – The Rietveld refinement of the XRD patterns of Al-7.5% Bi-2.5% In hydrolyzed at various mass ratios.

none of the intermetallic phases were hydrolyzed and that the total generated hydrogen content originated from the hydrolysis of Al. Bi that did not partake in intermetallic phase formation was oxidized to Bi_2O_3.

Table 3 – Parameter values of Rietveld structural refinement analysis of prepared Al-7.5% Bi-2.5% In hydrolyzed at various mass ratios.

Sample	Parameter (%)			
	R_{exp}	R_p	R_{wp}	GoF
1:20	3.24	5.02	6.74	2.08
1:50	3.24	6.62	10.06	3.10
1:200	3.29	4.09	5.70	1.73

Conclusions

Various Al composites were fabricated using Bi and In as activation compounds by a ball milling method. The reactivity of activated Al composites was investigated at room temperature with various water types (deionized, filtered, and tap). It was determined that In embrittled Al particles, and Bi formed Al–Bi micro-galvanic contact point. XRD analysis of milled composites indicated the presence of Al, BiIn, $BiIn_2$, and Bi_3In_5 phases. Phase formation between Bi and In depended on the Bi:In mol ratio. No phase formation between Al and Bi/In was observed. SEM-EDS analysis indicated complete dispersion of Bi and In onto the surface of Al, disrupting the protective layer present on the surface of Al.

Of all the investigated ternary Al composites, only Al-7.5% Bi-2.5% In, Al-5% Bi%-5% In, and Al-2.5% Bi-7.5% In had appreciable hydrogen yields of 93–96%. Other ternary composites had yields of 64–78%. The hydrogen yield of Al-7.5% Bi-2.5% In did not show a large dependence of reaction temperature. Rather, hydrolysis reaction rate was increased by an increase in reaction temperature. Thus, the mass ratio used during hydrolysis reactions should be used as a reaction controlling agent.

Acknowledgments

The Department of Science and Technology (DST) HySA Infrastructure Center of Competence at the North West University, South Africa, is acknowledged for financial support through KP5 program. The NRF Grant No: 85309 is also acknowledged.

REFERENCES

[1] Macanás J, Soler L, Candela AM, Muñoz M, Casado J. Hydrogen generation by aluminum corrosion in aqueous alkaline solutions of inorganic promoters: the AlHidrox process. Energy 2011;36:2493–501.
[2] Lattin W, Utgikar VP. Transition to hydrogen economy in the United States: a 2006 status report. Int J Hydrogen Energy 2007;32:3230–7.
[3] Chai YJ, Dong YM, Meng HX, Jia YY, Shen J, Huang YM, et al. Hydrogen generation by aluminum corrosion in cobalt (II) chloride and nickel (II) chloride aqueous solution. Energy 2014;68:204–9.
[4] Elam CC, Padró CEG, Sandrock G, Luzzi A, Lindblad P, Hagen EF. Realizing the hydrogen future: the International Energy Agency's efforts to advance hydrogen energy technologies. Int J Hydrogen Energy 2003;28:601–7.
[5] Ni M, Leung MK, Sumathy K, Leung DY. Potential of renewable hydrogen production for energy supply in Hong Kong. Int J Hydrogen Energy 2006;31:1401–12.
[6] Wang M, Wang Z, Gong X, Guo Z. The intensification technologies to water electrolysis for hydrogen production – a review. Renew Sustain Energy Rev 2014;29:573–88.
[7] Wang HZ, Leung DYC, Leung MKH, Ni M. A review on hydrogen production using aluminum and aluminum alloys. Renew Sustain Energy Rev 2009;13:845–53.
[8] Balat M. Potential importance of hydrogen as a future solution to environmental and transportation problems. Int J Hydrogen Energy 2008;33:4013–29.
[9] Ball M, Wietschel M. The future of hydrogen–opportunities and challenges. Int J Hydrogen Energy 2009;34:615–27.
[10] Damyanova S, Pawelec B, Arishtirova K, Fierro JLG. Ni-based catalysts for reforming of methane with CO2. Int J Hydrogen Energy 2012;37:15966–75.
[11] Reshetenko TV, Bethune K, Rocheleau R. Spatial proton exchange membrane fuel cell performance under carbon monoxide poisoning at a low concentration using a segmented cell system. J Power Sources 2012;218:412–23.
[12] Gosavi PV, Biniwale RB. Catalytic preferential oxidation of carbon monoxide over platinum supported on lanthanum ferrite–ceria catalysts for cleaning of hydrogen. J Power Sources 2013;222:1–9.
[13] Tzimas E, Filiou C, Peteves SD, Veyret J. Hydrogen storage: state-of-the-art and future perspective. 2003.
[14] Mahmoodi K, Alinejad B. Enhancement of hydrogen generation rate in reaction of aluminum with water. Int J Hydrogen Energy 2010;35:5227–32.
[15] Turner JA. Sustainable hydrogen production. Science 2004;305:972–4.
[16] Esswein AJ, Nocera DG. Hydrogen production by molecular photocatalysis. Chem Rev 2007;107:4022–47.
[17] Ilyukhina AV, Ilyukhin AS, Shkolnikov EI. Hydrogen generation from water by means of activated aluminum. Int J Hydrogen Energy 2012;37:16382–7.
[18] Sakintuna B, Lamari-Darkrim F, Hirscher M. Metal hydride materials for solid hydrogen storage: a review. Int J Hydrogen Energy 2007;32:1121–40.
[19] Elitzur S, Rosenband V, Gany A. On-board hydrogen production for auxiliary power in passenger aircraft. Int J Hydrogen Energy 2017;42:14003–9.
[20] Renouard-Vallet G, Saballus M, Schumann P, Kallo J, Friedrich KA, Müller-Steinhagen H. Fuel cells for civil aircraft application: on-board production of power, water and inert gas. Chem Eng Res Des 2012;90:3–10.
[21] Alinejad B, Mahmoodi K. A novel method for generating hydrogen by hydrolysis of highly activated aluminum nanoparticles in pure water. Int J Hydrogen Energy 2009;34:7934–8.
[22] Ilyukhina AV, Kravchenko OV, Bulychev BM. Studies on microstructure of activated aluminum and its hydrogen generation properties in aluminum/water reaction. J Alloys Compd 2017;690:321–9.
[23] Zou H, Chen S, Zhao Z, Lin W. Hydrogen production by hydrolysis of aluminum. J Alloys Compd 2013;578:380–4.
[24] Teng H, Lee T, Chen Y, Wang H, Cao G. Effect of $Al(OH)_3$ on the hydrogen generation of aluminum-water system. J Power Sources 2012;219:16–21.
[25] Czech E, Troczynski T. Hydrogen generation through massive corrosion of deformed aluminum in water. Int J Hydrogen Energy 2010;35:1029–37.
[26] Liu Y, Wang X, Liu H, Dong Z, Li S, Ge H, et al. Investigation on the improved hydrolysis of aluminum–calcium hydride-salt mixture elaborated by ball milling. Energy 2015;84:714–21.
[27] López-Miranda JL, Rosas G. Hydrogen generation by aluminum hydrolysis using the Fe2Al5 intermetallic compound. Int J Hydrogen Energy 2016;41:4054–9.
[28] Belitskus D. Reaction of aluminium with sodium hydroxide solution as a source of hydrogen. J Electrochem Soc 1970;117:1097–9.
[29] Soler L, Macanás J, Muñoz M, Casado J. Synergistic hydrogen generation from aluminum, aluminum alloys and sodium borohydride in aqueous solutions. Int J Hydrogen Energy 2007;32:4702–10.
[30] Martinez SS, Albañil Sánchez L, Álvarez Gallegos AA, Sebastian P. Coupling a PEM fuel cell and the hydrogen generation from aluminum waste cans. Int J Hydrogen Energy 2007;32:3159–62.
[31] Wang E-D, Shi P-F, Du C-Y, Wang X-R. A mini-type hydrogen generator from aluminum for proton exchange membrane fuel cells. J Power Sources 2008;181:144–8.
[32] El-Meligi A. Hydrogen production by aluminum corrosion in hydrochloric acid and using inhibitors to control hydrogen evolution. Int J Hydrogen Energy 2011;36:10600–7.
[33] Boukerche I, Djerad S, Benmansour L, Tifouti L, Saleh K. Degradability of aluminum in acidic and alkaline solutions. Corros Sci 2014;78:343–52.
[34] Dudoladov AO, Buryakovskaya OA, Vlaskin MS, Zhuk AZ, Shkolnikov EI. Generation of hydrogen by aluminium oxidation in aquaeous solutions at low temperatures. Int J Hydrogen Energy 2016;41:2230–7.

[35] Soler L, Macanás J, Muñoz M, Casado J. Aluminum and aluminum alloys as sources of hydrogen for fuel cell applications. J Power Sources 2007;169:144–9.
[36] Jung CR, Kundu A, Ku B, Gil JH, Lee HR, Jang JH. Hydrogen from aluminium in a flow reactor for fuel cell applications. J Power Sources 2008;175:490–4.
[37] Onwudili JA, Williams PT. Role of sodium hydroxide in the production of hydrogen gas from the hydrothermal gasification of biomass. Int J Hydrogen Energy 2009;34:5645–56.
[38] Vlaskin M, Shkolnikov E, Lisicyn A, Bersh A, Zhuk A. Computational and experimental investigation on thermodynamics of the reactor of aluminum oxidation in saturated wet steam. Int J Hydrogen Energy 2010;35:1888–94.
[39] Ivanov V, Leonov S, Savinov G, Gavrilyuk O, Glazkov O. Combustion of mixtures of ultradisperse aluminum and gel-like water. Combust Explos Shock Waves 1994;30:569–70.
[40] Huang X, Lv C, Huang Y, Liu S, Wang C, Chen D. Effects of amalgam on hydrogen generation by hydrolysis of aluminum with water. Int J Hydrogen Energy 2011;36:15119–24.
[41] Kliškić M, Radošević J, Gudić S, Šmith M. Cathodic polarization of Al–Sn alloy in sodium chloride solution. Electrochimica Acta 1998;43:3241–55.
[42] Fan M-Q, Sun L-X, Xu F. Study of the controllable reactivity of aluminum alloys and their promising application for hydrogen generation. Energy Convers Manag 2010;51:594–9.
[43] Bessone J. The activation of aluminium by mercury ions in non-aggressive media. Corros Sci 2006;48:4243–56.
[44] Senel E, Walmsley JC, Diplas S, Nisancioglu K. Liquid metal embrittlement of aluminium by segregation of trace element gallium. Corros Sci 2014;85:167–73.
[45] Nizovskii AI, Belkova SV, Novikov AA, Trenikhin MV. Hydrogen production for fuel cells in reaction of activated aluminum with water. Procedia Eng 2015;113:8–12.
[46] Baniamerian M, Moradi S. Al–Ga doped nanostructured carbon as a novel material for hydrogen production in water. J Alloys Compd 2011;509:6307–10.
[47] Wang H, Chang Y, Dong S, Lei Z, Zhu Q, Luo P, et al. Investigation on hydrogen production using multicomponent aluminum alloys at mild conditions and its mechanism. Int J Hydrogen Energy 2013;38:1236–43.
[48] Wang F-Q, Wang H-H, Wang J, Lu J, Luo P, Chang Y, et al. Effects of low melting point metals (Ga, In, Sn) on hydrolysis properties of aluminum alloys. Trans Nonferrous Met Soc China 2016;26:152–9.
[49] Ziebarth JT, Woodall JM, Kramer RA, Choi G. Liquid phase-enabled reaction of Al–Ga and Al–Ga–In–Sn alloys with water. Int J Hydrogen Energy 2011;36:5271–9.
[50] Kravchenko OV, Semenenko KN, Bulychev BM, Kalmykov KB. Activation of aluminum metal and its reaction with water. J Alloys Compd 2005;397:58–62.
[51] Jayaraman K, Chauveau C, Gökalp I. Effects of aluminum particle size, galinstan content and reaction temperature on hydrogen generation rate using activated aluminum and water. Energy Power Eng 2015;7:426.
[52] Parmuzina AV, Kravchenko OV. Activation of aluminium metal to evolve hydrogen from water. Int J Hydrogen Energy 2008;33:3073–6.
[53] Huang T, Gao Q, Liu D, Xu S, Guo C, Zou J, et al. Preparation of Al-Ga-In-Sn-Bi quinary alloy and its hydrogen production via water splitting. Int J Hydrogen Energy 2015;40:2354–62.
[54] Streletskii AN, Kolbanev IV, Borunova AB, Butyagin PY. Mechanochemically activated aluminium: preparation, structure, and chemical properties. J Mater Sci 2004;39:5175–9.
[55] Dupiano P, Stamatis D, Dreizin EL. Hydrogen production by reacting water with mechanically milled composite aluminum-metal oxide powders. Int J Hydrogen Energy 2011;36:4781–91.
[56] Wang H-W, Chung H-W, Teng H-T, Cao G. Generation of hydrogen from aluminum and water – effect of metal oxide nanocrystals and water quality. Int J Hydrogen Energy 2011;36:15136–44.
[57] Fan MQ, Xu F, Sun LX. Studies on hydrogen generation characteristics of hydrolysis of the ball milling Al-based materials in pure water. Int J Hydrogen Energy 2007;32:2809–15.
[58] Liu S, Fan M-Q, Wang C, Huang Y-X, Chen D, Bai L-Q, et al. Hydrogen generation by hydrolysis of Al–Li–Bi–NaCl mixture with pure water. Int J Hydrogen Energy 2012;37:1014–20.
[59] Fan MQ, Sun LX, Xu F, Mei D, Chen D, Chai WX, et al. Microstructure of Al–Li alloy and its hydrolysis as portable hydrogen source for proton-exchange membrane fuel cells. Int J Hydrogen Energy 2011;36:9791–8.
[60] Xiao Y, Wu C, Wu H, Chen Y. Hydrogen generation by CaH2-induced hydrolysis of Mg17Al12 hydride. Int J Hydrogen Energy 2011;36:15698–703.
[61] Liu Y, Wang X, Liu H, Dong Z, Li S, Ge H, et al. Improved hydrogen generation from the hydrolysis of aluminum ball milled with hydride. Energy 2014;72:421–6.
[62] Wang C, Yang T, Liu Y, Ruan J, Yang S, Liu X. Hydrogen generation by the hydrolysis of magnesium–aluminum–iron material in aqueous solutions. Int J Hydrogen Energy 2014;39:10843–52.
[63] Fan MQ, Sun Lx, Xu F. Experiment assessment of hydrogen production from activated aluminum alloys in portable generator for fuel cell applications. Energy 2010;35:2922–6.
[64] Fan M-Q, Xu F, Sun L-X. Hydrogen generation by hydrolysis reaction of ball-milled Al-Bi alloys. Energy fuels 2007;21:2294–8.
[65] Razavi-Tousi SS, Szpunar JA. Effect of structural evolution of aluminum powder during ball milling on hydrogen generation in aluminum–water reaction. Int J Hydrogen Energy 2013;38:795–806.
[66] Razavi-Tousi S, Szpunar J. Role of ball milling of aluminum powders in promotion of aluminum-water reaction to generate hydrogen. Metall Mater Trans E 2014:1–10.
[67] Suryanarayana C. Mechanical alloying and milling. Prog Mater Sci 2001;46:1–184.
[68] Benjamin J. Mechanical alloying. Sci Am 1976;234:40–8.
[69] Vargel C. Corrosion of aluminium. Elsevier; 2004.
[70] Caicedo-Martinez C, Koroleva E, Skeldon P, Thompson G, Hoellrigl G, Bailey P, et al. Behavior of impurity and minor alloying elements during surface treatments of aluminum. J Electrochem Soc 2002;149:B139–45.
[71] Fan MQ, Sun LX, Xu F. Hydrogen production for micro-fuel-cell from activated Al–Sn–Zn–X (X: hydride or halide) mixture in water. Renew Energy 2011;36:519–24.
[72] Fan MQ, Xu F, Sun L-X, Zhao J-N, Jiang T, Li W-X. Hydrolysis of ball milling Al–Bi–hydride and Al–Bi–salt mixture for hydrogen generation. J Alloys Compd 2008;460:125–9.
[73] Bessone JB, Flamini DO, Saidman SB. Comprehensive model for the activation mechanism of Al–Zn alloys produced by indium. Corros Sci 2005;47:95–105.
[74] Skrovan J, Alfantazi A, Troczynski T. Enhancing aluminum corrosion in water. J Appl Electrochem 2009;39:1695–702.
[75] Bhattacharya V, Chattopadhyay K. Morphology and phase transformation of nanoscaled indium–tin alloys in aluminium. Mater Sci Eng A 2004;375:932–5.
[76] Elitzur S, Rosenband V, Gany A. Electric energy storage using aluminum and water for hydrogen production on-demand. Int J Appl Sci Technol 2015;5:112–21.

CHAPTER 5: ARTICLE 3

Hydrogen generation by the hydrolysis of mechanochemically activated aluminum-tin-indium composites in pure water

5.1 Author list and contributions

Authors list

S.P. du Preez[a] and D.G. Bessarabov[a,*]

[a] HySA Centre of Competence, North-West University (NWU), Potchefstroom Campus, Private Bag X6001, Potchefstroom, 2520, South Africa

Contributions

Contributions of the various co-authors were as follows:

Experimental work, data processing and interpretation, research, and writing of the scientific paper, was performed mainly by the candidate, SP du Preez. DG Bessarabov (supervisor) made conceptual contributions and assisted with article preparation.

5.2 Formatting and current status of the article

The article presented in Chapter 5 was published in *International Journal of Hydrogen Energy* in 2018. Vol. 43, pages 21398-21413 (DOI: https://doi.org/10.1016/j.ijhydene.2018.09.133). The journal details can be found at https://www.journals.elsevier.com/international-journal-of-hydrogen-energy/ (Date of access: 11 October 2018).

Available online at www.sciencedirect.com

ScienceDirect

journal homepage: www.elsevier.com/locate/he

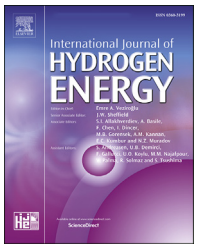

Hydrogen generation by the hydrolysis of mechanochemically activated aluminum-tin-indium composites in pure water

S.P. du Preez, D.G. Bessarabov *

HySA Centre of Competence, North-West University (NWU), Potchefstroom Campus, Private Bag X6001, Potchefstroom, 2520, South Africa

ARTICLE INFO

Article history:
Received 24 July 2018
Received in revised form
31 August 2018
Accepted 18 September 2018
Available online 10 October 2018

Keywords:
Mechanochemical activation
Activated aluminum
Hydrogen generation
Tin
Indium

ABSTRACT

This paper presents results of our continuing project on the mechanochemical activation of Al-based composites for hydrogen generation [1,2]. A series of bi- and ternary Al, Sn, and/or In composites were mechanochemically prepared and their reactivities towards neutral pH water at ambient conditions determined. Hydrogen generation was compared to previously reported data from related studies in Refs. [1] and [2]. Scanning electron microscopy (SEM) energy dispersive x-ray spectrometer (EDS) analysis suggests that Sn and In could be distributed relatively homogeneously onto and into Al particles exteriors and interiors, respectively. Such distribution allowed continuous micro-galvanic activity between anodic Al and cathodic Sn and In during hydrolysis reactions. X-ray diffraction indicated that *in-situ* Sn–In intermetallic phase formation was determined by the Sn:In mol ratio of each composite. The formed Sn–In phases included Sn_4In and $SnIn_3$. Some AlSn phases were detected in ternary composites. Reactive composites (>95% yield) exhibited relatively similar reactivities and it was found that composites containing various intermetallic phases had shorter induction periods than composites containing a single intermetallic phase.

Introduction

The adverse environmental impact of current world-wide fossil fuels combustion calls for the development and employment of alternative and efficient carbon-free energy systems [3]. Fuel cells (FCs) can serve as an alternative form of clean energy generation [4,5]. Several FC types exist, e.g. proton-exchange membrane (PEM), alkaline, phosphoric, molten carbonate, and solid oxide [6]. PEMFCs are considered advantageous over other FC types for mobile power applications (such as vehicles), stationary power units, and portable electrical devices [6–9]. PEMFCs convert the chemical energy associated with hydrogen gas into electrical energy, without combustion [10,11]. Hydrogen is an ideal near-zero emissions energy carrier and holds various attractive properties, e.g. abundant, environmentally friendly, and high calorific value [12]. Hydrogen generation processes include steam reformation, partial oxidation, water electrolysis, gasification of woody biomass conversion, biological processes, photo dissociation, and direct thermal or catalytically water splitting [13]. Currently, hydrogen is mainly produced

* *Corresponding author.*
E-mail address: dmitri.bessarabov@nwu.ac.za (D.G. Bessarabov).
https://doi.org/10.1016/j.ijhydene.2018.09.133

from hydrocarbons. Balat et al. (2008) stated that approximately 96% of hydrogen is produced from hydrocarbons (e.g. natural gas, oil, coal), and 4% from electrolysis [14]. However, hydrogen produced from hydrocarbons yields carbon dioxide and minute quantities of carbon monoxide as by-products [15,16]. Carbon monoxide can deteriorate PEMFCs [17,18], and poison platinum fuel cell catalysts [6]. Thus, it is necessary to decrease the carbon monoxide content to <50 ppm prior to fuel cell applications [4–6].

If the use of hydrogen as a future non-polluting energy carrier were to be realized, it has to be produced with relative ease from renewable sources using clean processes that limits or excludes carbon mon- and dioxide formation [19]. Water is an abundant source of hydrogen. The hydrogen content of water (111 kg m^{-3}) exceeds that of gasoline (84 kg m^{-3}) and liquid hydrogen (71 kg m^{-3}), making it a potential hydrogen source [20,21]. Several water-based hydrogen production methods exist, e.g. metal and metal hydride hydrolysis [22,23], water photo-catalysis [24,25], and water electrolysis [26,27]. Hydrogen has a very low gaseous density of 0.089 kg m^{-3} [28], complicating its storage. In fact, the major challenge in using hydrogen as an energy carrier is its storage. It is unlikely that any energy carrier can be handled and produced as easily as gasoline and diesel, which is especially true for gaseous energy carriers [15]. Currently, hydrogen is primarily stored as a pressurized gas, in its liquid state, or as a metal hydride [28]. Of these methods, pressurized gas is the most commonly applied storage method due to its simplicity and inexpensiveness [29]. To alleviate some of the technical complications associated with transport, handling and storing hydrogen gas, a route has to be developed in which hydrogen is generated on-demand and consumed on-site.

Hydrogen generation by reacting certain metals with water has received significant attention in recent years. Among the various metals studied, such as Al [22,30–33], Mg [34–39], Zn [40,41], to generate hydrogen from water, Al has been found to be the most promising candidate [42]. Al is the most abundant crustal metal on earth with a density and an energetic capacity of approximately 2700 kg m^{-3} and 2980 Ah kg^{-3}, respectively [43,44]. Al has a standard electrode potential of −1.66 V vs normal hydrogen electrode [45], potentially making Al an attractive anode metal in Al batteries [44]. Furthermore, Al possesses high hydrogen generation potential and is safer to store if compared to metal hydrides and other hydrogen generating materials [46]. Al hydrolysis primarily yields Al-hydroxides and hydrogen gas, according to the following reactions [1,2,46–51]:

$$2Al + 6H_2O \rightarrow 2Al(OH)_3 + 3H_2 \quad (1)$$

$$2Al + 4H_2O \rightarrow 2AlOOH + 3H_2 \quad (2)$$

The Al by-products of Reactions (1) to (2) are non-toxic and useable in various industrial applications [43], and can be can be fully re-metallized to Al^0 through the Hall-Héroult process [31,43]. Al hydrolysis is thermodynamically favorable [52]; however, a protective oxide layer (Al_2O_3) on Al's surface prevents hydrolysis from occurring spontaneously with neutral pH waters under ambient conditions. The corrosion potential of an Al electrode is shifted in the positive direction by approximately 1.0 V due to the presence of this oxide layer, significantly slowing Al's active dissolution [44].

In recent years, numerous methods have been investigated in an effort to produce hydrogen from water using Al as the hydrolyzing material, e.g. immersing Al in acidic or alkaline solutions [53–67], and hydrothermal processes to react Al with neutral pH waters at elevated temperatures and pressures [68–74]. However, such harsh experimental conditions limit their applications. Al amalgamation with mercury (Hg) and Hg-based composites is another approach to enable Al hydrolysis [75–77]. However, in its elemental and methylated form, Hg is toxic to humans and animals [78], which prevents the application of this method. Gallium (Ga) and Ga-based composites have a relatively similar effect as Hg on Al particles [22,42,79,80]. Numerous studies using Ga and combinations thereof with In, Sn, Zn, Bi, and/or Mg to thermally or mechanochemically activated Al have been performed [42,47,79–92]. However, Ga is expensive and the use thereof to activate Al greatly increases the cost of such composites. Furthermore, mechanochemical activation is less energy intensive and a simpler process if compared to thermal activation. If Al is to be considered as a hydrolyzing material to generate hydrogen, its activation has to be economically feasible, i.e. activated by inexpensive compounds using a mechanochemical route. Numerous studies have been performed to mechanochemically activate Al-based composites using compounds such as metal oxides, graphite, water-soluble salts, metal hydrides [93–103], and metals such as Li, Fe, Ca, and Mg [52,104–106].

Relatively few studies have been conducted on the mechanochemical activation of Al using metals (more specifically, low melting point metals) that excludes Ga. Xiao et al. (2018) mechanochemically prepared Al–Bi–Sn composites, achieving 84–86% hydrogen yields [107]. Du Preez and Bessarabov (2017a and b) produced several high hydrogen yielding (>90%) mechanochemical activated Al–In–Bi–Sn and Al–Bi–In composites [1,2]. However, relatively limited information is available in the public peer-reviewed domain on the mechanochemical activation of Al using only Sn and In. Several studies indicated the potential of using Sn and In to activate Al by a mechanochemical route [80,86]; however, reactive composites presented in these studies included between 1 and 3 wt% Ga. In this study, a series of Al–Sn/In composites where mechanochemically prepared to be hydrolyzed in neutral pH waters under ambient reaction conditions. The effects of these activation compounds on Al morphological changes and reactivity towards pure water were determined. Furthermore, the formation of intermetallic phases of binary Al–Sn/In, and ternary Al–Sn–In composites were determined.

Materials and methods

Materials

The following starting materials were supplied by Sigma-Aldrich (South Africa): Al powder (<200 μm, 99% purity), Sn powder (<150 μm, 99.99% purity), and In shots (between 5 and 2 mm, >99.9% purity). Pure deionized water (resistivity,

18.2 MΩ cm^{-1}), produced by a Milli-Q water purification system, was used for all hydrolysis reactions. Pure nitrogen gas (99.99%) (Afrox, South Africa) was used during all purging procedures.

Aluminum composite compositions and their mechanochemical activation

Binary Al–Sn and Al–In composites, and several ternary Al–Sn–In composites were prepared. The binary composite consisted of 10 wt% Sn/In with Al the balance. Ternary composites contained various amounts of Sn and In in the range of 0.5–9.5 wt% with Al the balance, and were divided into two groups, i.e. composites activated by 10 and 5 wt% activation compounds (henceforth referred to as 10 and 5% ternary composites). These ternary composites are indicated in Table 1. The total activation compound addition did not exceed 10 wt%, in an effort to maximize the Al content.

All ball milling procedures were performed in a high-energy Retsch Emax ball mill (Retsch, Germany). The as-received Al, Sn, and/or In were weight proportioned according to Table 1 and placed in a 125 mL stainless steel milling jar. Thereafter, 5 mm stainless steel milling balls were added to the milling jar at a ball to composite ratio of 30:1, i.e. 30 g milling balls per 1 g composite. The milling jars, with the as-received metals and milling balls loaded, where sealed using an airtight aeration lid and purged with a steady flow of N_2 for 2 min prior to commencing the milling procedure. For all composites, the as-received metals were milled at 1500 rpm for 30 min. After each milling procedure, the milling jar was allowed to cool down to room temperature before the composites were collected and stored in an air-tight container until further use. The composites reported in this study were obtained as visually very fine powders after milling procedures, void of any agglomerates and large particles, suggesting relatively homogeneous distribution of composite constituents. Prepared composites were experiment on as soon as possible to avoid any unwanted oxidation. Each composite was prepared in triplicate.

Hydrolysis reaction setup and hydrogen measurements

Hydrolysis reactions were performed at standard ambient temperature and pressure (i.e. 25 °C, 1 bar) in a 100 mL flask with three openings, one for water addition using a pressure equalizing addition funnel, one for a thermocouple for continuous temperature measurements, and one for the generated hydrogen to escape. The hydrogen then passed through a Drietite™ ($CaSO_4$) gas drier to remove water vapor prior to hydrogen measurements. Thereafter, the dried hydrogen was measured using a digital thermal gas mass flow meter to measure gas mass flow (Model GH-32654-12; Cole-Parmer, South Africa). Hydrogen measurements were performed by hydrolyzing 0.5 g composite using 25 mL deionized water, unless specified otherwise. The reaction solutions were left unagitated during hydrolysis reactions. Each composite was hydrolyzed in duplicate to determine the standard deviation. Thus, standard deviations were based on at least six hydrogen measurements, i.e. each composite prepared in triplicate and hydrolyzed in duplicate.

Table 1 – Composition of ternary Al composites.

Composites	Sn	In
Activation compounds (10 wt% total)		
Al-9.5% Sn-0.5% In	9.5	0.5
Al-8% Sn-2% In	8	2
Al-6.5% Sn-3.5% In	6.5	3.5
Al-5% Sn-5% In	5	5
Al-3.5% Sn-6.5% In	3.5	6.5
Al-2% Sn-8% In	2	8
Al-0.5% Sn-9.5% In	0.5	9.5
Activation compounds (5 wt% total)		
Al-4% Sn-1% In	4	1
Al-3.25% Sn-1.75% In	3.25	1.75
Al-2.5% Sn-2.5% In	2.5	2.5
Al-1.75% Sn-3.25% In	1.75	3.25

Expression for hydrogen generation

The hydrogen generated is expressed as a conversion yield %, which is defined as the total volume hydrogen produced over the theoretical hydrogen value that can be generated assuming the entire Al content is hydrolyzed. By applying the ideal gas law, approximately 1360 NmL hydrogen is theoretically achievable per gram Al (assuming complete Al hydrolysis) at standard ambient pressure and temperature. Thus, the hydrogen yield % reflects the volume hydrogen generated as a fraction of the obtainable 1360 NmL.

Sample characterization methods

X-ray diffraction (XRD) measurements were performed using a Röntgen diffraction system (PW3040/60 X'Pert Pro). Crystalline phases present in the Al composite were determined using a back-loading preparation method. Composites were scanned by X-rays generated by a copper (Cu) Kα X-ray tube and measurements were performed between variable divergence- and fixed-receiving slits. Detected phases were identified using X'Pert HighScore Plus software (PANalytical). The Rietveld method (Autoquan programme) was applied to refine the relative abundances of phases present in analyzed composites [108].

The morphological and chemical characterization of as-received Al and ball-milled Al composites were determined using scanning electron microscopy (SEM) equipped with an energy dispersive X-ray spectrometer (EDS). A FEI Quanta 250 FEG SEM incorporated with an Oxford X-map EDS system operation at 15 kV and a working distance of 10 mm was used. As-received Al and ball-milled composites were mounted on an Al stub using carbon-based adhesive tape. Thereafter, the samples were coated with an ultra-thin (approximately 3 nm) layer of gold-palladium. To evaluate the sub-surface chemical characteristics of ball-milled composites, a small amount of a composite was embedded in a carbon-based resin. Thereafter, the embedded particles were cross-sectioned by a series of grinding plates, and polished using cloth polishing sheets and ethanol as lubricant. Once a mirror-like surface was obtained, the samples were stored in an air-tight container until characterization.

Results and discussion

Effects of Sn and In additions on binary Al composite particles

The effects of Sn and In on Al particles during ball milling procedures were considered in this paper. Du Preez and Bessarabov (2017a and b) reported the effect of In on Al particles during ball milling procedures [1,2]. Is was determined that In can be distributed onto the surface of Al particles during ball milling procedures, and that In accelerated the strain-hardening process of Al particles, which promoted particle size reduction. Therefore, morphological investigations of Al-10% In composites were not repeated here. In this paper, Al particle morphological changes induced by Sn during ball milling were determined. Fig. 1 presents SEM micrographs depicting the morphology of as-received Al particles (a), and Al-10% Sn composite particles (b).

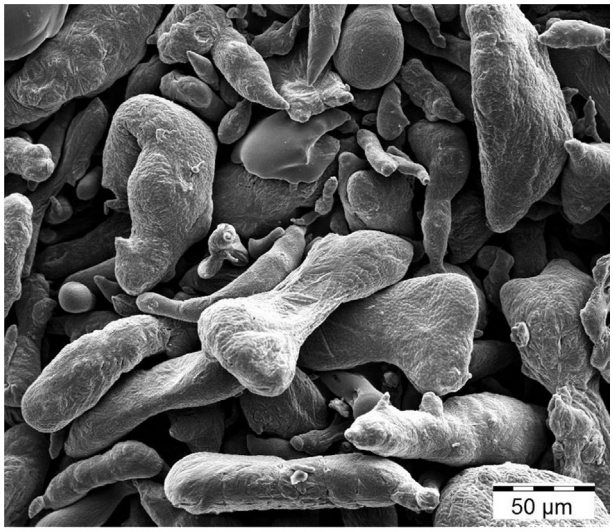

Fig. 1 – Backscatter SEM micrographs of as-received Al (a), and Al-10% Sn composite ball milled for 3 h at 1500 rpm (b).

It is evident that the binary Al-10% Sn composite particles (Fig. 1b) underwent appreciable particle size reduction if compared to the as-received Al particles (Fig. 1a). The as-received Al particles had a strand-like morphology and a particle size of approximately 100–300 μm. The Al-10% Sn composite particles consisted of small fractured particles with particle sizes of <80 μm and a significant fraction of particles <40 μm. The absence of unisize particles may be ascribed to a steady-state between particle cold-welding and particle fracturing. Large and ductile as-received particles tend to deform and/or under-go cold-welding, whereas smaller particle resist deformation and are more susceptible to fracturing due to strain-hardening. Fig. 1b suggests that the majority of particles have been strain-hardened to the point where the cold-welding/deformation mechanism has been substituted by the fracturing mechanism. Considering the morphology of the particle encircled in Fig. 1b, it is evident that fractured particles tend to agglomerate without undergoing cold-welding, driving the average particle size towards an intermediate size [109,110]. Cold-welding produces particles with a relatively smooth surface, whereas the encircled particle's surface contains many morphological deformities and irregularities. Such agglomerated particles allow water to freely penetrate particles, increasing the water:surface ratio.

It is evident from Fig. 1 that the particle size of as-received Al could be reduced by Sn during ball milling procedures. With regard to Al activation, size reduction alone does not guarantee that Al particles will undergo hydrolysis with neutral pH water under ambient conditions. To effectively disrupt Al's protective oxide layer, the activation compounds have to be distributed equally over the entire surface of Al particles. Fig. 2 shows the distribution of Sn on Al particle surfaces as determined by EDS-mapping. Al and Sn are presented in red and green, respectively. As stated earlier, In can be distributed onto the surface of Al particles [2]. Thus, EDS-mapping of Al-10% In was not repeated here.

It is evident from Fig. 2 that Sn was equally distributed onto the surface of Al particles. To determine the surface chemical composition of Al-10% Sn, SEM-EDS analysis was performed by scanning three wide rectangular areas of the sample in a raster-like pattern for 60 s. An average chemical composition of 91.17 wt% Al and 8.93 wt% Sn was revealed, which coincides well with the predetermined Al and Sn wt.% values. The treatment of Al with certain metals promotes the anodic dissolution of Al in ionic solutions [111,112]. Sn dispersion onto the surface of Al particles potentially increases the localized micro-galvanic activity of such composites, offering electron transfer from cathodic Sn (−0.136 V) to anodic Al (−1.663 V) during hydrolysis reactions. Furthermore, Sn has been proven the increase the thermodynamic activity of Al [113], and to enable Al to react with water under certain ambient conditions [96]. Additionally, Al–Sn has a more negative open circuit potential (OCP) than pure Al [111,114]. Kliškić et al. (1998) determined that the addition of 0.4 wt% Sn shifted the OCP by −0.35 V relative to pure Al. The Al-0.4 wt% Sn composite's lower OCP value may be ascribed to the more active anodic component of the corrosion process [111]. Polarization curves presented by Gudić et al. (2010) indicated that pure Al dissolution initiates at −0.74 V, whereas Al present in Al–In and Al–Sn composites initiates at

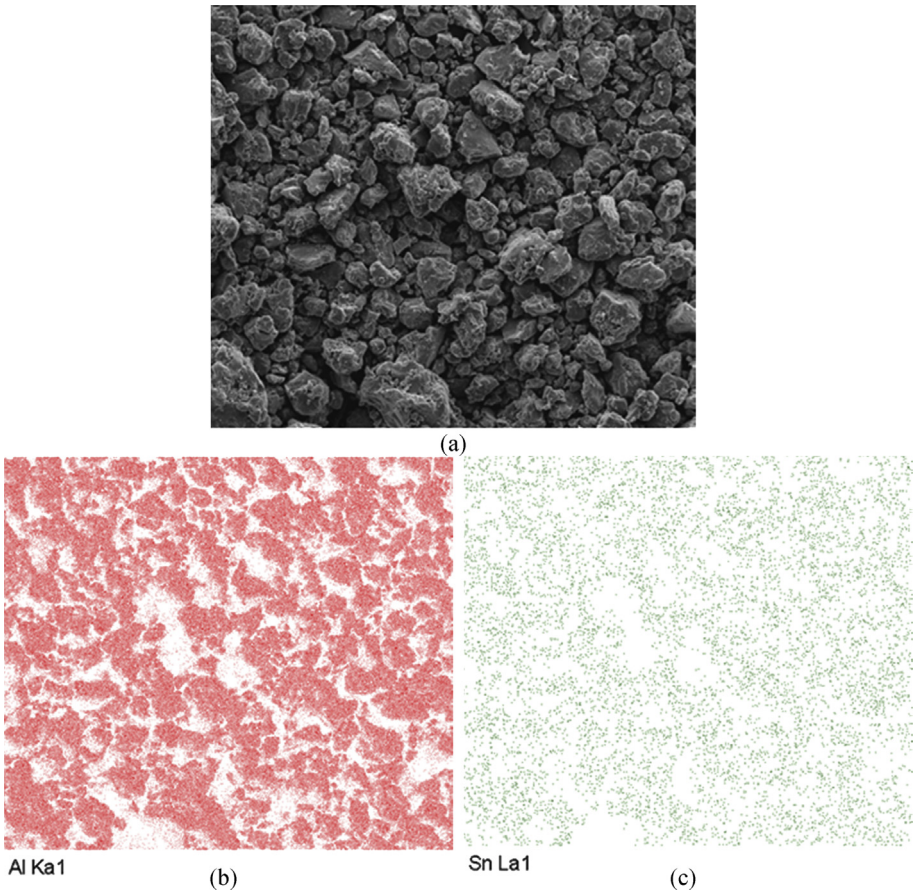

Fig. 2 – A backscatter SEM micrograph of a ball milled Al-10% Sn composite at 1200 times magnification (a) and the corresponding EDS mappings for Al (b) and Sn (c).

approximately −1.15 and −1.43 V, respectively [44]. The standard electrode potential of In is −0.34 V, meaning that micro-galvanic activity exist between Al and In. In addition to this, Eom et al. (2011) found that Sn addition to a Al–Fe alloy improved the breakdown of Al's protective oxide layer in a weak alkaline solution [115].

It is important to note that the solubilities of Sn and In in Al are considered negligible [44]. The solubility of Sn in Al at 232.2 °C is <0.01%, whereas the solubility of In in Al is 0.017% at 156 °C. The solubility of alloying elements can be improved by increasing the temperature, e.g. Sn in Al solubility increases to 0.1% at 600 °C [44,116]. Consequently, the low solubility of Sn and In suggests that a large majority of Sn and In is segregated on the surface of Al particles, and only minor quantities thereof are present within the Al particle interiors [44,116–118]. However, the latter-mentioned Sn and In solubilities refers to thermal alloying. Repetitive plastic deformation (e.g. ball milling) of metals is known to induce changes in residual stress, particle microstructure, and (of importance in this case) constituent redistribution [51]. Considering the ductile nature of the investigated elements (Al, Sn and In), it is expected that ball milled composite particle will consist of a relatively homogeneous solid-state distribution of composite constituents. Fig. 3 suggests a simplified schematic of how Al, Sn and In particles interact during ball-milling procedures, as well as SEM micrographs of Al-5% Sn-5% In particles recovered during different milling, i.e. particles presented in Fig. 3c and f were recovered after 10 and 30 min of ball milling, respectively.

Fig. 3a illustrates random starting positions of Al, Sn, and In particles. As ball milling initiates, Al, Sn, and In will cold-weld to one-another as they are caught between ball-ball and ball-jar interior collisions, forming larger coagulated particles consisting of a random, unequal distribution of initial constituents as shown in Fig. 3b and c. Fig. 3d and e illustrates how larger coagulated particles are further divided into smaller particles as a result of being forced apart by ball-ball and ball-jar interior collisions. These particles are further subjected to the cold-welding/dividing mechanism as ball milling continues, which further homogenizing the constituents. After a certain period of reparative plastic deformation, ductile particles start to harden (due to strain hardening) and fracture into smaller particles (as indicated in Fig. 3f) [1,2,119,120]. Thus, it is likely that the surface of ball milled particles will be representative of the particle interiors due to the afore-

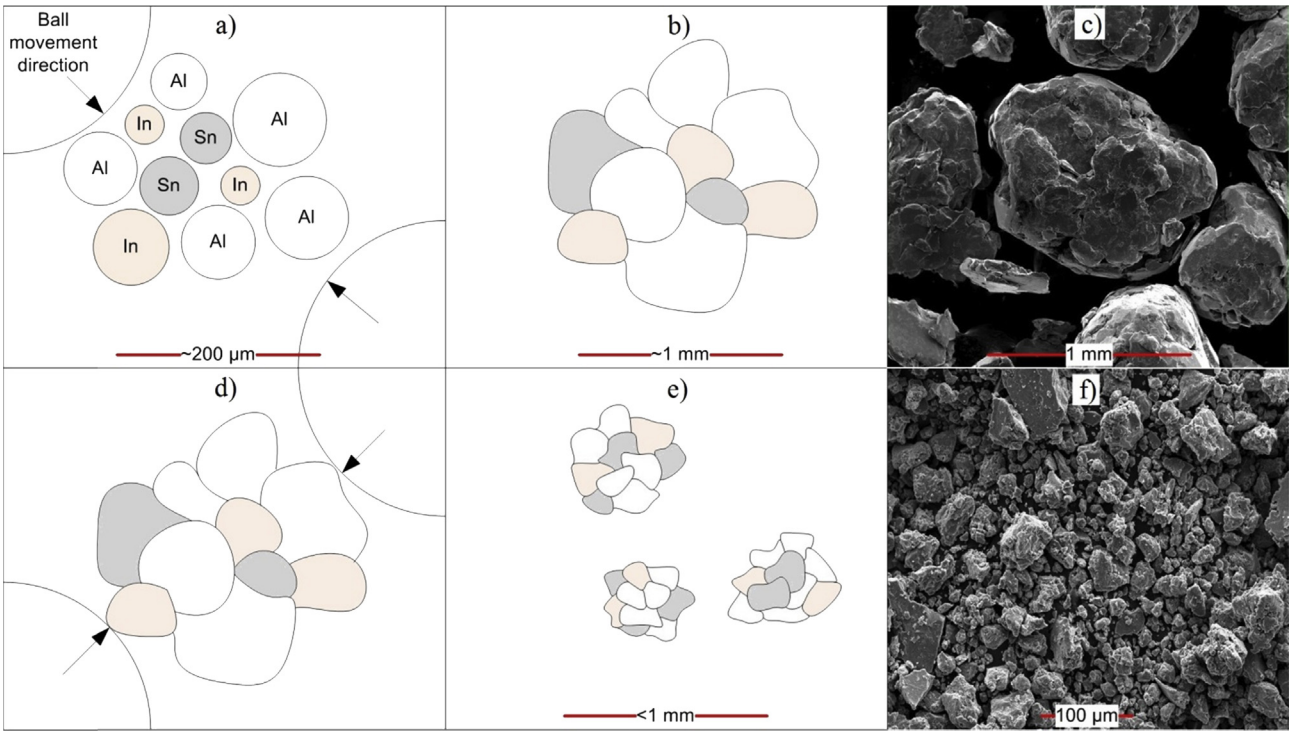

Fig. 3 – Simplified graphic illustration and SEM micrographs of Al, Sn, and In particles behaviors during ball milling procedures. Fig. 3c and f were prepared at 80 and 1200 times magnification, respectively. Fig. 3c and f presents Al-5% Sn-5% In composite particles after 10 and 30 min of milling, respectively.

mentioned constituent homogenization. To evaluate this, particles originating from the Al-5% Sn-5% In composite were cross-sectioned and investigated by SEM-EDS, as presented in Fig. 4.

It is evident from Fig. 4 that Sn and In could be distributed throughout the Al-5% Sn-5% Sn composite particles. SEM-EDS analyses were performed on at least two areas within eighteen cross-sectioned composite particle interiors similar to the particle presented in Fig. 4a, revealing an average chemical composition of 4.81 ± 0.11% Sn and 4.37 ± 0.19% In, coinciding well with the pre-determined 5% Sn and In contents. Thus, the presence of significant Sn and In fractions within Al particles is confirmed. Sn and In detected outside the Al particle interior (i.e. area labeled "Resin" in Fig. 4a) may be ascribed to the polishing process, resulting in some Sn and In particles being displaced from Al particles.

Considering the above discussed dispersion of Sn and In in Al particles, binary Al–Sn/In composites were investigated by XRD to determine if intermetallic phases between Al and Sn/In formed during ball milling procedures. Fig. 5 presents the Rietveld refined XRD patterns of binary Al-10% Sn and Al-10% In composites. Al peaks at 2θ position 44, 53 and 95 were partially excluded from Fig. 5 in an effort to increase the detail of surrounding peaks. The corresponding R-factors (R_{exp}, R_p, R_{wp}) and goodness-of-fit (GoF) values are summarized in Table 2. It may be concluded from Fig. 5 that Al did not form intermetallic phases with Sn or In when ball milled individually.

Activity of binary Al–Sn and Al–In composites

Reboul et al. (1984) proposed a mechanism explaining Al's activation by alloying elements, such as Sn and In Ref. [121]. Initially, anode dissolution caused by galvanic coupling oxidizes Al and the allowing element, according to Reaction (3):

$$Al(M) \rightarrow Al^{3+} + M^{n+},\ M = \text{alloying element} \quad (3)$$

M^{n+} cations produced by Reaction (3) re-deposits onto Al's surface due to the cathodic nature of alloying elements relative to Al, according to the electrochemical exchange reaction:

$$Al + M^{n+} \rightarrow Al^{3+} + M \quad (4)$$

During Reaction (4), simultaneous local separation of the Al oxide layer occurs, which shift the anodic potential closer to that of Al metal. Several studies have been performed on the electrochemical corrosion of Al by Sn/In. Equey et al. (1992) reported that the anodic current-potential curves of Al shifted by between 0.5 and 0.6 V towards more negative potentials when $InCl_3$ was introduced to a 2 M NaCl solution [122]. Breslin and Carroll (1993) stated that the breakdown potential of Al–In became more active in certain electrolytic solutions due to the effects of localized galvanic cells formation between Al–In solid solution [123]. Saidman et al. (1995) stated that Al activation by In is only possible when In comes into true metallic contact with Al within an active pit in the presence of

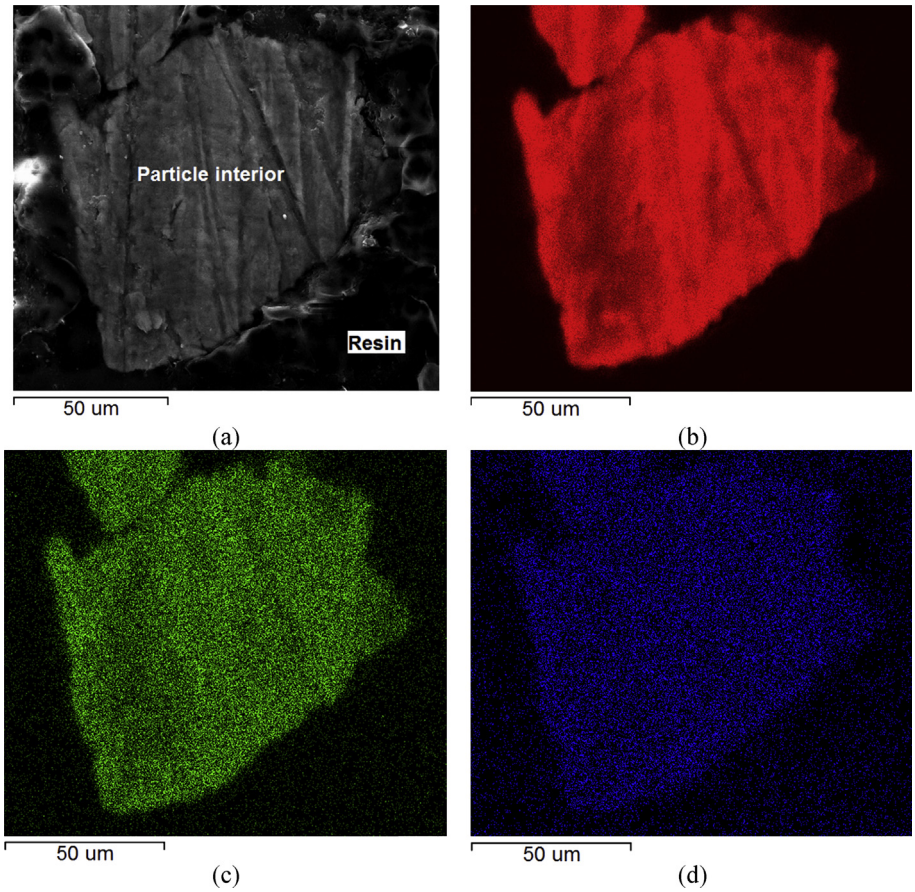

Fig. 4 – Backscatter SEM micrograph of a cross-sectioned Al-5% Sn-5% In particle (a) and the corresponding EDS mapping for Al (b), Sn (c) and In (d).

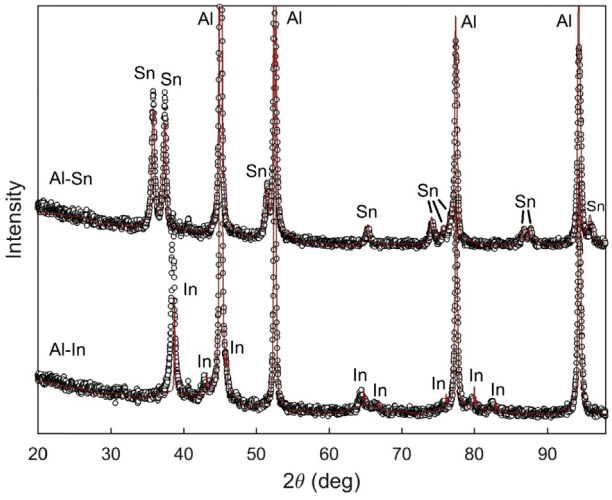

Fig. 5 – The Rietveld refinement of the XRD patterns of binary Al-10% In and Al-10% Sn composites. Observed and calculated values were indicated with black circles and a solid red line, respectively. (For interpretation of the references to color in this figure legend, the reader is referred to the Web version of this article.)

chloride ions [124]. Kliškić et al. (1998) stated that a low Sn content did not appreciably affect the open circuit potential of high purity Al in a 2 M NaCl solution and by increasing the Sn content, the anodic component activity increased substantially [111].

However, in this study mechanochemically activated binary Al-10% Sn and Al-10% In composites displayed very limited to no reactivity under the investigated conditions. Similarly, Wang et al. (2013) reported no hydrogen generation for mechanochemically activated Al-x wt.% Sn/In (x = 3, 5, 7, 10 wt%) composites exposed to tap water at room temperature [80]. Du Preez and Bessarabov (2017b) reported that Al-x wt.% In (x = 10, 20, 30 wt%) were non-reactive in deionized water at room temperature [2]. Fan et al. (2010) found that Al present in mechanochemically activated Al–In composites can be

Table 2 – Parameter values of Rietveld structural refinement analysis of binary Al composites.

Sample	Parameter (%)			
	R_{exp}	R_p	R_{wp}	GoF
Al–In	4.93	8.72	13.73	2.79
Al–Sn	5.01	7.46	10.03	2.00

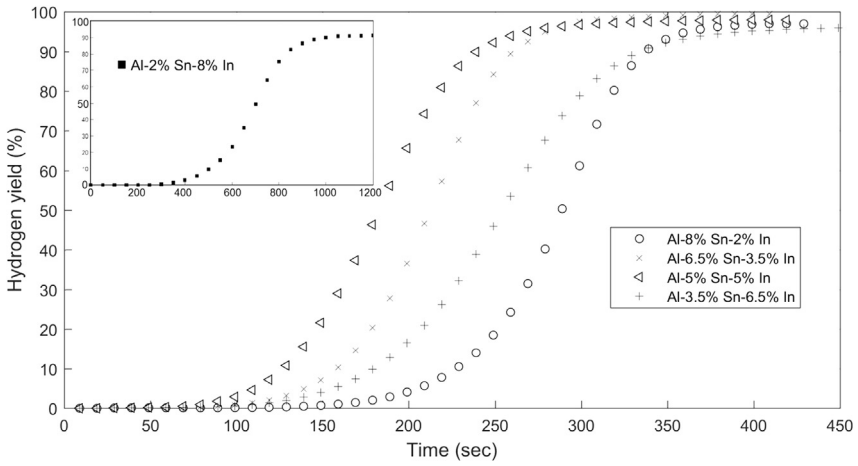

Fig. 6 – Hydrogen yields of 10% ternary Al–Sn–In composites hydrolyzed in pure water at ambient temperature and pressure.

hydrolyzed at elevated temperatures if free ion-transfers are possible [76]. Zhang et al. (2016) observed a near-theoretical hydrogen yield of a mechanochemically activated Al-80% Sn composite hydrolyzed in deionized water at 60 °C [125]. Thus, Al's mechanochemical activation by Sn and In is only achievable if: (i) a sufficient Sn/In content is present, (ii) Al–Sn/In is exposed to an ionic solution, and/or (iii) the reaction is performed at elevated temperatures. Only if such reaction conditions are present can the galvanic activity between Al and Sn/In be utilized to increase Al's anodic dissolution. However, such reaction conditions were not considered in this study. In summary, the prepared binary Al–Sn and Al–In composites were considered non-reactive under the conditions considered in this study.

Hydrolysis of ternary Al–Sn–In composites

Section Activity of binary Al–Sn and Al–In composites indicated that the Al contents of Al–Sn and Al–In composites could not be successfully hydrolyzed. Consequently, 10% ternary (Al–Sn–In) composites were prepared (as indicated in Table 1) in an effort to enable Al hydrolysis under ambient conditions. Fig. 6 presents these results. Standard deviations were excluded from Fig. 6 to prevent congestion of presented results. The maximum hydrogen yield standard deviation did not exceed 4.7%.

Fig. 6 presents the hydrogen yields of 10% ternary composites. The presented composites had hydrogen yields of between 96.5 and 99.5%, induction periods (time before reaction initiated) of 70–150 s, and total reaction times of 336–420 s. Al-2% Sn-8% In (included as an insert in Fig. 6) had a hydrogen yield of 90.5%, an induction period of 280 s, and a total reaction time of 1050 s. Al-9.5% Sn-0.5% In had a hydrogen yield of 25% after approximately 36 min. Al-0.5% Sn-9.5% In did not indicate any reactivity after 30 min of coming into contact with deionized water. Consequently, the two latter mention composites were excluded from Fig. 6. The reactivities of Al-9.5% Sn-0.5% In and Al-0.5% Sn-9.5% In

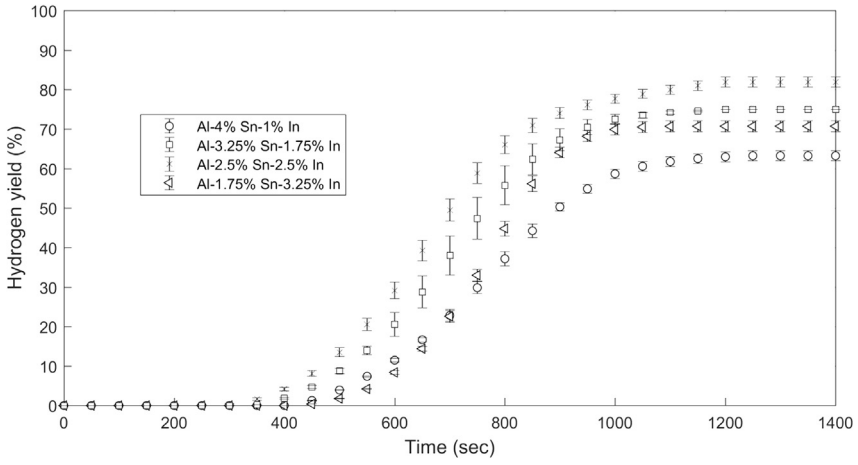

Fig. 7 – Hydrogen yields of 5% ternary Al–Sn–In composites hydrolyzed in pure water at ambient temperature and pressure.

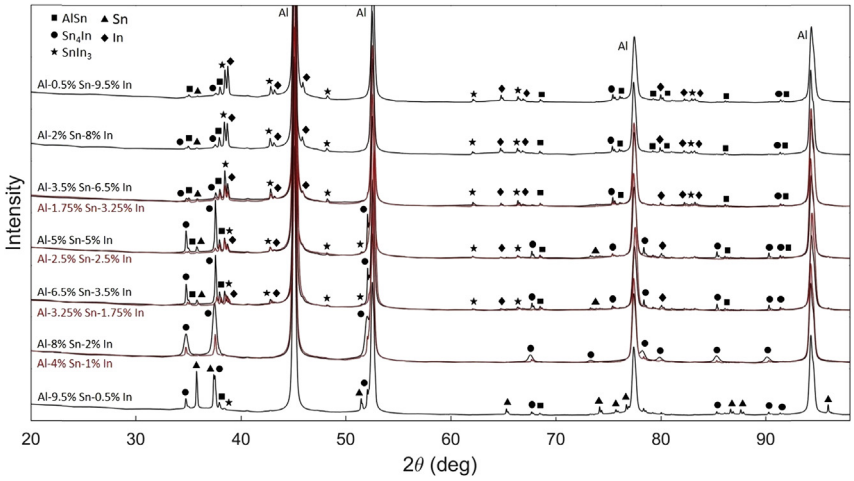

Fig. 8 – The Rietveld refinement of XRD patterns of 10% (indicated in black) and 5% (indicated in red) ternary composites. (For interpretation of the references to color in this figure legend, the reader is referred to the Web version of this article.)

reverted to their binary counterparts, i.e. Al-10% Sn and Al-10% In; thus explaining their low/no reactivity. It is evident from Fig. 6 that the effect of the Sn–In contents on Al's reactivity was non-linear. The composite reactivities, in order of fastest to slowest reaction kinetics, were as follows: Al-5% Sn-5% In, Al-6.5% Sn-3.5% In, Al-3.5% Sn-6.5% In, Al-8% Sn-2% In. This clearly indicated that a certain synergetic effect between Sn and In exists in their ability to enable Al to react with pure water. This Sn–In synergy is further contextualized in the following texts.

The composites presented in Fig. 6 (excluding Al-2% Sn-8% In) indicated relatively similar reaction kinetics and hydrogen yields, only slightly varying in induction period and total reaction time. In an effort to determine the effects of Sn and In on Al's reactivity towards water, the activation compound addition of the four most reactive composites was reduced from 10 to 5 wt%, and hydrolyzed in an exact similar way as the 10% ternary composites. These results are presented in Fig. 7 and the hydrogen yield standard deviations were included.

Table 3 – Parameter values of Rietveld structural refinement analysis of ternary composites.

Sample	Parameter (%)			
	R_{exp}	R_p	R_{wp}	GoF
Al-9.5% Sn-0.5% In	4.95	9.15	13.43	2.71
Al-8% Sn-2% In	4.83	6.98	9.62	1.99
Al-6.5% Sn-3.5% In	4.85	8.71	12.23	2.52
Al-5% Sn-5% In	4.86	9.41	13.67	2.81
Al-3.5% Sn-6.5% In	4.76	8.81	12.19	2.56
Al-2% Sn-8% In	4.82	8.87	14.16	2.94
Al-0.5% Sn-9.5% In	4.84	8.49	12.88	2.66
Al-4% Sn-1% In	4.78	8.09	11.14	2.33
Al-3.25% Sn-1.75% In	4.98	8.40	11.17	2.24
Al-2.5% Sn-2.5% In	4.75	7.89	11.18	2.35
Al-1.75% Sn-3.25% In	4.80	7.82	10.94	2.28

It is evident From Fig. 7 that a decrease in total activation compound addition had an adverse effect on the hydrogen yield and induction period. The Al-2.5% Sn-2.5% In composite had the highest hydrogen yield of 82.9 ± 1.2%. The Al-3.25% Sn-1.75% In and Al-1.75% Sn-3.25% In composites had yields of 75.0 ± 0.5 and 70.7 ± 1.4%, respectively. Al-4% Sn-1% In had the lowest yield of 63.2 ± 1.3%. In each case, the reaction completed within 1200 s (20 min). The 5% ternary composites exhibited similar reaction kinetics than the 10% ternary composites (Fig. 6). By increasing the Al content (reducing the total activation compound addition from 10 to 5 wt%), a larger fraction of composite is available to undergo the exothermic Al-hydrolysis reaction (ΔH = approximately −444 kJ mol^{-1} [104]), which is expected to promote the Al-hydrolysis reaction [2,20]. By considering the results presented in Figs. 6 and 7, this was clearly not the case. The observed decrease in composite reactivity may rather be ascribed to the inability of 5 wt% activation compound addition to sufficiently activate Al particles. Visually, the 5% ternary composites contained some large particles, suggesting incomplete distribution of composite constituents. Further decreasing the total activation compound addition to 2.5 wt% yielded non-reactive composites.

Of particular interest in Figs. 6 and 7 was the disagreement between composite Sn content and reactivity, i.e. high Sn/low In content composites were expected to be more reactive than low Sn/high In content composites. Gudić et al. (2010) thermally prepared Al–Sn and Al–In composites. They found that when such composites were exposed to a chlorine solution, In inhibited the cathodic reaction of hydrogen evolution, whereas Sn catalyzed it [44]. This is further indicative that a certain degree of synergy exists between Sn and In present in mechanochemically activated Al composites, either in terms of micro-galvanic cell formation, and/or Al particle size reduction and morphological changes induced during ball-milling. However, it is difficult to make feasible mechanistic deductions based solely on the hydrolysis kinetics, due to the

relatively similar hydrolysis kinetics of the presented composites (as shown in Figs. 6 and 7).

XRD analysis of ternary composites

XRD was performed on all of the ternary Al composites (as presented in Table 1) to determine if intermetallic phases formed between Al, Sn, and In. The presences of such intermetallic phases are likely to affect the hydrolysis kinetics of ternary Al composites, and may be applied (in conjuration with results shows in Figs. 6 and 7) to perform mechanistic deductions. Fig. 8 presents the Rietveld refined XRD patterns of ternary Al–Sn–In composites. In an effort to decrease cluttering, observed XRD values were excluded from Fig. 8 and only values calculated by the Rietveld method were presented. The corresponding R-factors and GoF values are summarized in Table 3. The Al peaks at 2θ positions 44 and 53 were partially excluded to improve surrounding peak detail.

It is evident from Fig. 8 that the detected phases (in no specific order) were residual Al, Sn, and In, intermetallic Sn–In phases (Sn_4In and $SnIn_3$), and minor AlSn peaks. Detected Sn and In phases indicates that some of the activation compounds did not partake in intermetallic phase formation, which is expected seeing as one of the activation compounds will likely be consumed in the intermetallic phase formation process and that the remaining activation

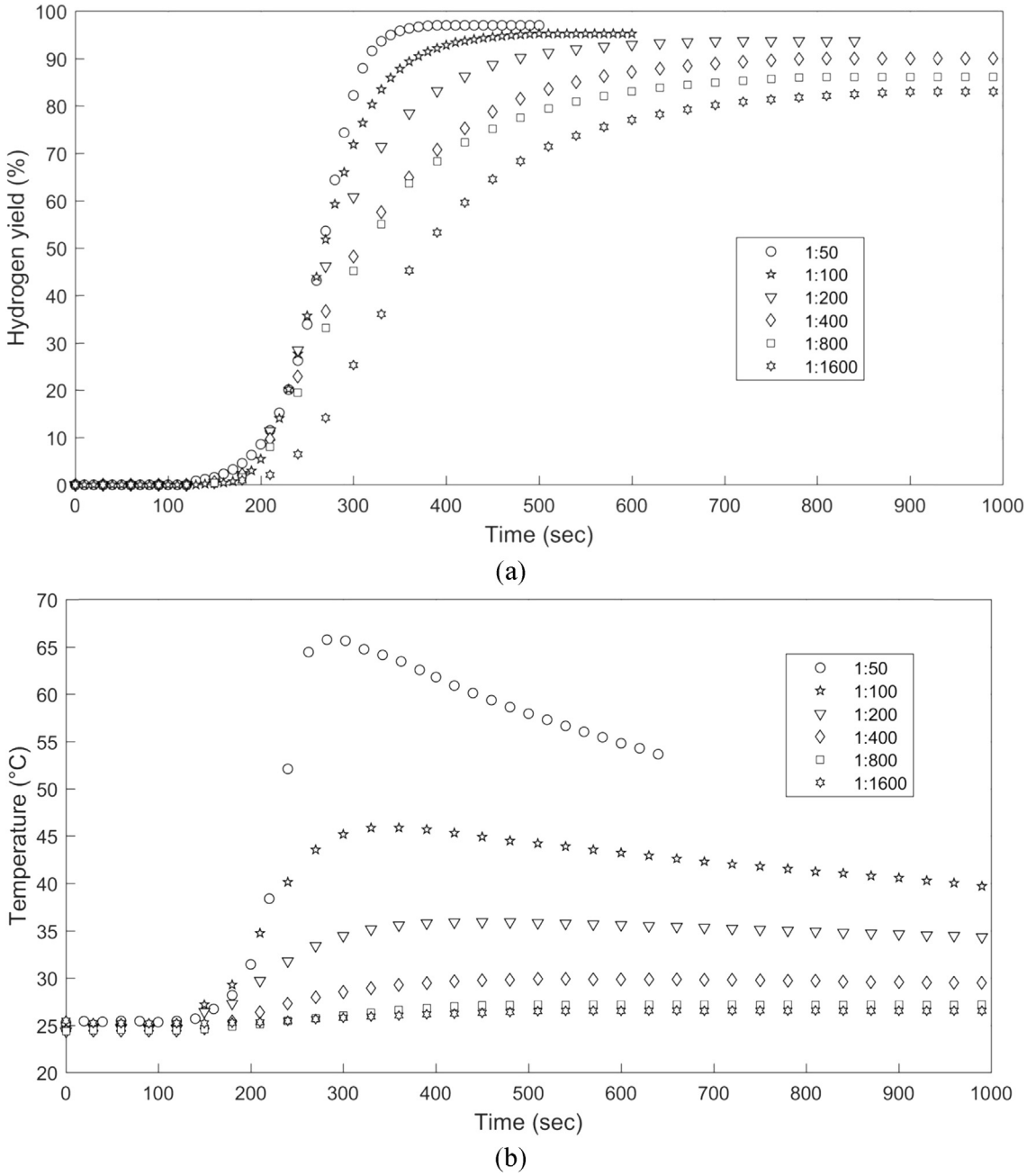

Fig. 9 – Hydrogen yields of Al-8% Sn-2% In hydrolyzed at various mass ratios of Al powder to mass pure water (a) and the observed changes in reaction temperature during hydrolysis (b).

compound could understandably no longer partake in this process. Both 10 and 5% ternary composites had similar peaks, only differing in peak intensity. This explains the observed similarities in reactivity (Section Hydrolysis of ternary Al–Sn–In composites, Figs. 6 and 7). Of particular interest in Fig. 8 is the presence of AlSn phases (with varying peak intensities), considering the absence of AlSn phases in binary Al-10% Sn composites (Fig. 5). This phenomenon may be due to the presence of In during the ball-milling process – currently it is impossible to say with certainty what promotes the AlSn phase formation process in ternary Al–Sn–In composites.

It is further evident from Fig. 8 that the Sn:In ratio determined the Sn–In phase formation. Sn_4In was the predominant Sn–In phase in composites with Sn:In ratios between 0.97 (Al-5% Sn-5% In) and 18.38 (Al-9.5% Sn-0.5% In). $SnIn_3$ was the dominant Sn–In phase in composites with a Sn:In ratio of <0.97.

Du Preez and Bessarabov (2017a) found that mechanochemically activated Al composites containing only Sn_4In had faster reaction kinetics if compared to composites containing only $SnIn_3$. When collectively considering the hydrogen yields presented in Fig. 6 and the XRD patters presented in Fig. 8, the following mechanistic deductions may be made: (i) composites containing Sn_4In as the major Sn–In phase were more reactive than composites containing $SnIn_3$ as the major Sn–In phase, (ii) composites containing only Sn_4In had the mildest reaction kinetics; however, this composite's milder reaction kinetics is likely due to it having a larger average particle size (if compared to composites containing multiple phases), rather than the absence of other intermetallic phases, and (iii) composites with Sn and/or In as the major phases exhibited low/no reactivity.

Considering the micrographs presented in Fig. 4, it is likely that the detected intermetallic Sn–In (i.e. Sn_4In and $SnIn_3$), Sn and In phases presented in Fig. 8 are distributed throughout Al particles, considering that such phases can only occur where Sn and In where detected by EDS. Thus, as the hydrolysis reaction initiates and the spend Al, i.e. $Al(OH)_3$ and/or AlOOH, separates from Al particles, fresh Al–Sn–In is exposed. Thus, micro-galvanic activity between Al and Sn/In will remain elevated throughout the hydrolysis reaction.

Table 4 – Ternary Al–Bi/Sn/In composites.

Comp.	Activation compound (wt.%)			Yield (%)	Reaction time (sec)	Reference
	Bi	Sn	In			
1	0	9.5	0.5	25	2160	This work
2	0	8	2	97	380	
3	0	6.5	3.5	96	370	
4	0	5	5	99	280	
5	0	3.5	6.5	97	300	
6	0	2	8	91	1050	
7	0	0.5	9.5	0	n.a	
8	0	4	1	63	1150	
9	0	3.25	1.75	75	1050	
10	0	2.5	2.5	83	1200	
11	0	1.75	3.25	71	1100	
1	0	8	2	~35[b]	7300[b]	[86]
2	0	6.7	3.3	~33[b]	550[b]	
3	0	5	5	~28[b]	3100[b]	
4	0	3.3	6.7	~29[b]	400[b]	
5	0	2	8	~31[b]	750[b]	
1	0	10.55	2.54	93	570	[1]
2	8.38	0	4.71	95	540	
3	0	3.27	9.82	93	810	
4	3.93	5.24	3.93	92	160	
5	6.54	2.62	3.93	96	100	
6	3.93	2.62	6.54	98	90	
7	3.93	6.54	2.62	93	130	
1	9.38	0	0.62	82	510	[2]
2	8.76	0	1.26	83	420	
3	7.5	0	2.5	95	450	
4	5	0	5	93	450	
5	3.74	0	6.26	77	378	
6	2.5	0	7.5	93	600	
7	1.26	0	8.76	66	720	
8	0.62	0	9.38	0	n.a	
1	7.5	2.5	0	86[a,b]	280[b]	[107]
2	5	5	0	84[a,b]	350[b]	

[a] Hydrolysis reaction performed at 35 °C.
[b] Values estimated from figure.

Effects of mass ratio ($m_{Al\ powder}/m_{water}$) and temperature on the hydrolysis reaction

To determine the effect of reaction temperature on the hydrolysis reaction of Al–Sn–In composites, the Al-8% Sn-2% In composite was hydrolyzed at various mass ratios, e.g. a 1:50 mass ratio is defined as 1 g Al composite hydrolyzed in 50 mL of deionized water. All mass ratios were derived similarly. The mass ratios investigated ranged from 1:50 to 1:1600. The Al-8% Sn-2% In was selected for this investigation due to its high hydrogen yield and low In content, decreasing the cost per unit volume hydrogen. A fit-for-purpose reaction vessel was used to perform large mass ratio experiments. Fig. 9 shows the effect of varying mass ratios on hydrogen yield (a) and reaction temperature (b). Maximum hydrogen yield standard deviation were <4.0%

Fig. 9a shows a steady decrease in hydrogen yield as the mass ratio was increased from 1:50 to 1:1600. Increasing the mass ratio from 1:50 to 1:100 decreased the hydrogen yield from 97.0% to 95.3%. A similar yield decrease, i.e. 95.3 to 93.8%, was observed when the mass ratio was increased from 1:100 to 1:200. Increasing the mass ratio to 1:400 and 1:800 further decreased the hydrogen yields to 90.0 and 86.1%, respectively. Finally, the hydrolysis reaction performed at a mass ratio of 1:1600 had a hydrogen yield of 83.0%.

Fig. 9b shows the hydrolysis reaction temperature of the various investigated mass ratios. It is evident from Fig. 9b that as the mass ratio was increased, the observed increases in reaction temperature decreased appreciably. The reaction temperature of the 1:50 mass ratio hydrolysis reaction increased by approximately 40 °C, whereas the 1:100 mass ratio reaction had a 20 °C increase. Further increasing the mass ratio resulted in smaller reaction temperature increases, i.e. 1:200 and 1:400 had temperature increases of 10 and 4 °C, respectively. The 1:800 and 1:1600 mass ratio reactions had temperature increases of approximately 2 and 1 °C, respectively. As stated earlier, Al hydrolysis is an exothermic reaction that releases *in-situ* generated heat, which subsequently promotes the hydrolysis reaction. By increasing the mass ratio, a larger volume of reaction solution is present to allow the generated heat to disperse into, mitigating away from immediate reaction sites (Al undergoing hydrolysis) [1,2,20]. Typically, a relatively large hydrogen yield decrease is expected when the reaction temperature is decreased, depending on the Al composite's temperature dependence. In this case the Al composite did not display a major dependence on temperature as only a 14% hydrogen yield decrease was observed as the mass ratio was increased from 1:50 to 1:1600, which corresponds to 3200% increase in water volume.

Recent work and future prospective

The results obtained in this study were compared to previous related studies, as well as some recent non-related studies. A listing of ternary Al-based composites is presented in Table 4. The Al-based composites presented here were activated by Bi, Sn, In and combinations, and were prepared by a mechanochemical route. Hydrolysis reactions were performed using neutral pH waters, which includes tap, distilled, and deionized water, and under ambient conditions, unless specified otherwise. Table 4 suggests good progress has been made towards determining the effects of Bi, Sn, In and combinations thereof on Al's reactivity with neutral pH waters. Future prospective should include identifying and developing methods to recover activation compounds from spent Al, and a fit-for-purpose hydrogen generation reactor designed to operate using neutral pH waters and activated Al-based composites.

Conclusions

A series of reactive ternary 10 wt% activation compound containing Al–Sn–In composites were prepared by high energy ball milling and hydrolyzed in deionized water under ambient conditions. SEM-EDS analysis indicated that Sn and In could be distributed onto and within Al particles. The presence of Sn and In on the surface disrupted Al's protective oxide layer, whereas Sn and In located on the surface and in the interior of Al particles promoted galvanic activity between Al and Sn/In. No intermetallic phases between Al and Sn/In were detected for binary Al–Sn/In composites, whereas ternary composites contained AlSn, Sn_4In and/or $SnIn_3$. Sn–In phase formation could partially be controlled by the Sn:In mol ratio.

Distinctive reactivity differences of ternary Al–Sn–In were not obvious, indicating some independence with regard to Sn and In contents. The 10% ternary composites had hydrogen yields of between 96.5 and 99.5%. Decreasing the composites' activation compound addition to 5 wt% decreased its reactivity. The 5% ternary composites had hydrogen yields of between 63.2 and 82.9%. Hydrogen generation rate during composite hydrolysis may be partially controlled by manipulating the mass ratio.

Acknowledgments

The Department of Science and Technology (DST) HySA Infrastructure Center of Competence at the North West University, South Africa, is acknowledged for financial support.

REFERENCES

[1] Du Preez SP, Bessarabov DG. Hydrogen generation by means of hydrolysis using activated Al-In-Bi-Sn composites for electrochemical energy applications. Int J Electrochem Sci 2017a;12:8663–82. https://doi.org/10.20964/2017.09.22.

[2] Du Preez SP, Bessarabov DG. Hydrogen generation of mechanochemically activated AlBiIn composites. Int J Hydrogen Energy 2017b;42:16589–602. https://doi.org/10.1016/j.ijhydene.2017.05.211.

[3] Kothari R, Buddhi D, Sawhney R. Comparison of environmental and economic aspects of various hydrogen production methods. Renew Sustain Energy Rev 2008;12:553–63. https://doi.org/10.1016/j.rser.2006.07.012.

[4] Edwards N, Ellis SR, Frost JC, Golunski SE, van Keulen ANJ, Lindewald NG, et al. On-board hydrogen generation for transport applications: the HotSpot™ methanol processor. J Power Sources 1998;71:123–8. https://doi.org/10.1016/S0378-7753(97)02797-3.

[5] Gray P, Petch M. Advances with HotSpot™ fuel processing efficient hydrogen production for use with solid polymer fuel cells. Platin Met Rev 2000;44:108.
[6] Faur Ghenciu A. Review of fuel processing catalysts for hydrogen production in PEM fuel cell systems. Curr Opin Solid State Mater Sci 2002;6:389–99. https://doi.org/10.1016/S1359-0286(02)00108-0.
[7] Kreuer KD. On the development of proton conducting polymer membranes for hydrogen and methanol fuel cells. J Membr Sci 2001;185:29–39. https://doi.org/10.1016/S0376-7388(00)00632-3.
[8] Barbir F, Gómez T. Efficiency and economics of proton exchange membrane (PEM) fuel cells. Int J Hydrogen Energy 1997;22:1027–37. https://doi.org/10.1016/S0360-3199(96)00175-9.
[9] Mousa G, Golnaraghi F, DeVaal J, Young A. Detecting proton exchange membrane fuel cell hydrogen leak using electrochemical impedance spectroscopy method. J Power Sources 2014;246:110–6. https://doi.org/10.1016/j.jpowsour.2013.07.018.
[10] Peighambardoust SJ, Rowshanzamir S, Amjadi M. Review of the proton exchange membranes for fuel cell applications. Int J Hydrogen Energy 2010;35:9349–84. https://doi.org/10.1016/j.ijhydene.2010.05.017.
[11] Divisek J, Oetjen HF, Peinecke V, Schmidt VM, Stimming U. Components for PEM fuel cell systems using hydrogen and CO containing fuels. Electrochim Acta 1998;43:3811–5. https://doi.org/10.1016/S0013-4686(98)00140-6.
[12] Wei C, Liu D, Xu S, Cui T, An Q, Liu Z, et al. Effects of Cu additives on the hydrogen generation performance of Al-rich alloys. J Alloy Comp 2018;738:105–10. https://doi.org/10.1016/j.jallcom.2017.12.152.
[13] Sørensen B, Spazzafumo G. Hydrogen and fuel cells: emerging technologies and applications. Academic Press; 2018.
[14] Balat M. Potential importance of hydrogen as a future solution to environmental and transportation problems. Int J Hydrogen Energy 2008;33:4013–29. https://doi.org/10.1016/j.ijhydene.2008.05.047.
[15] Ball M, Wietschel M. The future of hydrogen–opportunities and challenges. Int J Hydrogen Energy 2009;34:615–27. https://doi.org/10.1016/j.ijhydene.2008.11.014.
[16] Damyanova S, Pawelec B, Arishtirova K, Fierro JLG. Ni-based catalysts for reforming of methane with CO2. Int J Hydrogen Energy 2012;37:15966–75. https://doi.org/10.1016/j.ijhydene.2012.08.056.
[17] Reshetenko TV, Bethune K, Rocheleau R. Spatial proton exchange membrane fuel cell performance under carbon monoxide poisoning at a low concentration using a segmented cell system. J Power Sources 2012;218:412–23. https://doi.org/10.1016/j.jpowsour.2012.07.015.
[18] Gosavi PV, Biniwale RB. Catalytic preferential oxidation of carbon monoxide over platinum supported on lanthanum ferrite–ceria catalysts for cleaning of hydrogen. J Power Sources 2013;222:1–9. https://doi.org/10.1016/j.jpowsour.2012.07.095.
[19] Wang M, Wang Z, Gong X, Guo Z. The intensification technologies to water electrolysis for hydrogen production – a review. Renew Sustain Energy Rev 2014;29:573–88. https://doi.org/10.1016/j.rser.2013.08.090.
[20] Mahmoodi K, Alinejad B. Enhancement of hydrogen generation rate in reaction of aluminum with water. Int J Hydrogen Energy 2010;35:5227–32. https://doi.org/10.1016/j.ijhydene.2010.03.016.
[21] Tzimas E, Filiou C, Peteves SD, Veyret J. Hydrogen storage: state-of-the-art and future perspective. EU Commission, JRC Petten, EUR 20995EN; 2003.
[22] Ilyukhina AV, Ilyukhin AS, Shkolnikov EI. Hydrogen generation from water by means of activated aluminum. Int J Hydrogen Energy 2012;37:16382–7. https://doi.org/10.1016/j.ijhydene.2012.02.175.
[23] Sakintuna B, Lamari-Darkrim F, Hirscher M. Metal hydride materials for solid hydrogen storage: a review. Int J Hydrogen Energy 2007;32:1121–40. https://doi.org/10.1016/j.ijhydene.2006.11.022.
[24] Esswein AJ, Nocera DG. Hydrogen production by molecular photocatalysis. Chem Rev 2007;107:4022–47. https://doi.org/10.1021/cr050193e.
[25] Wang X, Maeda K, Thomas A, Takanabe K, Xin G, Carlsson JM, et al. A metal-free polymeric photocatalyst for hydrogen production from water under visible light. Nat Mater 2009;8:76–80. https://doi.org/10.1038/nmat2317.
[26] Turner JA. Sustainable hydrogen production. Science 2004;305:972–4. https://doi.org/10.1126/science.1103197.
[27] Bessarabov D, Human G, Kruger AJ, Chiuta S, Modisha PM, Du Preez SP, et al. South African hydrogen infrastructure (HySA infrastructure) for fuel cells and energy storage: overview of a projects portfolio. Int J Hydrogen Energy 2017;42:13568–88. https://doi.org/10.1016/j.ijhydene.2016.12.140.
[28] Elitzur S, Rosenband V, Gany A. On-board hydrogen production for auxiliary power in passenger aircraft. Int J Hydrogen Energy 2017;42:14003–9. https://doi.org/10.1016/j.ijhydene.2017.02.037.
[29] Renouard-Vallet G, Saballus M, Schumann P, Kallo J, Friedrich KA, Müller-Steinhagen H. Fuel cells for civil aircraft application: on-board production of power, water and inert gas. Chem Eng Res Des 2012;90:3–10. https://doi.org/10.1016/j.cherd.2011.07.016.
[30] Ilyukhina A, Kravchenko O, Bulychev B, Shkolnikov E. Mechanochemical activation of aluminum with gallams for hydrogen evolution from water. Int J Hydrogen Energy 2010;35:1905–10. https://doi.org/10.1016/j.ijhydene.2009.12.118.
[31] Liu Y, Wang X, Liu H, Dong Z, Li S, Ge H, et al. Investigation on the improved hydrolysis of aluminum–calcium hydride-salt mixture elaborated by ball milling. Energy 2015;84:714–21. https://doi.org/10.1016/j.energy.2015.03.035.
[32] Hiraki T, Yamauchi S, Iida M, Uesugi H, Akiyama T. Process for recycling waste aluminum with generation of high-pressure hydrogen. Environ Sci Technol 2007;41:4454–7. https://doi.org/10.1021/es062883l.
[33] Gai W-Z, Liu W-H, Deng Z-Y, Zhou J-G. Reaction of Al powder with water for hydrogen generation under ambient condition. Int J Hydrogen Energy 2012;37:13132–40. https://doi.org/10.1016/j.ijhydene.2012.04.025.
[34] Cho C-Y, Wang K-H, Uan J-Y. Evaluation of a new hydrogen generating system: Ni-rich magnesium alloy catalyzed by platinum wire in sodium chloride solution. Mater Trans 2005;46:2704–8. https://doi.org/10.2320/matertrans.46.2704.
[35] Grosjean M-H, Zidoune M, Roué L, Huot J-Y. Hydrogen production via hydrolysis reaction from ball-milled Mg-based materials. Int J Hydrogen Energy 2006;31:109–19. https://doi.org/10.1016/j.ijhydene.2005.01.001.
[36] Sun Q, Zou M, Guo X, Yang R, Huang H, Huang P, et al. A study of hydrogen generation by reaction of an activated Mg–CoCl2 (magnesium–cobalt chloride) composite with pure water for portable applications. Energy 2015;79:310–4. https://doi.org/10.1016/j.energy.2014.11.016.
[37] Huang M, Ouyang L, Ye J, Liu J, Yao X, Wang H, et al. Hydrogen generation via hydrolysis of magnesium with seawater using Mo, MoO 2, MoO 3 and MoS 2 as catalysts. J Mater Chem A 2017;5:8566–75. https://doi.org/10.1039/C7TA02457F.
[38] Oh S, Cho T, Kim M, Lim J, Eom K, Kim D, et al. Fabrication of Mg–Ni–Sn alloys for fast hydrogen generation in

seawater. Int J Hydrogen Energy 2017;42:7761–9. https://doi.org/10.1016/j.ijhydene.2016.11.138.
[39] Wang S, Sun L-X, Xu F, Jiao C-L, Zhang J, Zhou H-Y, et al. Hydrolysis reaction of ball-milled Mg-metal chlorides composite for hydrogen generation for fuel cells. Int J Hydrogen Energy 2012;37:6771–5. https://doi.org/10.1016/j.ijhydene.2012.01.099.
[40] Wegner K, Ly HC, Weiss RJ, Pratsinis SE, Steinfeld A. In situ formation and hydrolysis of Zn nanoparticles for production by the 2-step ZnO/Zn water-splitting thermochemical cycle. Int J Hydrogen Energy 2006;31:55–61. https://doi.org/10.1016/j.ijhydene.2005.03.006.
[41] Vishnevetsky I, Epstein M. Production of hydrogen from solar zinc in steam atmosphere. Int J Hydrogen Energy 2007;32:2791–802. https://doi.org/10.1016/j.ijhydene.2007.04.004.
[42] Kravchenko OV, Semenenko KN, Bulychev BM, Kalmykov KB. Activation of aluminum metal and its reaction with water. J Alloy Comp 2005;397:58–62. https://doi.org/10.1016/j.jallcom.2004.11.065.
[43] Wang HZ, Leung DYC, Leung MKH, Ni M. A review on hydrogen production using aluminum and aluminum alloys. Renew Sustain Energy Rev 2009;13:845–53. https://doi.org/10.1016/j.rser.2008.02.009.
[44] Gudić S, Smoljko I, Kliškić M. The effect of small addition of tin and indium on the corrosion behavior of aluminium in chloride solution. J Alloy Comp 2010;505:54–63. https://doi.org/10.1016/j.jallcom.2010.06.055.
[45] Pourbaix M. Atlas of electrochemical equilibria in aqueous solutions. Houston: National Association of Corrosion Engineers; 1974.
[46] Zou H, Chen S, Zhao Z, Lin W. Hydrogen production by hydrolysis of aluminum. J Alloy Comp 2013;578:380–4. https://doi.org/10.1016/j.jallcom.2013.06.016.
[47] Ilyukhina AV, Kravchenko OV, Bulychev BM. Studies on microstructure of activated aluminum and its hydrogen generation properties in aluminum/water reaction. J Alloy Comp 2017;690:321–9. https://doi.org/10.1016/j.jallcom.2016.08.151.
[48] Chai YJ, Dong YM, Meng HX, Jia YY, Shen J, Huang YM, et al. Hydrogen generation by aluminum corrosion in cobalt (II) chloride and nickel (II) chloride aqueous solution. Energy 2014;68:204–9. https://doi.org/10.1016/j.energy.2014.03.011.
[49] Alinejad B, Mahmoodi K. A novel method for generating hydrogen by hydrolysis of highly activated aluminum nanoparticles in pure water. Int J Hydrogen Energy 2009;34:7934–8. https://doi.org/10.1016/j.ijhydene.2009.07.028.
[50] Teng H, Lee T, Chen Y, Wang H, Cao G. Effect of $Al(OH)_3$ on the hydrogen generation of aluminum-water system. J Power Sources 2012;219:16–21. https://doi.org/10.1016/j.jpowsour.2012.06.077.
[51] Czech E, Troczynski T. Hydrogen generation through massive corrosion of deformed aluminum in water. Int J Hydrogen Energy 2010;35:1029–37. https://doi.org/10.1016/j.ijhydene.2009.11.085.
[52] López-Miranda JL, Rosas G. Hydrogen generation by aluminum hydrolysis using the Fe2Al5 intermetallic compound. Int J Hydrogen Energy 2016;41:4054–9. https://doi.org/10.1016/j.ijhydene.2016.01.012.
[53] Belitskus D. Reaction of aluminium with sodium hydroxide solution as a source of hydrogen. J Electrochem Soc 1970;117:1097–9. https://doi.org/10.1149/1.2407730.
[54] Soler L, Macanás J, Muñoz M, Casado J. Synergistic hydrogen generation from aluminum, aluminum alloys and sodium borohydride in aqueous solutions. Int J Hydrogen Energy 2007;32:4702–10. https://doi.org/10.1016/j.ijhydene.2007.06.019.
[55] Martinez SS, Albañil Sánchez L, Álvarez Gallegos AA, Sebastian P. Coupling a PEM fuel cell and the hydrogen generation from aluminum waste cans. Int J Hydrogen Energy 2007;32:3159–62. https://doi.org/10.1016/j.ijhydene.2006.03.015.
[56] Wang E-D, Shi P-F, Du C-Y, Wang X-R. A mini-type hydrogen generator from aluminum for proton exchange membrane fuel cells. J Power Sources 2008;181:144–8. https://doi.org/10.1016/j.jpowsour.2008.02.088.
[57] El-Meligi A. Hydrogen production by aluminum corrosion in hydrochloric acid and using inhibitors to control hydrogen evolution. Int J Hydrogen Energy 2011;36:10600–7. https://doi.org/10.1016/j.ijhydene.2011.05.111.
[58] Boukerche I, Djerad S, Benmansour L, Tifouti L, Saleh K. Degradability of aluminum in acidic and alkaline solutions. Corrosion Sci 2014;78:343–52. https://doi.org/10.1016/j.corsci.2013.10.019.
[59] Dudoladov AO, Buryakovskaya OA, Vlaskin MS, Zhuk AZ, Shkolnikov EI. Generation of hydrogen by aluminium oxidation in aquaeous solutions at low temperatures. Int J Hydrogen Energy 2016;41:2230–7. https://doi.org/10.1016/j.ijhydene.2015.11.122.
[60] Soler L, Macanás J, Muñoz M, Casado J. Aluminum and aluminum alloys as sources of hydrogen for fuel cell applications. J Power Sources 2007;169:144–9. https://doi.org/10.1016/j.jpowsour.2007.01.080.
[61] Jung CR, Kundu A, Ku B, Gil JH, Lee HR, Jang JH. Hydrogen from aluminium in a flow reactor for fuel cell applications. J Power Sources 2008;175:490–4. https://doi.org/10.1016/j.jpowsour.2007.09.064.
[62] Yang B, Chai Y, Yang F, Zhang Q, Liu H, Wang N. Hydrogen generation by aluminum-water reaction in acidic and alkaline media and its reaction dynamics. Int J Energy Res 2018;42:1594–602. https://doi.org/10.1002/er.3953.
[63] El-Meligi A. Hydrogen production by aluminum alloy in sulphuric acid solutions. Recent Pat Mater Sci 2017;10:75–81. https://doi.org/10.2174/1874464810666170605113128.
[64] Liu H, Yang F, Yang B, Zhang Q, Chai Y, Wang N. Rapid hydrogen generation through aluminum-water reaction in alkali solution. Catal Today 2018. https://doi.org/10.1016/j.cattod.2018.03.030.
[65] Hurtubise DW, Klosterman DA, Morgan AB. Development and demonstration of a deployable apparatus for generating hydrogen from the hydrolysis of aluminum via sodium hydroxide. Int J Hydrogen Energy 2018;43:6777–88. https://doi.org/10.1016/j.ijhydene.2018.02.087.
[66] Ho C-Y, Huang C-H. Enhancement of hydrogen generation using waste aluminum cans hydrolysis in low alkaline de-ionized water. Int J Hydrogen Energy 2016;41:3741–7. https://doi.org/10.1016/j.ijhydene.2015.11.083.
[67] Ambaryan GN, Vlaskin MS, Dudoladov AO, Meshkov EA, Zhuk AZ, Shkolnikov EI. Hydrogen generation by oxidation of coarse aluminum in low content alkali aqueous solution under intensive mixing. Int J Hydrogen Energy 2016;41:17216–24. https://doi.org/10.1016/j.ijhydene.2016.08.005.
[68] Vlaskin M, Shkolnikov E, Lisicyn A, Bersh A, Zhuk A. Computational and experimental investigation on thermodynamics of the reactor of aluminum oxidation in saturated wet steam. Int J Hydrogen Energy 2010;35:1888–94. https://doi.org/10.1016/j.ijhydene.2009.12.061.
[69] Ivanov V, Leonov S, Savinov G, Gavrilyuk O, Glazkov O. Combustion of mixtures of ultradisperse aluminum and gel-like water. Combust Explos Shock Waves 1994;30:569–70. https://doi.org/10.1007/BF00790170.

[70] Setiani P, Watanabe N, Sondari RR, Tsuchiya N. Mechanisms and kinetic model of hydrogen production in the hydrothermal treatment of waste aluminum. Mater Renew Sustain Energy 2018;7:10. https://doi.org/10.1007/s40243-018-0118-8.
[71] Vlaskin MS, Shkolnikov EI, Bersh AV. Oxidation kinetics of micron-sized aluminum powder in high-temperature boiling water. Int J Hydrogen Energy 2011;36:6484–95. https://doi.org/10.1016/j.ijhydene.2011.02.131.
[72] Bersh AV, Lisitsyn AV, Sorokovikov AI, Vlaskin MS, Mazalov YA, Shkol'nikov EI. Study of the processes of steam-hydrogen mixture generation in a reactor for hydrothermal aluminum oxidation for power units. High Temp 2010;48:866–73. https://doi.org/10.1134/s0018151x10060131.
[73] Potapova YV, Tikhov SF, Sadykov VA, Fenelonov VB. Kinetics of aluminium powder oxidation by water vapor at moderate temperatures. React Kinet Catal Lett 2001;73:55–61. https://doi.org/10.1023/a:1013964602995.
[74] Yavor Y, Goroshin S, Bergthorson JM, Frost DL, Stowe R, Ringuette S. Enhanced hydrogen generation from aluminum–water reactions. Int J Hydrogen Energy 2013;38:14992–5002. https://doi.org/10.1016/j.ijhydene.2013.09.070.
[75] Bessone J. The activation of aluminium by mercury ions in non-aggressive media. Corrosion Sci 2006;48:4243–56. https://doi.org/10.1016/j.corsci.2006.03.013.
[76] Fan M-q, Sun L-x, Xu F. Study of the controllable reactivity of aluminum alloys and their promising application for hydrogen generation. Energy Convers Manag 2010;51:594–9. https://doi.org/10.1016/j.enconman.2009.11.005.
[77] Huang X, Lv C, Huang Y, Liu S, Wang C, Chen D. Effects of amalgam on hydrogen generation by hydrolysis of aluminum with water. Int J Hydrogen Energy 2011;36:15119–24. https://doi.org/10.1016/j.ijhydene.2011.08.073.
[78] Venter A, Beukes J, Van Zyl P, Brunke E-G, Labuschagne C, Slemr F, et al. Statistical exploration of gaseous elemental mercury (GEM) measured at Cape Point from 2007 to 2011. Atmos Chem Phys 2015;15:10271–80. https://doi.org/10.5194/acp-15-10271-2015.
[79] Parmuzina AV, Kravchenko OV. Activation of aluminium metal to evolve hydrogen from water. Int J Hydrogen Energy 2008;33:3073–6. https://doi.org/10.1016/j.ijhydene.2008.02.025.
[80] Wang H, Chang Y, Dong S, Lei Z, Zhu Q, Luo P, et al. Investigation on hydrogen production using multicomponent aluminum alloys at mild conditions and its mechanism. Int J Hydrogen Energy 2013;38:1236–43. https://doi.org/10.1016/j.ijhydene.2012.11.034.
[81] Senel E, Walmsley JC, Diplas S, Nisancioglu K. Liquid metal embrittlement of aluminium by segregation of trace element gallium. Corrosion Sci 2014;85:167–73. https://doi.org/10.1016/j.corsci.2014.04.012.
[82] Nizovskii AI, Belkova SV, Novikov AA, Trenikhin MV. Hydrogen production for fuel cells in reaction of activated aluminum with water. Procedia Eng 2015;113:8–12. https://doi.org/10.1016/j.proeng.2015.07.278.
[83] Baniamerian M, Moradi S. Al–Ga doped nanostructured carbon as a novel material for hydrogen production in water. J Alloy Comp 2011;509:6307–10. https://doi.org/10.1016/j.jallcom.2011.03.069.
[84] Nizovskii A, Kulikov A, Trenikhin M, Bukhtiyarov V. Material for compact hydrogen cartridges based on commercial aluminium alloys activated by Ga-in eutectics. Catal Sustain Energy 2017;4:62–6. https://doi.org/10.1515/cse-2017-0010.
[85] Ying C, Bei L, Huihu W, Shijie D. Effects of preparation parameters and alloy elements on the hydrogen generation performance of aluminum Alloy-0° C pure water reaction. Rare Metal Mater Eng 2017;46:2428–32. https://doi.org/10.1016/S1875-5372(17)30210-2.
[86] Wang F-Q, Wang H-H, Wang J, Lu J, Luo P, Chang Y, et al. Effects of low melting point metals (Ga, In, Sn) on hydrolysis properties of aluminum alloys. Trans Nonferrous Metals Soc China 2016;26:152–9. https://doi.org/10.1016/S1003-6326(16)64100-6.
[87] Ziebarth JT, Woodall JM, Kramer RA, Choi G. Liquid phase-enabled reaction of Al–Ga and Al–Ga–In–Sn alloys with water. Int J Hydrogen Energy 2011;36:5271–9. https://doi.org/10.1016/j.ijhydene.2011.01.127.
[88] Du B, Wang W, Chen W, Chen D, Yang K. Grain refinement and Al-water reactivity of AlGaInSn alloys. Int J Hydrogen Energy 2017;42:21586–96. https://doi.org/10.1016/j.ijhydene.2017.07.105.
[89] Jayaraman K, Chauveau C, Gökalp I. Effects of aluminum particle size, galinstan content and reaction temperature on hydrogen generation rate using activated aluminum and water. Energy Power Eng 2015;7:426. https://doi.org/10.4236/epe.2015.79041.
[90] Huang T, Gao Q, Liu D, Xu S, Guo C, Zou J, et al. Preparation of Al-Ga-In-Sn-Bi quinary alloy and its hydrogen production via water splitting. Int J Hydrogen Energy 2015;40:2354–62. https://doi.org/10.1016/j.ijhydene.2014.12.034.
[91] Yang B, Zhu J, Jiang T, Gou Y, Hou X, Pan B. Effect of heat treatment on AlMgGaInSn alloy for hydrogen generation through hydrolysis reaction. Int J Hydrogen Energy 2017;42:24393–403. https://doi.org/10.1016/j.ijhydene.2017.07.091.
[92] Du BD, He TT, Liu GL, Chen W, Wang YM, Wang W, et al. Al-water reactivity of AlMgGaInSn alloys used for hydraulic fracturing tools. Int J Hydrogen Energy 2018;43:7201–15. https://doi.org/10.1016/j.ijhydene.2018.02.090.
[93] Dupiano P, Stamatis D, Dreizin EL. Hydrogen production by reacting water with mechanically milled composite aluminum-metal oxide powders. Int J Hydrogen Energy 2011;36:4781–91. https://doi.org/10.1016/j.ijhydene.2011.01.062.
[94] Wang H-W, Chung H-W, Teng H-T, Cao G. Generation of hydrogen from aluminum and water – effect of metal oxide nanocrystals and water quality. Int J Hydrogen Energy 2011;36:15136–44. https://doi.org/10.1016/j.ijhydene.2011.08.077.
[95] Streletskii AN, Kolbanev IV, Borunova AB, Butyagin PY. Mechanochemically activated aluminium: preparation, structure, and chemical properties. J Mater Sci 2004;39:5175–9. https://doi.org/10.1023/B:JMSC.0000039205.46608.1a.
[96] Fan MQ, Xu F, Sun LX. Studies on hydrogen generation characteristics of hydrolysis of the ball milling Al-based materials in pure water. Int J Hydrogen Energy 2007;32:2809–15. https://doi.org/10.1016/j.ijhydene.2006.12.020.
[97] Liu S, Fan M-q, Wang C, Huang Y-x, Chen D, Bai L-q, et al. Hydrogen generation by hydrolysis of Al–Li–Bi–NaCl mixture with pure water. Int J Hydrogen Energy 2012;37:1014–20. https://doi.org/10.1016/j.ijhydene.2011.03.029.
[98] Fan Mq, Sun Lx, Xu F. Experiment assessment of hydrogen production from activated aluminum alloys in portable generator for fuel cell applications. Energy 2010;35:2922–6. https://doi.org/10.1016/j.energy.2010.03.023.
[99] Xiao Y, Wu C, Wu H, Chen Y. Hydrogen generation by CaH2-induced hydrolysis of Mg17Al12 hydride. Int J Hydrogen Energy 2011;36:15698–703. https://doi.org/10.1016/j.ijhydene.2011.09.022.

[100] Liu Y, Wang X, Liu H, Dong Z, Li S, Ge H, et al. Improved hydrogen generation from the hydrolysis of aluminum ball milled with hydride. Energy 2014;72:421–6. https://doi.org/10.1016/j.energy.2014.05.060.
[101] Jia Y, Shen J, Meng H, Dong Y, Chai Y, Wang N. Hydrogen generation using a ball-milled Al/Ni/NaCl mixture. J Alloy Comp 2014;588:259–64. https://doi.org/10.1016/j.jallcom.2013.11.058.
[102] Huang X-N, Lv C-J, Wang Y, Shen H-Y, Chen D, Huang Y-X. Hydrogen generation from hydrolysis of aluminum/graphite composites with a core–shell structure. Int J Hydrogen Energy 2012;37:7457–63. https://doi.org/10.1016/j.ijhydene.2012.01.126.
[103] Fan M-q, Liu S, Sun L-X, Xu F, Wang S, Zhang J, et al. Synergistic hydrogen generation from AlLi alloy and solid-state NaBH4 activated by CoCl2 in water for portable fuel cell. Int J Hydrogen Energy 2012;37:4571–9. https://doi.org/10.1016/j.ijhydene.2011.06.040.
[104] Fan MQ, Sun LX, Xu F, Mei D, Chen D, Chai WX, et al. Microstructure of Al–Li alloy and its hydrolysis as portable hydrogen source for proton-exchange membrane fuel cells. Int J Hydrogen Energy 2011;36:9791–8. https://doi.org/10.1016/j.ijhydene.2011.05.096.
[105] Wang C, Yang T, Liu Y, Ruan J, Yang S, Liu X. Hydrogen generation by the hydrolysis of magnesium–aluminum–iron material in aqueous solutions. Int J Hydrogen Energy 2014;39:10843–52. https://doi.org/10.1016/j.ijhydene.2014.05.047.
[106] Zhao Z, Chen X, Hao M. Hydrogen generation by splitting water with Al–Ca alloy. Energy 2011;36:2782–7. https://doi.org/10.1016/j.energy.2011.02.018.
[107] Xiao F, Guo Y, Li J, Yang R. Hydrogen generation from hydrolysis of activated aluminum composites in tap water. Energy 2018;157:608–14. https://doi.org/10.1016/j.energy.2018.05.201.
[108] Hill R, Howard C. Quantitative phase analysis from neutron powder diffraction data using the Rietveld method. J Appl Crystallogr 1987;20:467–74. https://doi.org/10.1107/S0021889887086199.
[109] Suryanarayana C. Mechanical alloying and milling. Prog Mater Sci 2001;46:1–184. https://doi.org/10.1016/S0079-6425(99)00010-9.
[110] Benjamin J. Mechanical alloying. Sci Am 1976;234:40–8.
[111] Kliškić M, Radošević J, Gudić S, Šmith M. Cathodic polarization of Al–Sn alloy in sodium chloride solution. Electrochim Acta 1998;43:3241–55. https://doi.org/10.1016/S0013-4686(98)00001-2.
[112] Reding J, Newport J. The influence of alloying elements on aluminum anodes in sea water. Mater Prot 1966;5:15–8. https://doi.org/10.3323/jcorr1954.16.2_68.
[113] Taranets NY, Nizhenko V, Poluyanskaya V, Naidich YV. Ge–Al and Sn–Al alloys capillary properties in contact with aluminum nitride. Acta Mater 2002;50:5147–54. https://doi.org/10.1016/S1359-6454(02)00383-X.
[114] Lee K-K, Kim K-B. Electrochemical impedance characteristics of pure Al and Al–Sn alloys in NaOH solution. Corrosion Sci 2001;43:561–75. https://doi.org/10.1016/S0010-938X(00)00060-3.
[115] Eom K, Kim M, Oh S, Cho E, Kwon H. Design of ternary Al–Sn–Fe alloy for fast on-board hydrogen production, and its application to PEM fuel cell. Int J Hydrogen Energy 2011;36:11825–31. https://doi.org/10.1016/j.ijhydene.2011.06.072.
[116] Parsons R. Handbook of electrochemical constants. 1959.
[117] Gundersen J, Aytac A, Nordlien J, Nişancıoğlu K. Effect of heat treatment on electrochemical behaviour of binary aluminium model alloys. Corrosion Sci 2004;46:697–714. https://doi.org/10.1016/S0010-938X(03)00179-3.
[118] Graver B, van Helvoort ATJ, Nisancioglu K. Effect of heat treatment on anodic activation of aluminium by trace element indium. Corrosion Sci 2010;52:3774–81. https://doi.org/10.1016/j.corsci.2010.07.029.
[119] Razavi-Tousi SS, Szpunar JA. Effect of structural evolution of aluminum powder during ball milling on hydrogen generation in aluminum–water reaction. Int J Hydrogen Energy 2013;38:795–806. https://doi.org/10.1016/j.ijhydene.2012.10.106.
[120] Razavi-Tousi S, Szpunar J. Role of ball milling of aluminum powders in promotion of aluminum-water reaction to generate hydrogen. Metall Mater Trans E 2014:1–10. https://doi.org/10.1007/s40553-014-0024-7.
[121] Reboul M, Gimenez P, Rameau J. A proposed activation mechanism for Al anodes. Corrosion 1984;40:366–71.
[122] Equey JF, Müller S, Desilvestro J, Haas O. Electrochemical properties of aluminum in weakly acidic sodium chloride solutions: II . Influence of the electrolyte additives Hg2+, In3+, Ga3+, and Sn2+. J Electrochem Soc 1992;139:1499–502. https://doi.org/10.1149/1.2069444.
[123] Breslin CB, Carroll WM. The effects of indium precipitates on the electrochemical dissolution of Al-In alloys. Corrosion Sci 1993;34:1099–109. https://doi.org/10.1016/0010-938X(93)90291-N.
[124] Saidman SB, Garcia SG, Bessone JB. Electrochemical behaviour of Al-In alloys in chloride solutions. J Appl Electrochem 1995;25:252–8. https://doi.org/10.1007/bf00262964.
[125] Zhang F, Yonemoto R, Arita M, Horita Z. Hydrogen generation from pure water using Al–Sn powders consolidated through high-pressure torsion. J Mater Res 2016;31:775–82. https://doi.org/10.1557/jmr.2016.74.

CHAPTER 6: ARTICLE 4

Mechanochemical processing of aluminum-based composites for hydrogen generation purposes: Effects of bismuth and tin

6.1 Author list and contributions

Authors list

S.P. du Preez[a] and D.G. Bessarabov[a,*]

[a] HySA Centre of Competence, North-West University (NWU), Potchefstroom Campus, Private Bag X6001, Potchefstroom, 2520, South Africa

Contributions

Contributions of the various co-authors were as follows:

Experimental work, data processing and interpretation, research, and writing of the scientific paper, was performed mainly by the candidate, SP du Preez. DG Bessarabov (supervisor) made conceptual contributions and assisted with article preparation.

6.2 Formatting and current status of the article

The article presented in Chapter 6 was submitted to *Journal of Alloys and Compounds* in 2018, and was under review when this dissertation was submitted for examination. The journal details can be found at https://www.journals.elsevier.com/journal-of-alloys-and-compounds (Date of access: 13 September 2018).

Mechanochemical processing of aluminum-based composites for hydrogen generation purposes: Effects of bismuth and tin

S.P. du Preez[a] and D.G. Bessarabov[a,*]

[a] HySA Centre of Competence, North-West University (NWU), Potchefstroom Campus, Private Bag X6001, Potchefstroom, 2520, South Africa

*Corresponding author. E-mail address: dmitri.bessarabov@nwu.ac.za;
telephone: (+27) 18 285 2460; fax: (+27) 18 299 1667

ABSTRACT

The work described in this paper forms part of a study on the mechanochemical processing of Al with dissimilar metals for hydrogen generation purposes [1-3]. Specifically, we describe here the microstructural properties and hydrolysis reactivities of activated Al composites. Binary and ternary Al, Bi, and/or Sn composites were fabricated by a high-energy mechanochemical processing route and their reactivities towards pure water under standard ambient conditions were determined. The microstructures of the composites were characterized by scanning electron microscopy with energy dispersive X-ray spectroscopy and X-ray diffraction (XRD). It was found that Bi and Sn intruded Al particles via Al's repetitive plastic deformation that occurred during mechanochemical processing. Bi and Sn intrusion resulted in continuous galvanic activity between anodic Al and cathodic Bi/Sn during hydrolysis reactions. XRD revealed some minor intermetallic phases between Al and Sn, and between Bi and Sn. However, the major phases detected were Al, Bi, and Sn, which suggested that intermetallic phases do not govern morphology changes (occurring during mechanochemical processing) and hydrolysis reactivity.

Keywords: Aluminum; Mechanochemical processing; Composite material; Intermetallic phases; Hydrogen generation.

1. Introduction

Hydrogen is the ideal candidate to replace traditional fossil fuels as an energy carrier due to its high energy density and environmental friendliness. A number of processes are used to produce hydrogen, e.g., thermochemical [4, 5], electrochemical [6, 7], photochemical [8], photocatalytic [9], and photo-electrochemical [10], and also numerous nanoparticle-assisted bio-hydrogen production processes [11]. Hydrogen is mainly produced from methane steam reformation and hydrocarbon partial oxidation, both of which yield carbon dioxide (CO_2) and minute quantities of carbon monoxide (CO) as by-products [12, 13]. This hydrogen can subsequently be fed to proton exchange membrane fuel cells (PEMFCs), which consume hydrogen and oxygen to produce an electrical circuit without the need for combustion [14, 15]. PEMFCs offer a technology for clean energy production [16, 17]. However, if PEMFCs are supplied with CO-containing hydrogen streams, the CO can lead to the deterioration in performance of PEMFCs [18, 19], and poison platinum fuel cell catalysts [20].

In recent years, the hydrolysis of metals such as Al, Mg, and Zn for pure hydrogen generation purposes has attracted much interest [21-28]. Al has shown potential as a hydrolyzing metal due to its abundance, low cost, and light weight. An example of the application of Al in the energy field is its use in batteries. The discharge potential of pure Al can be as low as –2.33V with respect to a standard hydrogen electrode if a strong alkaline electrolyte (pH 14) is present [29]. According to Li and Bjerrum, Al–air batteries consisting of an Al-based anode, gas diffusion cathode, and aqueous alkaline electrolyte comprise possibly the only battery system with a range and refueling time comparable to that of

internal combustion engines [30]. Of importance here is the potential of Al and Al-based composites to be used as hydrolyzing material. It has been reported that Al hydrolysis can be performed using water of varying qualities, e.g., pure, filtered, tap, sea, and urine [31-33]. Utilization of the generated hydrogen yields pure water, in certain cases, e.g., in combustion and fuel cell (FC) applications.

Al hydrolysis is a spontaneous reaction; it yields Al hydroxides (and to a lesser extent Al_2O_3), hydrogen, and heat. Reactions 1–3 show these reactions [34]:

$$2Al + 6H_2O \rightarrow 2Al(OH)_3 + 3H_2 + 16.3 \text{ MJ/kg Al} \quad (1)$$

$$2Al + 4H_2O \rightarrow 2AlOOH + 3H_2 + 15.5 \text{ MJ/kg Al} \quad (2)$$

$$2Al + 3H_2O \rightarrow Al_2O_3 + 3H_2 + 15.1 \text{ MJ/kg Al} \quad (3)$$

Al can essentially be rehydrolyzed indefinitely because the Al hydroxides can be converted to Al_2O_3, which can then be fully metallized to the metallic state (Al^0) by the Hall–Héroult process [23, 35, 36]. It is well known that a thin oxide layer on the Al surface prevents Reactions 1–3 from taking place under mild conditions (e.g., neutral pH water and standard ambient temperature/pressure) [1, 37].

Numerous studies have been performed on the removal/disruption of Al's oxide layer, by various means, e.g., submersing Al in acidic or alkaline solutions [38-41], amalgamation with Hg [42-44], and hydrothermal processes [45-51]. An attractive approach to removing this oxide layer is the mechanochemical or thermal processing of Al with various metals, metal oxides, salts, and combinations thereof, e.g., Al-x (x = combinations of Ga, Bi, In, Sn, Zn, Mg, Cu) [33, 34, 37, 52-65], Al-$BaCl_2$ [66], Al-KCl [67], Al-Ni-NaCl [68], and Al-Bi-hydride/salt [69]. However, the utilization of some Al composites is restricted to laboratory scale, for several reasons, e.g., corrosive reaction conditions when acidic/alkaline solutions are used, toxicity (e.g., Hg activated Al composites) and high cost (e.g., Ga activated Al composites) of activation compounds, requirement for expensive equipment for hydrothermal

reactions, Al composites exhibit too slow/fast hydrogen generation rates, and prolonged/energy intensive Al activation procedures.

Some research has been carried out on mechanochemically activating Al with metals such as Bi, Sn, In, Bi-In, Sn-In and Bi-Sn-In [1-3]. As far as the authors could assess, limited literature is available on Al's activation by Bi-Sn. A recent study by Xiao et al. presented the physical and chemical properties of ternary composites Al-7.5% Bi-2.5% Sn and Al-5% Bi-5% Sn, achieving hydrogen yields of 84–86% [70]. From literature, Bi is known to enable Al's reactivity towards pure water under ambient conditions [2], whereas Al-Sn composites show non-appreciable reactivity under the same conditions [71].

In an effort to better understand the effects of Bi and Sn on Al during mechanochemical processing, a series of Al-Bi-Sn composites was mechanochemically processed, their microstructures characterized, and the hydrolysis properties determined. A specific goal was to minimize the activation compound addition. Furthermore, a preliminary method for recovering Bi and Sn from hydrolyzed Al is discussed.

2. Material and methods

2.1. Materials

The following commercially available starting materials were obtained from Sigma-Aldrich (South Africa): Al powder (<200 μm, 99% purity), Bi granules (>99.99% purity), and Sn powder (<150 μm, 99.99% purity). Hydrochloric acid (HCl, 37%), nitric acid (HNO_3, 55%), and sulfuric acid (H_2SO_4, 98%) acid were obtained from Sigma-Aldrich (South Africa). Pure deionized water (18.2 $M\Omega.cm^{-1}$ resistivity) produced by a Milli-Q water purification system was used for all hydrolysis reactions. Pure nitrogen gas (99.99%) (Afrox, South Africa) was used during all purging procedures.

2.2. Composite preparation

Binary Al-Bi/Sn composites, containing 10 wt % Bi/Sn and with Al the balance, were prepared. A series of ternary Al-Bi-Sn composites was prepared; the composites contained various amounts of Sn and In in the range 0.8–9 wt %, with Al comprising the balance. These composites were divided into three groups: composites activated by a total of 10, 5, and 2.5 wt % activation compounds, and henceforth referred to as 10, 5, and 2.5% ternary composites, respectively. Table 1 summarizes the compositions of these composites. In an effort to maximize the Al content, activation compound addition did not exceed 10 wt %.

Table 1: Compositions of ternary Al composites

Composites	Activation compounds (10 wt % total)	
	Bi	Sn
Al-9% Bi-1% Sn	9	1
Al-7.5% Bi-2.5% Sn	7.5	2.5
Al-5% Bi-5% Sn	5	5
Al-2.5% Bi-7.5% Sn	2.5	7.5
Al-1% Bi-9% Sn	1	9
	Activation compounds (5 wt % total)	
Al-4.5% Bi-0.5% Sn	4.5	0.5
Al-3.75% Bi-1.25% Sn	3.75	1.25
Al-2.5% Bi-2.5% Sn	2.5	2.5
	Activation compounds (2.5 wt % total)	
Al-2.25% Bi-0.25% Sn	2.25	0.25
Al-1.7% Bi-0.8% Sn	1.7	0.8
Al-1.25% Bi-1.25% Sn	1.25	1.25

All composites were prepared by high-energy mechanochemical processing using a Retsch Emax ball mill (Retsch, Germany). Each composite was weight proportioned according to Table 1, and placed in a 125 mL stainless steel milling jar. Stainless steel milling balls (5 mm diameter) were added to the milling jar at a ball-to-composite ratio of 30:1 (30 g milling balls per 1 g composite). Thereafter, the milling jar was sealed with a

stainless steel aerated lid and purged with nitrogen. Each composite was milled for 30 min at 1500 rpm. After each milling procedure, the jar was allowed to cool to room temperature before the composites were recovered. Samples were stored in an airtight container until required for use in hydrolysis experiments. Each composite was prepared in duplicate.

2.3. Experimental setup and hydrogen measurements

All hydrolysis experiments were performed at standard ambient temperature and pressure in a 100 mL three-neck round-bottom flask. The three openings served the following purposes: i) one for water addition, using a pressure equalizing addition funnel, ii) one for insertion of a thermocouple for continuous temperature measurements, and iii) one for allowing the generated hydrogen to escape. Prior to hydrogen measurements, the generated hydrogen was dried using a Drietite^{TM} ($CaSO_4$) gas drier. The dried hydrogen gas flow was then measured with a digital thermal gas mass flow meter (Model GH-32654-12; Cole-Parmer, South Africa). Each hydrogen measurement was performed by hydrolyzing 0.5 g composite in 25 mL deionized water. During the hydrolysis reactions, the reaction solution was left unagitated. Each hydrolysis reaction was performed in duplicate to determine the standard deviation (SD). Thus, SD values are based on four hydrogen measurements, i.e., each composite prepared and hydrolyzed in duplicate.

The generated hydrogen was expressed as a conversion yield %, defined as the total volume hydrogen generated over the total theoretical hydrogen volume obtainable. By applying the ideal gas law, approximately 1360 NmL hydrogen is theoretically achievable per gram Al (assuming 100% Al hydrolysis) at standard ambient pressure and temperature. Thus, the hydrogen yield % presented in this study reflects the hydrogen obtained as a fraction of the obtainable 1360 NmL.

2.4. Characterization of samples

X-ray diffraction (XRD) measurements were performed using a Röntgen diffraction system (PW3040/60 X'Pert Pro). A back-loading preparation method was applied to determine the crystalline phases present in Al composites. X-rays generated by a Cu Kα X-ray tube were used to scan composites, and measurements were performed between variable divergence- and fixed-receiving slits. Identification of detected phases was performed using X'Pert HighScore Plus software (PANalytical). Relative abundances of composite phases were refined by the Rietveld method (Autoquan programme) [72].

The morphological and/or chemical characterization of prepared composites and as-received Al was carried out using a scanning electron microscope equipped with an energy dispersive X-ray spectrometer. A FEI Quanta 250 FEG scanning electron microscope incorporated with an Oxford X-map energy dispersive X-ray spectrometer system, operating at 15 kV and at a working distance of approximately 10 mm, was used. Samples considered for investigation were mounted on a sample stub using a carbon-based adhesive tape, and coated with a thin layer of gold–palladium (approximately 3 nm). For subsurface chemical characterization, composites were embedded in a carbon-based resin and cross-sectioned. Cross-sectioning was performed using a series of grinding plates and polishing cloths with ethanol as lubricant. Cross-sectioned samples were stored in an airtight container until required for characterization.

2.4. Leaching procedure

Acid leaching was applied in an effort to determine whether the activation compounds could be separated from hydrolyzed mechanochemically processed Al. For each leaching procedure, 0.5 g hydrolysis product was contacted with 100 mL of 25% H_2SO_4, 25% HCl, or 25% HNO_3 solution for 6 h. After contact, the solid residue was separated from the acid solutions by means of vacuum filtration. The leachate and residues were collected and

analyzed by inductive coupled plasma optical emission spectroscopy (ICP-OES) and scanning electron microscopy/energy dispersive X-ray spectroscopy (SEM-EDS), respectively. The samples designated for ICP-OES analysis were prepared by diluting the leachate to 1 L using deionized water. An Agilent 5110 ICP-OES instrument was used to determine the Al, Bi, and Sn contents in the leachates. ICP-OES calibration was performed using Ultraspec aqueous single (Al) and multielement (Bi and Sn) certified reference standards (De Bruyn Spectroscopic Solutions, South Africa).

3. Results and discussion

3.1. Characterization of processed composites

The general particle size and morphological changes of ductile, brittle, and ductile–brittle metals occurring during mechanochemical processing are explained in Refs. [73] and [74]. The behavior of Al-based composite particles during mechanochemical processing is relatively well understood and may be summarized as follows: i)initially, Al particles cold-weld to one another to form large particles and non-Al particles are distributed unevenly throughout these particles, ii) repetitive plastic deformation increases the degree of composite constituent distribution and induces work hardening of particles, which causes particles to fracture, and iii) fractured particles do not cold-weld, they rather agglomerate to other particles. Earlier studies investigated the behavior of Al during mechanochemical processing with certain metals: Al-Sn, Al-In, Al-Sn-In, Al-Bi, Al-Bi-In, and Al-Bi-Sn-In [1-3].

Of particular importance in our study is the particle size reduction and morphological changes that occur during the mechanochemical processing of Al and Sn (ductile metals), and Bi (brittle metal). Fig. 1 presents secondary electron SEM micrographs of the particle morphology of as-received Al (a) and the Al-2.5% Bi-2.5% Sn composite (b).

(a)

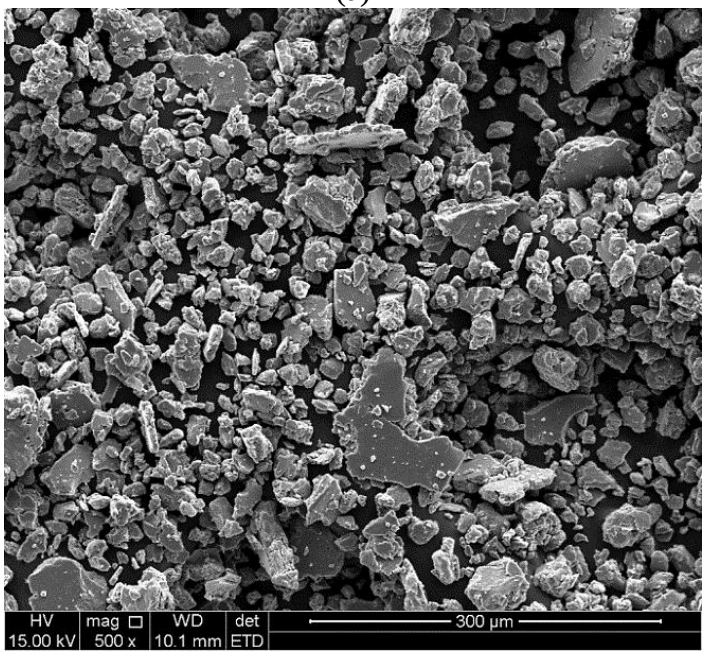

(b)

Fig. 1. Secondary electron SEM micrographs of particles: as-received Al (a) and mechanochemically processed Al-2.5% Bi-2.5% Sn composite (b).

Fig. 1 shows that Al underwent particle size reduction when mechanochemically processed with relatively small quantities of Bi and Sn (each 2.5 wt %). The as-received Al particles had uneven, strand-like morphologies, and diameters of 100–300 μm. The Al-2.5% Bi-2.5% Sn composite consisted of particles <100 μm, with a large fraction of particles <25 μm. However, particle size reduction alone does not necessarily mean that Al will react

with pure water under standard ambient conditions. The uniform distribution of Bi and Sn is likely to promote the hydrolysis reactivity of Al by disrupting the coherent oxide layer of Al and by forming micro-galvanic couplings with Al. The solubilities of Bi and Sn in Al are limited. For instance, Sn has a 0.1% solubility in Al at 600 °C [75, 76], whereas Bi has no appreciable solubility in Al and forms a segregated film on the surface of an Al melt [77]. However, these solubilities are only true for thermally treated Al-Bi/Sn composites. The distribution mechanism of Sn and In in Al particles during mechanochemical processing is presented and discussed by Ref. [3], and it is likely that Bi and Sn will behave in a similar manner.

EDS mapping was performed on the surface of Al-2.5% Bi-2.5% Sn particles to determine the distribution of Bi and Sn. Results are presented in Fig. 2. EDS mapping suggests that Bi and Sn could be distributed relatively evenly onto the surface of Al particles by mechanochemical processing, disrupting the coherent oxide layer, and that Bi/Sn does not occur as large particles (agglomerates/chunks). The potential difference between Al and a dissimilar metal controls Al's localized micro-galvanic corrosion [78, 79]. The standard electrode potentials of Al (–1.662 V), Bi (0.308 V) and Sn (–0.136 V) suggests that galvanic couplings between Al and Bi/Sn are likely to occur, which promote Al's dissolution in aqueous solutions.

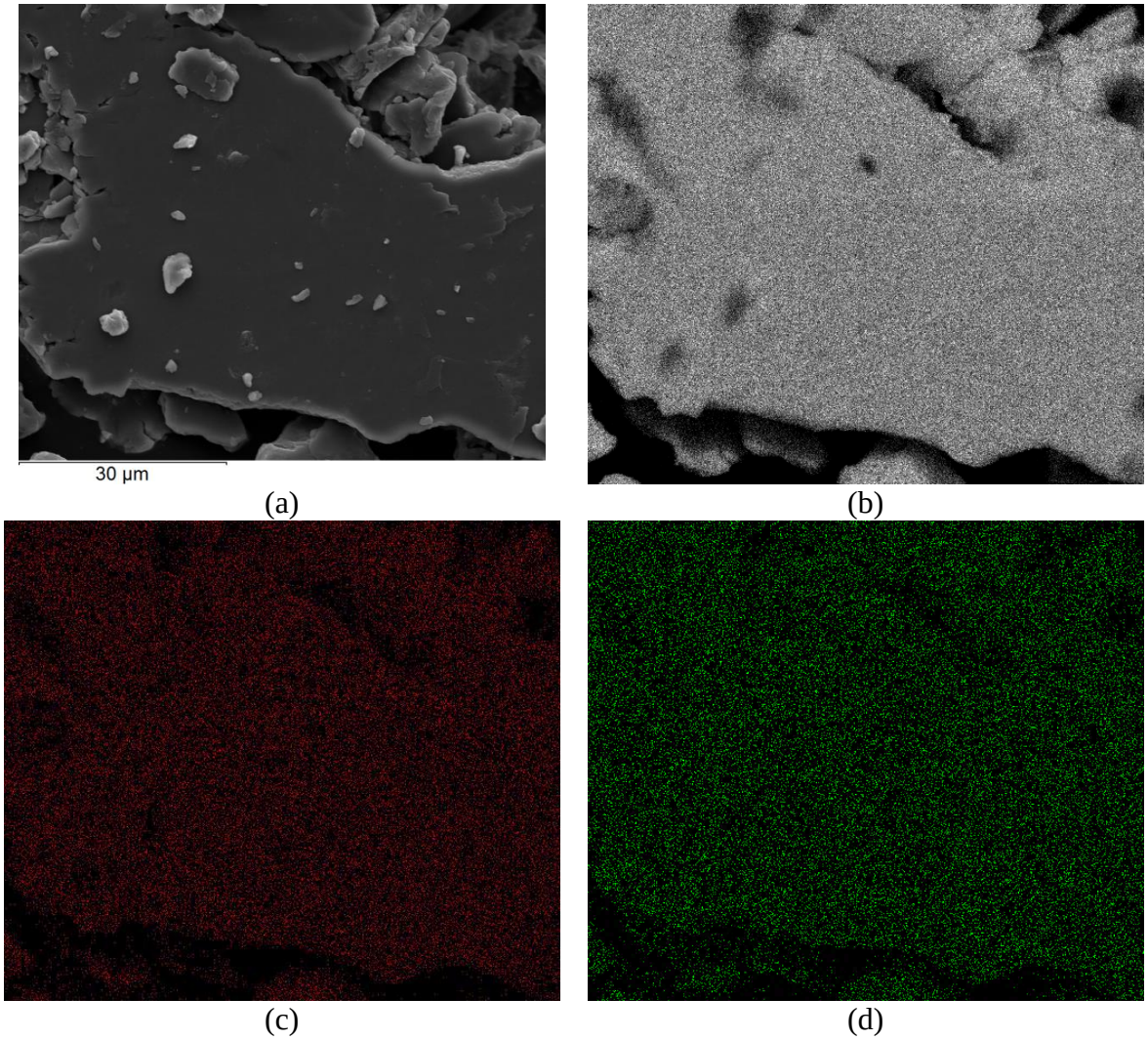

Fig. 2. Backscatter SEM micrograph of the surface of Al-2.5% Bi-2.5% Sn (a) and the corresponding EDS mappings for Al (b), Bi (c), and Sn (d).

Reboul et al. proposed a mechanism to explain Al's dissolution by activation compounds [80]. Initial galvanic coupling oxidizes Al and the activation compound, according to Reaction 4:

$$Al(M) \rightarrow Al^{3+} + M^{n+}, \text{ M = activation compound} \quad (4)$$

M^{n+} cations redeposit onto fresh Al surfaces due to the cathodic nature of the activation compounds relative to Al, according to the following electrochemical exchange reaction:

$$Al + M^{n+} \rightarrow Al^{3+} + M \quad (5)$$

Thus, Al is oxidized to Al^{3+} and migrates from the solid matrix into solution where it is hydrolyzed.

The mappings shown in Fig. 2 do not elucidate the subsurface Bi and Sn distribution. To determine whether the mechanism above only occurs on the surface of Al composite particles, Al-2.5% Bi-2.5% Sn particles were cross-sectioned and characterized in a similar manner to the particles presented in Fig. 2. This characterization is presented in Fig. 3.

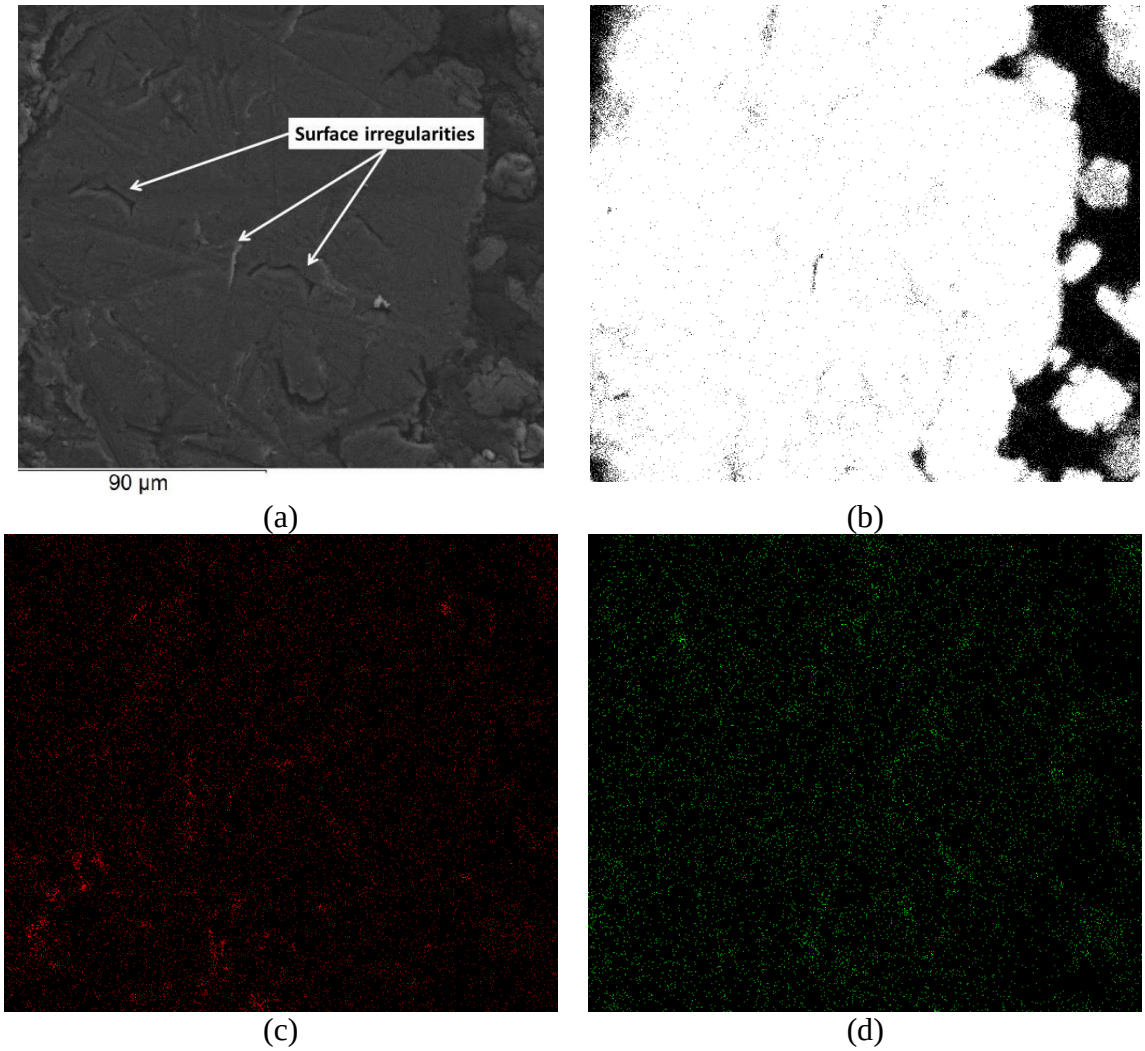

Fig. 3. Backscatter SEM micrograph of a cross-sectioned Al-2.5% Bi-2.5% Sn particle (a) and the corresponding EDS mapping for Al (b), Bi (c), and Sn (d).

The areas with higher particle contents observed in Fig. 3c and d may be ascribed to surface irregularities (cavities and hills, as indicated in Fig. 3a) on the cross-sectioned Al particle's surface. These irregularities are formed during the cross-sectioning procedure.

Nevertheless, Fig. 3 shows that Bi and Sn may be distributed throughout Al particles. EDS analysis of several areas within particles similar to the particle presented in Fig. 3b revealed Bi and Sn wt % contents of 2.26 and 1.99 wt %, respectively. Although, EDS analysis is a semi-quantitative method, with the oxygen determined by difference, the detected Bi and Sn contents showed some similarity to the predetermined values (indicated in Table 1). The Bi and Sn distributions presented in Fig. 3 were similar to Sn and In distributions [3]. Such a distribution may be ascribed to redistribution of composite constituents occurring during Al's repetitive plastic deformation induced by mechanochemical processing [81], enabling Bi and Sn intrusion of Al particles. During Al hydrolysis, it is likely that the presence of Al-Bi/Sn couplings will promote continuous galvanic activity throughout the reaction and related Al dissolution. Figs 2 and 3 suggest that Bi and Sn could be distributed relatively uniformly throughout Al particles.

Considering the observed Bi and Sn in Al distributions, binary Al-Bi/Sn composites were investigated by Rietveld refined XRD analysis to determine whether any intermetallic phases formed between Al and Bi/Sn. Fig. 4 shows these XRD patterns. Some Al peaks (2θ positions 44, 53, and 95) were partially excluded from Fig. 4 to increase detail of surrounding peaks. The corresponding R-factors (R_{exp}, R_p, R_{wp}) and goodness-of-fit (GoF) values are summarized in Table 2. It is evident from Fig. 4 that the only detected phases were Al, Bi, and Sn, which suggests that no reactions occurred between Al and Bi/Sn during mechanochemical processing.

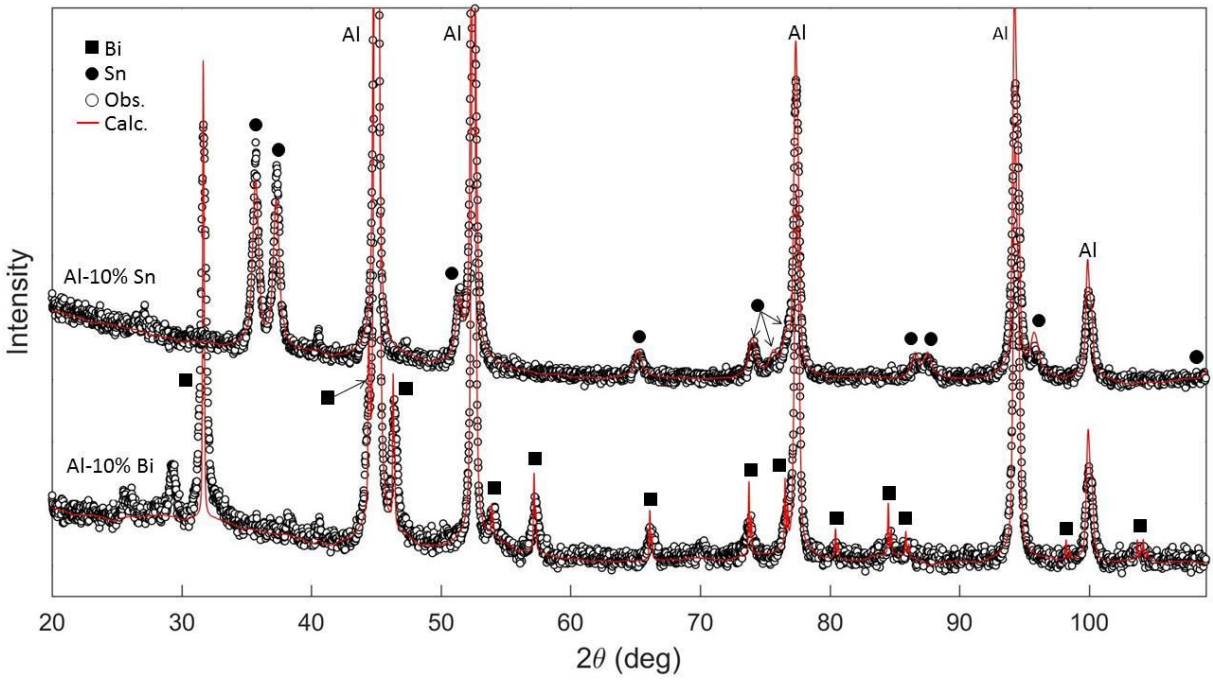

Fig. 4. Rietveld refinement of the XRD patterns of mechanochemically processed binary Al-10% Bi and Al-10% Sn composites. Observed and calculated values are indicated with black circles and a solid red line, respectively.

Table 2: Parameter values of Rietveld structural refinement analysis of binary Al composites

Sample	Parameter (%)			
	R_{exp}	R_p	R_{wp}	GoF
Al-Bi	4.20	7.96	12.08	2.88
Al-Sn	5.04	7.24	9.92	1.97

3.2. Hydrolysis of Al composites

The reactivities of mechanochemically processed Al-Bi and/or Al-Sn composites in neutral pH water at room temperature have been reported in Refs [2], [3], [33], and [70]. Binary composite reactivities are therefore not repeated in this study. The hydrogen yield curves and change in reaction temperature curves of 10% ternary composites are shown in Fig. 5. The SDs are excluded from Fig. 5 to prevent congestion of the results presented here. The SDs of maximum hydrogen yield and temperature did not exceed 3.9% and 2.1 °C, respectively.

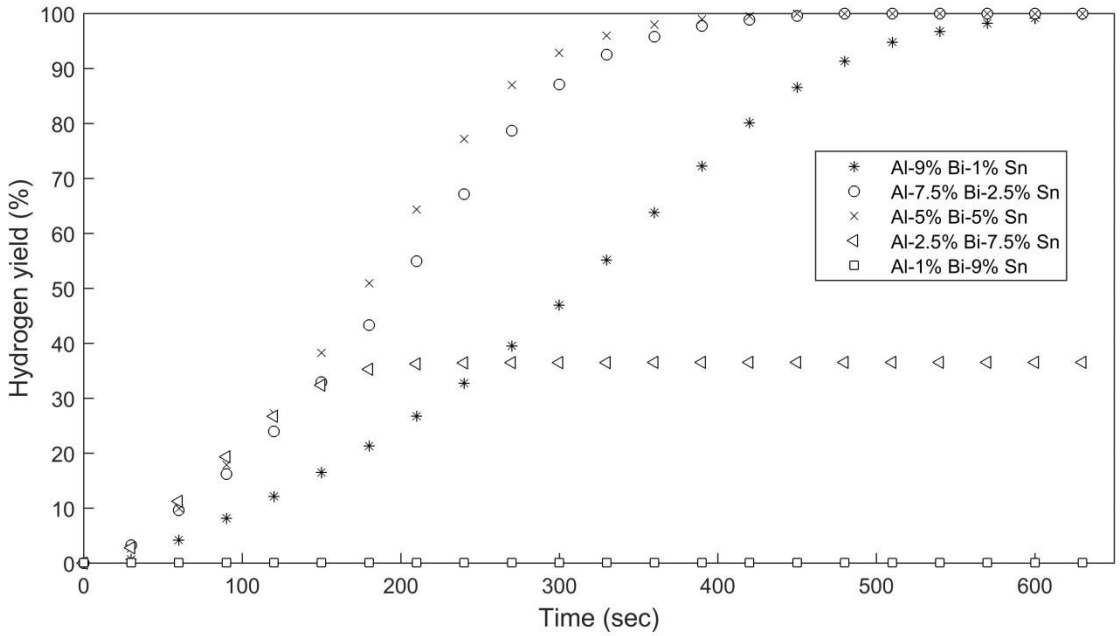

(a)

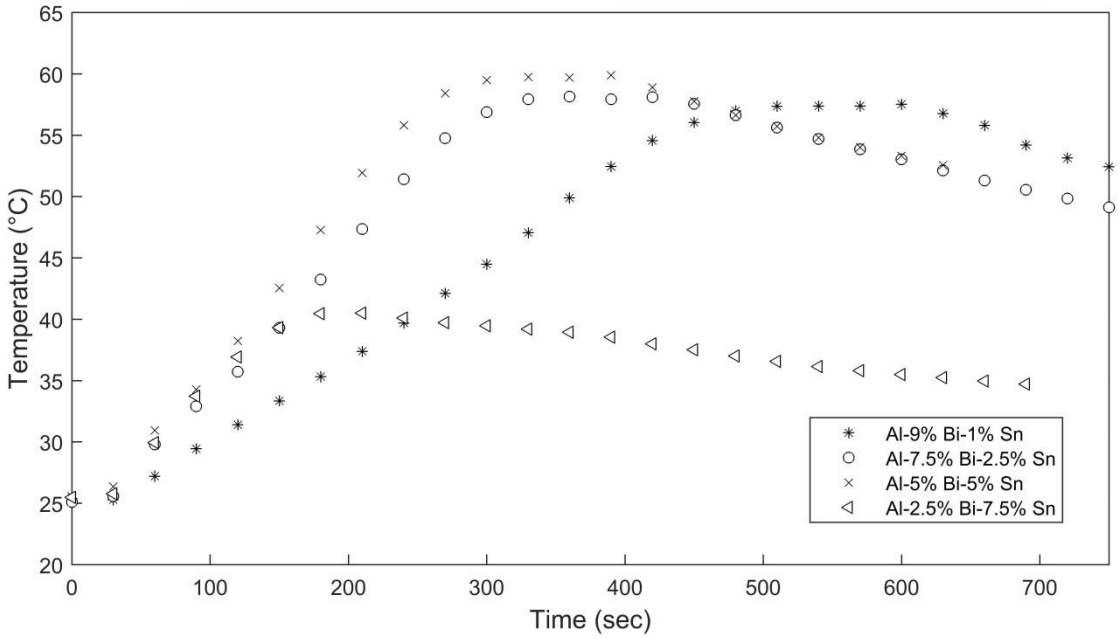

(b)

Fig. 5. The hydrogen yield (a) and changes in temperature curves (b) of 10% ternary Al-Bi-Sn composites.

It is evident from Fig. 5a that the Al-1% Bi-9% Sn composite was nonreactive in pure water at 25 °C. Al-2.5% Bi-7.25% Sn achieved a hydrogen yield of 38.5 ± 2.5%, while the other ternary composites achieved >99% yields. Al-5% Bi-5% Sn and Al-7.5% Bi-2.5% Sn had similar reaction kinetics and their hydrolysis reactions were completed after 430 and 480 sec, respectively. Al-9% Bi-1% Sn achieved a >99% hydrogen yield after approximately 640

sec. Bi is known to be superior to Sn in promoting the hydrolysis reactivity of Al [2, 71]. This was evident when comparing the reactivities of the Al-1% Bi-9% Sn and Al-9% Bi-1% Sn composites. However, when considering that Al-5% Bi-5% Sn is more reactive than Al-7.5% Bi-2.5% Sn, it is clear that a certain degree of synergy between Bi and Sn exists when enabling Al's hydrolysis reactivity. Bi-Sn synergy will be contextualized in the following texts.

It is evident from Fig. 5b that the reactivity of a composite is reflected in its increase in reaction temperature curve. For the two most reactive composites, Al-5% Bi-5% Sn and Al-7.5% Bi-2.5% Sn, reaction temperature increases of approximately 35 and 33 °C, respectively, were observed. Similarly, for Al-9% Bi-1% Sn, a reaction temperature increase of 32 °C was observed; however, this increase was observed over a longer period, corresponding with this composite's hydrolysis reaction time. Al-2.5% Bi-7.5% Sn showed a relatively small temperature increase of 15 °C, ascribed to its relatively low hydrolysis reactivity.

An objective of this study was to maximize the hydrogen volume obtainable from a mass unit of composite by minimizing the composite non-Al constituency. Therefore, the activation compound addition of the three most reactive Al composites presented in Fig. 5a was reduced to 5%. These 5% ternary composites were hydrolyzed in the same manner as the 10% ternary composites. Results of hydrogen yields of the 5% ternary Al-Bi-Sn composites are presented in Fig. 6. The hydrogen yield curves of 10% ternary composites as presented in Fig. 5a are included here as dashed lines, for reference purposes. The SD of the maximum hydrogen yield did not exceed 3.5%.

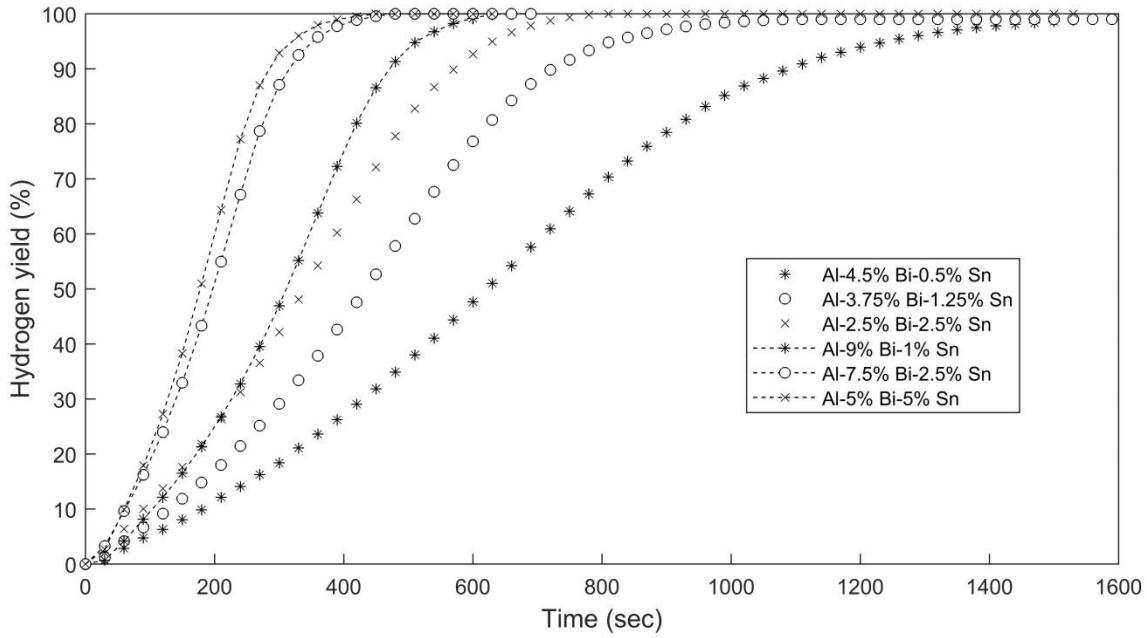

Fig. 6. Hydrogen yields of 5% ternary Al-Bi-Sn composites. The hydrogen yield curves of 10% ternary composites are included (indicated by dashed lines) and serve as references.

It is evident from Fig. 6 that the 5% ternary composites had >99% yields and that their hydrogen yield curves resembled that of their 10 wt % counterparts. The only major difference observed was the slower hydrogen release rates, as is evident from the prolonged reaction times. Decreasing the amount of activation compound addition to composites would reduce associated effects of such activation compounds; specifically, Al's protective oxide layer disruption caused by Bi and Sn and the amount of micro-galvanic Al-Bi/Sn cell formation, which could decrease Al's reactivity towards neutral pH water. However, when considering the high hydrogen yields of the 5% ternary composites, this was not the case. Elevated reaction temperatures are known to promote Al hydrolysis [2, 82]. When taking this and the increase in Al content of the 5% ternary composites into consideration, it is likely that Al's exothermic hydrolysis reaction was adequately self-catalyzing to achieve >99% hydrogen yields. Al-2.5% Bi-2.5% Sn and Al-3.75% Bi-1.25% Sn exhibited reaction temperature increases of 31 and 29 °C, respectively, while Al-4.5% Bi-0.5% Sn exhibited a 23 °C increase. These temperature increases were 4–9 °C lower than with the 10% ternary

composites. However, it is evident that such temperature increases still promoted the hydrolysis reaction sufficiently, as is evident from the >99% hydrogen yields.

A further decrease in activation compound addition to 2.5 wt % yielded nonreactive composites. The 2.5% ternary composites mainly consisted of large chunks of seemingly agglomerated material, indicating that the composite constituents did not undergo homogenization. These composites were nonreactive or exhibited very limited reactivity in neutral pH waters, and were not considered further.

3.4. Ternary composites: intermetallic phases

The XRD patterns of binary Al and Bi/Sn presented in Fig. 4 (Section 3.1) showed that no intermetallic phases formed between Al and Bi/Sn during the mechanochemical processing of binary Al-Bi and Al-Sn. To determine whether intermetallic phases formed between Al, Bi, and/or Sn, XRD analysis was performed on 10% ternary composites. Fig. 7 presents the Rietveld refined XRD patterns. Only the Rietveld refined calculated values are presented here, to prevent cluttering. The corresponding R-factors and GoF values are summarized in Table 3.

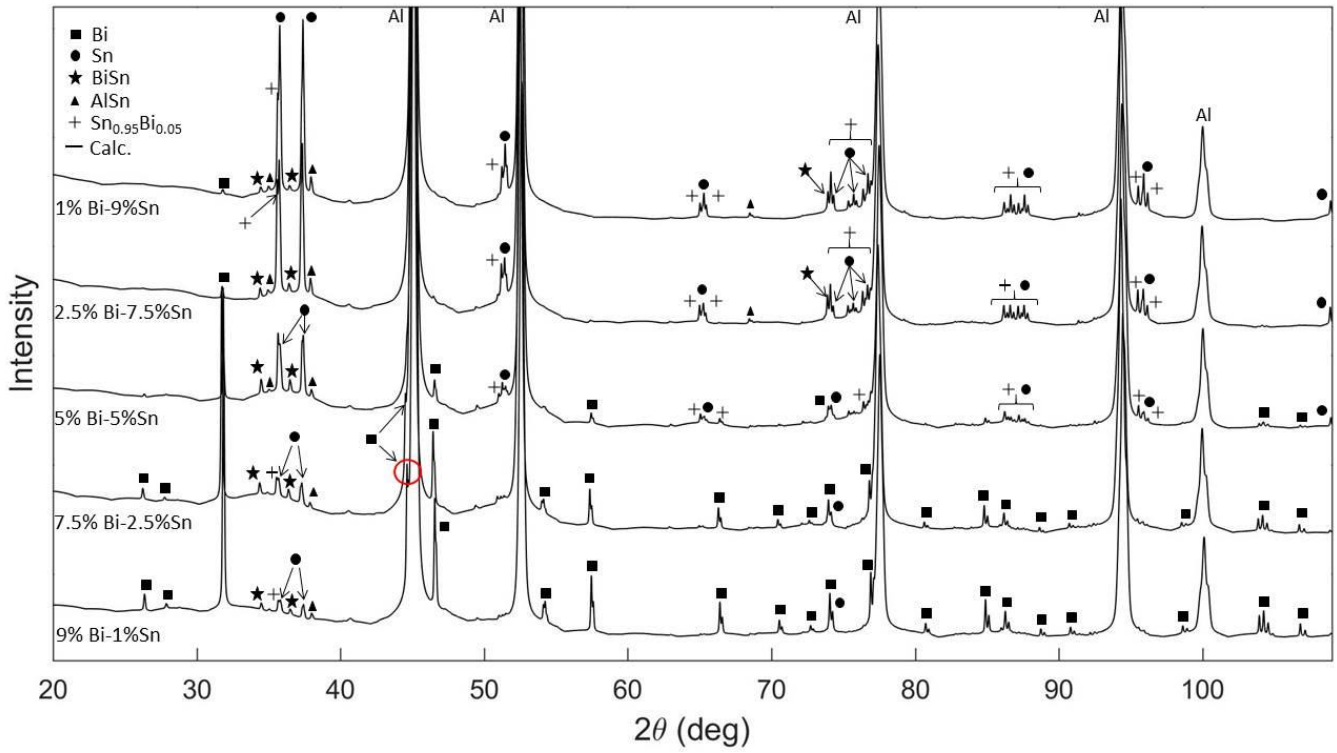

Fig. 7. The Rietveld refinement of XRD patterns of 10% ternary composites.

Table 3: Parameter values of Rietveld structural refinement analysis of 10% ternary composites

Sample	Parameter (%)			
	R_{exp}	R_p	R_{wp}	GoF
Al-1% Bi-9% Sn	4.47	7.24	10.13	2.27
Al-2.5% Bi-7.5% Sn	4.25	7.12	10.16	2.39
Al-5% Bi-5% Sn	4.62	7.53	10.76	2.33
Al-7.5% Bi-2.5% Sn	4.23	7.73	11.28	2.65
Al-9% Bi-1% Sn	4.84	8.06	11.79	2.44

Fig. 7 shows that the detected phases were (in no specific order) Al, Bi, and Sn, intermetallic Bi-Sn phases (BiSn and $Sn_{0.95}Bi_{0.05}$), and AlSn phases. The following deductions are made from Fig. 8: i) when considering relative peak intensities, it is clear that Bi and Sn did not readily form intermetallic phases with each other or Al, ii) the dominant Bi and Sn phases of samples with Bi>Sn and Bi<Sn were Bi and Sn, respectively, and for Bi=Sn, large Bi and Sn peaks were present, iii) minor AlSn, BiSn, and $Sn_{0.95}Bi_{0.05}$ phases were detected in all cases, vi) AlSn and $Sn_{0.95}Bi_{0.05}$ peak intensity decreased with increasing Bi content, and v) the presence of BiSn phases were independent of Bi:Sn ratio, as in all

cases, minor BiSn phases were detected. It is also noteworthy that the previously indicated Sn in Al and Bi in Al liquidus solubilities (Section 3.1) are reflected in Fig. 7, i.e., Sn has very limited solubility in Al and is reflected as minor AlSn peaks, and no AlBi phases are detected due to the insolubility of Bi in Al. Furthermore, Fig. 4 shows that no AlSn phases were formed during the mechanochemical processing of Al-Sn binary composites; however, AlSn phases were observed in ternary Al-Bi-Sn composites. This suggests that the presence of Bi may have had an influence on Al-Sn interparticle behavior during mechanochemical processing. However, it is currently unclear how Bi promoted/enabled AlSn phase formation (this may be considered further in future studies).

From Figs 5a and 7, it is evident that composites with Bi as the dominant phase were more reactive than phases with Sn as the dominant phase. For instance, the reactivities of the composites (in decreasing order) were Al-5% Bi-5% Sn, Al-7.5% Bi-2.5% Sn, Al-9% Bi-1% Sn, Al-2.5% Bi-7.5% Sn, and Al-1% Bi-9% Sn. It is also evident that certain Bi:Sn wt % ratios were more effective at activating Al. For example, a Bi:Sn wt % ratio of 1 produced the most reactive composite, whereas composites with wt % ratios of 3 and 9 were less reactive. In the cases were the Bi:Sn wt % ratios were <1, composites exhibited low/no reactivities, as is evident from the reactivities of Al-2.5% Bi-7.5% Sn and Al-1% Bi-9% Sn.

3.5. Effects of initial water temperature

To determine the effects of the initial reaction temperature on the hydrolysis reaction, Al-5% Bi-5% Sn was hydrolyzed at starting temperatures of 8, 14, 25, 45, and 55 °C. Fig. 8 shows the hydrogen yield (a) and reaction temperature changes (b). The SDs of maximum hydrogen yield for initial temperature reactions of ≤25 °C and >25 °C were <3.0 and <6.3%, respectively. Maximum standard temperature deviations were <4.2 °C in all cases. The inherent temperature increase of 8 °C reaction solution is included as a dashed line in Fig. 8(b) to show heat transfer from the ambient environment to the reaction solution.

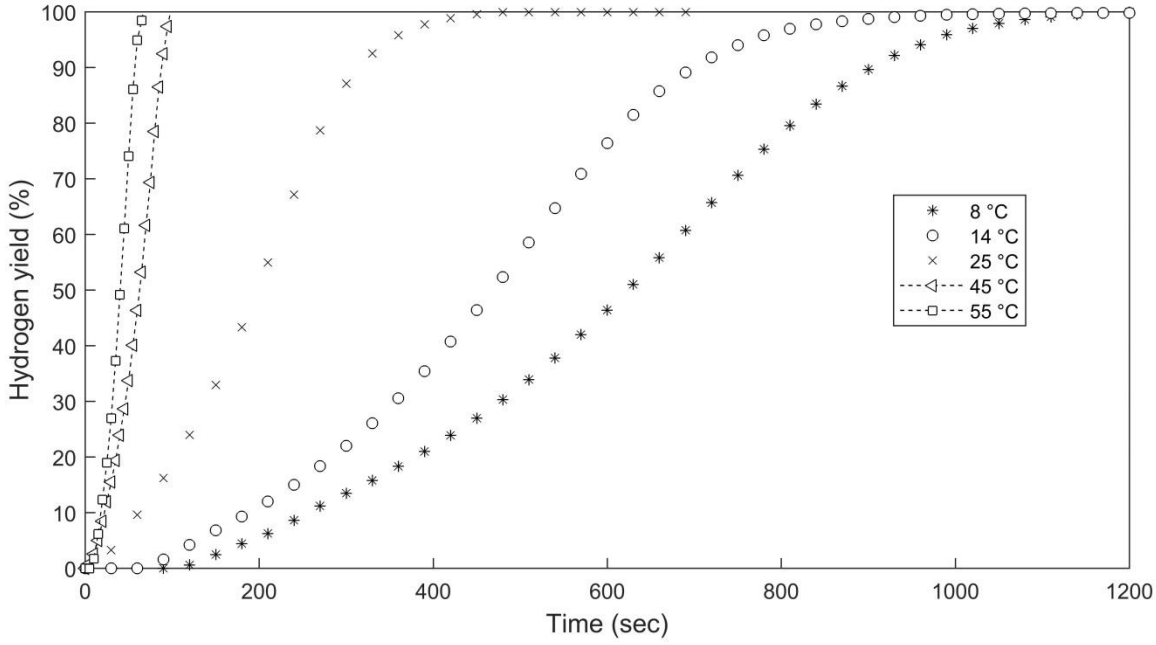

(a)

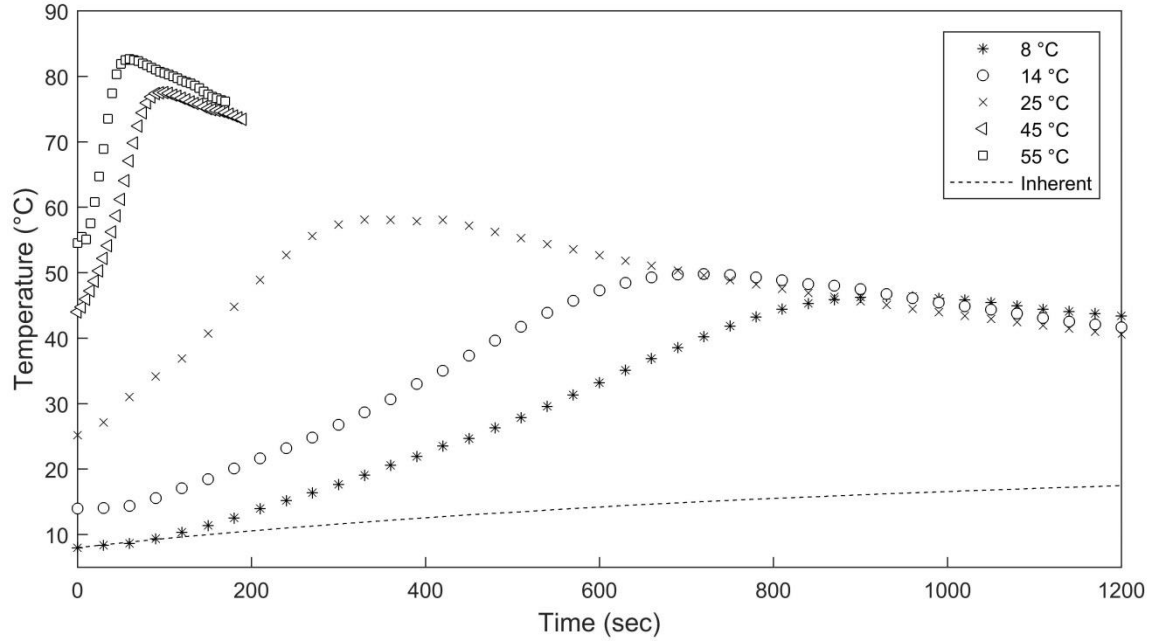

(b)

Fig. 8. Hydrogen yields of Al-5% Bi-5% Sn hydrolyzed at starting temperatures of 8, 14, 25, 45, and 55 °C (a) and the observed changes in reaction temperature during hydrolysis (b).

Fig. 8a suggests that the hydrogen release rate of Al-5% Bi-5% Sn may be partially reduced by decreasing the initial reaction temperature, without sacrificing hydrogen yield, i.e. the hydrogen yield is >99%, regardless of initial reaction temperature. The induction period increased with a decrease in initial reaction temperature. The 8, 14, and 25 °C hydrolysis

reactions initiated after approximately 100, 60, and 20 sec, respectively, whilst the 45 and 55 °C reactions initiated almost instantly when the composite came into contact with water.

Fig. 8b shows that the average temperature increase for the 8, 14, 25, 45, and 55 °C hydrolysis reactions were 38, 35, 33, 34, and 28 °C, respectively. The dotted line in Fig. 8b illustrates the heat transfer from the reaction to the environment, which explains why the 8 °C reaction had such a large increase in reaction temperature. The opposite is evident for the 55 °C reaction, i.e., this reaction exhibits the smallest reaction temperature increase due to heat transfer from the reaction to the environment. Considering these heat transfers mentioned, it can be said that the reaction temperature increases for each reaction were relatively similar.

3.6. Recovery of activation compounds

The recovery of activation compounds from spend mechanochemically activated Al is a topic that has been largely unexplored to date. Three common acids (HCl, H_2SO_4, HNO_3) were used in efforts to separate the activation compounds from the spent Al. Al-5% Bi-5% Sn was selected for this investigation because it has equal Bi and Sn content. Table 4 presents the chemical analysis of the leachates (determined by ICP-OES) and the surface chemical composition of the residues (determined by SEM-EDS). The leachate results are presented in units of wt % and solubilized % (amount determined by ICP-OES, expressed as a fraction of the total theoretical amount). As stated earlier, SEM-EDS results should be considered as semi-quantitative.

Table 4: Chemical analysis of Al-5% Bi-5% Sn leachates and residues				
Acid solution	ICP-OES (wt %, % solubilized)			
	Al	Bi	Sn	
HCl	89.54 (91.04)	5.16 (94.52)	5.30 (97.00)	
HNO_3	93.96 (96.29)	5.23 (96.52)	0.81 (14.88)	
H_2SO_4	92.96 (92.24)	1.41 (25.16)	5.63 (100.56)	
	SEM-EDS (wt %)			
	Al	Bi	Sn	O
HCl	4.19±0.72	4.39±1.22	2.72±1.26	88.70±2.98
HNO_3	0.52±0.10	0.29±0.15	55.57±0.64	43.62±0.85
H_2SO_4	0.82±0.05	71.89±0.38	1.75±0.08	25.53±0.37

It is evident for Table 4 that the acid solutions under consideration dissolved the majority of composite constituents; however, the HNO_3 and H_2SO_4 solutions only partially solubilized Sn (14.88% solubilized) and Bi (25.16% solubilized). SEM-EDS analysis of the HNO_3 and H_2SO_4 residues suggests that these particles were rich in Sn and Bi, respectively. Selective Al dissolution or collective Bi and Sn dissolution were not achieved using the acids considered. Ideally, a leaching procedure should selectively solubilize either Al or the activation compounds, with minimal dissolution of the nonselected compound(s). Furthermore, for a leaching procedure to be attractive, the leaching parameters and extraction chemical concentration should be as mild/low as possible.

It is recommended that the use of other extraction chemicals (including alkaline chemicals), and the development and optimization of a selective leaching procedure should be addressed in future research.

4. Conclusions

A series of ternary Al-Bi-Sn composites was prepared by mechanochemical processing. SEM micrographs suggest that Bi and Sn promoted the structural failure of Al during mechanochemical processing, which then readily decreased Al's overall particle size.

Surface and subsurface SEM-EDS analysis suggest that Bi and Sn were distributed relatively evenly throughout the Al particles, hence promoting continuous micro-galvanic activity between anodic Al and cathodic Bi/Sn during hydrolysis reactions. XRD analysis revealed minor intermetallic phases, i.e., AlSn, BiSn, and $Sn_{0.95}Bi_{0.05}$, with the major phases being Al, Bi, and Sn. This indicated that formation of intermetallic phases between Al, Bi and Sn did not occur readily during mechanochemical processing. High hydrogen yielding ternary composites (>99%) were prepared and the activation compound addition could be reduced from 10 to 5 wt % without affecting the hydrogen yield. Decreasing the initial reaction temperature to 8 °C did not affect the hydrogen yield of Al-5% Bi-5% Sn. Preliminary results indicate that Bi and Sn could be partially recovered from hydrolyzed Al using H_2SO_4 and HNO_3, respectively.

Acknowledgements

The Department of Science and Technology (DST) HySA Infrastructure Center of Competence at the North West University, South Africa, is acknowledged for financial support.

References

[1] S.P. Du Preez, D.G. Bessarabov, Hydrogen generation by means of hydrolysis using activated Al-In-Bi-Sn composites for electrochemical energy applications, Int. J. Electrochem. Sci. 12 (2017a) 8663-8682. DOI: https://doi.org/10.20964/2017.09.22

[2] S.P. Du Preez, D.G. Bessarabov, Hydrogen generation of mechanochemically activated AlBiIn composites, Int. J. Hydrogen Energy. 42 (2017b) 16589-16602. DOI: https://doi.org/10.1016/j.ijhydene.2017.05.211

[3] S.P. Du Preez, D.G. Bessarabov, Hydrogen generation by the hydrolysis of mechanochemically activated aluminum-tin-indium composites in pure water, Int. J. Hydrogen Energy. In press (2018). DOI: https://doi.org/10.1016/j.ijhydene.2018.09.133

[4] J. E. Funk, Thermochemical hydrogen production: past and present, Int. J. Hydrogen Energy. 26 (2001) 185-190. DOI: https://doi.org/10.1016/S0360-3199(00)00062-8

[5] H. Kaneko, N. Gokon, N. Hasegawa, Y. Tamaura, Solar thermochemical process for hydrogen production using ferrites, Energy. 30 (2005) 2171-2178. DOI: https://doi.org/10.1016/j.energy.2004.08.020

[6] A.V. Levchenko, Y.A. Dobrovolsky, N.G. Bukun, L.S. Leonova, T.S. Zyubina, V.S. Neudachina, et al., Chemical and electrochemical processes in low-temperature superionic hydrogen sulfide sensors, Rus. J. Electrochem. 43 (2007) 552-560. DOI: https://doi.org/10.1134/S1023193507050084

[7] D.G. Bessarabov, G. Human, A.J. Kruger, S. Chiuta, P.M. Modisha, S.P. du Preez, et al., South African hydrogen infrastructure (HySA infrastructure) for fuel cells and energy storage: Overview of a projects portfolio, Int. J. Hydrogen Energy. 42 (2017) 13568-13588. DOI: https://doi.org/10.1016/j.ijhydene.2016.12.140

[8] Y. Amao, Y. Tomonou, I. Okura, Highly efficient photochemical hydrogen production system using zinc porphyrin and hydrogenase in CTAB micellar system, Sol. Energy

Mater Sol. Cells. 79 (2003) 103-111. DOI: https://doi.org/10.1016/S0927-0248(02)00373-2

[9] A.A. Nada, M.H. Barakat, H.A. Hamed, N.R. Mohamed, T.N. Veziroglu, Studies on the photocatalytic hydrogen production using suspended modified TiO2 photocatalysts, Int. J. Hydrogen Energy. 30 (2005) 687-691. DOI: https://doi.org/10.1016/j.ijhydene.2004.06.007

[10] V. Sediroglu, İ. Eroglu, M. Yücel, L. Türker, U. Gündüz, The biocatalytic effect of Halobacterium halobium on photoelectrochemical hydrogen production, J. Biotechnol. 70 (1999) 115-124. DOI: https://doi.org/10.1016/S0168-1656(99)00065-6

[11] P.T. Sekoai, C.N.M. Ouma, S.P. du Preez, P. Modisha, N. Engelbrecht, D.G. Bessarabov, et al., Application of nanoparticles in biofuels: An overview, Fuel. 237 (2019) 380-397. DOI: https://doi.org/10.1016/j.fuel.2018.10.030

[12] S. Damyanova, B. Pawelec, K. Arishtirova, J. Fierro, Ni-based catalysts for reforming of methane with CO_2, Int. J. Hydrogen Energy. 37 (2012) 15966-15975. DOI: https://doi.org/10.1016/j.ijhydene.2012.08.056

[13] M. Balat, Potential importance of hydrogen as a future solution to environmental and transportation problems, Int. J. Hydrogen Energy. 33 (2008) 4013-4029. DOI: https://doi.org/10.1016/j.ijhydene.2008.05.047

[14] S.J. Peighambardoust, S. Rowshanzamir, M. Amjadi, Review of the proton exchange membranes for fuel cell applications, Int. J. Hydrogen Energy. 35 (2010) 9349-9384. DOI: https://doi.org/10.1016/j.ijhydene.2010.05.017

[15] J. Divisek, H.F. Oetjen, V. Peinecke, V.M. Schmidt, U. Stimming, Components for PEM fuel cell systems using hydrogen and CO containing fuels, Electrochim. Acta. 43 (1998) 3811-3815. DOI: https://doi.org/10.1016/S0013-4686(98)00140-6

[16] N. Edwards, S.R. Ellis, J.C. Frost, S.E. Golunski, A.N.J. van Keulen, N.G. Lindewald, et al., On-board hydrogen generation for transport applications: the HotSpot™ methanol processor, J. Power Sources. 71 (1998) 123-128. DOI: https://doi.org/10.1016/S0378-7753(97)02797-3

[17] P. Gray, M. Petch, Advances with HotSpot™ Fuel Processing Efficient Hydrogen Production for use with Solid Polymer Fuel Cells, Platin. Met. Rev. 44 (2000) 108.

[18] T.V. Reshetenko, K. Bethune, R. Rocheleau, Spatial proton exchange membrane fuel cell performance under carbon monoxide poisoning at a low concentration using a segmented cell system, J. Power Sources. 218 (2012) 412-423. DOI: http://dx.doi.org/10.1016/j.jpowsour.2012.07.015

[19] P.V. Gosavi, R.B. Biniwale, Catalytic preferential oxidation of carbon monoxide over platinum supported on lanthanum ferrite–ceria catalysts for cleaning of hydrogen, J. Power Sources. 222 (2013) 1-9. DOI: https://doi.org/10.1016/j.jpowsour.2012.07.095

[20] A. Faur Ghenciu, Review of fuel processing catalysts for hydrogen production in PEM fuel cell systems, Curr. Opin. Solid State Mater. Sci. 6 (2002) 389-399. DOI: https://doi.org/10.1016/S1359-0286(02)00108-0

[21] A.V. Ilyukhina, A.S. Ilyukhin, E.I. Shkolnikov, Hydrogen generation from water by means of activated aluminum, Int. J. Hydrogen Energy. 37 (2012) 16382-16387. DOI: http://dx.doi.org/10.1016/j.ijhydene.2012.02.175

[22] W.-Z. Gai, W.-H. Liu, Z.-Y. Deng, J.-G. Zhou, Reaction of Al powder with water for hydrogen generation under ambient condition, Int. J. Hydrogen Energy. 37 (2012) 13132-13140. DOI: https://doi.org/10.1016/j.ijhydene.2012.04.025

[23] Y. Liu, X. Wang, H. Liu, Z. Dong, S. Li, H. Ge, et al., Investigation on the improved hydrolysis of aluminum–calcium hydride-salt mixture elaborated by ball milling, Energy. 84 (2015) 714-721. DOI: http://dx.doi.org/10.1016/j.energy.2015.03.035

[24] T. Hiraki, S. Yamauchi, M. Iida, H. Uesugi, T. Akiyama, Process for recycling waste aluminum with generation of high-pressure hydrogen, Environ. Sci. Tech. 41 (2007) 4454-4457. DOI: http://dx.doi.org/10.1021/es062883l

[25] C.-Y. Cho, K.-H. Wang, J.-Y. Uan, Evaluation of a new hydrogen generating system: Ni-rich magnesium alloy catalyzed by platinum wire in sodium chloride solution, Mater. Trans. 46 (2005) 2704-2708. DOI: https://doi.org/10.2320/matertrans.46.2704

[26] S. Wang, L.-X. Sun, F. Xu, C.-L. Jiao, J. Zhang, H.-Y. Zhou, et al., Hydrolysis reaction of ball-milled Mg-metal chlorides composite for hydrogen generation for fuel cells, Int. J. Hydrogen Energy. 37 (2012) 6771-6775. DOI: https://doi.org/10.1016/j.ijhydene.2012.01.099

[27] K. Wegner, H.C. Ly, R.J. Weiss, S.E. Pratsinis, A. Steinfeld, In situ formation and hydrolysis of Zn nanoparticles for production by the 2-step ZnO/Zn water-splitting thermochemical cycle, Int. J. Hydrogen Energy. 31 (2006) 55-61. DOI: http://dx.doi.org/10.1016/j.ijhydene.2005.03.006

[28] I. Vishnevetsky, M. Epstein, Production of hydrogen from solar zinc in steam atmosphere, Int. J. Hydrogen Energy. 32 (2007) 2791-2802. DOI: https://doi.org/10.1016/j.ijhydene.2007.04.004

[29] D. Rand, R. Woods, R. Dell, Batteries for Electric Vehicles, Research Studies Press Ltd, Somerset, 1998.

[30] Q. Li, N.J. Bjerrum, Aluminum as anode for energy storage and conversion: a review, J. Power Sources. 110 (2002) 1-10. DOI: https://doi.org/10.1016/S0378-7753(01)01014-X

[31] M.-S. Zou, X.-Y. Guo, H.-T. Huang, R.-J. Yang, P. Zhang, Preparation and characterization of hydro-reactive Mg–Al mechanical alloy materials for hydrogen production in seawater, J. Power Sources. 219 (2012) 60-64. DOI: https://doi.org/10.1016/j.jpowsour.2012.07.008

[32] S. Elitzur, V. Rosenband, A. Gany, Urine and aluminum as a source for hydrogen and clean energy, Int. J. Hydrogen Energy. 41 (2016) 11909-11913. DOI: https://doi.org/10.1016/j.ijhydene.2016.05.259

[33] H. Wang, Y. Chang, S. Dong, Z. Lei, Q. Zhu, P. Luo, et al., Investigation on hydrogen production using multicomponent aluminum alloys at mild conditions and its mechanism, Int. J. Hydrogen Energy. 38 (2013) 1236-1243. DOI: http://dx.doi.org/10.1016/j.ijhydene.2012.11.034

[34] A.V. Ilyukhina, O.V. Kravchenko, B.M. Bulychev, Studies on microstructure of activated aluminum and its hydrogen generation properties in aluminum/water reaction, J. Alloys Compd. 690 (2017) 321-329. DOI: http://dx.doi.org/10.1016/j.jallcom.2016.08.151

[35] H.Z. Wang, D.Y.C. Leung, M.K.H. Leung, M. Ni, A review on hydrogen production using aluminum and aluminum alloys, Renewable Sustainable Energy Rev. 13 (2009) 845-853. DOI: http://dx.doi.org/10.1016/j.rser.2008.02.009

[36] W.E. Haupin, Electrochemistry of the Hall-Heroult process for aluminum smelting, J. Chem. Educ. 60 (1983) 279. DOI: https://doi.org/10.1021/ed060p279

[37] M. Baniamerian, S. Moradi, Al–Ga doped nanostructured carbon as a novel material for hydrogen production in water, J. Alloys Compd. 509 (2011) 6307-6310. DOI: https://doi.org/10.1016/j.jallcom.2011.03.069

[38] D. Belitskus, Reaction of Aluminium with Sodium Hydroxide Solution as a Source of Hydrogen, J. Electrochem. Soc. 117 (1970) 1097-1099. DOI: http://dx.doi.org/10.1149/1.2407730

[39] L. Soler, J. Macanás, M. Muñoz, J. Casado, Synergistic hydrogen generation from aluminum, aluminum alloys and sodium borohydride in aqueous solutions, Int. J.

Hydrogen Energy. 32 (2007) 4702-4710. DOI: http://dx.doi.org/10.1016/j.ijhydene.2007.06.019

[40] E.-D. Wang, P.-F. Shi, C.-Y. Du, X.-R. Wang, A mini-type hydrogen generator from aluminum for proton exchange membrane fuel cells, J. Power Sources. 181 (2008) 144-148. DOI: http://dx.doi.org/10.1016/j.jpowsour.2008.02.088

[41] A.O. Dudoladov, O.A. Buryakovskaya, M.S. Vlaskin, A.Z. Zhuk, E.I. Shkolnikov, Generation of hydrogen by aluminium oxidation in aquaeous solutions at low temperatures, Int. J. Hydrogen Energy. 41 (2016) 2230-2237. DOI: http://dx.doi.org/10.1016/j.ijhydene.2015.11.122

[42] J. Bessone, The activation of aluminium by mercury ions in non-aggressive media, Corros. Sci. 48 (2006) 4243-4256. DOI: https://doi.org/10.1016/j.corsci.2006.03.013

[43] M.-q. Fan, L.-x. Sun, F. Xu, Study of the controllable reactivity of aluminum alloys and their promising application for hydrogen generation, Energy Convers. Manage. 51 (2010) 594-599. DOI: http://dx.doi.org/10.1016/j.enconman.2009.11.005

[44] X. Huang, C. Lv, Y. Huang, S. Liu, C. Wang, D. Chen, Effects of amalgam on hydrogen generation by hydrolysis of aluminum with water Int. J. Hydrogen Energy. 36 (2011) 15119-15124. DOI: http://dx.doi.org/10.1016/j.ijhydene.2011.08.073

[45] M. Vlaskin, E. Shkolnikov, A. Lisicyn, A. Bersh, A. Zhuk, Computational and experimental investigation on thermodynamics of the reactor of aluminum oxidation in saturated wet steam, Int. J. Hydrogen Energy. 35 (2010) 1888-1894. DOI: https://doi.org/10.1016/j.ijhydene.2009.12.061

[46] V. Ivanov, S. Leonov, G. Savinov, O. Gavrilyuk, O. Glazkov, Combustion of mixtures of ultradisperse aluminum and gel-like water, Combus. Explo. Shock Waves. 30 (1994) 569-570. DOI: https://doi.org/10.1007/BF00790170

[47] P. Setiani, N. Watanabe, R.R. Sondari, N. Tsuchiya, Mechanisms and kinetic model of hydrogen production in the hydrothermal treatment of waste aluminum, Mater. Renewable Sustainable Energy. 7 (2018) 10. DOI: https://doi.org/10.1007/s40243-018-0118-8

[48] M.S. Vlaskin, E.I. Shkolnikov, A.V. Bersh, Oxidation kinetics of micron-sized aluminum powder in high-temperature boiling water, Int. J. Hydrogen Energy. 36 (2011) 6484-6495. DOI: https://doi.org/10.1016/j.ijhydene.2011.02.131

[49] A.V. Bersh, A.V. Lisitsyn, A.I. Sorokovikov, M.S. Vlaskin, Y.A. Mazalov, E.I. Shkol'nikov, Study of the processes of steam-hydrogen mixture generation in a reactor for hydrothermal aluminum oxidation for power units, High Temp. 48 (2010) 866-873. DOI: https://doi.org/10.1134/s0018151x10060131

[50] Y.V. Potapova, S.F. Tikhov, V.A. Sadykov, V.B. Fenelonov, Kinetics of Aluminium Powder Oxidation by Water Vapor at Moderate Temperatures, React. Kinet. Catal. Lett. 73 (2001) 55-61. DOI: https://doi.org/10.1023/a:1013964602995

[51] Y. Yavor, S. Goroshin, J.M. Bergthorson, D.L. Frost, R. Stowe, S. Ringuette, Enhanced hydrogen generation from aluminum–water reactions, Int. J. Hydrogen Energy. 38 (2013) 14992-15002. DOI: http://dx.doi.org/10.1016/j.ijhydene.2013.09.070

[52] O.V. Kravchenko, K.N. Semenenko, B.M. Bulychev, K.B. Kalmykov, Activation of aluminum metal and its reaction with water, J. Alloys Compd. 397 (2005) 58-62. DOI: http://dx.doi.org/10.1016/j.jallcom.2004.11.065

[53] A.V. Parmuzina, O.V. Kravchenko, Activation of aluminium metal to evolve hydrogen from water, Int. J. Hydrogen Energy. 33 (2008) 3073-3076. DOI: http://dx.doi.org/10.1016/j.ijhydene.2008.02.025

[54] E. Senel, J.C. Walmsley, S. Diplas, K. Nisancioglu, Liquid metal embrittlement of aluminium by segregation of trace element gallium, Corros. Sci. 85 (2014) 167-173. DOI: http://dx.doi.org/10.1016/j.corsci.2014.04.012

[55] A.I. Nizovskii, S.V. Belkova, A.A. Novikov, M.V. Trenikhin, Hydrogen Production for Fuel Cells in Reaction of Activated Aluminum with Water, Procedia Eng. 113 (2015) 8-12. DOI: http://dx.doi.org/10.1016/j.proeng.2015.07.278

[56] A. Nizovskii, A. Kulikov, M. Trenikhin, V. Bukhtiyarov, Material for Compact Hydrogen Cartridges Based on Commercial Aluminium Alloys Activated by Ga-In Eutectics, Catal. Sustain. Energy. 4 (2017) 62-66. DOI: https://doi.org/10.1515/cse-2017-0010

[57] C. Ying, L. Bei, W. Huihu, D. Shijie, Effects of Preparation Parameters and Alloy Elements on the Hydrogen Generation Performance of Aluminum Alloy-0° C Pure Water Reaction, Rare Metal Mat. Eng. 46 (2017) 2428-2432. DOI: https://doi.org/10.1016/S1875-5372(17)30210-2

[58] F.-Q. Wang, H.-H. Wang, J. Wang, J. Lu, P. Luo, Y. Chang, et al., Effects of low melting point metals (Ga, In, Sn) on hydrolysis properties of aluminum alloys, Trans. Nonferrous Met. Soc. China. 26 (2016) 152-159. DOI: http://dx.doi.org/10.1016/S1003-6326(16)64100-6

[59] J.T. Ziebarth, J.M. Woodall, R.A. Kramer, G. Choi, Liquid phase-enabled reaction of Al–Ga and Al–Ga–In–Sn alloys with water, Int. J. Hydrogen Energy. 36 (2011) 5271-5279. DOI: http://dx.doi.org/10.1016/j.ijhydene.2011.01.127

[60] B. Du, W. Wang, W. Chen, D. Chen, K. Yang, Grain refinement and Al-water reactivity of AlGaInSn alloys, Int. J. Hydrogen Energy. 42 (2017) 21586-21596. DOI: https://doi.org/10.1016/j.ijhydene.2017.07.105

[61] K. Jayaraman, C. Chauveau, I. Gökalp, Effects of Aluminum Particle Size, Galinstan Content and Reaction Temperature on Hydrogen Generation Rate Using Activated Aluminum and Water, Energy and Power Engineering. 7 (2015) 426. DOI: http://dx.doi.org/10.4236/epe.2015.79041

[62] T. Huang, Q. Gao, D. Liu, S. Xu, C. Guo, J. Zou, et al., Preparation of Al-Ga-In-Sn-Bi quinary alloy and its hydrogen production via water splitting, Int. J. Hydrogen Energy. 40 (2015) 2354-2362. DOI: http://dx.doi.org/10.1016/j.ijhydene.2014.12.034

[63] B. Yang, J. Zhu, T. Jiang, Y. Gou, X. Hou, B. Pan, Effect of heat treatment on AlMgGaInSn alloy for hydrogen generation through hydrolysis reaction, Int. J. Hydrogen Energy. 42 (2017) 24393-24403. DOI: https://doi.org/10.1016/j.ijhydene.2017.07.091

[64] B.D. Du, T.T. He, G.L. Liu, W. Chen, Y.M. Wang, W. Wang, et al., Al-water reactivity of AlMgGaInSn alloys used for hydraulic fracturing tools, Int. J. Hydrogen Energy. 43 (2018) 7201-7215. DOI: https://doi.org/10.1016/j.ijhydene.2018.02.090

[65] C. Wei, D. Liu, S. Xu, T. Cui, Q. An, Z. Liu, et al., Effects of Cu additives on the hydrogen generation performance of Al-rich alloys, J. Alloys Compd. 738 (2018) 105-110. DOI: https://doi.org/10.1016/j.jallcom.2017.12.152

[66] A. Irankhah, S.M. Seyed Fattahi, M. Salem, Hydrogen generation using activated aluminum/water reaction, Int. J. Hydrogen Energy. 43 (2018) 15739-15748. DOI: https://doi.org/10.1016/j.ijhydene.2018.07.014

[67] S.S. Razavi-Tousi, J.A. Szpunar, Effect of addition of water-soluble salts on the hydrogen generation of aluminum in reaction with hot water, J. Alloys Compd. 679 (2016) 364-374. DOI: https://doi.org/10.1016/j.jallcom.2016.04.038

[68] Y. Jia, J. Shen, H. Meng, Y. Dong, Y. Chai, N. Wang, Hydrogen generation using a ball-milled Al/Ni/NaCl mixture, J. Alloys Compd. 588 (2014) 259-264. DOI: http://dx.doi.org/10.1016/j.jallcom.2013.11.058

[69] M.Q. Fan, F. Xu, L.-X. Sun, J.-N. Zhao, T. Jiang, W.-X. Li, Hydrolysis of ball milling Al–Bi–hydride and Al–Bi–salt mixture for hydrogen generation, J. Alloys Compd. 460 (2008) 125-129. DOI: http://dx.doi.org/10.1016/j.jallcom.2007.05.077

[70] F. Xiao, Y. Guo, J. Li, R. Yang, Hydrogen generation from hydrolysis of activated aluminum composites in tap water, Energy. 157 (2018) 608-614. DOI: https://doi.org/10.1016/j.energy.2018.05.201

[71] M.Q. Fan, F. Xu, L.X. Sun, Studies on hydrogen generation characteristics of hydrolysis of the ball milling Al-based materials in pure water, Int. J. Hydrogen Energy. 32 (2007) 2809-2815. DOI: https://doi.org/10.1016/j.ijhydene.2006.12.020

[72] R. Hill, C. Howard, Quantitative phase analysis from neutron powder diffraction data using the Rietveld method, J. Appl. Crystallogr. 20 (1987) 467-474. DOI: https://doi.org/10.1107/S0021889887086199

[73] J. Benjamin, Mechanical alloying, Sci. Am. 234 (1976) 40-48.

[74] C. Suryanarayana, Mechanical alloying and milling, Prog. Mater Sci. 46 (2001) 1-184. DOI: http://dx.doi.org/10.1016/S0079-6425(99)00010-9

[75] S. Gudić, I. Smoljko, M. Kliškić, The effect of small addition of tin and indium on the corrosion behavior of aluminium in chloride solution, J. Alloys Compd. 505 (2010a) 54-63. DOI: https://doi.org/10.1016/j.jallcom.2010.06.055

[76] R. Parsons, Handbook of electrochemical constants, Butterworths, London, 1959.

[77] A. Papworth, P. Fox, The disruption of oxide defects within aluminium alloy castings by the addition of bismuth, Electron. Mater. Lett. 35 (1998) 202-206. DOI: https://doi.org/10.1016/S0167-577X(97)00244-9

[78] C. Vargel. Corrosion of aluminium, Elsevier Ltd, Oxfort, 2004.

[79] C. Caicedo-Martinez, E. Koroleva, P. Skeldon, G. Thompson, G. Hoellrigl, P. Bailey, et al., Behavior of impurity and minor alloying elements during surface treatments of aluminum, J. Electrochem. Soc. 149 (2002) B139-B145. DOI: https://doi.org/10.1149/1.1457982

[80] M. Reboul, P. Gimenez, J. Rameau, A proposed activation mechanism for Al anodes, Corrosion. 40 (1984) 366-371. DOI: https://doi.org/10.5006/1.3593939

[81] E. Czech, T. Troczynski, Hydrogen generation through massive corrosion of deformed aluminum in water, Int. J. Hydrogen Energy. 35 (2010) 1029-1037. DOI: http://dx.doi.org/10.1016/j.ijhydene.2009.11.085

[82] K. Mahmoodi, B. Alinejad, Enhancement of hydrogen generation rate in reaction of aluminum with water, Int. J. Hydrogen Energy. 35 (2010) 5227-5232. DOI: http://dx.doi.org/10.1016/j.ijhydene.2010.03.016

CHAPTER 7: PROJECT EVALUATION AND CONCLUSIONS

The project evaluation is presented in Section 7.1. Therein the project is evaluated against the general aims and specific objectives as presented in Chapter 1, Section 1.2. Additionally, future prospective for continued research is presented in Section 7.2.

7.1 Project evaluation and main conclusions

In order to do a self-evaluation, the candidate evaluated the study against the objectives that were set in Chapter 1. The points listed below correlate with the objectives set in Section 1.2.

Objective 1: Identify suitable activation compounds to activate Al using a mechanochemical approach.

An in-depth literature survey indicated several low melting point metals that could be used to activate Al. However, in many cases the activation process included gallium (Ga) as an activation compound and/or the use of a thermal activation route. Ga is an expensive material, which greatly increases the cost of Al activation. Furthermore, a thermal activation route is more energy intensive if compare to mechanochemical activation. Regardless, the use of In and Sn in conjuration with Ga is widely reported in the peer-reviewed public domain. Similarly, the use of Bi with various other materials has also been reported. Thus, it was decided to investigate the use of Bi, In and Sn (and combinations thereof) as activation compounds.

Objective 2: Determine the efficiency of identified activation compounds in terms of enabling Al's reactivity towards neutral pH waters under ambient conditions.

In order to address this objective, the individual and combined effects of the identified activation compounds, i.e. Bi, In and Sn, were determined. The combinations considered for investigation were Bi-In-Sn, Bi-In, Sn-In, and Bi-Sn. For each investigation, a series of

binary and ternary composites were prepared and characterized by SEM-EDS and XRD, and their hydrolysis reactivities determined. Table 7-1 presents a listing of ternary composites prepared in this dissertation, their respective yields and reaction times, and the relevant chapters they were presented in. It is clear from Table 7-1 that numerous composites were fabricated and that the efficiencies of the considered compounds were investigated in depth.

Table 7-1: Ternary composites prepared in this dissertation						
Composition	Activation compound (wt.%)			Yield (%)	Reaction time (sec)	Reference
	Bi	Sn	In			
1	0	10.55	2.54	93	570	Chapter 3
2	8.38	0	4.71	95	540	
3	0	3.27	9.82	93	810	
4	3.93	5.24	3.93	92	160	
5	6.54	2.62	3.93	96	100	
6	3.93	2.62	6.54	98	90	
7	3.93	6.54	2.62	93	130	
8	9.38	0	0.62	82	510	Chapter 4
9	8.76	0	1.26	83	420	
10	7.5	0	2.5	95	450	
11	5	0	5	93	450	
12	3.74	0	6.26	77	378	
13	2.5	0	7.5	93	600	
14	1.26	0	8.76	66	720	
15	0.62	0	9.38	0	n.a	
16	0	9.5	0.5	25	2160	Chapter 5
17	0	8	2	97	380	
18	0	6.5	3.5	96	370	
19	0	5	5	99	280	
20	0	3.5	6.5	97	300	
21	0	2	8	91	1050	
22	0	0.5	9.5	0	n.a	
23	0	4	1	63	1150	
24	0	3.25	1.75	75	1050	
25	0	2.5	2.5	83	1200	
26	0	1.75	3.25	71	1100	
27	9	1	0	99	640	Chapter 6
28	7.5	2.5	0	99	480	
29	5	5	0	99	430	
30	2.5	7.5	0	38.5	220	
31	1	9	0	0	n.a	
32	4.5	0.5	0	99	740	
33	3.75	1.25	0	99	1100	
34	2.5	2.5	0	99	1550	

Objective 3: Investigate the various reaction parameters that may affect the performance of prepared composites.

The following reaction parameters were considered:

i) Activation energy (E_a). This energy was determined for several composites presented in Chapter 3 and ranged between 47.2 to 62.1 kJ/mol.

ii) Mass ratio, which is defined as the ratio of composite mass to volume water used during hydrolysis reactions (e.g. a mass ratio of 1:50 is defined as 1 g composite per 50 mL water). The effects of mass ratio were determined in Chapters 3, 4 and 5. It was found that by increasing the mass ratio, the increase in reaction temperature was greatly decreased. However, in all cases, a higher mass ratio adversely affected hydrogen yield. In addition to this, the hydrogen generation rate could be partially controlled by manipulating the mass ratio.

iii) Water quality. The effects of water quality on hydrogen yield were determined in Chapter 4. The water qualities considered were deionized, filtered and tap. It was found that water quality only marginally affected the hydrogen generation rate.

iv) Initial reaction temperature. Chapter 6 investigated the effect of initial reaction temperature on the hydrolysis reaction. Though the idea was to perform all hydrolysis reactions under standard ambient conditions, the effects of initial reaction temperature was consider in cases where activated Al were to be used in cold (i.e. 8 and 14°C) or hot (i.e. 45 and 55°C environments. Results suggested that a lower initial reaction temperature could retard the hydrogen release rate, whilst not affecting the hydrogen yield. A very exothermic reaction was observed when the initial reaction temperature was increase to >45°C, resulting in explosion-like reactivity.

Objective 4: Develop a method to recover activation compounds from hydrolyzed Al composites.

This objective was addressed in Chapter 7. Three common acids, i.e. hydrochloric (HCl), nitric (HNO_3) and sulphuric (H_2SO_4), were considered to recover activation compounds from hydrolysed Al. Hydrolysed Al-5% Bi-5% Sn was considered for this investigation. Hydrolysis products were contacted with an individual acid for 6 hrs. Thereafter, the leachate and residues were analysed by ICP-OES and SEM-EDS, respectively. The results suggested

that the acids consider dissolved the majority of the hydrolysis product; however, HNO_3 and H_2SO_4 solutions only solubilized 14.88% Sn and 25.16% Bi, respectively.

7.2 Future prospects

Relatively good progress has been made towards determining the effects of Bi, In, and Sn and combinations thereof on Al's morphological characteristics and its reactivity towards neutral pH waters under standard ambient conditions caused by mechanochemical processing. However, several topics have yet to be addressed/explored. Of major importance is the lack of a suitable reactor that operates on such Al composites. Several reactors have been reported that operate on Al-alkaline solution, but as far as the candidate could assess, no reactor operating on activated Al has been reported in the peer-reviewed public domain. An important factor to consider when designing such a reactor will be the uncontrollability of Al's reactivity, i.e. as soon as the hydrolysis reaction is initiated, it cannot easily be stopped. Thus, such a reactor will be based upon a high pressure design, i.e. hydrogen is generated at a faster rate as what it can be consumed and unconsumed hydrogen is systematically released from the reactor to be utilized. Finally, a preliminary approach towards the recovery of activation compounds from hydrolysed Al was proposed here; however, this process requires further development and optimization. Activation compound recovery would greatly increase the attractiveness of this hydrogen generation method.

BIBLIOGRAPHY

[1] Damyanova S, Pawelec B, Arishtirova K, Fierro J. Ni-based catalysts for reforming of methane with CO_2. International Journal of Hydrogen Energy. 2012;37:15966-75. DOI: https://doi.org/10.1016/j.ijhydene.2012.08.056

[2] Balat M. Potential importance of hydrogen as a future solution to environmental and transportation problems. International Journal of Hydrogen Energy. 2008;33:4013-29. DOI: https://doi.org/10.1016/j.ijhydene.2008.05.047

[3] Peighambardoust SJ, Rowshanzamir S, Amjadi M. Review of the proton exchange membranes for fuel cell applications. International Journal of Hydrogen Energy. 2010;35:9349-84. DOI: https://doi.org/10.1016/j.ijhydene.2010.05.017

[4] Divisek J, Oetjen HF, Peinecke V, Schmidt VM, Stimming U. Components for PEM fuel cell systems using hydrogen and CO containing fuels. Electrochimica Acta. 1998;43:3811-5. DOI: https://doi.org/10.1016/S0013-4686(98)00140-6

[5] Reshetenko TV, Bethune K, Rocheleau R. Spatial proton exchange membrane fuel cell performance under carbon monoxide poisoning at a low concentration using a segmented cell system. Journal of Power Sources. 2012;218:412-23. DOI: http://dx.doi.org/10.1016/j.jpowsour.2012.07.015

[6] Gosavi PV, Biniwale RB. Catalytic preferential oxidation of carbon monoxide over platinum supported on lanthanum ferrite–ceria catalysts for cleaning of hydrogen. Journal of Power Sources. 2013;222:1-9. DOI: https://doi.org/10.1016/j.jpowsour.2012.07.095

[7] Edwards N, Ellis SR, Frost JC, Golunski SE, van Keulen ANJ, Lindewald NG, et al. On-board hydrogen generation for transport applications: the HotSpot™ methanol processor.

Journal of Power Sources. 1998;71:123-8. DOI: https://doi.org/10.1016/S0378-7753(97)02797-3

[8] Gray P, Petch M. Advances with HotSpot™ Fuel Processing Efficient Hydrogen Production for use with Solid Polymer Fuel Cells. Platinum Metals Rev. 2000;44:108.

[9] Faur Ghenciu A. Review of fuel processing catalysts for hydrogen production in PEM fuel cell systems. Current Opinion in Solid State and Materials Science. 2002;6:389-99. DOI: https://doi.org/10.1016/S1359-0286(02)00108-0

[10] Kreuer KD. On the development of proton conducting polymer membranes for hydrogen and methanol fuel cells. Journal of Membrane Science. 2001;185:29-39. DOI: https://doi.org/10.1016/S0376-7388(00)00632-3

[11] Elitzur S, Rosenband V, Gany A. On-board hydrogen production for auxiliary power in passenger aircraft. International Journal of Hydrogen Energy. 2017;42:14003-9. DOI: https://doi.org/10.1016/j.ijhydene.2017.02.037

[12] Ilyukhina AV, Ilyukhin AS, Shkolnikov EI. Hydrogen generation from water by means of activated aluminum. International Journal of Hydrogen Energy. 2012;37:16382-7. DOI: http://dx.doi.org/10.1016/j.ijhydene.2012.02.175

[13] Gai W-Z, Liu W-H, Deng Z-Y, Zhou J-G. Reaction of Al powder with water for hydrogen generation under ambient condition. International Journal of Hydrogen Energy. 2012;37:13132-40. DOI: https://doi.org/10.1016/j.ijhydene.2012.04.025

[14] Liu Y, Wang X, Liu H, Dong Z, Li S, Ge H, et al. Investigation on the improved hydrolysis of aluminum–calcium hydride-salt mixture elaborated by ball milling. Energy. 2015;84:714-21. DOI: http://dx.doi.org/10.1016/j.energy.2015.03.035

[15] Hiraki T, Yamauchi S, Iida M, Uesugi H, Akiyama T. Process for recycling waste aluminum with generation of high-pressure hydrogen. Environmental Science & Technology. 2007;41:4454-7. DOI: http://dx.doi.org/10.1021/es062883l

[16] Cho C-Y, Wang K-H, Uan J-Y. Evaluation of a new hydrogen generating system: Ni-rich magnesium alloy catalyzed by platinum wire in sodium chloride solution. Materials transactions. 2005;46:2704-8. DOI: https://doi.org/10.2320/matertrans.46.2704

[17] Wang S, Sun L-X, Xu F, Jiao C-L, Zhang J, Zhou H-Y, et al. Hydrolysis reaction of ball-milled Mg-metal chlorides composite for hydrogen generation for fuel cells. International Journal of Hydrogen Energy. 2012;37:6771-5. DOI: https://doi.org/10.1016/j.ijhydene.2012.01.099

[18] Wegner K, Ly HC, Weiss RJ, Pratsinis SE, Steinfeld A. In situ formation and hydrolysis of Zn nanoparticles for production by the 2-step ZnO/Zn water-splitting thermochemical cycle. International Journal of Hydrogen Energy. 2006;31:55-61. DOI: http://dx.doi.org/10.1016/j.ijhydene.2005.03.006

[19] Vishnevetsky I, Epstein M. Production of hydrogen from solar zinc in steam atmosphere. International Journal of Hydrogen Energy. 2007;32:2791-802. DOI: https://doi.org/10.1016/j.ijhydene.2007.04.004

[20] Mahmoodi K, Alinejad B. Enhancement of hydrogen generation rate in reaction of aluminum with water. International Journal of Hydrogen Energy. 2010;35:5227-32. DOI: http://dx.doi.org/10.1016/j.ijhydene.2010.03.016

[21] Tzimas E, Filiou C, Peteves SD, Veyret J. Hydrogen storage: state-of-the-art and future perspective. EU Commission, JRC Petten, EUR 20995EN. 2003.

[22] Kothari R, Buddhi D, Sawhney R. Comparison of environmental and economic aspects of various hydrogen production methods. Renewable and Sustainable Energy Reviews. 2008;12:553-63. DOI: https://doi.org/10.1016/j.rser.2006.07.012

[23] Kulkarni SH, Anil TR, Gowdar RD. Wind Energy Development in India and a Methodology for Evaluating Performance of Wind Farm Clusters. Journal of Renewable Energy. 2016;2016.

[24] Karmakar DK, Dasari L, Swaroop KMP, Raju N. Power Balance Theory Control of an Integrated Electronic Load Controller with Zig-Zag Transformer for Stand-Alone Wind Farm with PV Array Connected to Three-Phase Four-Wire Load. Power. 2016;6.

[25] Song J, Choi Y. Design of photovoltaic systems to power aerators for natural purification of acid mine drainage. Renewable Energy. 2015;83:759-66. DOI: http://dx.doi.org/10.1016/j.renene.2015.05.014

[26] Song J, Choi Y. Analysis of the Potential for Use of Floating Photovoltaic Systems on Mine Pit Lakes: Case Study at the Ssangyong Open-Pit Limestone Mine in Korea. Energies. 2016;9:102.

[27] Uemura Y, Kai T, Natori R, Takahashi T, Hatate Y, Yoshida M. Potential of renewable energy sources and its applications in Yakushima Island. Renewable Energy. 2004;29:581-91. DOI: http://dx.doi.org/10.1016/j.renene.2003.09.005

[28] Sakaguchi T, Tabata T. 100% electric power potential of PV, wind power, and biomass energy in Awaji island Japan. Renewable and Sustainable Energy Reviews. 2015;51:1156-65. DOI: http://dx.doi.org/10.1016/j.rser.2015.06.056

[29] Suh J, Brownson J. Solar Farm Suitability Using Geographic Information System Fuzzy Sets and Analytic Hierarchy Processes: Case Study of Ulleung Island, Korea. Energies. 2016;9:648.

[30] Judd R, Pinchbeck D. Power to Gas Research Roadmap. Offering a solution to the energy storage problem.

[31] Momirlan M, Veziroglu TN. The properties of hydrogen as fuel tomorrow in sustainable energy system for a cleaner planet. International Journal of Hydrogen Energy. 2005;30:795-802. DOI: https://doi.org/10.1016/j.ijhydene.2004.10.011

[32] Macanás J, Soler L, Candela AM, Muñoz M, Casado J. Hydrogen generation by aluminum corrosion in aqueous alkaline solutions of inorganic promoters: The AlHidrox process. Energy. 2011;36:2493-501. DOI: http://dx.doi.org/10.1016/j.energy.2011.01.041

[33] Lattin W, Utgikar VP. Transition to hydrogen economy in the United States: a 2006 status report. International Journal of Hydrogen Energy. 2007;32:3230-7.

[34] Dupont V. Steam reforming of sunflower oil for hydrogen gas production. Helia. 2007;30:103-32.

[35] Sharma S, Ghoshal SK. Hydrogen the future transportation fuel: From production to applications. Renewable and Sustainable Energy Reviews. 2015;43:1151-8. DOI: http://dx.doi.org/10.1016/j.rser.2014.11.093

[36] Mueller-Langer F, Tzimas E, Kaltschmitt M, Peteves S. Techno-economic assessment of hydrogen production processes for the hydrogen economy for the short and medium term. International Journal of Hydrogen Energy. 2007;32:3797-810.

[37] Barreto L, Makihira A, Riahi K. The hydrogen economy in the 21st century: a sustainable development scenario. International Journal of Hydrogen Energy. 2003;28:267-84.

[38] Ramachandran R, Menon RK. An overview of industrial uses of hydrogen. International Journal of Hydrogen Energy. 1998;23:593-8.

[39] Eliaz N, Eliezer D, Olson D. Hydrogen-assisted processing of materials. Materials Science and Engineering: A. 2000;289:41-53.

[40] Eliezer D, Eliaz N, Senkov O, Froes F. Positive effects of hydrogen in metals. Materials Science and Engineering: A. 2000;280:220-4.

[41] Elam CC, Padró CEG, Sandrock G, Luzzi A, Lindblad P, Hagen EF. Realizing the hydrogen future: the International Energy Agency's efforts to advance hydrogen energy technologies. International Journal of Hydrogen Energy. 2003;28:601-7. DOI: http://dx.doi.org/10.1016/S0360-3199(02)00147-7

[42] Ni M, Leung MK, Sumathy K, Leung DY. Potential of renewable hydrogen production for energy supply in Hong Kong. International Journal of Hydrogen Energy. 2006;31:1401-12.

[43] Wang C, Yang T, Liu Y, Ruan J, Yang S, Liu X. Hydrogen generation by the hydrolysis of magnesium–aluminum–iron material in aqueous solutions. International Journal of Hydrogen energy. 2014;39:10843-52. DOI: https://doi.org/10.1016/j.ijhydene.2014.05.047

[44] Das L. Hydrogen engines: a view of the past and a look into the future. International Journal of Hydrogen Energy. 1990;15:425-43.

[45] Barbir F, Gómez T. Efficiency and economics of proton exchange membrane (PEM) fuel cells. International Journal of Hydrogen Energy. 1997;22:1027-37. DOI: https://doi.org/10.1016/S0360-3199(96)00175-9

[46] Mousa G, Golnaraghi F, DeVaal J, Young A. Detecting proton exchange membrane fuel cell hydrogen leak using electrochemical impedance spectroscopy method. Journal of Power Sources. 2014;246:110-6. DOI: https://doi.org/10.1016/j.jpowsour.2013.07.018

[47] Veziroğlu TN, Şahi S. 21st Century's energy: Hydrogen energy system. Energy Conversion and Management. 2008;49:1820-31.

[48] Edwards PP, Kuznetsov VL, David WIF, Brandon NP. Hydrogen and fuel cells: Towards a sustainable energy future. Energy Policy. 2008;36:4356-62. DOI: http://dx.doi.org/10.1016/j.enpol.2008.09.036

[49] Ball M, Wietschel M. The future of hydrogen–opportunities and challenges. International Journal of Hydrogen Energy. 2009;34:615-27. DOI: https://doi.org/10.1016/j.ijhydene.2008.11.014

[50] Wang M-Y, Wang Z, Gong X-Z, Guo Z-C. The intensification technologies to water electrolysis for hydrogen production–A review. Renewable and Sustainable Energy Reviews. 2014;29:573-88.

[51] Trasatti S. Water electrolysis: who first? Journal of Electroanalytical Chemistry. 1999;476:90-1.

[52] Zeng K, Zhang D. Recent progress in alkaline water electrolysis for hydrogen production and applications. Progress in Energy and Combustion Science. 2010;36:307-26.

[53] Lipman T. An overview of hydrogen production and storage systems with renewable hydrogen case studies. Clean Energy States Alliance. 2011.

[54] Herzog A, Tatsutani M. A hydrogen future? An economic and environmental assessment of hydrogen production pathways. Natural Resources Defense Council. 2005:23.

[55] Yildiz B, Kazimi MS. Efficiency of hydrogen production systems using alternative nuclear energy technologies. International Journal of Hydrogen Energy. 2006;31:77-92. DOI: http://dx.doi.org/10.1016/j.ijhydene.2005.02.009

[56] Stojić DL, Marčeta MP, Sovilj SP, Miljanić ŠS. Hydrogen generation from water electrolysis—possibilities of energy saving. Journal of Power Sources. 2003;118:315-9.

[57] Shakya B, Aye L, Musgrave P. Technical feasibility and financial analysis of hybrid wind–photovoltaic system with hydrogen storage for Cooma. International Journal of Hydrogen Energy. 2005;30:9-20.

[58] Modisha PM, Jordaan JHL, Bösmann A, Wasserscheid P, Bessarabov D. Analysis of reaction mixtures of perhydro-dibenzyltoluene using two-dimensional gas chromatography and single quadrupole gas chromatography. International Journal of Hydrogen Energy. 2018;43:5620-36. DOI: https://doi.org/10.1016/j.ijhydene.2018.02.005

[59] Bessarabov DG, Human G, Kruger AJ, Chiuta S, Modisha PM, du Preez SP, et al. South African hydrogen infrastructure (HySA infrastructure) for fuel cells and energy storage: Overview of a projects portfolio. International Journal of Hydrogen Energy. 2017;42:13568-88. DOI: https://doi.org/10.1016/j.ijhydene.2016.12.140

[60] Renouard-Vallet G, Saballus M, Schumann P, Kallo J, Friedrich KA, Müller-Steinhagen H. Fuel cells for civil aircraft application: On-board production of power, water and inert gas. Chemical Engineering Research and Design. 2012;90:3-10. DOI: https://doi.org/10.1016/j.cherd.2011.07.016

[61] Wang HZ, Leung DYC, Leung MKH, Ni M. A review on hydrogen production using aluminum and aluminum alloys. Renewable and Sustainable Energy Reviews. 2009;13:845-53. DOI: http://dx.doi.org/10.1016/j.rser.2008.02.009

[62] Wang X, Maeda K, Thomas A, Takanabe K, Xin G, Carlsson JM, et al. A metal-free polymeric photocatalyst for hydrogen production from water under visible light. Nature Materials. 2009;8:76-80. DOI: https://doi.org/10.1038/nmat2317

[63] Chen X, Shen S, Guo L, Mao SS. Semiconductor-based photocatalytic hydrogen generation. Chemical reviews. 2010;110:6503-70.

[64] Zou Z, Ye J, Sayama K, Arakawa H. Direct splitting of water under visible light irradiation with an oxide semiconductor photocatalyst. Nature. 2001;414:625-7.

[65] Esswein AJ, Nocera DG. Hydrogen production by molecular photocatalysis. Chemical Reviews. 2007;107:4022-47. DOI: https://doi.org/10.1021/cr050193e

[66] Barbir F. PEM electrolysis for production of hydrogen from renewable energy sources. Solar Energy. 2005;78:661-9.

[67] Doenitz W, Schmidberger R, Steinheil E, Streicher R. Hydrogen production by high temperature electrolysis of water vapour. International Journal of Hydrogen Energy. 1980;5:55-63.

[68] Sakintuna B, Lamari-Darkrim F, Hirscher M. Metal hydride materials for solid hydrogen storage: a review. International Journal of Hydrogen Energy. 2007;32:1121-40. DOI: https://doi.org/10.1016/j.ijhydene.2006.11.022

[69] Liu BH, Li ZP, Suda S. Nickel-and cobalt-based catalysts for hydrogen generation by hydrolysis of borohydride. Journal of Alloys and Compounds. 2006;415:288-93.

[70] Hua D, Hanxi Y, Xinping A, Chuansin C. Hydrogen production from catalytic hydrolysis of sodium borohydride solution using nickel boride catalyst. International Journal of Hydrogen Energy. 2003;28:1095-100.

[71] Ilyukhina AV, Kravchenko OV, Bulychev BM. Studies on microstructure of activated aluminum and its hydrogen generation properties in aluminum/water reaction. Journal of Alloys and Compounds. 2017;690:321-9. DOI: http://dx.doi.org/10.1016/j.jallcom.2016.08.151

[72] Parmuzina AV, Kravchenko OV. Activation of aluminium metal to evolve hydrogen from water. International Journal of Hydrogen Energy. 2008;33:3073-6. DOI: http://dx.doi.org/10.1016/j.ijhydene.2008.02.025

[73] Kravchenko OV, Semenenko KN, Bulychev BM, Kalmykov KB. Activation of aluminum metal and its reaction with water. Journal of Alloys and Compounds. 2005;397:58-62. DOI: http://dx.doi.org/10.1016/j.jallcom.2004.11.065

[74] Ilyukhina A, Kravchenko O, Bulychev B, Shkolnikov E. Mechanochemical activation of aluminum with gallams for hydrogen evolution from water. International Journal of Hydrogen Energy. 2010;35:1905-10. DOI: https://doi.org/10.1016/j.ijhydene.2009.12.118

[75] Grosjean M-H, Zidoune M, Roué L, Huot J-Y. Hydrogen production via hydrolysis reaction from ball-milled Mg-based materials. International Journal of Hydrogen Energy. 2006;31:109-19. DOI: https://doi.org/10.1016/j.ijhydene.2005.01.001

[76] Du Preez SP, Bessarabov DG. Hydrogen generation by means of hydrolysis using activated Al-In-Bi-Sn composites for electrochemical energy applications. International Journal of Electrochemical Sciences. 2017a;12:8663-82. DOI: https://doi.org/10.20964/2017.09.22

[77] Du Preez SP, Bessarabov DG. Hydrogen generation of mechanochemically activated AlBiIn composites. International Journal of Hydrogen Energy. 2017b;42:16589-602. DOI: https://doi.org/10.1016/j.ijhydene.2017.05.211

[78] Parthasarathy N, Buffle J. Study of polymeric aluminium(III) hydroxide solutions for application in waste water treatment. Properties of the polymer and optimal conditions of preparation. Water Research. 1985;19:25-36. DOI: http://dx.doi.org/10.1016/0043-1354(85)90319-7

[79] Alinejad B, Mahmoodi K. A novel method for generating hydrogen by hydrolysis of highly activated aluminum nanoparticles in pure water. International Journal of Hydrogen Energy. 2009;34:7934-8. DOI: http://dx.doi.org/10.1016/j.ijhydene.2009.07.028

[80] Rand D, Woods R, Dell R. Batteries for Electric Vehicles. Somerset. England, 1998 Research Studies Press Ltd. 1998.

[81] Li Q, Bjerrum NJ. Aluminum as anode for energy storage and conversion: a review. Journal of Power Sources. 2002;110:1-10. DOI: https://doi.org/10.1016/S0378-7753(01)01014-X

[82] Dražić D, Popić J. Corrosion rates and negative difference effects for Al and some Al alloys. Journal of Applied Electrochemistry. 1999;29:43-50.

[83] Belitskus D. Reaction of Aluminium with Sodium Hydroxide Solution as a Source of Hydrogen. Journal of The Electrochemical Society. 1970;117:1097-9. DOI: http://dx.doi.org/10.1149/1.2407730

[84] Soler L, Macanás J, Muñoz M, Casado J. Synergistic hydrogen generation from aluminum, aluminum alloys and sodium borohydride in aqueous solutions. International Journal of Hydrogen Energy. 2007;32:4702-10. DOI: http://dx.doi.org/10.1016/j.ijhydene.2007.06.019

[85] Martinez SS, Albañil Sánchez L, Álvarez Gallegos AA, Sebastian P. Coupling a PEM fuel cell and the hydrogen generation from aluminum waste cans. International Journal of Hydrogen Energy. 2007;32:3159-62. DOI: https://doi.org/10.1016/j.ijhydene.2006.03.015

[86] Wang E-D, Shi P-F, Du C-Y, Wang X-R. A mini-type hydrogen generator from aluminum for proton exchange membrane fuel cells. Journal of Power Sources. 2008;181:144-8. DOI: http://dx.doi.org/10.1016/j.jpowsour.2008.02.088

[87] El-Meligi A. Hydrogen production by aluminum corrosion in hydrochloric acid and using inhibitors to control hydrogen evolution. International Journal of Hydrogen Energy. 2011;36:10600-7. DOI: https://doi.org/10.1016/j.ijhydene.2011.05.111

[88] Boukerche I, Djerad S, Benmansour L, Tifouti L, Saleh K. Degradability of aluminum in acidic and alkaline solutions. Corrosion Science. 2014;78:343-52. DOI: http://dx.doi.org/10.1016/j.corsci.2013.10.019

[89] Dudoladov AO, Buryakovskaya OA, Vlaskin MS, Zhuk AZ, Shkolnikov EI. Generation of hydrogen by aluminium oxidation in aquaeous solutions at low temperatures. International Journal of Hydrogen Energy. 2016;41:2230-7. DOI: http://dx.doi.org/10.1016/j.ijhydene.2015.11.122

[90] Soler L, Macanás J, Muñoz M, Casado J. Aluminum and aluminum alloys as sources of hydrogen for fuel cell applications. Journal of Power Sources. 2007;169:144-9. DOI: http://dx.doi.org/10.1016/j.jpowsour.2007.01.080

[91] Jung CR, Kundu A, Ku B, Gil JH, Lee HR, Jang JH. Hydrogen from aluminium in a flow reactor for fuel cell applications. Journal of Power Sources. 2008;175:490-4. DOI: https://doi.org/10.1016/j.jpowsour.2007.09.064

[92] Yang B, Chai Y, Yang F, Zhang Q, Liu H, Wang N. Hydrogen generation by aluminum-water reaction in acidic and alkaline media and its reaction dynamics. International Journal of Energy Research. 2018;42:1594-602. DOI: https://doi.org/10.1002/er.3953

[93] El-Meligi A. Hydrogen Production by Aluminum Alloy in Sulphuric Acid Solutions. Recent Patents on Materials Science. 2017;10:75-81. DOI: https://doi.org/10.2174/1874464810666170605113128

[94] Liu H, Yang F, Yang B, Zhang Q, Chai Y, Wang N. Rapid hydrogen generation through aluminum-water reaction in alkali solution. Catalysis Today. 2018. DOI: https://doi.org/10.1016/j.cattod.2018.03.030

[95] Hurtubise DW, Klosterman DA, Morgan AB. Development and demonstration of a deployable apparatus for generating hydrogen from the hydrolysis of aluminum via sodium

hydroxide. International Journal of Hydrogen Energy. 2018;43:6777-88. DOI: https://doi.org/10.1016/j.ijhydene.2018.02.087

[96] Ho C-Y, Huang C-H. Enhancement of hydrogen generation using waste aluminum cans hydrolysis in low alkaline de-ionized water. International Journal of Hydrogen Energy. 2016;41:3741-7. DOI: https://doi.org/10.1016/j.ijhydene.2015.11.083

[97] Ambaryan GN, Vlaskin MS, Dudoladov AO, Meshkov EA, Zhuk AZ, Shkolnikov EI. Hydrogen generation by oxidation of coarse aluminum in low content alkali aqueous solution under intensive mixing. International Journal of Hydrogen Energy. 2016;41:17216-24. DOI: https://doi.org/10.1016/j.ijhydene.2016.08.005

[98] Hiraki T, Takeuchi M, Hisa M, Akiyama T. Hydrogen production from waste aluminum at different temperatures, with LCA. Materials Transactions. 2005;46:1052-7.

[99] Soler L, Macanás J, Munoz M, Casado J. Hydrogen generation from aluminum in a non-consumable potassium hydroxide solution. Proceedings International Hydrogen Energy Congress and Exhibition IHEC2005. p. 13-5.

[100] Bunker CE, Smith MJ. Nanoparticles for hydrogen generation. Journal of Materials Chemistry. 2011;21:12173-80.

[101] Brindley GF. Composition of matter for generating hydrogen. Google Patents; 1909.

[102] Gill GC. Hydrogen generator. Google Patents; 1955.

[103] Checketts JH. Hydrogen generation system and pelletized fuel. Google Patents; 1998.

[104] Vlaskin M, Shkolnikov E, Lisicyn A, Bersh A, Zhuk A. Computational and experimental investigation on thermodynamics of the reactor of aluminum oxidation in saturated wet steam. International Journal of Hydrogen Energy. 2010;35:1888-94. DOI: https://doi.org/10.1016/j.ijhydene.2009.12.061

[105] Ivanov V, Leonov S, Savinov G, Gavrilyuk O, Glazkov O. Combustion of mixtures of ultradisperse aluminum and gel-like water. Combustion, Explosion, and Shock Waves. 1994;30:569-70. DOI: https://doi.org/10.1007/BF00790170

[106] Setiani P, Watanabe N, Sondari RR, Tsuchiya N. Mechanisms and kinetic model of hydrogen production in the hydrothermal treatment of waste aluminum. Materials for Renewable and Sustainable Energy. 2018;7:10. DOI: https://doi.org/10.1007/s40243-018-0118-8

[107] Vlaskin MS, Shkolnikov EI, Bersh AV. Oxidation kinetics of micron-sized aluminum powder in high-temperature boiling water. International Journal of Hydrogen Energy. 2011;36:6484-95. DOI: https://doi.org/10.1016/j.ijhydene.2011.02.131

[108] Bersh AV, Lisitsyn AV, Sorokovikov AI, Vlaskin MS, Mazalov YA, Shkol'nikov EI. Study of the processes of steam-hydrogen mixture generation in a reactor for hydrothermal aluminum oxidation for power units. High Temperature. 2010;48:866-73. DOI: https://doi.org/10.1134/s0018151x10060131

[109] Potapova YV, Tikhov SF, Sadykov VA, Fenelonov VB. Kinetics of Aluminium Powder Oxidation by Water Vapor at Moderate Temperatures. Reaction Kinetics and Catalysis Letters. 2001;73:55-61. DOI: https://doi.org/10.1023/a:1013964602995

[110] Yavor Y, Goroshin S, Bergthorson JM, Frost DL, Stowe R, Ringuette S. Enhanced hydrogen generation from aluminum–water reactions. International Journal of Hydrogen Energy. 2013;38:14992-5002. DOI: http://dx.doi.org/10.1016/j.ijhydene.2013.09.070

[111] Foote JP, Lineberry JT, Thompson BR, Winkelman BC. Investigation of aluminum particle combustion for underwater propulsion applications. AIAA paper. 1996;3086:1996.

[112] Ingenito A, Bruno C. Using aluminum for space propulsion. Journal of Propulsion and Power. 2004;20:1056-63.

[113] Brousseau P, Anderson CJ. Nanometric aluminum in explosives. Propellants, Explosives, Pyrotechnics. 2002;27:300-6.

[114] Reboul M, Gimenez P, Rameau J. A proposed activation mechanism for Al anodes. Corrosion. 1984;40:366-71.

[115] Kliškić M, Radošević J, Gudić S, Šmith M. Cathodic polarization of Al–Sn alloy in sodium chloride solution. Electrochimica Acta. 1998;43:3241-55. DOI: https://doi.org/10.1016/S0013-4686(98)00001-2

[116] El Shayeb HA, Abd El Wahab FM, Zein El Abedin S. Electrochemical behaviour of Al, Al–Sn, Al–Zn and Al–Zn–Sn alloys in chloride solutions containing stannous ions. Corrosion Science. 2001;43:655-69. DOI: http://dx.doi.org/10.1016/S0010-938X(00)00101-3

[117] Smith I. Hydrogen generation by means of the aluminum/water reaction. Journal of Hydronautics. 1972;6:106-9.

[118] Bessone J. The activation of aluminium by mercury ions in non-aggressive media. Corrosion Science. 2006;48:4243-56. DOI: https://doi.org/10.1016/j.corsci.2006.03.013

[119] Fan M-q, Sun L-x, Xu F. Study of the controllable reactivity of aluminum alloys and their promising application for hydrogen generation. Energy Conversion and Management. 2010;51:594-9. DOI: http://dx.doi.org/10.1016/j.enconman.2009.11.005

[120] Huang X, Lv C, Huang Y, Liu S, Wang C, Chen D. Effects of amalgam on hydrogen generation by hydrolysis of aluminum with water. International Journal of Hydrogen Energy. 2011;36:15119-24. DOI: http://dx.doi.org/10.1016/j.ijhydene.2011.08.073

[121] Breslin C, Friery L, Carroll W. The electrochemical behaviour of Al-Zn-In and Al-Zn-Hg alloys in aqueous halide solutions. Corrosion science. 1994;36:85-97.

[122] El-Shafey E. Removal of Zn (II) and Hg (II) from aqueous solution on a carbonaceous sorbent chemically prepared from rice husk. Journal of Hazardous Materials. 2010;175:319-27.

[123] Wilhelm SM, McArthur A, Kane RD. Methods to combat liquid metal embrittlement in cryogenic aluminum heat exchangers. American Inst. of Chemical Engineers, New York, NY (United States); 1994.

[124] Baniamerian M, Moradi S. Al–Ga doped nanostructured carbon as a novel material for hydrogen production in water. Journal of Alloys and Compounds. 2011;509:6307-10. DOI: https://doi.org/10.1016/j.jallcom.2011.03.069

[125] Huang X, Gao T, Pan X, Wei D, Lv C, Qin L, et al. A review: Feasibility of hydrogen generation from the reaction between aluminum and water for fuel cell applications. Journal of Power Sources. 2013;229:133-40. DOI: http://dx.doi.org/10.1016/j.jpowsour.2012.12.016

[126] Seo K, Nishikawa Y, Naitoh K. A method of generating hydrogen gas by aluminum dissolution in water. Technol Rep Osaka Univ. 1988;38:179-86.

[127] Venter A, Beukes J, Van Zyl P, Brunke E-G, Labuschagne C, Slemr F, et al. Statistical exploration of gaseous elemental mercury (GEM) measured at Cape Point from 2007 to 2011. Atmospheric Chemistry and Physics. 2015;15:10271-80. DOI: https://doi.org/10.5194/acp-15-10271-2015

[128] Wang H, Chang Y, Dong S, Lei Z, Zhu Q, Luo P, et al. Investigation on hydrogen production using multicomponent aluminum alloys at mild conditions and its mechanism. International Journal of Hydrogen Energy. 2013;38:1236-43. DOI: http://dx.doi.org/10.1016/j.ijhydene.2012.11.034

[129] Villars P, Prince A, Okamoto H. Handbook of ternary alloy phase diagrams: Asm Intl; 1995.

[130] Senel E, Walmsley JC, Diplas S, Nisancioglu K. Liquid metal embrittlement of aluminium by segregation of trace element gallium. Corrosion Science. 2014;85:167-73. DOI: http://dx.doi.org/10.1016/j.corsci.2014.04.012

[131] Ziebarth JT, Woodall JM, Kramer RA, Choi G. Liquid phase-enabled reaction of Al–Ga and Al–Ga–In–Sn alloys with water. International Journal of Hydrogen Energy. 2011;36:5271-9. DOI: http://dx.doi.org/10.1016/j.ijhydene.2011.01.127

[132] Nizovskii AI, Belkova SV, Novikov AA, Trenikhin MV. Hydrogen Production for Fuel Cells in Reaction of Activated Aluminum with Water. Procedia Engineering. 2015;113:8-12. DOI: http://dx.doi.org/10.1016/j.proeng.2015.07.278

[133] Nizovskii A, Kulikov A, Trenikhin M, Bukhtiyarov V. Material for Compact Hydrogen Cartridges Based on Commercial Aluminium Alloys Activated by Ga-In Eutectics. Catalysis for Sustainable Energy. 2017;4:62-6. DOI: https://doi.org/10.1515/cse-2017-0010

[134] Du B, Wang W, Chen W, Chen D, Yang K. Grain refinement and Al-water reactivity of AlGaInSn alloys. International Journal of Hydrogen Energy. 2017;42:21586-96. DOI: https://doi.org/10.1016/j.ijhydene.2017.07.105

[135] Wang W, Chen D, Yang K. Investigation on microstructure and hydrogen generation performance of Al-rich alloys. International Journal of Hydrogen Energy. 2010;35:12011-9.

[136] Jayaraman K, Chauveau C, Gökalp I. Effects of Aluminum Particle Size, Galinstan Content and Reaction Temperature on Hydrogen Generation Rate Using Activated Aluminum and Water. Energy and Power Engineering. 2015;7:426. DOI: http://dx.doi.org/10.4236/epe.2015.79041

[137] Huang T, Gao Q, Liu D, Xu S, Guo C, Zou J, et al. Preparation of Al-Ga-In-Sn-Bi quinary alloy and its hydrogen production via water splitting. International Journal of Hydrogen Energy. 2015;40:2354-62. DOI: http://dx.doi.org/10.1016/j.ijhydene.2014.12.034

[138] Yang B, Zhu J, Jiang T, Gou Y, Hou X, Pan B. Effect of heat treatment on AlMgGaInSn alloy for hydrogen generation through hydrolysis reaction. International Journal of Hydrogen Energy. 2017;42:24393-403. DOI: https://doi.org/10.1016/j.ijhydene.2017.07.091

[139] Du BD, He TT, Liu GL, Chen W, Wang YM, Wang W, et al. Al-water reactivity of AlMgGaInSn alloys used for hydraulic fracturing tools. International Journal of Hydrogen Energy. 2018;43:7201-15. DOI: https://doi.org/10.1016/j.ijhydene.2018.02.090

[140] Papworth A, Fox P. The disruption of oxide defects within aluminium alloy castings by the addition of bismuth. Materials Letters. 1998;35:202-6. DOI: https://doi.org/10.1016/S0167-577X(97)00244-9

[141] Gudić S, Smoljko I, Kliškić M. The effect of small addition of tin and indium on the corrosion behavior of aluminium in chloride solution. Journal of Alloys and Compounds. 2010a;505:54-63. DOI: https://doi.org/10.1016/j.jallcom.2010.06.055

[142] Parsons R. Handbook of electrochemical constants. 1959.

[143] Benjamin J. Mechanical alloying. Scientific American. 1976;234:40-8.

[144] Suryanarayana C. Mechanical alloying and milling. Progress in Materials Science. 2001;46:1-184. DOI: http://dx.doi.org/10.1016/S0079-6425(99)00010-9

[145] Razavi-Tousi SS, Szpunar JA. Effect of structural evolution of aluminum powder during ball milling on hydrogen generation in aluminum–water reaction. International Journal of Hydrogen Energy. 2013;38:795-806. DOI: http://dx.doi.org/10.1016/j.ijhydene.2012.10.106

[146] Du Preez SP, Bessarabov DG. Hydrogen generation by the hydrolysis of mechanochemically activated aluminum-tin-indium composites in pure water. International

Journal of Hydrogen Energy. 2018;43:21398-413. DOI: https://doi.org/10.1016/j.ijhydene.2018.09.133

[147] Ying C, Bei L, Huihu W, Shijie D. Effects of Preparation Parameters and Alloy Elements on the Hydrogen Generation Performance of Aluminum Alloy-0° C Pure Water Reaction. Rare Metal Materials and Engineering. 2017;46:2428-32. DOI: https://doi.org/10.1016/S1875-5372(17)30210-2

[148] Wang F-Q, Wang H-H, Wang J, Lu J, Luo P, Chang Y, et al. Effects of low melting point metals (Ga, In, Sn) on hydrolysis properties of aluminum alloys. Transactions of Nonferrous Metals Society of China. 2016;26:152-9. DOI: http://dx.doi.org/10.1016/S1003-6326(16)64100-6

[149] Fan MQ, Xu F, Sun LX. Studies on hydrogen generation characteristics of hydrolysis of the ball milling Al-based materials in pure water. International Journal of Hydrogen Energy. 2007;32:2809-15. DOI: https://doi.org/10.1016/j.ijhydene.2006.12.020

[150] Dupiano P, Stamatis D, Dreizin EL. Hydrogen production by reacting water with mechanically milled composite aluminum-metal oxide powders. International Journal of Hydrogen Energy. 2011;36:4781-91. DOI: http://dx.doi.org/10.1016/j.ijhydene.2011.01.062

[151] Deng ZY, Tang YB, Zhu LL, Sakka Y, Ye J. Effect of different modification agents on hydrogen-generation by the reaction of Al with water. International Journal of Hydrogen Energy. 2010;35:9561-8. DOI: http://dx.doi.org/10.1016/j.ijhydene.2010.07.027

[152] Wang H-W, Chung H-W, Teng H-T, Cao G. Generation of hydrogen from aluminum and water – Effect of metal oxide nanocrystals and water quality. International Journal of Hydrogen Energy. 2011;36:15136-44. DOI: http://dx.doi.org/10.1016/j.ijhydene.2011.08.077

[153] Czech E, Troczynski T. Hydrogen generation through massive corrosion of deformed aluminum in water. International Journal of Hydrogen Energy. 2010;35:1029-37. DOI: http://dx.doi.org/10.1016/j.ijhydene.2009.11.085

[154] Fan MQ, Xu F, Sun L-X, Zhao J-N, Jiang T, Li W-X. Hydrolysis of ball milling Al–Bi–hydride and Al–Bi–salt mixture for hydrogen generation. Journal of Alloys and Compounds. 2008;460:125-9. DOI: http://dx.doi.org/10.1016/j.jallcom.2007.05.077

[155] Huang X-N, Lv C-J, Wang Y, Shen H-Y, Chen D, Huang Y-X. Hydrogen generation from hydrolysis of aluminum/graphite composites with a core–shell structure. International Journal of Hydrogen Energy. 2012;37:7457-63. DOI: http://dx.doi.org/10.1016/j.ijhydene.2012.01.126

[156] Streletskii AN, Kolbanev IV, Borunova AB, Butyagin PY. Mechanochemically activated aluminium: Preparation, structure, and chemical properties. Journal of Materials Science. 2004;39:5175-9. DOI: 10.1023/B:JMSC.0000039205.46608.1a

[157] Wu N, Wu J, Wang G-X, Li Z. Amorphization in the Al-C system by mechanical alloying. Journal of Alloys and Compounds. 1997;260:121-6.

[158] Streletskii A, Kolbanev I, Borunova A, Butyagin PY. Mechanochemical activation of aluminum: 3. Kinetics of interaction between aluminum and water. Colloid Journal. 2005;67:631-7.

[159] Pivkina A, Streletskii A, Kolbanev I, Ul'Yanova P, Frolov Y, Butyagin P, et al. Mechanochemically activated nano-aluminium: Oxidation behaviour. Journal of Materials Science. 2004;39:5451-3.

[160] Zhao Z, Chen X, Hao M. Hydrogen generation by splitting water with Al–Ca alloy. Energy. 2011;36:2782-7. DOI: http://dx.doi.org/10.1016/j.energy.2011.02.018

[161] Fan MQ, Sun LX, Xu F, Mei D, Chen D, Chai WX, et al. Microstructure of Al–Li alloy and its hydrolysis as portable hydrogen source for proton-exchange membrane fuel cells. International Journal of Hydrogen Energy. 2011;36:9791-8. DOI: http://dx.doi.org/10.1016/j.ijhydene.2011.05.096

[162] Rosenband V, Gany A. Compositions and methods for hydrogen generation. Google Patents; 2014.

[163] Chen X, Zhao Z, Liu X, Hao M, Chen A, Tang Z. Hydrogen generation by the hydrolysis reaction of ball-milled aluminium–lithium alloys. Journal of Power Sources. 2014;254:345-52. DOI: http://dx.doi.org/10.1016/j.jpowsour.2013.12.113

[164] Fan Mq, Sun Lx, Xu F. Experiment assessment of hydrogen production from activated aluminum alloys in portable generator for fuel cell applications. Energy. 2010;35:2922-6. DOI: http://dx.doi.org/10.1016/j.energy.2010.03.023

[165] Fan M-Q, Xu F, Sun L-X. Hydrogen generation by hydrolysis reaction of ball-milled Al-Bi alloys. Energy & Fuels. 2007;21:2294-8.

[166] Liu S, Fan M-q, Wang C, Huang Y-x, Chen D, Bai L-q, et al. Hydrogen generation by hydrolysis of Al–Li–Bi–NaCl mixture with pure water. International Journal of Hydrogen Energy. 2012;37:1014-20. DOI: http://dx.doi.org/10.1016/j.ijhydene.2011.03.029

APPENDIX A: PATENT

Activation compounds for hydrogen generation

A.1 Author list and contributions

Authors list

D.G. Bessarabov[a,*] and S.P. du Preez[a]

[a] HySA Centre of Competence, North-West University (NWU), Potchefstroom Campus, Private Bag X6001, Potchefstroom, 2520, South Africa

Contributions

Contributions of the various co-authors were as follows:

DG Bessarabov (supervisor) made conceptual contributions and assisted with scientific paper preparation. Experimental work, data processing and interpretation, research, and writing of the scientific paper was performed by the candidate, SP du Preez.

A.2 Patent Status

The patent presented in Appendix A was granted by the Netherlands Patent office (Publication number: NL2017962B1). Only the front page and claims of the patent was presented here. The full patent can be found at https://patents.google.com/patent/NL2017962B1/en?inventor=bessarabov&oq=bessarabov.

(19) Octrooicentrum Nederland

(11) **2017962**

(12) B1 **OCTROOI**

(21) Aanvraagnummer: **2017962**

(22) Aanvraag ingediend: **09/12/2016**

(51) Int. Cl.:
C01B 3/08 (2017.01)

(41) Aanvraag ingeschreven:
19/06/2018

(43) Aanvraag gepubliceerd:
-

(47) Octrooi verleend:
19/06/2018

(45) Octrooischrift uitgegeven:
20/06/2018

(73) Octrooihouder(s):
North-West University
te POTCHEFSTROOM, South Africa, ZA.

(72) Uitvinder(s):
Dmitri Georgievich Bessarabov
te POTCHEFSTROOM (ZA).
Stephanus Petrus Du Preez te BRITS (ZA).

(74) Gemachtigde:
ir. H.V. Mertens c.s. te Rijswijk.

(54) **ACTIVATION COMPOUNDS FOR HYDROGEN GENERATION**

(57) The invention relates to a mechanochemical activated compound for producing hydrogen via hydrolysis, the compound comprising aluminium consisting of at least 90 wt% of the compound, and at least two non-identical additional elements, each of said two additional elements being independently selected from the group consisting of In, Bi and Sn and wherein said two elements collectively consist of not more than 10 wt% of the compound. The invention further relates to a process and the use of the mechanochemical activated compound during hydrolysis.

NL B1 2017962

Clauses:

1. A mechanochemical activated compound for producing hydrogen via hydrolysis, the compound comprising;
   - aluminium consisting of at least 90 wt% of the compound, and
   - at least two non-identical additional elements, each of said two additional elements being independently selected from the group consisting of In, Bi and Sn and wherein said two elements collectively consist of not more than 10 wt% of the compound.

2. The compound of clause 1, wherein the at least two non-identical additional elements are In and Bi, respectively.

3. The compound of clause 2, wherein the wt% of In is in the range from, both values inclusive, between 8.76 wt% and 0.62 wt%, and whereby the Bi has a corresponding wt% value that together with the In wt% consist of not more than 10 wt% of the compound.

4. The compound of clause 2, wherein the compound consists of 90 wt% Al, 0.62 wt% In and 9.38 wt% Bi for achieving hydrogen generation during hydrolysis.

5. The compound of clause 2, wherein the compound consists of 90 wt% Al, 1.26 wt% In and 8.76 wt% Bi for achieving hydrogen generation during hydrolysis.

6. The compound of clause 2, wherein the compound consists of 90 wt% Al, 2.5 wt% In and 7.5 wt% Bi for achieving hydrogen yields exceeding 93% during hydrolysis.

7. The compound of clause 2, wherein the compound consists of 90 wt% Al, 5 wt% In and 5 wt% Bi for achieving hydrogen yields exceeding 93% during hydrolysis.

8. The compound of clause 2, wherein the compound consists of 90 wt% Al, 6.26 wt% In and 3.74 wt% Bi for achieving hydrogen generation during hydrolysis.

9. The compound of clause 2, wherein the compound consists of 90 wt% Al, 7.5 wt% In and 2.5 wt% Bi for achieving hydrogen yields exceeding 93% during hydrolysis.

10. The compound of clause 2, wherein the compound consists of 90 wt% Al, 8.76 wt% In and 1.26 wt% Bi for achieving hydrogen generation during hydrolysis.

11. The compound of clause 1, wherein the at least two non-identical additional elements are In and Sn, respectively.

12. The compound of clause 11, wherein the compound consists of 90 wt% Al, 7.5 wt% In and 2.5 wt% Sn for achieving hydrogen yields exceeding 93% during hydrolysis.

13. A mechanochemical activated compound for producing hydrogen via hydrolysis, the compound comprising;
- aluminium consisting of at least 86.91 wt% of the compound, and
- at least two non-identical additional elements, each of said two additional elements being independently selected from the group consisting of In, Bi and Sn and wherein said two elements collectively consist of not more than 13.09 wt% of the compound.

14. The compound of clause 13, wherein the compound consists of 86.91 wt% Al, 4.71 wt% In and 8.38 wt% Bi for achieving hydrogen yields exceeding 93% during hydrolysis.

15. The compound of clause 13, wherein the compound consists of 86.91 wt% Al, 2.54 wt% In and 10.55 wt% Sn for achieving hydrogen yields exceeding 93% during hydrolysis.

16. The compound of clause 13, wherein the compound consists of 86.91 wt% Al, 9.82 wt% In and 3.27 wt% Sn for achieving hydrogen yields exceeding 93 wt% during hydrolysis.

17. A mechanochemical activated compound for producing hydrogen via hydrolysis, the compound comprising;
- aluminium consisting of at least 86.91 wt% of the compound, and
- three additional elements being independently selected from the group consisting of In, Bi and Sn and wherein said three elements collectively consists of not more than 13.09 wt% of the compound.

18. The compound of clause 17, wherein the compound consist of 86.91 wt% Al, 3.93 wt% In, 3.93 wt% Bi and 5.24 wt% Sn for achieving hydrogen yields exceeding 93% during hydrolysis.

19. The compound of clause 17, wherein the compound consists of 86.91 wt% Al, 3.93 wt% In, 6.54 wt% Bi and 2.62 wt% Sn for achieving hydrogen yields exceeding 93% during hydrolysis.

20. The compound of clause 17, wherein the compound consists of 86.91 wt% Al, 6.54 wt% In, 3.93 wt% Bi and 2.62 wt% Sn for achieving hydrogen yields exceeding 93% during hydrolysis.

21. The compound of clause 17, wherein the compound consists of 86.91 wt% Al, 2.62 wt% In, 3.93 wt% Bi and 6.54 wt% Sn for achieving hydrogen yields exceeding 93% during hydrolysis.

22. The compound of any one of the preceding clauses, wherein the mechanochemical activation is ball milling.

23. A process for producing hydrogen via hydrolysis, the process including the following steps in non-sequential order;
    - providing a mechanochemical activated compound as described herein above;
    - providing a source of water; and
    - producing hydrogen via hydrolysis.

24. Use of the compound of any one of the preceding clauses in a hydrolysis reaction.

25. Use of the compound of any one of the preceding clauses for proton exchange membrane fuel cell (PEMFC) applications.

26. The compound of any one of clauses 1, 13 or 17, substantially as herein described with reference to the accompanying figures.

27. The process of clause 23, substantially as herein described with reference to the accompanying figures.

28. The use of clause 24 or clause 25, substantially as herein described with reference to the accompanying figures.